AWARD NUMBER: W81XWH-16-1-0068
(BC150847)

TITLE: Targeting the Mevalonate Pathway and its Restorative Feedback Loop in Breast Cancer

PRINCIPAL INVESTIGATOR: Linda Penn, PhD

CONTRACTING ORGANIZATION: University Health Network, 200 Elizabeth St, Toronto, Ontario, CANADA M5G 2C4

REPORT DATE: July 2021

TYPE OF REPORT: Final Report

PREPARED FOR: U.S. Army Medical Research and Development Command
Fort Detrick, Maryland 21702-5012

REPORT DOCUMENTATION PAGE

Form Approved
OMB No. 0704-0188

1. REPORT DATE	2. REPORT TYPE	3. DATES COVERED
JULY 2021	Final Report	1-APR-2016 to 31-MAR-2021

4. TITLE AND SUBTITLE

Targeting the Mevalonate Pathway and Its Restorative Feedback Loop in Breast Cancer

5a. CONTRACT NUMBER
W81XWH-16-1-0068

5b. GRANT NUMBER
BC150847

5c. PROGRAM ELEMENT NUMBER

6. AUTHOR(S)
Linda Penn, PhD

E-Mail: lpenn@uhnresearch.ca

5d. PROJECT NUMBER

5e. TASK NUMBER

5f. WORK UNIT NUMBER

7. PERFORMING ORGANIZATION NAME(S) AND ADDRESS(ES)
University Health Network
200 Elizabeth St
Toronto, Ontario, CANADA
M5G 2C4

8. PERFORMING ORGANIZATION REPORT NUMBER

9. SPONSORING / MONITORING AGENCY NAME(S) AND ADDRESS(ES)

U.S. Army Medical Research and Development Command
Fort Detrick, Maryland 21702-5012

10. SPONSOR/MONITOR'S ACRONYM(S)

11. SPONSOR/MONITOR'S REPORT NUMBER(S)

12. DISTRIBUTION / AVAILABILITY STATEMENT

Approved for Public Release; Distribution Unlimited

13. SUPPLEMENTARY NOTES

14. ABSTRACT.

We have shown that targeting the mevalonate pathway with fluvastatin preferentially induces apoptosis in breast cancer (BrCa) cells that have undergone epithelial-to-mesenchyme transition (EMT), a critical process for the initiation of metastasis. Moreover, we have identified that EMT gene expression is bimodally distributed and is a biomarker of fluvastatin sensitivity. Mechanistically, we have shown that fluvastatin can induce apoptosis by limiting production of an important end-product of the mevalonate pathway essential for protein *N*-glycosylation associated with EMT. We have also shown that dipyridamole(DP) potentiates fluvastatin-induced apoptosis of BrCa cells by blocking the statin-induced restorative feedback loop. We have also identified additional agents that can potentiate statin-induced BrCa cell death, thereby expanding this class of anti-cancer agents. We have published 3 manuscripts (2 at *Cancer Research* and *Molecular Oncology*), have another nearly ready for resubmission to *Nature Communications*, and have published a review article in *Clinical Cancer Research*. Thus, we have been highly productive and made advances that are actionable and have potential to immediately impact BrCa patient outcome.

15. SUBJECT TERMS
statins, dipyridamole, apoptosis, breast cancer, metastasis, mouse models, therapeutics, FDA-approved agents

16. SECURITY CLASSIFICATION OF:			17. LIMITATION OF ABSTRACT	18. NUMBER OF PAGES	19a. NAME OF RESPONSIBLE PERSON
a. REPORT	b. ABSTRACT	c. THIS PAGE			USAMRMC
Unclassified	Unclassified	Unclassified	Unclassified	122	19b. TELEPHONE NUMBER *(include area code)*

Table of Contents

Page

1. Introduction……. 4

2. Keywords……. 4

3. Accomplishments……..……... 5

4. Impact……...…… 14

5. Changes/Problems...…..…… 16

6. Products…….…….…..……. 17

7. Participants & Other Collaborating Organizations……. 19

8. Appendices…… 21

INTRODUCTION:

Background: In early stage breast cancer (BrCa) treated with frontline therapy, 20-30% reoccur as distant metastases, despite intensive treatment. Metastatic BrCa accounts for nearly all BrCa deaths, and has no cure. Development of new and effective metastasis prevention strategies will clearly mark a key advance. We aim to fill this gap and address two overarching challenges in BrCa: 1) prevention of metastatic BrCa spread and elimination of the mortality associated with metastatic BrCa; and 2) replacing toxic interventions with ones that are safe and effective. Specifically, we aim to provide essential preclinical data to advance two families of Federal Drug Administration (FDA)-approved drugs, statins and dipyridamole (DP), as metastatic BrCa prevention agents. Our preliminary data show that statins are cytotoxic to BrCa cells that have undergone epithelial-to-mesenchymal transition (EMT) and mesenchymal-to-epithelial transition (MET), two processes that form the initiation and completion of the invasion-metastasis cascade in malignant tumors. We have also shown that DP potentiates the cytotoxic activity of statins by blocking the statin-triggered restorative feedback response. Interrogating the efficacy and mechanism of the statin+DP combination in BrCa will provide preclinical evidence to support further evaluation of this novel drug combination in human clinical trials, and for the development of predictive and dynamic biomarkers of drug sensitivity.

Hypothesis and objectives: We *hypothesize* that statins, alone or in combination with DP, can be effective therapeutics to prevent BrCa recurrence. Our *objectives* are to evaluate statins +/- DP for their efficacy and mechanism of action in BrCa cells *in vitro*, *in vivo* in a relevant mouse model, and in a cohort of patient derived xenografts (PDXs). Upon completion of this BCRP grant, we will have pre-clinical evidence of efficacy and biomarkers to support a follow-up, short time-frame clinical trial to test the use of statins +/- DP to treat metastatic disease. Our long-term goal is to leverage positive results from these pre-clinical and clinical studies to support a larger, longer, and resource-intensive trial for the use of statins+/-DP following surgery, with the goal of metastasis prevention. We believe that prescription of these effective, well-tolerated, and inexpensive therapeutics in patients with high risk of metastatic recurrence after surgery, will provide clinical benefit and improve BrCa patient survival and quality of life.

Specific Aims:

1. Delineate the efficacy and mechanism of the fluvastatin+DP combination in BrCa cells that have undergone EMT and/or MET.

2. Delineate the mechanism by which DP potentiates statin-induced tumor cell apoptosis.

3. Evaluate the efficacy of fluvastatin+DP in relevant mouse models of BrCa metastasis.

KEYWORDS: statins, dipyridamole, statin-induced feedback inhibitors, apoptosis, breast cancer, metastasis, mouse models, therapeutics, FDA-approved agents

ACCOMPLISHMENTS:

With support from the DOD, the research outlined in the original proposal has progressed in a steady and productive manner. To delineate the accomplishments, the tasks outlined in the original Statement of Work (SOW) of the proposal are itemized below (italics) and a final report for each task provided.

Aim 1. Delineate the efficacy and mechanism of the fluvastatin+DP combination in BrCa cells that have undergone EMT and/or MET (months 1-36).
Milestones to Achieve: We will delineate the efficacy and mechanism of the fluvastatin/DP combination in BrCa cells that have undergone EMT (months 1-36).

Complete. We have delineated the efficacy and mechanism of fluvastatin-induced apoptosis in BrCa cells that have undergone EMT. Our results indicate that BrCa cells that have undergone EMT become more sensitive to the pro-apoptotic effects of fluvastatin. This anti-BrCa activity is reversible with exogenous mevalonate, showing the effect is on-target. Moreover, we have shown that expression of genes associated with EMT serves as a robust biomarker of statin sensitivity, not only in BrCa, but across a broad range of cancers. Our manuscript describing these findings has been published in the journal *Cancer Research*. A copy of this manuscript has been appended (Appendix 1). Mechanistically, we had shown that the anti-proliferative effects of fluvastatin on cells undergoing EMT is dependent on a specific product of the mevalonate pathway; geranylgeranyl pyrophosphate (GGPP). GGPP can serve as a substrate for protein isoprenylation or as a building block for the production of co-enzyme Q or dolichol. Unexpectedly, the mechanism did not involve protein isoprenylation as anticipated. Instead, we have shown that key end-product in cell undergoing EMT is dolichol, which is essential for protein *N*-glycosylation. Moreover, as EMT can be a critical component of BrCa metastasis, we have demonstrated that statins inhibit BrCa metastasis. A manuscript describing these results has been published in the journal *Cancer Research*. A copy of this manuscript has been appended (Appendix 2). Once we discovered this new paradigm for how and why fluvastatin preferentially targets tumor cells undergoing EMT, and thereby inhibits BrCa metastasis, we next focused on delineating the efficacy and mechanism of the fluvastatin/DP combination in BrCa cells that have undergone EMT.

Subtask 1: Develop and validate HPLC/MS assays to measure the intracellular concentration of MVA, GGPP and FPP, as well as DP, (Fluvastatin already established), using MCF10A cell lines overexpressing Snail and H-Ras (months 1-12; Site 1, Penn)
Complete. In collaboration with Dr. Eric Chen, we have successfully developed HPLC/MS assays to detect MVA, GGPP, FPP and DP.

Subtask 2: Establish and validate IHC assays for HMGCS1 and SREBP2, (HMGCR already established) (months 1-12; Site 1, Penn)
Complete. We have established and validated an IHC assay for SREBP2. Assay development for HMGCS1 has been terminated as all commercially available antibodies have failed at the level of sensitivity and/or specificity. Thus, we will go forward with IHC assays for the transcription factors SREBP2 and its target gene HMGCR. While having an IHC assay for another SREBP2 target, HMGCS1, would have been ideal, it is not essential to conduct our research as two out of three probes have been successfully validated.

Subtask 3: Develop titratable inducible system to express dominant active (DA) alleles, and DA alleles fused to a myristoylation tag (myr-DA) of five isoprenylated proteins (months 1-12; Site 1, Penn)
Complete. We have successfully used a retroviral transgene expression system to express DA alleles and/or myr-DA alleles of five isoprenylated proteins (K-Ras, RhoA, RhoB, Rac1, and Rap1A) in the MCF10A cell line (Appendix 1).

Subtask 4: Express DA and myr-DA alleles in MCF10A and assay for activity, EMT and fluvastatin sensitivity in 2D and 3D culture conditions (months 6-18; Site 1, Penn).
Complete. The DA alleles of five isoprenylated proteins did not all sensitize MCF10A cells to fluvastatin-induced apoptosis or -decreased colony growth. Moreover, expression of the myr-alleles did not overcome sensitivity to fluvastatin-induced death as expected, yet this tumor cell death was rescued with exogenous GGPP. Taken together, this data suggested that protein isoprenylation was not contributing to the increased sensitivity to fluvastatin (Appendix 1).

Subtask 5: Express DA and myr-DA alleles in MCF10A Snail and H-Ras cells and assay for activity, EMT and fluvastatin sensitivity in 2D and 3D culture conditions (months 12-24; Site 1, Penn).
Complete. Based on the results of Aim1, Subtask 4 (Appendix 1), this series of experiments was no longer required as we have shown that fluvastatin-induced apoptosis in BrCa cells was uncoupled from protein isoprenylation, yet still functionally rescued by exogenous GGPP. Further interrogation showed that GGPP was not required for isoprenylation but for the production of dolichol. Thus, the model changed and evaluating the role of these isoprenylated proteins, as originally outlined, became obsolete. Instead, we determined that dolichol was the essential end-product downstream of GGPP that was essential for fluvastatin-induced kill of cells that have undergone EMT (Apppendix 2).

Subtask 6: Conduct RNAseq on cells grown in 3D on Matrigel, this include MCF10A cells that have (Snail, H-ras) and have not undergone EMT (vector control, MycT58A), as well as MCF10A cells expressing DA or myr-DA that undergo EMT (months 6-18; Site 1, Penn).
Complete. The goal of this subtask was to develop a mRNA expression-based biomarker of cells that have undergone EMT and are highly sensitive to the anti-proliferative activity of fluvastatin. Indeed, we have identified that expression of genes associated with EMT are bimodally distributed and serve as a robust biomarker of statin sensitivity in BrCa. Moreover, we have shown that this biomarker shows efficacy across large panel of cancer types, beyond BrCa (Appendix 1).

Subtask 7: Conduct Bioinformatics analysis on RNAseq data (months 9-21; Site 1, Penn).
Complete. Bioinformatic analysis led to the discovery the EMT gene mRNA expression was robustly bimodally distributed and was associated with statin sensitivity. This discovery was evident in multiple cancer subtypes, including BrCa, and with multiple statin drugs, including fluvastatin, simvastatin and lovastatin (Appendix 1).

Subtask 8: Evaluate metastatic potential of EMT cells (MCF10As overexpressing Snail or H-Ras) in response to fluvastatin+DP (months 18-24; Site 1, Penn)
Complete. To further evaluate the association of fluvastatin sensitivity with cells having undergone EMT, we have shown that BrCa cells that are epithelial (e.g. MCF-7) or mesenchymal (e.g. MDA-MB-231) in nature are relatively insensitive and sensitive to fluvastatin-induced apoptosis in tissue culture, respectively. To model metastasis we therefore used a derivative of the MDA-MB-231 cells that metastasize to the lung (LM2-4) and have

shown that fluvastatin decreases metastasis *in vivo* (Appendix 2). We used this LM2-4 (MDA-MB-231) model system rather than the MCF10A cells expressing exogenous Snail or H-Ras as we were concerned that the ability of the MCF10A models to metastasize would not be sufficiently robust, which would delay these experiments as metastatic clones would have to be identified and serially propagated to first establish the model, and then evaluate efficacy of fluvastatin+DP. Thus, the well-established LM2-4 (MDA-MB-231) cells were successfully used to model mesenchymal BrCa cells that undergo metastasis and show that fluvastatin has anti-metastatic properties (Appendix 2).

With the model established using fluvastatin alone we went on to evaluate efficacy of fluvastatin+DP. However, when we were evaluating DP dosing, we unexpectedly observed liver-associated toxicities in the cohort of mice receiving DP after 3-4 weeks of daily treatment. Thus, optimization of the dose and treatment schedule for DP was required, which is particularly important for the longer duration treatments that were planned using the resection/metastases prevention models. Unfortunately, this issue was not able to be resolved. Notably, this phenomenon is not expected to impact the potential clinical translation of our results, as DP is delivered to patients in an oral, extended-release formulation, and the combined use with statins is well established for secondary stroke prevention.

Subtask 9: Determine mechanism of cell death in EMT cells (MCF10As overexpressing Snail or H-Ras) vs non-EMT cells (vector control, MycT58A) (months 18-24; Site 1, Penn)
Complete. The mechanism of fluvastatin-induced cell death in EMT cells is apoptosis due to depletion of GGPP/dolichol (Appendices 1 and 2). Non-EMT cells are relatively insensitive to fluvastatin.

Subtask 10: Validate in independent breast cell systems using the following TNBC cell lines: MDA-MB-231, HCC1500, SUM159PT, SUM149PT, BT20, HCC1937, HS578T, MDAMB468, MDAMB436 (months 24-36; Site 1, Penn)
Complete. To determine whether the fluvastatin+DP combination was synergistic across a panel of BrCa cell lines, a concentration range of DP was evaluated in combination with a sub-lethal dose of fluvastatin. From this data a synergy score was determined using the Bliss Index model. Remarkably the fluvastatin+DP combination was synergistic across the majority of cell lines. Even cell lines that were only weakly sensitive to fluvastatin were responsive to the fluvastatin+DP combination. This is consistent with our previous data showing the mevalonate pathway feedback response was intact across a panel of 25 breast cell lines (Goard et al., PMID:24337703). Interestingly, gene set enrichment analysis demonstrated that an EMT gene signature predicted sensitivity to the fluvastatin+DP combination as well as fluvastatin alone. These data have been incorporated into a manuscript recently posted on BioRxiv, which was also submitted and favorably reviewed at the journal *Nature Communications*. A copy of this manuscript has been appended (Appendix 3).

Aim 2: Delineate the mechanism by which DP potentiates statin-induced tumor cell apoptosis (months 1-36).
Milestones To Achieve: We will identify the mechanism of DP action that potentiates fluvastatin induced apoptosis and identify molecular mechanism at the level of SREBP2 feedback response.

Novel agents and pathways that sensitize fluvastatin anti-BrCa activity will be identified (months 1-36).

Original Strategy: Complete. We have shown DP blocks SREBP translocation and the restorative feedback response to statin exposure, however, the mechanism of action remained unclear. To address this gap, our original strategy was to identify agents that blocked each of the many reported activities of DP individually, to determine which of these would phenocopy DP potentiation of statin-induced cell death. We started our analyses in cell lines derived from acute myelogenous leukemia (AML) and multiple myeloma (MM) as this is where our original identification of DP was discovered and studies could begin without delay (Pandyra, et al.; PMID 24994712). Our data in AML suggested that a phosphodiesterase (PDE) inhibitor, cilostazol, phenocopied DP by elevating intracellular cAMP levels. Since cAMP activates a major signaling cascade through Protein Kinase A (PKA), we further investigated whether modulation of PKA activities played a role in the inhibition of the sterol feedback response and potentiation of fluvastatin-induced cancer cell death. To our surprise, however, when we functionally assessed whether the activation of PKA was the key response to DP-induced elevated cAMP, we found that PKA activation is not functionally important in DP potentiation of statin activity. The activity of DP and cilostazol was intact in both wild-type and PKA null cells at the level of statin potentiation of tumor cell kill and inhibition of the statin-induced feedback response. Thus, this line of investigation hit a dead-end and was not been as fruitful as anticipated. To ensure these well-performed experiments were disseminated broadly, so others can conduct research knowing these results, a manuscript describing these data has been published in the *Molecular Oncology* (Appendix 4).

New Strategy: Complete. As the primary goal of this Aim was to identify "Novel agents and pathways that sensitize fluvastatin anti-BrCa activity" and we could not evaluate statin+DP in mouse models of BrCa as anticipated (see Aim 1, Subtask 8), we decided to take a pharmacogenomics approach with Dr. Ben Haibe-Kains to ask whether other drugs are "DP-like" in terms of i) Structure; by identifying compounds that have a shared chemical structure with DP, ii) Perturbation; by identifying compounds that when exposed to cells triggered similar changes to mRNA expression of six mevalonate pathway genes, determined by interrogating the LINCS L1000 dataset, and iii) Sensitivity Screening; by identifying compounds that triggered a similar profile of cell death in response to DP exposure across the NCI-60 panel of cell lines. This resulted in a Mevalonate (MVA) Pathway-specific Drug Network Fusion (MVA-DNF; Appendix 3).

Twenty-three drugs were identified as hits based on statistical significance. The top five hits included doxorubicin, which we had previously published as a potentiator of lovastatin (PMID:20298590), thus providing confidence in our *in silico* approach and the results obtained. The additional drugs in the top five (selumetinib, nelfinavir, mitoxantrone, honokiol) were advanced for experimental validation. Three of these four drugs were validated as potentiators of fluvastatin-induced cell death, including selumetinib (Selu), nelfinavir (NFV), and honokiol (HNK), based on: i) MTT Assays; ii) propidium iodide staining of cellular DNA followed by flow-cytometry to determine the percent 'Pre-G1' population; and, iii) PARP cleavage. We investigated these three agents for their mechanism of action and showed that two (NFV, HNK) do indeed behave like DP and inhibit the statin-triggered feedback response based on MVA gene mRNA expression and SREBP2 activation. As before (Aim1, Subtask 10), we evaluated the

synergy of these agents in combination with fluvastatin (Fluva) across 47 breast cancer cell lines and compared this to DP (positive control). We have also shown that basal mRNA gene expression as a predictor for each of the drug combinations (Fluva+NFV vs. Fluva+DP, Fluva+HNK vs. Fluva+DP, and Fluva+NFV vs. Fluva+HNK) across this cell line panel were highly correlated, consistent with a common mechanism of action underlying the observed synergy. By ranking genes according to their correlation to the fluvastatin IC_{50} value or to the synergy score (Fluva+DP, Fluva+NFV and Fluva+HNK) using gene set enrichment analysis (GSEA) with the Hallmark gene set collection, we have shown that genes associated with Epithelial to Mesenchymal Transition (EMT) were associated with sensitivity. This association was evident across multiple gene set collections, which shows this signal is robust. Validation of specific EMT genes has been performed and E-cadherin is significant across all conditions.

In summary, we have achieved our goal to identify "Novel agents and pathways that sensitize fluvastatin anti-BrCa activity". Using our new MVA-DNF strategy we validated that four of the top five hits potentiate the pro-apoptotic activity of fluvastatin and, mechanistically, two inhibit the statin-induced feedback mechanism. This provides confidence in our approach that has unveiled two FDA-approved drugs, Fluva+NFV, can synergize to trigger cell death of mesenchymal-enriched BCa cells. Moreover, additional hits for future evaluation have been uncovered through this approach (Appendix 3). Further *in vivo* testing in PDX organoids and mouse models of BCa is now warranted and will be performed over the next year, during a no cost extension of my partnering PI (Dave Cescon). These data have been incorporated into a manuscript recently posted on BioRxiv, which was also submitted and favorably reviewed at the journal *Nature Communications*. A copy of this manuscript has been appended (Appendix 3). We are just finishing this up by addressing reviewers' comments and anticipate re-submission of this revised manuscript in the next 2-3 months.

Subtask 1: Evaluate pharmacological agents for their ability to phenocopy DP and potentiate fluvastatin anti-BrCa activity (MCF10As overexpressing Snail or H-Ras; other TNBC cell lines including MDA-MB-231, HCC1500, SUM159PT, SUM149PT, BT20, HCC1937, HS578T, MDAMB468, MDAMB436 (months 1-12; Site 1, Penn)

Original Strategy: Complete. DP has been reported to alter several biochemical pathways. To identify the mechanism of DP potentiation of fluvastatin anti-cancer activity it was important to validate across a panel of different types of cancers, including acute myeloid leukemia (AML), multiple myeloma (MM), prostate and BrCa. Our preliminary data in AML suggest that a PDE inhibitor, cilostazol, phenocopies DP by elevating intracellular cAMP levels. Since cAMP activates signaling cascades through PKA, we further investigated whether modulation of PKA activities plays a role in the inhibition of the sterol feedback response and potentiation of fluvastatin-induced cancer cell death. To our surprise, PKA activation was not mechanistically involved in this DP activity, nor was the DP induction of cAMP evident in other cancer types, including BrCa. Despite this line of investigation not being as productive as anticipated, we felt it was important to report our results and share this knowledge with the community. A manuscript describing these results was published in *Molecular Oncology* and has been appended (Appendix 4)

New Strategy: Complete. To investigate whether the drugs identified as DP-like using our pharmacogenomics approach, MVA-DNF, could potentiate fluvastatin induced cell death, we further investigated the top five hits from the ranked list of drugs similar to DP ($p<0.05$). As Doxorubicin scored as a top hit and we had previously published this agent as a potentiator of lovastatin (Martirosyan et al., PMID:20298590), this provided confidence in our results, and the top four drugs were advanced for validation (selumetinib, nelfinavir, mitoxantrone and honokiol). We investigated the sensitivity to sub-lethal statin exposure in combination with the novel DP-like drugs in a statin-sensitive (MDA-MB-231) and insensitive (HCC1937) BrCa cell lines. As seen with DP, we observed similar potentiation of statins when combined with nelfinavir, honokiol or selumetinib, but not mitoxantrone. To determine the nature of the anti-proliferative activity of statins+drugs, we evaluated cell cycle arrest and cell death by fixed propidium-iodide/flow cytometry and apoptosis by PARP-cleavage, respectively. Our data indicates that all three drugs mimic DP as potentiators of the pro-apoptotic activity of fluvastatin (Appendix 3).

Subtask 2: Validate results using independent pharmacological inhibitors and RNAi approach (months 9-24; Site 1, Penn)

Original Strategy: Complete. We validated the above preliminary results in AML using an independent PDE inhibitor, sildenafil, and an activator of cAMP, forskolin, and showed these agents could phenocopy DP to potentiate fluvastatin-induced cancer cell apoptosis in some but not all cancer types, including BrCa. We also used RNAi and CRISPR-Cas9 technologies to knockdown and knockout PKA, respectively, to evaluate the role of PKA activity in inhibition of the sterol feedback response and potentiation of fluvastatin-induced cancer cell death. To our surprise, PKA was not mechanistically involved in this DP activity. This line of investigation has been quite disappointing, and we are no longer pursuing this approach. Nonetheless, we disseminated this knowledge through publication of a manuscript in *Molecular Oncology* (Appendix 4).

New Strategy: Essentially Complete. Selumetinib is an inhibitor of MEK, and we had previously shown that statin inhibition of the MAPK-ERK-MEK pathway contributed to the AML cell death in response to lovastatin exposure (Wu et al. PMID:15374955). Moreover, we had shown that the MEK1 inhibitor PD98059 sensitized AML cells to low, physiologically achievable concentrations of lovastatin. Thus, our new data shows another MEK inhibitor (selumetinib) can potentiate fluvastatin-induced cell death of BrCa cell lines and validates statin+MEKi as a combination for further evaluation. Honokial is a natural product derived from Mahogany tree bark whose mechanism of action remains unclear, therefore we are not able to further evaluate mechanism at a molecular level using a genetic approach. Nelfinavir is a S1P protease inhibitor approved for the treatment of HIV with a well-defined mechanism of action. Therefore, we will further validate its action in this setting by establishing inducible shRNAs targeting this protease to evaluate whether this on-target effect is mechanistically critical for nelfinavir to potentiate fluvastatin tumor cell death. These experiments will be incorporated into the manuscript (Appendix 3) that is now being prepared for re-submission within the next 2-3 months.

Subtask 3: Determine molecular mechanism of action of novel DP-like molecules that can potentiate fluvastatin-induced apoptosis by assaying statin-induced feedback loop at the molecular level (MCF10As overexpressing Snail or H-Ras) (months 24-36; Site 1, Penn).

New Strategy: Complete. We investigated the top three agents (Selu, NFV, HNK) that potentiated fluvastatin cell death for their mechanism of action and showed that two (NFV, HNK) behaved like DP and inhibited the statin-triggered feedback response based on MVA gene mRNA expression (Appendix 3).

Subtask 4: Conduct biochemical analyses to determine point of SREBP2 translocation that is blocked by DP (MCF10As overexpressing Snail or H-Ras) (months 1-12; Site 1, Penn).
New Strategy: Complete. We investigated the top three agents (Selu, NFV, HNK) that potentiated fluvastatin cell death for their mechanism of action and showed that two (NFV, HNK) behaved like DP and inhibited SREBP2 activation (Appendix 3).

Subtask 5: Evaluate precise point of SREBP2 inhibition by DP using fluorescence strategies (months 13-24; Site 1, Penn).
70% Complete. We have used a complementary approach to Aim2, Subtask 4 by using high-content image analysis using a novel fluorescent probe to track SREBP2 within living BrCa cells in response to fluvastatin +/- DP. The probes (SCAP-GFP, SREBEP2-Venus) have now been built and the assay validated for further evaluation of DP and DP-like agents (NFV, HNK). These new data will be incorporated into the resubmission of Appendix 3 scheduled for completion within the next 2-3 months.

Subtask 6: Determine whether novel agents and RNAi block at similar or dissimilar points of SREBP2 feedback control (months 24-36; Site 1, Penn).
Complete. The mechanism of DP (positive control) remains unclear (Appendix 2), so RNAi cannot be used to phenocopy the DP mechanism of action as an inhibitor of SREBP2 activation in response to statin exposure.

Aim 3: Evaluate the efficacy of fluvastatin+DP in relevant mouse models of BrCa metastasis (months 1-36).
Milestones To Achieve: Evaluate the effects of fluvastatin +/- DP treatment in cell line and BrCa patient-derived xenografts (PDX) using both a conventional and resection model to evaluate activity on primary and metastatic tumor (months 1-36).

Progress: 35%. We have completed the initial planned experiments evaluating the effects of fluvastatin treatment of cell line xenografts by the resection models (Appendix 2, Figure 4). To evaluate fluvastatin+/- DP combination we first evaluated DP dosing and unexpectedly observed liver-associated toxicities in the cohort of mice receiving DP after 3-4 weeks of daily treatment. Thus, optimization of the dose and treatment schedule for DP was required, which is particularly important for the longer duration treatments planned using the resection/metastases prevention models. Unfortunately, this issue was not able to be resolved. Notably, this phenomenon is not expected to impact the potential clinical translation of our results, as DP is delivered clinically in an oral, slow-release formulation, and the combined use with statins is well established in secondary stroke prevention. Having completed the characterization of the models, and recognizing that synergistic combination therapies are likely to be necessary (vs statin monotherapy), we plan to proceed with a mitigation strategy of evaluating alternative combinations from the DP-like agents (Appendix 3) that block the statin-induced feedback response. To that end, following identification and in vitro validation of these DP-like agents, we have conducted a pilot experiment of NFV and HNK as single agents in a BrCa (LN2-4) cell line

xenograft models (n=3) to establish a dose that is well-tolerated and can be evaluated in combination with fluvastatin (Appendix6; Figure 1A). Based on the prioritization as outlined from the in vitro experiments, we are advancing NFV for further studies as, like fluvastatin, it is FDA-approved. To that end, we have shown that NFV can be measured in both serum and tumor (Appendix6; Figure 1B). In addition, the combinations of fluvastatin+DP and fluvastatin+NFV can be evaluated in the patient-derived models using 3D organoid approach. These experiment are ongoing and results will be incorporated into the resubmission of Appendix 3 in the coming months. Further evaluation in PDXs predicted to be responsive to these fluvastatin-drug combinations will be performed during the no cost extension of my Partnering PI (Dave Cescon).

Subtask 1: Conduct dose escalation experiments to identify maximum tolerated and effective dose of fluvastatin in the resection model using two cell lines: Luc+14 and Luc+16 (months 1-2; Site 1, Penn).
Complete. We have shown that in the resection model using the MDA-MB-231 derived cell line LM2-4, that 50 mg/kg daily oral fluvastatin treatment is effective and well-tolerated for long-term treatment in the post-surgical adjuvant setting in SCID mice. This dose of fluvastatin treatment has been used for all subsequent animal studies (Appendix 2).

Subtask 2: Establish and treat PDX #1-8 in (A) conventional PDX models and (B) resection models (months 3-12; Site 2, Cescon).
20% Complete. While DP optimization was underway, we evaluated the effect of fluvastatin monotherapy in (A) conventional and (B) resection models as proposed (Appendix 2). While model characterization has been completed (Subtask 4 below), given the limitations encountered with DP administration, we have refocussed on evaluating the fluvastatin+NFV combination for *in vivo* testing. Development of *in vitro* patient-derived xenograft organoids using a chemically-defined matrix has successfully generated alternative models to evaluate the fluvastatin+DP and other novel combinations such as fluvastatin+NFV. This work will continue under the no cost extension of my Partnering PI (Dave Cescon).

Subtask 3: Establish and treat PDX #9-25 with control, fluvastatin+DP (2 treatment arms) in (A) conventional PDX models and (B) resection models (months 8-28; Site 2, Cescon).
Yet to complete. Given the limitations as encountered above, mitigation strategies have been successfully pursued, including the generation of PDX-derived organoids and the refocus on novel DP-like combinations (e.g. fluvastatin+NFV) to be evaluated. This work will be conducted during the no cost extension phase of my Partnering PI (Dave Cescon).

Subtask 4: Conduct RNAseq on 25 PDX donor mouse primary tumors (months 3-28; Site 1, Penn)
Complete. Basal RNAseq data has been collected on over 45 PDX models, and informatic and pharmacologic data have been integrated in a bespoke pharmacogenomics platform. These data will permit the interrogation of gene expression predictors of responsiveness to guide experimental evaluation of statin combinations *in vivo* (NFV) and/or *in vitro* organoid cultures (DP, NFV).

Subtask 5: Conduct Bioinformatics analysis on RNAseq data (months 18-36; Site 1, Penn)
Yet to complete. We will next distinguish patient-derived models with the EMT signature. These will be prioritized for testing with fluvastatin in combination with feedback inhibitors *in vivo* (NFV) and/or *in vitro* organoid cultures (DP, NFV). This will be completed during the no cost extension.

Subtask 6: Measure the intracellular concentration of MVA, GGPP and FPP, as well as fluvastatin and DP, as well as cholesterol, triglycerides; pilot on MDA-MB-231 metastasis model, then evaluate PDX models (month 3-36; Site 1, Penn)
50% Complete. We have measured fluvastatin in the MDA-MB-231 metastasis model. Assay development for DP and NFV detection and quantification *in vivo* is complete. The assay for cholesterol and triglycerides measurement is already developed by our collaborator Dr. Richard Lehner. Detection of these metabolites in the PDX models will be conducted after the PDXs are established and treated with the new fluvastatin+feedback inhibitor regimen (e.g. NFV).

Subtask 7: Conduct RNA analysis and IHC assays for mevalonate genes including HMGCR, HGMCS1 and SREBP2; pilot on MDA-MB-231 metastasis model, then evaluate PDX models (months 3-36; Site 1, Penn).
On-going. We have collected RNA for HMGCR, HMGCS1 and SREBP2 analysis in the MDA-MB-231 metastasis model, and baseline expression data for all of these targets has been collected through RNAseq analyses of patient derived models. Evaluation of the dynamic changes in the expression of these genes in the PDX models will be conducted after the PDXs are established and treated with fluvastatin and the new feedback inhibitor regimen.

Subtask 8: Analyze all data and publish papers (months 12-36; Site 1 and 2, Penn and Cescon)
Nearly Complete. Funding from the DOD has resulted in the publication of 3 manuscripts (Appendix 1, 2, 4) and another is nearly ready for resubmission (Appendix 3). During the COVID-19 lockdown we also wrote a review article, published in *Clinical Cancer Research* (Appendix 5).

IMPACT:

We have shown that fluvastatin specifically induces apoptosis in BrCa cells that have undergone EMT, a critical process for the initiation of metastatic spread. These results have direct medical **impact**, as the addition of fluvastatin to the standard of care for BrCa in the adjuvant setting is novel and an actionable outcome that can be readily and affordably implemented.

We have shown that the mechanism of fluvastatin-induced apoptosis in cells undergoing EMT is independent of protein isoprenylation. These results directly **impact** disciplines involving the study of the anti-cancer effects of statins, isoprenylation of RAS family members, metabolic reprogramming and cancer cell EMT. For decades, it has been unclear whether statins kill tumour cells by inhibiting the synthesis of FPP and GGPP, thereby limiting the function of RAS family oncoproteins. This has been a major obstacle in accelerating statins into the BrCa clinic. Our work has resolved the discrepancy surrounding this open question by showing that although statins can inhibit isoprenylation of RAS family members, this is not the cause of statin-induced cell death. Instead, we identified EMT gene expression as a robust biomarker of statin sensitivity, which has **impact** and clinical utility as it will inform which patients are most likely to benefit from statin treatment to inhibit aggressive and/or metastatic cancers.

We have delineated the mechanism of action of DP and additional feedback inhibitors that potentiate fluvastatin induced apoptosis. These results have important conceptual, technical and clinical **impact**, i) being the first indication that the MVA pathway and its homeostatic feedback regulation are both essential to cells with increased epithelial-mesenchymal plasticity, and ii) uncovering novel experimental approaches to identify new strategies to inhibit the SREBP family of transcription factors that drive expression of mevalonate pathway genes and the statin-induced feedback response.

While we have encountered challenges in the *in vivo* evaluation of the fluvastatin+DP combination therapy, due to mouse-specific delivery/tolerability issues, we believe our data characterizing the anticancer effects of these well-tolerated and clinically actionable agents (in humans) supports the potential for clinical translation. In addition, we have identified additional novel FDA-approved and well-tolerated agents such as nelfinavir, which have superior synergy with fluvastatin to drive BrCa cell death. These novel fluvastatin-drug combinations have been validated and prioritized using the systems and models developed in this project. Evaluating the efficacy of these therapeutics in relevant mouse models that closely mimic, not only the human disease and course of metastatic spread, but also the patient treatment and recovery experience adds strength to our results. These relevant and innovative research approaches significantly **impact** BrCa treatment and metastasis prevention.

We have prepared three manuscripts describing our research results from this DOD funding. Two in Cancer Research (Appendix 1 & 2) and one in *Molecular Oncology* (Appendix 4). A fourth manuscript was favorably reviewed at *Nature Communications* (Appendix 3) and will be resubmitted in the next 2-3 months. We have also published a comprehensive review in *Clinical Cancer Research* focused on "Statins as Anticancer Agents in the Era of Precision Medicine".

Publishing our work in top-flight journals such as these with wide readership significantly **impacts** technology transfer, allowing us to communicate our ideas and successes, and to move the tools and treatments we have developed forward to clinical application. Presenting our results in local seminars and international conferences to scientists as well as the lay public also **impacts** society at large by engaging a global and diverse audience.

CHANGES/PROBLEMS:

One of our goals has been to address the mechanism of DP action from a bottom-up and top-down approach. To address the former we used mass spectrometry and image analysis tools that we have developed and revealed that DP blocks SREBP2 translocation from the ER to the Golgi, thus blocking this transcription factor from reaching the nucleus. By taking a top-down approach we anticipated that we could determine which of the many biochemical pathways affected by DP may be important for DPs ability to potentiate statin-induced apoptosis of BrCa cells. We evaluated agents that block each of the pathways downstream of DP and thought that inhibition of phosphodiesterases, leading to elevation of cAMP was the key. However, further work showed that cAMP activation of PKA was not functionally important. Thus, this work was not fruitful and lead to a dead end. To overcome this problem, we adopted pharmacogenomic approaches to identify other agents that can potentiate statin anti-proliferative activity of BrCa cells by inhibiting the statin-induced feedback response. This strategy has increased the arsenal of inhibitors that can potentiate the anti-BrCa activity of statins.

As noted, chronic DP administration *in vivo* for the duration required to evaluate the effects of interest (on metastases) presented an unexpected challenge. We have addressed this in several ways: (i) developing relevant in vitro models (PDX-derived organoids) amenable to the evaluation of drug synergy and (ii) characterization of novel DP-like combinations, such as nelfinavir, which could offer new therapeutic opportunities.

PRODUCTS:

Manuscript published:

Appendix 1: Yu, R., Longo, J., van Leeuwen, J.E., Mullen, P.J., Ba-Alawi, W., Haibe-Kains, B., Penn, L.Z. Statin-induced cancer cell death can be mechanistically uncoupled from prenylation of RAS family proteins. *Cancer Res.* 2018 Mar 1;78(5):1347-1357.

Appendix 2: Yu, R., Longo, J., van Leeuwen, JE., Zhang, J., Branchard, E., Elbaz, M., Cescon, DW., Drake, R., Dennis, JW., Penn, LZ. Mevalonate pathway inhibition slows breast cancer metastasis via reduced N-glycosylation abundance and branching. *Cancer Res*. 2021 May 15;81(10):2625-2635.

Appendix 3: van Leeuwen, J., Ba-Alawi, W., Branchard, E., Longo, J., Silvester, J., Cescon, DW., Haibe-Kains, B., Penn, LZ., Gendoo, DMA. Computational pharmacogenomics screen identifies synergistic statin-compound combinations as anti-breast cancer therapies. *bioRxiv*. 2020 September. Favorably reviewed at *Nature Communications* with anticipated resubmission in 2-3 months.

Appendix 4: Longo, J., Pandyra, AA., Stachura, P., Minden, MD., Schimmer, AD., Penn, LZ. Cyclic AMP-hydrolyzing phosphodiesterase inhibitors potentiate statin-induced cancer cell death. *Mol Oncol.* 2020 Oct;14(10):2533-2545.

Appendix 5: Longo, J., van Leeuwen, JE., Elbaz, M., Branchard, E., Penn, LZ. Statins as anti-cancer agents in the era of precision medicine. *Clin Cancer Res.* 2020 Nov 15;26(22):5791-5800.

Conference Participation:

Yu, R., Longo, J., van Leeuwen, J., Mullen, PJ., Penn, LZ. "Metabolic reprogramming during initiation of metastasis sensitizes breast cancer cells to the cytotoxic effects of fluvastatin." *Metabolic and transcriptional reprogramming leads to cancer vulnerabilities,* Abcam Conference, Toronto, Ontario, Canada. Oct 3, 2016.

Yu, R., Longo, J., van Leeuwen, J., Mullen, PJ., Penn, LZ. "Reducing breast cancer metastasis with fluvastatin as an adjuvant therapeutic." *Personalizing Cancer Medicine Conference 2017: Harnessing the Cross Disciplinary Approach,* Toronto, Ontario, Canada. Feb 6-7, 2017.

van Leeuwen, J., Pandyra, A., Goard, C., Mullen, P., Yu, R. and Penn, LZ. "Targeting the metabolic mevalonate pathway with statins as anti-breast cancer agents." *American Association for Cancer Research*. Washington, D.C., USA. April 1-5, 2017.

van Leeuwen, JE., Yu, R., Longo, J., Zhang, C., Zhang, W., Cescon, D., Chen, E., Dennis, J., Penn, LZ. "Mechanism and efficacy of statins as metastasis-prevention agents in breast cancer." *Terry Fox Research Institute Annual Scientific Meeting*. Vancouver, British Columbia, Canada. November 4, 2017.

van Leeuwen, JE., Yu, R., Longo, J., Zhang, C., Zhang, W., Cescon, D., Chen, E., Dennis, J., Penn, LZ. "Mechanism and efficacy of statins as metastasis-prevention agents in breast cancer." *Canadian Cancer Research Conference*, Vancouver, BC. November 5-7, 2017.

van Leeuwen, JE., Pandyra, A., Goard, C., Mullen, PJ., Yu, R., Penn, LZ. "Targeting the metabolic mevalonate pathway with statins as anti-breast cancer agents." *Accelerating Precision Medicine*, Toronto, ON. January 19, 2018.

van Leeuwen, JE, Yu, R., Longo, J., Zhang, C., Zhang, W-J., Cescon, DW., Chen, E., Drake, RR., Dennis, JW., Penn, LZ. "Mechanism and efficacy of statins as metastasis-prevention agents in breast cancer." *Metabolism in Health and Disease Conference.* Puerto Vallarta, Mexico. May 22-29, 2019.

van Leeuwen, JE., Ba-Alawi, W., Branchard, E., Longo, J., Silvester, J., Cescon, DW., Haibe-Kains, B., Penn, LZ., Gendoo, DM. "Computational pharmacogenomics screen identifies synergistic statin-drug combinations as anti-breast cancer therapies." *Terry Fox Research Institute Ontario Node Symposium*. Toronto, ON. December 12, 2019.

Elbaz, M., Branchard, E., Longok J., Van Leeuwen, J., **Penn, LZ**. "Blocking the restorative feedback response by novel drugs potentiates the anti-cancer activity of statins." *Terry Fox Research Institute Ontario Node Symposium*. Toronto, ON. December 12, 2019. Winner of the only poster prize, generously provided by Lab150.

PARTICIPANTS & OTHER COLLABORATING ORGANIZATIONS

Name:	*Linda Penn*
Project Role:	*PI (Site 1)*
Researcher Identifier (e.g. ORCID ID):	0000-0001-8133-5459
Nearest person month worked:	60
Contribution to Project:	*Dr. Penn is the leading PI of this project.*
Funding Support:	Salary is not covered by the DOD grant

Name:	*David Cescon*
Project Role:	*Partnering PI (Site 2)*
Researcher Identifier (e.g. ORCID ID):	
Nearest person month worked:	60
Contribution to Project:	*Dr. Cescon is the partnering PI of this project.*
Funding Support:	Salary is not covered by the DOD grant

Name:	*Joseph Longo*
Project Role:	*Graduate Student*
Researcher Identifier (e.g. ORCID ID):	*n/a*
Nearest person month worked:	48
Contribution to Project:	*Mr. Longo has performed work in delineating the mechanism by which DP potentiates statin-induced tumor cell apoptosis, and evaluating the efficacy of fluvastatin in a relevant mouse model of BrCa metastasis.*
Funding Support:	*CIHR Fellowship + DOD grant*

Name:	*Jenna E. van Leeuwen*
Project Role:	*Graduate Student*
Researcher Identifier (e.g. ORCID ID):	*n/a*
Nearest person month worked:	60
Contribution to Project:	*Ms. van Leeuwen has performed work in delineating the efficacy and mechanism of the fluvastatin+DP combination in BrCa cell lines, and evaluating the efficacy of fluvastatin in a relevant mouse model of BrCa metastasis.*
Funding Support:	*DOD grant*

Name:	*Aaliya Tamachi*
Project Role:	*Research Technician*
Researcher Identifier (e.g. ORCID ID):	*n/a*
Nearest person month worked:	60
Contribution to Project:	*Ms. Tamachi has contributed to this project by supporting the animal work and lab work.*
Funding Support:	*DOD grant*

Name:	*Mohamad Elbaz*
Project Role:	*Post-Doctoral Fellow*
Researcher Identifier (e.g. ORCID ID):	*n/a*
Nearest person month worked:	41
Contribution to Project:	*Dr. Elbaz has performed work to identify DP-like molecules that potentiate fluvastatin anti-BrCa activity by inhibiting the fluvastatin restorative feedback response, and evaluating the efficacy of fluvastatin in a relevant mouse model of BrCa metastasis.*
Funding Support:	*DOD grant*

APPENDICES:

Appendix 1: Yu, R., Longo, J., van Leeuwen, J.E., Mullen, P.J., Ba-Alawi, W., Haibe-Kains, B., Penn, L.Z. Statin-induced cancer cell death can be mechanistically uncoupled from prenylation of RAS family proteins. *Cancer Res.* 2018 Mar 1;78(5):1347-1357.

Appendix 2: Yu, R., Longo, J., van Leeuwen, JE., Zhang, J., Branchard, E., Elbaz, M., Cescon, DW., Drake, R., Dennis, JW., Penn, LZ. Mevalonate pathway inhibition slows breast cancer metastasis via reduced N-glycosylation abundance and branching. *Cancer Res*. 2021 May 15;81(10):2625-2635.

Appendix 3: van Leeuwen, J., Ba-Alawi, W., Branchard, E., Longo, J., Silvester, J., Cescon, DW., Haibe-Kains, B., Penn, LZ., Gendoo, DMA. Computational pharmacogenomics screen identifies synergistic statin-compound combinations as anti-breast cancer therapies. *bioRxiv*. 2020 September. Favorably reviewed at *Nature Communications* with anticipated resubmission in 2-3 months.

Appendix 4: Longo, J., Pandyra, AA., Stachura, P., Minden, MD., Schimmer, AD., Penn, LZ. Cyclic AMP-hydrolyzing phosphodiesterase inhibitors potentiate statin-induced cancer cell death. *Mol Oncol.* 2020 Oct;14(10):2533-2545.

Appendix 5: Longo, J., van Leeuwen, JE., Elbaz, M., Branchard, E., Penn, LZ. Statins as anti-cancer agents in the era of precision medicine. *Clin Cancer Res.* 2020 Nov 15;26(22):5791-5800.

Published OnlineFirst December 11, 2017; DOI: 10.1158/0008-5472.CAN-17-1231

Translational Science

Cancer Research

Statin-Induced Cancer Cell Death Can Be Mechanistically Uncoupled from Prenylation of RAS Family Proteins

Rosemary Yu[1,2], Joseph Longo[1,2], Jenna E. van Leeuwen[1,2], Peter J. Mullen[1], Wail Ba-Alawi[1], Benjamin Haibe-Kains[1,2,3,4], and Linda Z. Penn[1,2]

Abstract

The statin family of drugs preferentially triggers tumor cell apoptosis by depleting mevalonate pathway metabolites farnesyl pyrophosphate (FPP) and geranylgeranyl pyrophosphate (GGPP), which are used for protein prenylation, including the oncoproteins of the RAS superfamily. However, accumulating data indicate that activation of the RAS superfamily are poor biomarkers of statin sensitivity, and the mechanism of statin-induced tumor-specific apoptosis remains unclear. Here we demonstrate that cancer cell death triggered by statins can be uncoupled from prenylation of the RAS superfamily of oncoproteins. Ectopic expression of different members of the RAS superfamily did not uniformly sensitize cells to fluvastatin, indicating that increased cellular demand for protein prenylation cannot explain increased statin sensitivity. Although ectopic expression of HRAS increased statin sensitivity, expression of myristoylated HRAS did not rescue this effect. HRAS-induced epithelial-to-mesenchymal transition (EMT) through activation of zinc finger E-box binding homeobox 1 (ZEB1) sensitized tumor cells to the antiproliferative activity of statins, and induction of EMT by ZEB1 was sufficient to phenocopy the increase in fluvastatin sensitivity; knocking out ZEB1 reversed this effect. Publicly available gene expression and statin sensitivity data indicated that enrichment of EMT features was associated with increased sensitivity to statins in a large panel of cancer cell lines across multiple cancer types. These results indicate that the anticancer effect of statins is independent from prenylation of RAS family proteins and is associated with a cancer cell EMT phenotype.

Significance: The use of statins to target cancer cell EMT may be useful as a therapy to block cancer progression. *Cancer Res; 78(5); 1347–57. ©2017 AACR.*

Introduction

Statins are inhibitors of 3-hydroxy-3-methylglutaryl coenzyme A reductase (HMGCR; Fig. 1A), and have been widely prescribed to lower cholesterol levels (1). Epidemiologic evidence indicate that statins have anticancer activities, particularly in breast and prostate cancers (2–5). Preclinical and clinical data demonstrate that statin treatment induces cancer cells to undergo apoptosis and lowers disease burden (6–9). Despite the promising potential to repurpose statins as anticancer agents, the molecular mechanism of how inhibition of HMGCR can specifically kill cancer cells remains unclear.

HMGCR catalyzes the conversion of HMG-CoA to mevalonate (MVA), the sole precursor for the *de novo* synthesis of sterols, geranylgeranyl pyrophosphate (GGPP), farnesyl pyrophosphate (FPP), and several other metabolic endproducts (Fig. 1A; refs. 1, 10). Statin-induced apoptosis can be rescued by coadministration with MVA (8, 11), demonstrating that this is an on-target effect, or with GGPP or FPP (8, 11–15). Sterols cannot rescue cancer cell apoptosis induced by statins (8). These results have led to a model where statins induce apoptosis by inhibiting GGPP and FPP synthesis.

GGPP and FPP are essential substrates for protein geranylgeranylation and farnesylation, respectively, together referred to as protein prenylation (16). Prenylation with the hydrophobic geranylgeranyl or farnesyl moiety localizes proteins to cellular membranes (16). Prenylation-driven membrane localization is required for all proteins in the RAS GTPase superfamily, and several groups have shown that statin treatment decreases the prenylated and membrane-associated forms of RAS, RHO, RAC, RAP, and RAB subfamily proteins (12, 17–20). However, evidence for the functional importance of these small GTPases in conferring statin sensitivity has been conflicting. For example, cancer cells with upregulated or hyperactivated RAS or RHO demonstrate increased statin sensitivity in some studies (17–19), but not others (8, 14, 21). Understanding the mechanism driving these discrepancies has remained a challenge and has been an area of debate for many years (10).

In this manuscript, we directly address these discrepancies and show that inhibition of RAS family protein prenylation is not essential for, and can be uncoupled from, statin-induced cell death. We chose MCF10A cells as our model system as they are an immortal, nontransformed basal breast cell line that possesses a highly stable genome, allowing for the evaluation of ectopic gene expression in the absence of gross genetic instability (22). We

[1]Princess Margaret Cancer Centre, University Health Network, Toronto, Ontario, Canada. [2]Department of Medical Biophysics, University of Toronto, Toronto, Ontario, Canada. [3]Department of Computer Science, University of Toronto, Toronto, Ontario, Canada. [4]Ontario Institute of Cancer Research, Toronto, Ontario, Canada.

Note: Supplementary data for this article are available at Cancer Research Online (http://cancerres.aacrjournals.org/).

Corresponding Author: Linda Z. Penn, Princess Margaret Cancer Centre, 13th Floor 13-706, 101 College St., Toronto, Ontario M5G 1L7, Canada. Phone: 416-634-8770; E-mail: Linda.Penn@uhnresearch.ca

doi: 10.1158/0008-5472.CAN-17-1231

Published OnlineFirst December 11, 2017; DOI: 10.1158/0008-5472.CAN-17-1231

systematically introduced several members of the RAS superfamily in the MCF10A cell line to produce a panel of sublines with increased demand for GGPP and/or FPP. This did not uniformly sensitize cells to inhibition of GGPP and FPP synthesis, as only $HRAS^{G12V}$ and $KRAS^{G12V}$ exhibited an increased sensitivity to fluvastatin. $HRAS^{G12V}$ and myristoylated-$HRAS^{G12V}$ sensitized cells to statins to a similar extent, indicating that statin-induced cell death is independent of RAS prenylation, even in RAS-transformed cells. We then showed that overexpression of RAS induced epithelial-to-mesenchymal transition (EMT) in these cells, in part by upregulating the EMT driver zinc finger E-box binding homeobox 1 (ZEB1). Exogenous expression or knockout of ZEB1 conferred or rescued statin sensitivity, respectively, suggesting that EMT was the critical feature that was functionally important for statin-induced cell death. Taking a computational pharmacogenomics approach, we discovered that EMT was associated with statin sensitivity across a large panel of cancer cell lines. Taken together, our results provide a rationale for why RAS-related oncogenes have been poor biomarkers of statin sensitivity, and suggest that a set of EMT-associated genes should be further evaluated in the preclinical and clinical setting as biomarkers of statin sensitivity.

Materials and Methods

Reagents

Fluvastatin and TGFβ were purchased from US Biologicals and PeproTech, respectively. Other chemicals were purchased from Sigma unless otherwise specified.

Cell culture

MCF10A cells were a kind gift of Dr. Senthil Muthuswamy; MGH8, H1264, and RVH6849 were kind gifts of Dr. Ming Tsao; Mia-Paca-2 was a kind gift of Dr. David Hedley; KP-4 was a kind gift of Dr. Bradley Wouters; and HT-29 was a kind gift of Dr. Catherine O'Brien. All cell lines were cultured as recommended by ATCC. All cell lines were authenticated by short-tandem repeat (STR) profiling, and routinely tested to be free of mycoplasma by Lonza MycoAlert Mycoplasma Detection Kit. All cell lines were used within 20 passages from thawing for the described experiments. Transgene expression was stably introduced into MCF10A cells using retroviral insertion with pBabe-Puro. Cells were imaged on the Leica MZ FLIII Stereomicroscope.

MTT assays

3-(4,5-Dimethylthiazol-2-yl)-2,5-diphenyltetrazolium bromide (MTT) assays were performed as previously described (6). Briefly, MCF10A cells were seeded at 750 cells/well in 96-well plates overnight, then treated in triplicate with 0 to 200 μmol/L fluvastatin for 72 hours. IC_{50} values were computed using GraphPad Prism with a bottom constraint equal to 0.

Immunoblotting

Cell lysates were prepared by lysing directly in boiling SDS lysis buffer (1% SDS, 11% glycerol, 10% β-mercaptoethanol, 0.1 mol/L Tris pH 6.8). The following antibodies were used: E-Cadherin (CST 3195), vimentin (CST 5741), actin (Sigma A2066), tubulin (Millipore CP06), FLAG (Sigma F1804), EGFR (CST 2232), ERK (CST 4695), p-ERK (CST 4370), AKT (CST 9272), p-AKT (CST 9271), HMGCS1 (SCB sc-32423), RALA (BD 610221), BRAF (Sigma HPA001328), MYC (MAb 9E10 prepared in-house using ATCC CRL-1729), ZEB1 (Sigma HPA027524), HMGCR (MAb A9 prepared in-house using ATCC CRL-1811).

Soft agar colony formation

Anchorage-independent colony growth of MCF10A sublines in soft agar was evaluated as previously described (23). Colonies were imaged at 1.2× magnification on the Leica MZ FLIII Stereomicroscope after 14 to 18 days of fluvastatin treatment. Colony number and average colony size were quantified using ImageJ.

Membrane fractionation

Cell were seeded at 2×10^6/plate overnight and treated as indicated. Harvested cells were resuspended in 1 mL HEPES buffer (0.25 mol/L sucrose, 50 mmol/L HEPES pH 7.5, 5 mmol/L NaF, 5 mmol/L EDTA, 2 mmol/L DTT) and lysed by sonication. Homogenate was cleared at 2,000 × *g* for 20 minutes at 4°C, then ultracentrifuged at 115,000 × *g* for 70 min at 4°C for membrane fractionation. Membrane protein pellet was resuspended in Triton buffer (1% TritonX-114, 50 mmol/L Tris pH 7.5, 0.1 mmol/L NaCl, 5 mmol/L EDTA, 5 mmol/L NaF, 2 mmol/L DTT).

Cell death assay

Cells were seeded at 2.5×10^5/plate overnight and treated as indicated. After 72 hours, cells were fixed in 70% ethanol for >24 hours, stained with propidium iodide, and analyzed by flow cytometry for the % sub-diploid DNA population as % cell death, as previously described (6).

qRT-PCR

Total RNA was harvested from subconfluent cells using TRIzol Reagent (Invitrogen). cDNA was synthesized from 500 ng of RNA using SuperScript III (Invitrogen). Real-time quantitative RT-PCR was performed using TaqMan probes for HMGCR (ABI Hs00168352), HMGCS1 (ABI Hs00266810), and GAPDH (ABI Hs99999905), and using SYBR Green for TWIST, SNAIL, ZEB1, and 18S rRNA with the following primers:

TWIST_fw 5′-CCGGAGACCTAGATGTCATTG-3′
TWIST_rv 5′-CCACGCCCTGTTTCTTTG-3′
SNAIL_fw 5′-CACTATGCCGCGCTCTTTC-3′
SNAIL_rv 3′-GGTCGTAGGGCTGCTGGAA-3′
ZEB1_fw 5′-GCCAATAAGCAAACGATTCTG-3′
ZEB1_rv 5′-TTTGGCTGGATCACTTTCAAG-3′
18S_rRNA_fw 5′-GTAACCCGTTGAACCCCATT-3′
18S_rRNA_rv 3′-CCATCCAATCGGTAGTAGCG-3′

CRISPR/Cas9-mediated gene knockout

Two sgRNAs were designed using CRISPOR (24) and cloned into LentiGuide-Puro following the established protocol (25). ZEB1 knockout lines were generated as previously described (25). LentiGuide-Puro (Addgene #52963) and LentiCas9-Blast (Addgene #52962) were kind gifts from Dr. Feng Zhang (Broad Institute of MIT and Harvard, Cambridge, MA). Sequences of ZEB1 sgRNAs cloned were:

sgRNA A: TGCTTTCTGCGCTTACACCT GGG
sgRNA B: GCAGAAAGCAGGCGAACCCG CGG

Pharmacogenomic analysis

RNA-seq and drug sensitivity data were retrieved and curated from the Cancer Cell Line Encyclopedia (CCLE; ref. 26) and the

Published OnlineFirst December 11, 2017; DOI: 10.1158/0008-5472.CAN-17-1231

Cancer Therapeutics Portal version 2 (CTRPv2; refs. 27–29) databases, and were mined using the R/Bioconductor PharmacoGx package (30). To calculate the bimodality index (31, 32), a mixture of two Gaussian models was used to fit the RNA-seq expression values of each gene across all cell lines in CCLE, as implemented in the bimod function in the R/Bioconductor genefu package (version 2.6.0; ref. 32). The cutoff was calculated by finding the midpoint between the maximum value of the first Gaussian model (left distribution) and the minimum value of the second Gaussian model (right distribution). The cutoff was used to classify cell lines into either showing low or high expression of a gene. A binary classification rule was developed to determine whether a cell line is "enriched" with EMT phenotype or not. Cell lines from tumors of hematopoietic and lymphoid tissues, and those with unknown origin, were excluded from this analysis. If expression of any of *VIM*, *ZEB1*, *FN1*, or *CDH2* was high, or if expression of *CDH1* was low, in a cell line according to the bimodality cutoff, then it was classified as "enriched" with EMT phenotype. Concordance index (CI) and *P*-value were calculated to measure the association between statin sensitivity, obtained from CTRPv2 database, and cell lines that were classified as either "enriched" with EMT phenotype or "not enriched." *P*-value was calculated using the nonparametric Wilcoxon rank sum test, comparing statin response on cell lines "enriched" versus "not enriched" with the EMT phenotype. The script and data used for the generation of these figures can be downloaded at https://github.com/bhklab/StatinEMT.

Results

$HRAS^{G12V}$ and $KRAS^{G12V}$, but not other proteins in the RAS superfamily, sensitize MCF10A cells to fluvastatin

Using the MCF10A breast epithelial cell line as a nontransformed, genomically stable cell background (22), we ectopically expressed representative proteins from the RAS, RHO, RAC, and RAP subfamilies in their dominantly active forms (Fig. 1B; ref. 16). These mutants remain dependent on prenylation for activity, allowing us to simulate an increase in demand for FPP and/or GGPP as a result of aberrant activation of these GTPases. The increase in demand for FPP and/or GGPP did not universally sensitize cells to fluvastatin (Fig. 1C), as only cells overexpressing $HRAS^{G12V}$ or $KRAS^{G12V}$ had significantly lowered fluvastatin IC_{50} values (13.6 and 13.2 μmol/L, respectively) compared to the vector control (22.2 μmol/L), which indicated an increased sensitivity to fluvastatin (Fig. 1C). A colony formation assay in soft agar was used to test the inhibitory effect of fluvastatin treatment on the transformation potential of these cells (Fig. 1D; Supplementary Fig. S1A). In this and all subsequent colony formation assays, 20 μmol/L fluvastatin was used to allow for adequate penetrance into the soft agar. Fluvastatin treatment significantly reduced both colony count (Fig. 1E) and colony size (Fig. 1F) of cells overexpressing $HRAS^{G12V}$ and $KRAS^{G12V}$, but not those expressing other proteins in the RAS superfamily (Supplementary Fig. S1B–S1D). Thus, compared to other members of the RAS superfamily, activated HRAS and KRAS preferentially sensitize MCF10A cells to the anticancer activity of fluvastatin.

Inhibition of RAS prenylation is uncoupled from fluvastatin-induced cell death

If inhibition of RAS localization was the mechanism of fluvastatin-induced cell death, cells overexpressing myristoylated $HRAS^{G12V}$ (myr-HRAS), which localizes to the cell membrane independently of prenylation with FPP or GGPP, should remain insensitive to fluvastatin. Figure 2A shows that overexpression of $HRAS^{G12V}$ and myristoylated $HRAS^{G12V}$ both activated downstream signaling to a similar extent, as seen by the increase in Erk and Akt phosphorylation. Although the mislocalization of $HRAS^{G12V}$ from the membrane to the cytoplasm was evident after treatment with 10 μmol/L of fluvastatin for 24 hours, myr-$HRAS^{G12V}$ remained in the membrane fraction, confirming that myristoylation occurs independent of FPP and GGPP (Fig. 2B). EGFR, HMGCS1, and actin were used as controls for membrane-localized, cytosol-localized, and total proteins, respectively (Fig. 2B). Unexpectedly, the fluvastatin IC_{50} value of cells overexpressing myr-$HRAS^{G12V}$ was significantly decreased similarly to $HRAS^{G12V}$ (Fig. 2C). Colony formation was also inhibited by fluvastatin treatment in cells overexpressing myr-$HRAS^{G12V}$ (Fig. 2D–F), to the same extent as cells overexpressing $HRAS^{G12V}$ (Fig. 1D–F). Addition of MVA, GGPP, or FPP rescued the fluvastatin-induced cell death in both $HRAS^{G12V}$ and myr-$HRAS^{G12V}$ cells (Fig. 2G–I). Together, these data uncouple statin-induced cell death from GGPP and FPP demand for prenylation of RAS family proteins, and implicate that events downstream of RAS signaling are responsible for the increase in statin sensitivity in this cell system.

The RAS–ZEB1–EMT signaling axis underlies increased sensitivity to fluvastatin

We next addressed several potential models to understand the mechanism of RAS sensitization of MCF10A cells to the antiproliferative activity of fluvastatin. Overexpression of $HRAS^{G12V}$ or myr-$HRAS^{G12V}$ in MCF10A cells did not affect the expression of MVA pathway genes HMGCR and HMGCS1, either basally or in response to fluvastatin exposure (Supplementary Fig. S2A and S2B). This rules out impairment of the sterol feedback response as the mechanism of increased statin sensitivity in this model, which were previously reported to be associated with statin sensitivity in multiple myeloma (6).

Because RAS signaling, rather than RAS localization, was implicated as the driver of fluvastatin sensitivity, we overexpressed constitutively active forms of several classic effectors of RAS signaling ($RALA^{G23V}$, $BRAF^{V600E}$, PI3K-$p110\alpha^{E545K}$, PI3K-$p110\alpha^{H1047R}$, and MYC^{T58A}), to determine which of these, if any, phenocopied the increase in fluvastatin sensitivity in RAS-overexpressing cells. None of these sublines exhibited a lowered fluvastatin IC_{50} (Supplementary Fig. S3A–S3C). By contrast, overexpression of PI3K-p110α led to significant increases in IC_{50} values (Supplementary Fig. S3A–S3C). Similar results were evident in soft agar colony formation assays (Supplementary Fig. S3D–S3F). Therefore, the observed increase in fluvastatin sensitivity in RAS-transformed cells was not mediated through these downstream mediators of RAS signaling.

The RAS sublines were phenotypically distinct from the MCF10A parental cells. Instead of an epithelial phenotype with a cobblestone-like appearance, the RAS sublines appeared more mesenchymal, with an elongated and spindle-shaped morphology (Fig. 3A). These cells had undergone EMT, with a dramatic loss of E-cadherin expression and a gain of vimentin expression (Fig. 3B). By contrast, sublines overexpressing other members of the RAS superfamily (Supplementary Fig. S1D) and classic effectors of RAS signaling (Supplementary Fig. S3C) remained

Published OnlineFirst December 11, 2017; DOI: 10.1158/0008-5472.CAN-17-1231

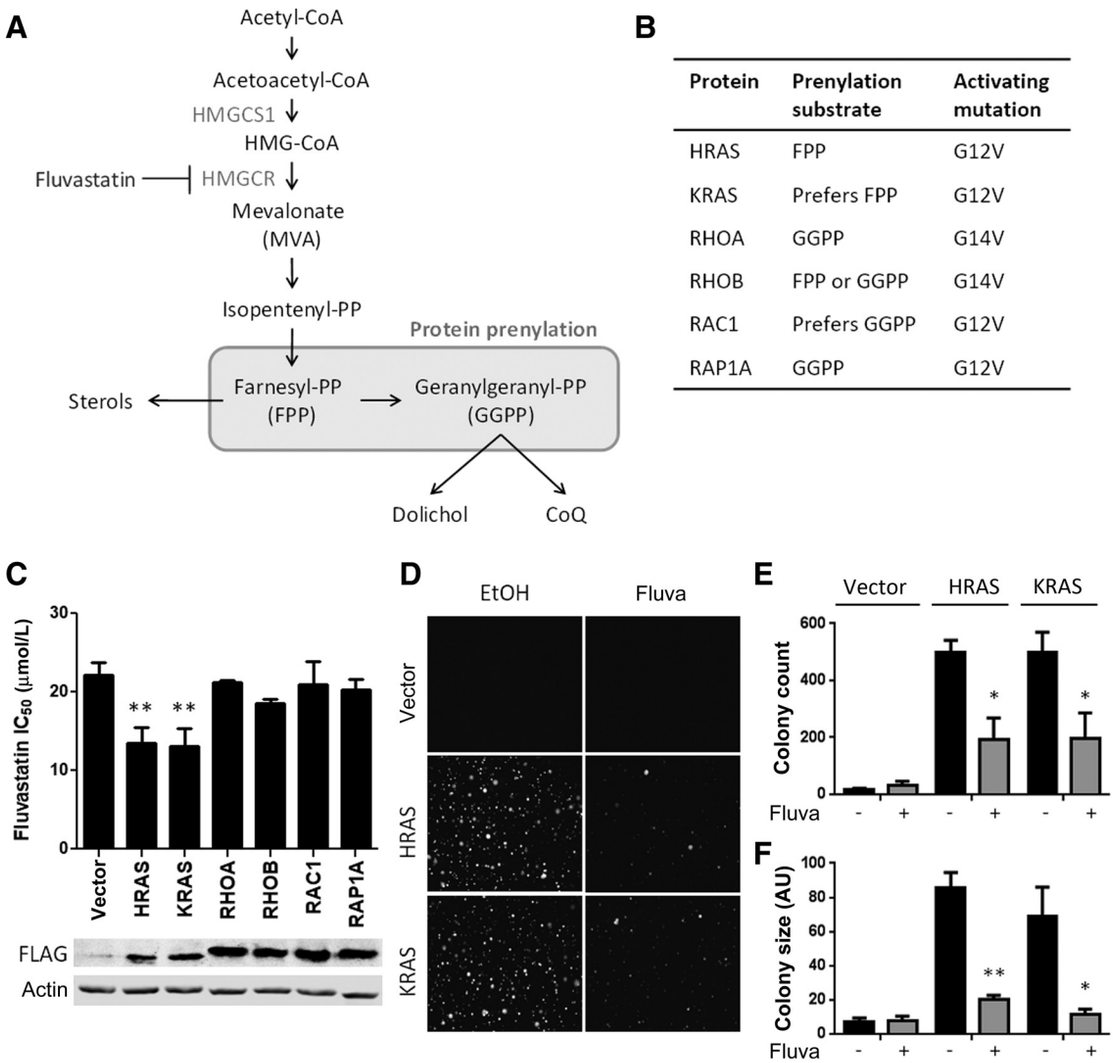

Figure 1.

HRAS^{G12V} and KRAS^{G12V}, but not other prenylated proteins, sensitize MCF10A cells to fluvastatin. **A,** A simplified schematic of the MVA pathway. **B,** Representative RAS family proteins selected for ectopic expression in MCF10A cell lines. **C,** Ectopic expression of HRAS^{G12V} and KRAS^{G12V} sensitized MCF10A cells to fluvastatin, as assessed by MTT assay following 72 hours of treatment. Bars, mean + SD, $n = 3$. **, $P < 0.01$ (one-way ANOVA with a Dunnett posttest, comparing all columns vs. vector control column). **D–F,** Treatment with fluvastatin decreased colony count and colony size of RAS-driven anchorage-independent growth in soft agar. Colonies were treated with 20 μmol/L fluvastatin 2× weekly for 18 days. Bars, mean + SD, $n = 4$. *, $P < 0.05$; **, $P < 0.01$ (unpaired, two-tailed *t* test, comparing fluvastatin-treated vs. no treatment control).

epithelial, expressing E-cadherin and vimentin at similar levels to the vector controls. To test whether induction of EMT confers sensitivity to fluvastatin, we treated MCF10A cells with TGFβ for 3 days, which induces EMT independently of RAS status (Fig. 3C). This led to an increased sensitivity to fluvastatin, as indicated by a decrease in fluvastatin IC_{50} in TGFβ-treated cells (Fig. 3D). After TGFβ treatment, removal of TGFβ from the culture media gradually reverses EMT (Supplementary Fig. S4). MCF10A cells fully reverted back to an epithelial phenotype 7 days after the removal of TGFβ, and sensitivity to fluvastatin was restored to control levels (Supplementary Fig. S4). These data indicate that a mesenchymal state is sufficient to confer sensitivity to fluvastatin.

RAS induces EMT by upregulating the EMT-driving transcription factor ZEB1, and not by other EMT regulators such as SNAIL or TWIST in our MCF10A system (Fig. 3E). ZEB1-overexpression in MCF10As led to a loss of E-cadherin and gain of vimentin expression independent of RAS status (Fig. 3F), and decreased the fluvastatin IC_{50} value similarly to the RAS sublines (Fig. 3G). ZEB1 overexpression had no effect on the IC_{50} value of GGTI-298 (Fig. 3H), a specific inhibitor to geranylgeranyltransferase I, reinforcing the model that prenylation of RAS family proteins is uncoupled from fluvastatin-induced tumor cell death. We then knocked out ZEB1 in cells with ectopic expression of HRAS^{G12V} and myr-HRAS^{G12V}, and showed that ZEB1 knockout reversed cells to epithelial state, as evidenced by

Published OnlineFirst December 11, 2017; DOI: 10.1158/0008-5472.CAN-17-1231

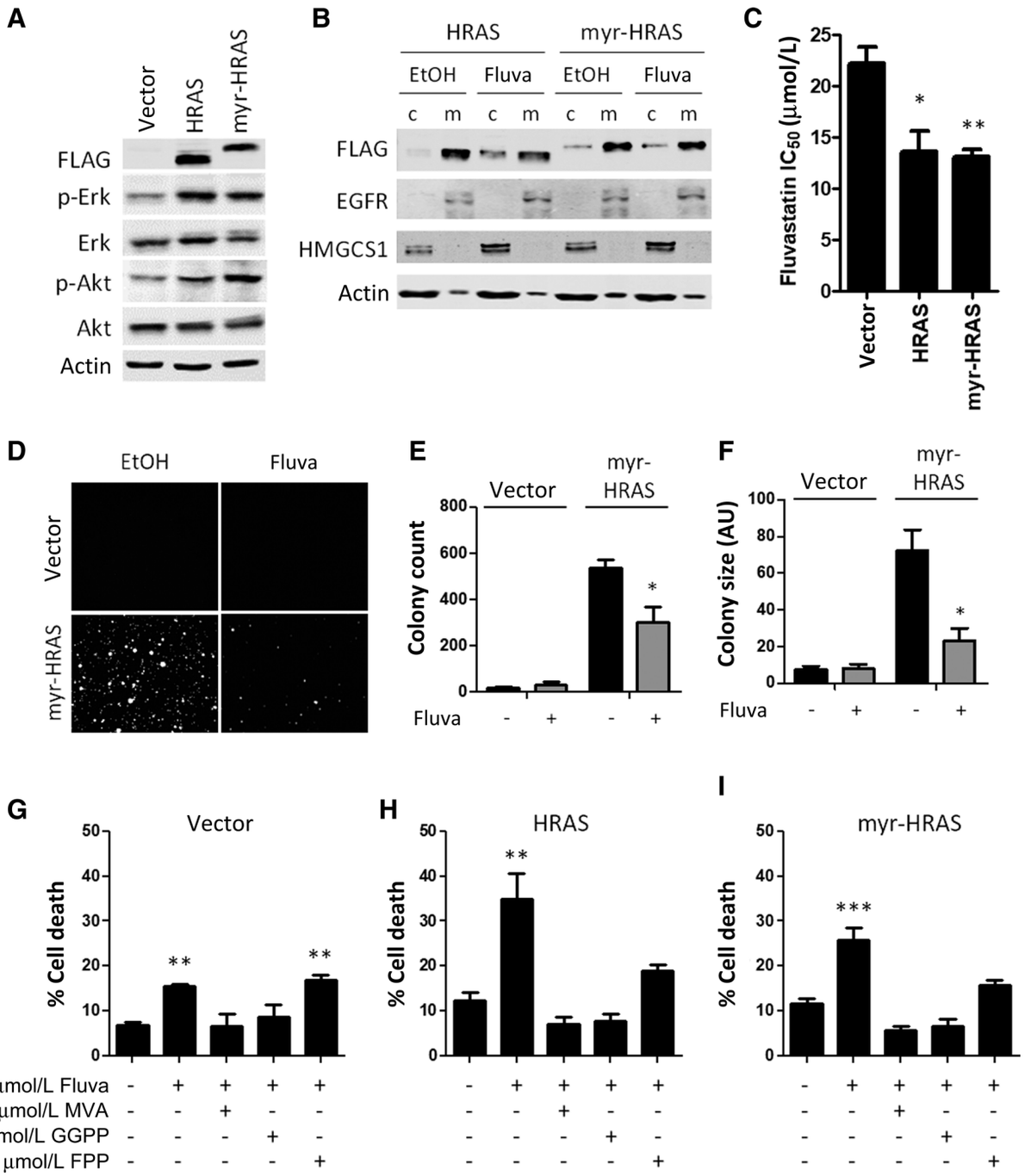

Figure 2.

Inhibition of RAS prenylation is uncoupled from fluvastatin-induced cell death. **A,** Overexpression of HRAS^{G12V} and myr-HRAS^{G12V} activated Erk phosphorylation and Akt phosphorylation to a similar extent. **B,** The proportion of HRAS^{G12V} in the cytoplasmic (c) fraction was increased, and the proportion in the membrane (m) proportion was decreased after 24 hours of treatment with 10 μmol/L fluvastatin. In contrast, the localization of myr-HRAS^{G12V} was unaffected by fluvastatin treatment. **C,** Both HRAS^{G12V} and myr-HRAS^{G12V} sensitized MCF10As to fluvastatin as assessed by MTT assay following 72 hours of treatment. Bars, mean + SD, $n = 3$. *, $P < 0.05$; **, $P < 0.01$ (one-way ANOVA with a Dunnett posttest, comparing all columns vs. vector control column). **D–F,** Treatment with fluvastatin decreased colony count and colony size of myr-HRAS^{G12V}-driven anchorage-independent growth in soft agar. Colonies were treated with 20 μmol/L fluvastatin 2× weekly for 18 days. Bars, mean + SD, $n = 4$. *, $P < 0.05$ (unpaired, two-tailed t test, comparing fluvastatin-treated vs. no treatment control). **G–I,** Ten μmol/L fluvastatin induced cell death in MCF10A cells overexpressing HRAS^{G12V} and myr-HRAS^{G12V}, which was reversed by coadministration with MVA, GGPP, or FPP. Bars, mean + SD, $n = 3$. **, $P < 0.01$; ***, $P < 0.001$ (one-way ANOVA with a Dunnett posttest, comparing all columns vs. no treatment control column).

Published OnlineFirst December 11, 2017; DOI: 10.1158/0008-5472.CAN-17-1231

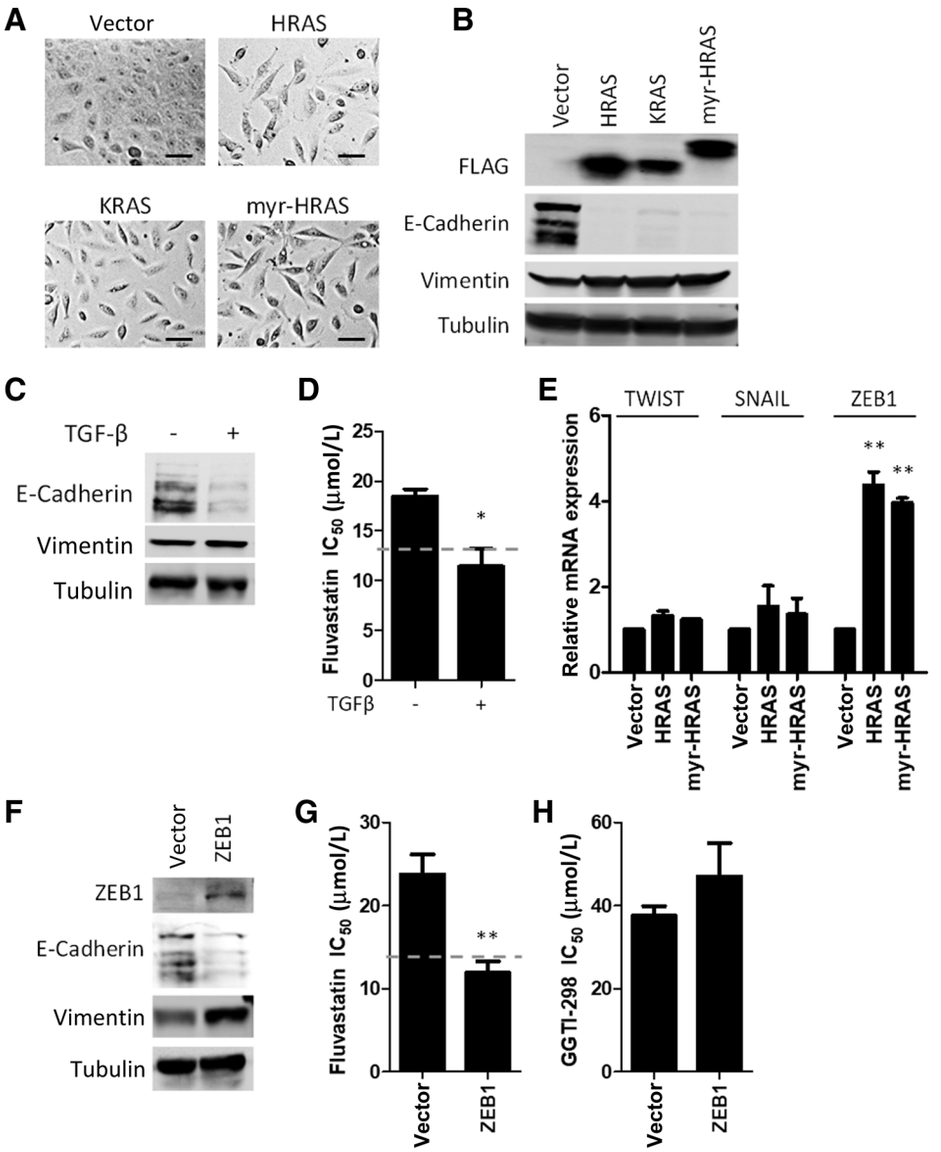

Figure 3.
RAS induces EMT through ZEB1, and induction of EMT is sufficient for sensitizing cells to fluvastatin. **A,** RAS-overexpressing cells appear more mesenchymal than the vector control cells. Representative images are shown. Scale bar, 50 μm. **B,** RAS overexpression reduced expression of E-cadherin, an epithelial cell marker, and increased expression of vimentin, a mesenchymal cell marker. **C,** Treating MCF10A cells with 5 ng/mL TGFβ for 3 days induced EMT. **D,** Induction of EMT by 5 ng/mL TGFβ treatment sensitized MCF10A cells to fluvastatin, as assessed by MTT assay following 72 hours of treatment. Dashed line represents IC_{50} of $HRAS^{G12V}$-overexpressing cells. Bars, mean + SD, $n = 3$. *, $P < 0.05$ (unpaired, two-tailed t test, comparing TGFβ-treated vs. no treatment control). **E,** $HRAS^{G12V}$ and myr-$HRAS^{G12V}$ cells upregulate the EMT transcription factor ZEB1. Bars, mean + SD, $n = 3$. **, $P < 0.01$ (one-way ANOVA with a Dunnett posttest, comparing all columns vs. vector control column). **F,** Ectopic expression of ZEB1 induced EMT. **G,** ZEB1 overexpression sensitized MCF10A cells to fluvastatin, as assessed by MTT assay following 72 hours of treatment. Dashed line represents IC_{50} of $HRAS^{G12V}$-overexpressing cells. Bars, mean + SD, $n = 3$. **, $P < 0.01$ (unpaired, two-tailed t test, comparing TGFβ-treated vs. no treatment control). **H,** ZEB1 overexpression did not sensitize cells to GGTI-298. Bars, mean + SD, $n = 3$.

the increased expression of E-cadherin and decreased expression of vimentin (Fig. 4A). Knocking out ZEB1 rescued the RAS-driven fluvastatin sensitivity, both by IC_{50} measurements (Fig. 4B) and by colony formation in soft agar (Fig. 4C–E).

Enrichment of EMT phenotype is associated with sensitivity to statins in a large panel of cancer cell lines

The CCLE database (26) contains RNA-seq data of 927 cancer cell lines across >20 cancer types (Supplementary Fig. S5A). Mining this large database, we observed that although the expression pattern for most genes follow a unimodal (Gaussian) distribution, as exemplified by *POLR2A* (RNA polymerase II, subunit A; Fig. 5A), some genes are bimodally expressed, such as *ESR1* (estrogen receptor α; Fig. 5A; Supplementary Fig. S5B). *ESR1* is known for a strong bimodal expression in breast tissue (32, 33), representing ERα-low (left peak) and ERα-high (right peak) cell lines (Fig. 5A; Supplementary Fig. S5B). We then examined the expression profile of 11 well-characterized EMT-associated genes, and observed that their expression were strongly bimodal, with bimodality indices (31, 32) higher than that of *ESR1*, our positive control (Supplementary Fig. S5C). The distribution of the top five bimodally expressed genes (*VIM*, *CDH1*, *ZEB1*, *FN1*, and *CDH2*) is shown in Fig. 5A. For each gene, we computed the cutoff optimally discriminating between the two modes of expression distribution, and classified the cell lines with either low or high expression of the gene of interest (Fig. 5A). Each cell line was therefore characterized by a binary vector representing the activation of the top five bimodally expressed EMT-associated genes.

Using the top five bimodally expressed EMT-associated genes as features, we built a binary classification rule that classified each solid tumor cell line as enriched with an EMT phenotype if at least one of the EMT-associated genes was activated (Fig. 5A, right peak for *VIM*, *ZEB1*, *FN1*, and *CDH2*; left peak for *CDH1*). We then mined the CTRPv2 database (27–29) using the PharmacoGx R/

Published OnlineFirst December 11, 2017; DOI: 10.1158/0008-5472.CAN-17-1231

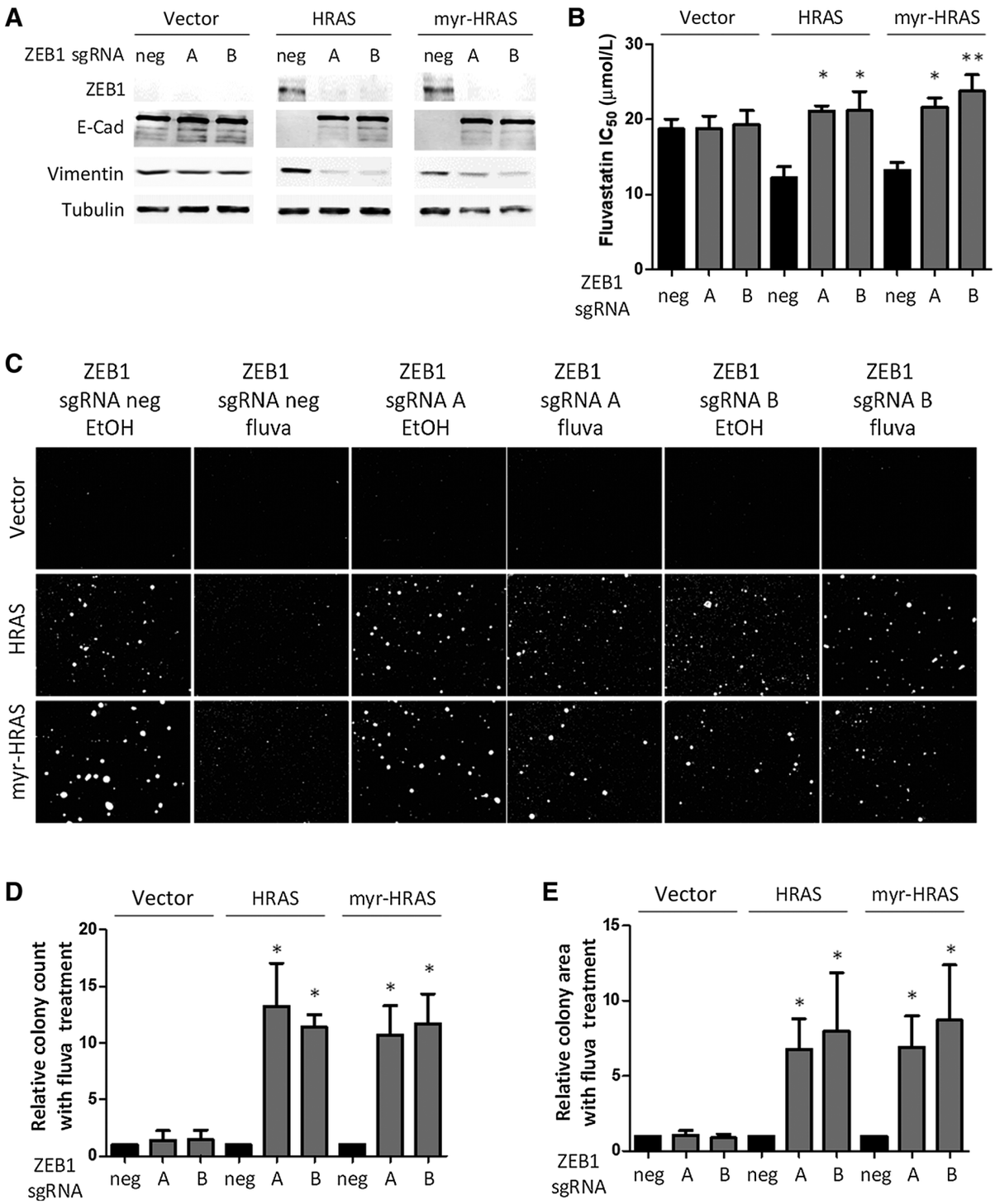

Figure 4.

CRISPR/Cas9-mediated knockout of ZEB1 reverses EMT and rescues the increased sensitivity in HRAS^{G12V} and myr-HRAS^{G12V} cells. **A,** Two independent sgRNAs (**A** and **B**) were used to knockout ZEB1 in MCF10A cells overexpressing HRAS^{G12V} and myr-HRAS^{G12V}. Knocking out ZEB1 reversed cells to epithelial state, as seen by the increased expression of E-cadherin and decreased expression of vimentin. **B,** ZEB1 knockout rescued the decreased fluvastatin IC_{50} observed in HRAS^{G12V} and myr-HRAS^{G12V} cells. Bars, mean + SD, $n = 3$. *, $P < 0.05$; **, $P < 0.01$ (one-way ANOVA with a Dunnett posttest, comparing all columns vs. vector control column). **C–E,** ZEB1 knockout in HRAS^{G12V} and myr-HRAS^{G12V} cells led to increased colony formation in soft agar under fluvastatin treatment. Colonies were treated with 20 μmol/L fluvastatin 2× weekly for 14 to 16 days. Bars, mean + SD, $n = 3$. *, $P < 0.05$ (one-way ANOVA with a Dunnett posttest, comparing all columns vs. vector control column).

Published OnlineFirst December 11, 2017; DOI: 10.1158/0008-5472.CAN-17-1231

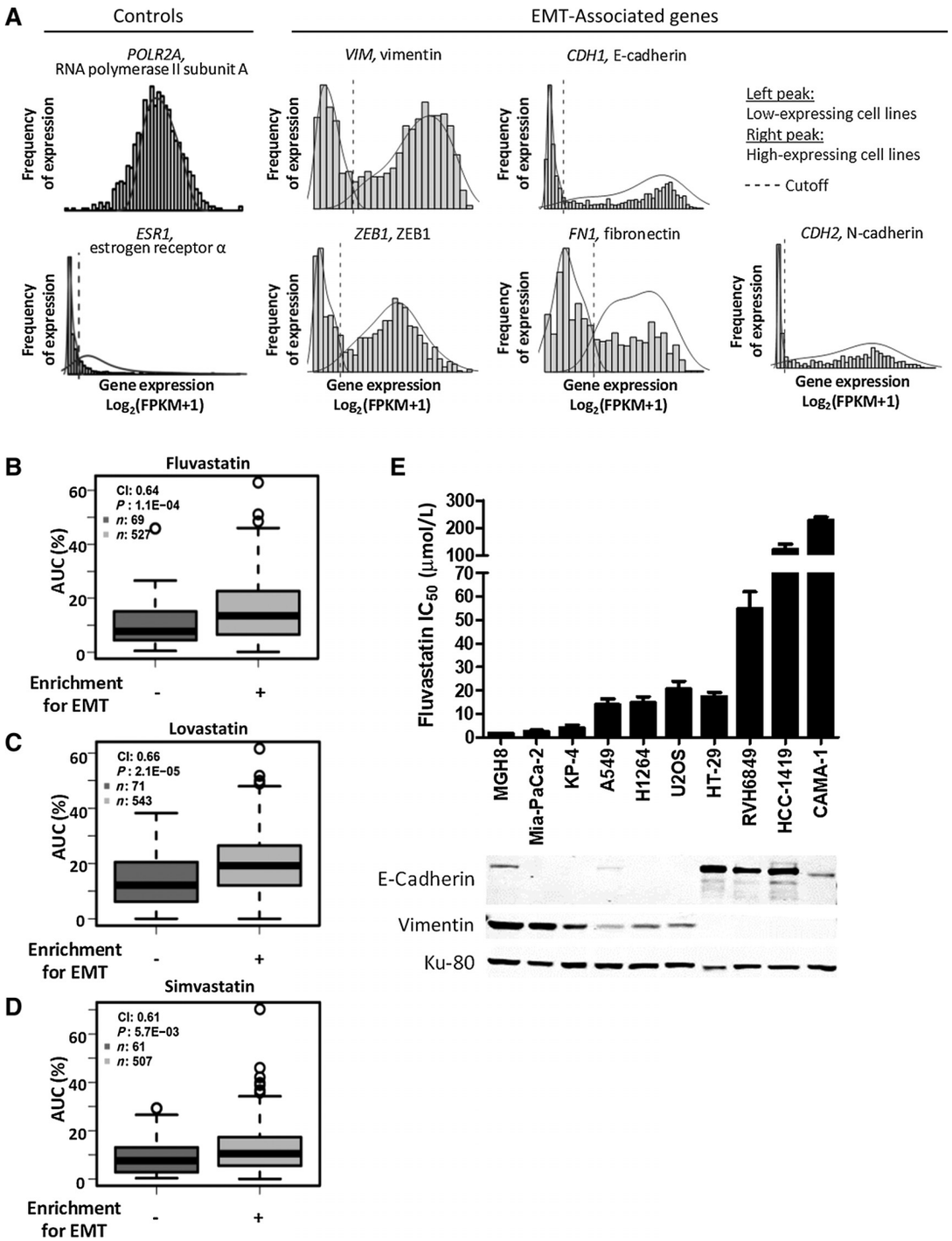

Figure 5.

Statin sensitivity is associated with cancer cell EMT. **A,** Unimodal (Gaussian) distribution of *POLR2A* and bimodal distribution of *ESR1* (left) are used as controls for gene expression distribution analyses. Bimodal expression of the five EMT-associated genes (right) was used to classify cell lines. Gene expression values are $\log_2$(FPKM+1) with fragments per kilobase of transcript per million mapped reads (FPKM). **B–D,** Sensitivity to three statin family members are significantly associated with cell lines enriched for EMT features. AUC, area under the curve (higher values represent higher drug sensitivity); *P* value, Wilcoxon rank sum test, comparing statin response on EMT "enriched" vs. "not-enriched" cell lines; *n*, number of cell lines. Of a total of 631 cancer cell lines derived from solid tumors, 596 have been evaluated for sensitivity to fluvastatin, 614 have been evaluated for sensitivity to lovastatin, and 568 have been evaluated for sensitivity to simvastatin. The script and data used for the generation of these figures can be downloaded at https://github.com/bhklab/StatinEMT. **E,** Sensitivity to fluvastatin (lower IC_{50} values) is positively associated with E-cadherin expression and negatively associated with vimentin expression across a panel of cancer-derived cell lines.

Published OnlineFirst December 11, 2017; DOI: 10.1158/0008-5472.CAN-17-1231

Bioconductor package (30), and demonstrated that the EMT-enriched cell lines were associated with significantly higher AUC (more sensitive) to all three statin family members that have been assessed in CTRPv2: fluvastatin (Fig. 5B), lovastatin (Fig. 5C), and simvastatin (Fig. 5D; Wilcoxon rank sum test P-value < 0.001). Thus, cancer cell EMT is associated with sensitivity to multiple statin family members in a large panel of cancer cell lines, across multiple cancer types. As a negative control, we showed that *ESR1* expression levels are not correlated with statin sensitivity (Supplementary Fig. S5D–S5F). Finally, using a panel of 10 cancer-derived cell lines, we showed that fluvastatin IC_{50} is positively associated with E-cadherin expression and negatively associated with vimentin expression (Fig. 5E), strengthening our conclusion that statin sensitivity is associated with an enrichment of EMT phenotype.

Discussion

Previously, the increased cancer cell sensitivity to statins was thought to be mediated by inhibiting prenylation of proteins in the RAS superfamily. This model was built on three observations: (i) statins inhibit prenylation of RAS family proteins (8, 11, 12, 17–21); (ii) coadministration of GGPP or FPP with statins reverses the effect on protein prenylation (8, 11, 13, 17–21); and (iii) coadministration of GGPP or FPP can rescue statin kill (8, 13–15, 18–20). However, most epidemiological studies and clinical trials do not support an association between response to statins and RAS mutations (34–39). Additionally, in cell lines that were sensitive to statins, rescuing RAS localization (8, 40) or RAF–MEK–ERK signaling (41) did not decrease statin sensitivity, and intrinsic sensitivity to statin kill was largely independent of RAS function (8, 42). These contradicting data raise the possibility that inhibition of RAS family protein prenylation is not the sole contributor to statin sensitivity, implicating not only an alternative mechanism of statin-induced apoptosis, but also the potential to develop better biomarkers for the identification of patients that will benefit from statin treatment.

We show here that statin-induced cell death can indeed be uncoupled from inhibition of RAS family protein prenylation. First, increased cellular demand for GGPP and FPP for ectopic expression of RAS family proteins requiring prenylation for activity did not always sensitize MCF10A cells to fluvastatin (Fig. 1). Although RAS overexpression led to an increased sensitivity to fluvastatin, this effect was independent from RAS prenylation and localization to the cell membrane (Fig. 2). Instead, RAS induced EMT by upregulating ZEB1, which was the underlying cause of the increased sensitivity to fluvastatin-induced cell death (Figs. 3 and 4). This can, in part, explain why statins have been reported to be more effective in more aggressive (invasive/metastatic) cancer subtypes (2, 3, 42), while mutations in RAS family proteins are poorly associated with statin response (33–38).

Interestingly, when we assayed for the expression profile of a cohort of 11 genes known to be strongly associated with EMT (43), we observed that they followed a bimodal distribution (Supplementary Fig. S5C). Bimodal distribution of *VIM*, *CDH1*, *ZEB1*, *FN1*, or *CDH2* were used as features to classify all solid tumor cell lines in the CCLE (26) into high expression and low expression populations (Fig. 5A). As a comparison, *ESR1* (estrogen receptor α) is known to be bimodally expressed in breast cancer (32, 33), which could be used as a classifier of estrogen receptor-positive and -negative breast tumors in large bioinformatics databases (Supplementary Fig. S5B; ref. 32). CTRPv2 (27–29), we interrogated sensitivity to three statin family members in >500 solid tumor cell lines for any association with an EMT phenotype. Cell lines enriched with EMT features were associated with significantly higher AUC in response to statin treatment (Fig. 5B–D), indicating that they were more sensitive to the antiproliferative effects of statins. Thus, our original observation in the MCF10A model system is expanded to include >20 cancer types and three statin family members, suggesting that the association between EMT and increased sensitivity to statins can be generalized across a broad range of solid tumor cell lines.

Activation of EMT is proposed to be the critical initiating step in metastatic dissemination of late-stage cancers (43). Although it is still debated whether this process is required for metastasis, as opposed to being a phenotype of aggressive/metastatic disease (44, 45), it is nevertheless known to be associated with cell de-differentiation, stem-like properties, and antiapoptotic signaling (46). Importantly, activation of EMT is typically associated with therapeutic resistance (44–46). We show here that activation of EMT increased cell sensitivity to fluvastatin (Fig. 3; Supplementary Fig. S4), consistent with previous reports (47–49). This suggests the intriguing possibility that statins may be used to target disseminated and/or dormant cancer cells (that is, those that presumably have undergone EMT) that are responsible for therapeutic failure and refractory disease. Several epidemiological studies have reported supporting evidence, showing that statin use in breast cancer patients following front-line treatment was associated with better disease-free survival and overall survival (5, 7). Further testing of statins as adjuvant therapeutics in the preclinical and clinical setting is warranted.

It is perhaps tempting to ask which prenylated protein(s), other than the ones selected for testing in this study, is/are responsible for the anticancer effects of statins in the context of EMT. Indeed, we show that coadministration of GGPP or FPP could rescue fluvastatin kill in both $HRAS^{G12V}$- and myr-$HRAS^{G12V}$-overexpressing cells (Fig. 2G–I). However, the two isoprenoids did not rescue to the same extent: GGPP and MVA completely rescued cell death to control levels, but FPP was less effective (Fig. 2G–I). This is reminiscent of previous studies, where GGPP consistently rescued statin effects (8, 11, 13–15, 18–20), while FPP did so less consistently, rescuing completely (11), partially (8, 13, 14, 18), or not at all (15, 18, 21). Nonetheless, the observation that FPP did not rescue as well as GGPP in an $HRAS^{G12V}$-overexpressing system was unexpected, since HRAS prefers FPP over GGPP for prenylation (16). Two explanations are possible for this observation. First, because FPP also acts as the precursor to sterols (1, 10), a portion of the supplemented FPP could be shunted towards cholesterol production, which does not play a role in statin-induced apoptosis (8). However, the observation that MVA consistently rescues statin-induced cell death (8, 11) (Fig. 2G–I) argues against this interpretation. Alternatively, GGPP also functions as the precursor for other isoprenoids such as dolichols and isoprenoid moieties on coenzyme Q (1, 10), and depletion of these larger isoprenoids could be contributing to statin sensitivity. Consistent with this is the observation that cells overexpressing ZEB1 were more sensitive to fluvastatin, but not to inhibition of geranylgeranylation itself through GGTI (Fig. 3G and H). Taken together, our data reinforce the new model presented here that, in the context of cancer cell EMT,

fluvastatin-induced cell death is uncoupled from inhibition of RAS family protein prenylation. Why cells become dependent on the MVA pathway when undergoing EMT, and are therefore sensitive to fluvastatin inhibition, remains to be elucidated and will be an interesting area for future investigation that could lead to the identification of additional biomarkers of fluvastatin-responsive cancers.

Disclosure of Potential Conflicts of Interest

No potential conflicts of interest were disclosed.

Authors' Contributions

Conception and design: R. Yu, L.Z. Penn
Development of methodology: R. Yu, B. Haibe-Kains
Acquisition of data (provided animals, acquired and managed patients, provided facilities, etc.): R. Yu, J.E. van Leeuwen, P.J. Mullen, B. Haibe-Kains
Analysis and interpretation of data (e.g., statistical analysis, biostatistics, computational analysis): R. Yu, J. Longo, W. Ba-Alawi, B. Haibe-Kains
Writing, review, and/or revision of the manuscript: R. Yu, J. Longo, J.E. van Leeuwen, W. Ba-Alawi, B. Haibe-Kains, L.Z. Penn
Study supervision: L.Z. Penn

Acknowledgments

We thank Drs. David Hedley, Senthil Muthuswamy, Catherine O'Brien, Ming Tsao, and Bradley Wouters for providing reagents. We also thank Lindsay Lustig and Aaliya Tamachi for technical assistance, and all members of the Penn lab for helpful discussion and critical review of the manuscript. This work was supported by funding from the Canada Research Chairs Program (to L.Z. Penn; 950-229872), Canadian Institutes of Health Research (to L.Z. Penn; MOP-142263), Terry Fox Research Institute (to L.Z. Penn, B. Haibe-Kains, and W. Ba-Alawi; 1064), CIHR Canada Graduate Scholarship (to R. Yu), Ontario Graduate Scholarship (to J. Longo), and Ontario Student Opportunity Trust Fund (to J.E. van Leeuwen). This work was also supported by the Office of the Assistant Secretary of Defense for Health Affairs, through the Breast Cancer Research Program under Award No. W81XWH-16-1-0068 (to L.Z. Penn). Opinions, interpretations, conclusions and recommendations are those of the author and are not necessarily endorsed by the Department of Defense.

The costs of publication of this article were defrayed in part by the payment of page charges. This article must therefore be hereby marked *advertisement* in accordance with 18 U.S.C. Section 1734 solely to indicate this fact.

Received April 25, 2017; revised October 4, 2017; accepted November 30, 2017; published OnlineFirst December 11, 2017.

References

1. Goldstein JL, Brown MS. Regulation of the mevalonate pathway. Nature 1990;343:425–30.
2. Kumar AS, Benz CC, Shim V, Minami CA, Moore DH, Esserman LJ. Estrogen receptor-negative breast cancer is less likely to arise among lipophilic statin users. Cancer Epidemiol Biomarkers Prev 2008;17:1028–33.
3. Loeb S, Kan D, Helfand BT, Nadler RB, Catalona WJ. Is statin use associated with prostate cancer aggressiveness? BJU Int 2010;105:1222–5.
4. Nielsen SF, Nordestgaard BG, Bojesen SE. Statin use and reduced cancer-related mortality. N Engl J Med 2012;367:1792–802.
5. Ahern TP, Pedersen L, Tarp M. Statin prescriptions and breast cancer recurrence risk: a Danish nationwide prospective cohort study. J Natl Cancer Inst 2011;103:1461–8.
6. Clendening JW, Pandyra A, Li Z, Boutros PC, Martirosyan A, Lehner R, et al. Exploiting the mevalonate pathway to distinguish statin-sensitive multiple myeloma. Blood 2010;115:4787–97.
7. Campbell MJ, Esserman LJ, Zhou Y, Shoemaker M, Lobo M, Borman E, et al. Breast cancer growth prevention by statins. Cancer Res 2006;66:8707–14.
8. Wong WW, Clendening JW, Martirosyan A, Boutros PC, Bros C, Khosravi F, et al. Determinants of sensitivity to lovastatin-induced apoptosis in multiple myeloma. Mol Cancer Ther 2007;6:1886–97.
9. Garwood ER, Kumar AS, Baehner FL, Moore DH, Au A, Hylton N, et al. Fluvastatin reduces proliferation and increases apoptosis in women with high grade breast cancer. Breast Cancer Res Treat 2010;119:137–44.
10. Mullen PJ, Yu R, Longo J, Archer MC, Penn LZ. The interplay between cell signalling and the mevalonate pathway in cancer. Nat Rev Cancer 2016;16:718–31.
11. Kaneko R, Tsuji N, Asanuma K, Tanabe H, Kobayashi D, Watanabe N. Survivin down-regulation plays a crucial role in 3-hydroxy-3-methylglutaryl coenzyme A reductase inhibitor-induced apoptosis in cancer. J Biol Chem 2007;282:19273–81.
12. Tsubaki M, Mashimo K, Takeda T, Kino T, Fujita A, Itoh T, et al. Statins inhibited the MIP-1alpha expression via inhibition of Ras/ERK and Ras/Akt pathways in myeloma cells. Biomed Pharmacother 2016;78:23–9.
13. Finlay GA, Malhowski AJ, Liu Y, Fanburg BL, Kwiatkowski DJ, Toksoz D. Selective inhibition of growth of tuberous sclerosis complex 2 null cells by atorvastatin is associated with impaired Rheb and Rho GTPase function and reduced mTOR/S6 kinase activity. Cancer Res 2007;67:9878–86.
14. Araki M, Maeda M, Motojima K. Hydrophobic statins induce autophagy and cell death in human rhabdomyosarcoma cells by depleting geranylgeranyl diphosphate. Eur J Pharmacol 2012;674:95–103.
15. Taylor-Harding B, Orsulic S, Karlan BY, Li AJ. Fluvastatin and cisplatin demonstrate synergistic cytotoxicity in epithelial ovarian cancer cells. Gynecol Oncol 2010;119:549–56.
16. Berndt N, Hamilton AD, Sebti SM. Targeting protein prenylation for cancer therapy. Nat Rev Cancer 2011;11:775–91.
17. Tsubaki M, Takeda T, Sakamoto K, Shimaoka H, Fujita A, Itoh T, et al. Bisphosphonates and statins inhibit expression and secretion of MIP-1alpha via suppression of Ras/MEK/ERK/AML-1A and Ras/PI3K/Akt/AML-1A pathways. Am J Cancer Res 2015;5:168–79.
18. Elsayed M, Kobayashi D, Kubota T, Matsunaga N, Murata R, Yoshizawa Y, et al. Synergistic antiproliferative effects of zoledronic acid and fluvastatin on human pancreatic cancer cell lines: an in vitro study. Biol Pharm Bull 2016;39:1238–46.
19. Rigoni M, Riganti C, Vitale C, Griggio V, Campia I, Robino M, et al. Simvastatin and downstream inhibitors circumvent constitutive and stromal cell-induced resistance to doxorubicin in IGHV unmutated CLL cells. Oncotarget 2015;6:29833–46.
20. Moriceau G, Roelofs AJ, Brion R, Redini F, Ebetion FH, Rogers MJ, et al. Synergistic inhibitory effect of apomine and lovastatin on osteosarcoma cell growth. Cancer 2012;118:750–60.
21. Kusama T, Mukai M, Tatsuta M, Nakamura H, Inoue M. Inhibition of transendothelial migration and invasion of human breast cancer cells by preventing geranylgeranylation of Rho. Int J Oncol 2006;29:217–23.
22. Soule HD, Maloney TM, Wolman SR, Peterson WD Jr, Brenz R, McGrath CM, et al. Isolation and characterization of a spontaneously immortalized human breast epithelial cell line, MCF-10. Cancer Res 1990;50:6075–86.
23. Wasylishen AR, Stojanova A, Oliveri S, Rust AC, Schimmer AD, Penn LZ. New model systems provide insights into Myc-induced transformation. Oncogene 2011;30:3727–34.
24. Haeussler M, Schonig K, Eckert H, Eschstruth A, Mianne J, Renaud JB, et al. Evaluation of off-target and on-target scoring algorithms and integration into the guide RNA selection tool CRISPOR. Genome Biol 2016;17:148.
25. Sanjana NE, Shalem O, Zhang F. Improved vectors and genome-wide libraries for CRISPR screening. Nat Methods 2014;11:783–4.
26. Barretina J, Caponigro G, Stransky N, Venkatesan K, Margolin AA, Kim S, et al. The Cancer Cell Line Encyclopedia enables predictive modelling of anticancer drug sensitivity. Nature 2012;483:603–7.
27. Rees MG, Seashore-Ludlow B, Cheah JH, Adams DJ, Price EV, Gill S, et al. Correlating chemical sensitivity and basal gene expression reveals mechanism of action. Nat Chem Biol 2016;12:109–16.

28. Seashore-Ludlow B, Rees MG, Cheah JH, Cokol M, Price EV, Coletti ME, et al. Harnessing connectivity in a large-scale small-molecule sensitivity dataset. Cancer Discov 2015;5:1210–23.
29. Basu A, Bodycombe NE, Cheah JH, Price EV, Liu K, Schaefer GI, et al. An interactive resource to identify cancer genetic and lineage dependencies targeted by small molecules. Cell 2013;154:1151–61.
30. Smirnov P, Safikhani Z, El-Hachem N, Wang D, She A, Olsen C, et al. PharmacoGx: an R package for analysis of large pharmacogenomic datasets. Bioinformatics 2016;32:1244–6.
31. Wang J, Wen S, Symmans WF, Pusztai L, Coombes KR. The bimodality index: a criterion for discovering and ranking bimodal signatures from cancer gene expression profiling data. Cancer Inform 2009;7:199–216.
32. Gendoo DM, Ratanasirigulchai N, Schroder MS, Pare L, Parker JS, Prat A, et al. Genefu: an R/Bioconductor package for computation of gene expression-based signatures in breast cancer. Bioinformatics 2016;32:1097–9.
33. Muftah AA, Aleskandarany M, Sonbul SN, Nolan CC, Diez Rodriguez M, Caldas C, et al. Further evidence to support bimodality of oestrogen receptor expression in breast cancer. Histopathology 2017;70:456–65.
34. Krens LL, Simkens LH, Baas JM, Koomen ER, Gelderblom H, Punt CJ, et al. Statin use is not associated with improved progression free survival in cetuximab treated KRAS mutant metastatic colorectal cancer patients: results from the CAIRO2 study. PLoS One 2014;9:e112201.
35. Lee JE, Baba Y, Ng K, Giovannucci E, Fuchs CS, Ogino S, et al. Statin use and colorectal cancer risk according to molecular subtypes in two large prospective cohort studies. Cancer Prev Res 2011;4:1808–15.
36. Baas JM, Krens LL, ten Tije AJ, Erdkamp F, van Wezel T, Morreau H, et al. Safety and efficacy of the addition of simvastatin to cetuximab in previously treated KRAS mutant metastatic colorectal cancer patients. Invest New Drugs 2015;33:1242–7.
37. Baas JM, Krens LL, Bos MM, Portielje JE, Batman E, van Wezel T, et al. Safety and efficacy of the addition of simvastatin to panitumumab in previously treated KRAS mutant metastatic colorectal cancer patients. Anticancer Drugs 2015;26:872–7.
38. Hong JY, Nam EM, Lee J, Park JO, Lee SC, Song SY, et al. Randomized double-blinded, placebo-controlled phase II trial of simvastatin and gemcitabine in advanced pancreatic cancer patients. Cancer Chemother Pharmacol 2014;73:125–30.
39. Ng K, Ogino S, Meyerhardt JA, Chan JA, Chan AT, Niedzwiecki D, et al. Relationship between statin use and colon cancer recurrence and survival: results from CALGB 89803. J Natl Cancer Inst 2011;103:1540–51.
40. DeClue JE, Vass WC, Papageorge AG, Lowy DR, Willumsen BM. Inhibition of cell growth by lovastatin is independent of ras function. Cancer Res 1991;51:712–7.
41. Wu J, Wong WW, Khosravi F, Minden MD, Penn LZ. Blocking the Raf/MEK/ERK pathway sensitizes acute myelogenous leukemia cells to lovastatin-induced apoptosis. Cancer Res 2004;64:6461–8.
42. Goard CA, Chan-Seng-Yue M, Mullen PJ, Quiroga AD, Wasylishen AR, Clendening JW, et al. Identifying molecular features that distinguish fluvastatin-sensitive breast tumor cells. Breast Cancer Res Treat 2014;143:301–12.
43. Thiery JP. Epithelial-mesenchymal transitions in tumour progression. Nat Rev Cancer 2002;2:442–54.
44. Fischer KR, Durrans A, Lee S, Sheng J, Li F, Wong STC, et al. Epithelial-to-mesenchymal transition is not required for lung metastasis but contributes to chemoresistance. Nature 2015;527:472–6.
45. Zheng X, Carstens JL, Kim J, Scheible M, Kaye J, Sugimoto H, et al. Epithelial-to-mesenchymal transition is dispensable for metastasis but induces chemoresistance in pancreatic cancer. Nature 2015;527:525–30.
46. Pattabiraman DR, Weinberg RA. Targeting the epithelial-to-mesenchymal transition: the case for differentiation-based therapy. Cold Spring Harb Symp Quant Biol 2016;81:11–19.
47. Kang S, Kim ES, Moon A. Simvastatin and lovastatin inhibit breast cell invasion induced by H-Ras. Oncol Rep 2009;21:1317–22.
48. Warita K, Warita T, Beckwitt CH, Schurdak ME, Vazquez A, Wells A, et al. Statin-induced mevalonate pathway inhibition attenuates the growth of mesenchymal-like cancer cells that lack functional E-cadherin mediated cell cohesion. Sci Rep 2014;4:7593.
49. Fan Z, Jiang H, Wang Z, Qu J. Atorvastatin partially inhibits the epithelial-mesenchymal transition in A549 cells induced by TGF-β1 by attenuating the upregulation of SphK1. Oncol Rep 2016;36:1016–22.

Published OnlineFirst December 11, 2017; DOI: 10.1158/0008-5472.CAN-17-1231

Cancer Research
The Journal of Cancer Research (1916–1930) | The American Journal of Cancer (1931–1940)

AACR American Association for Cancer Research

Statin-Induced Cancer Cell Death Can Be Mechanistically Uncoupled from Prenylation of RAS Family Proteins

Rosemary Yu, Joseph Longo, Jenna E. van Leeuwen, et al.

Cancer Res 2018;78:1347-1357. Published OnlineFirst December 11, 2017.

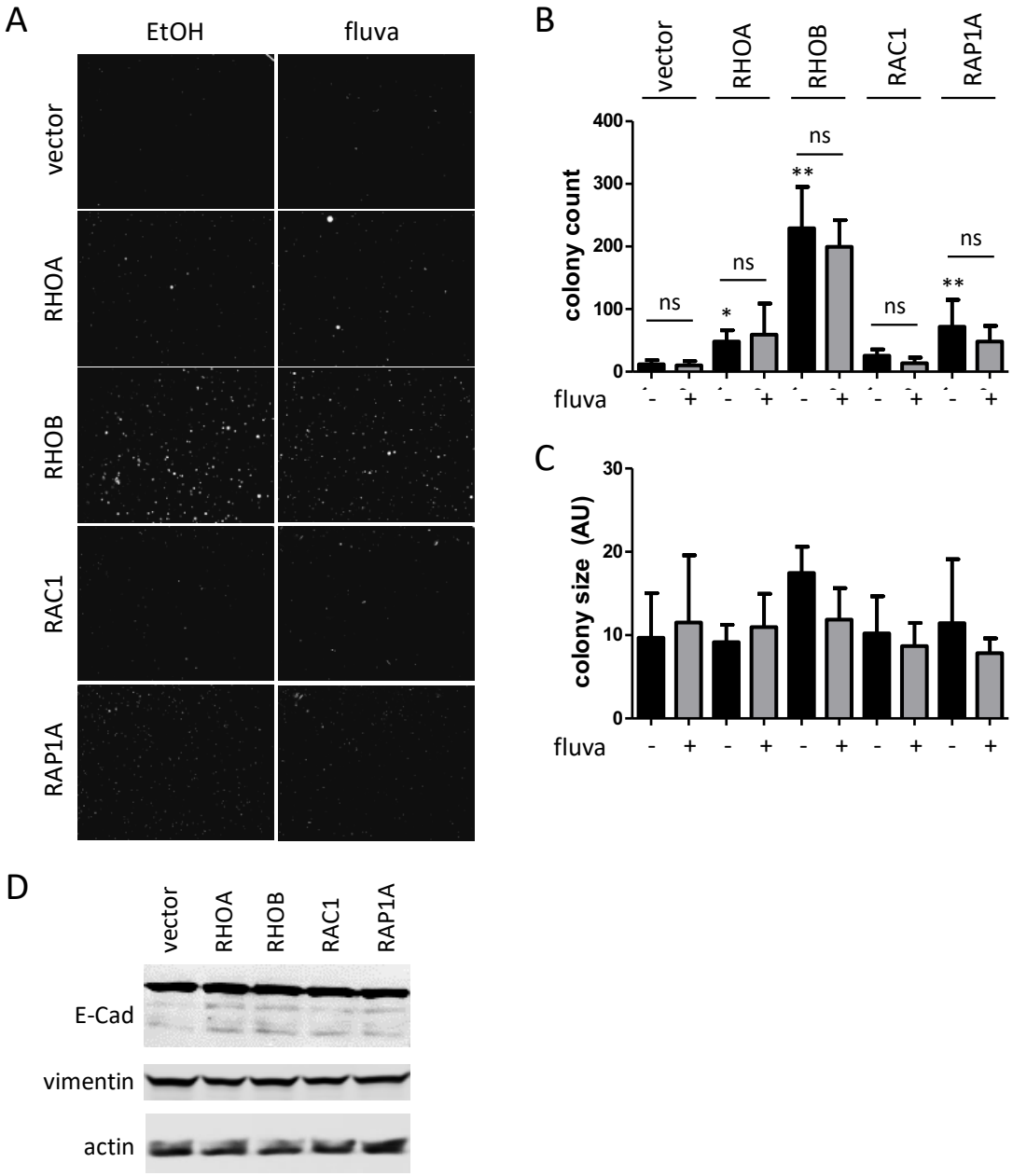

Supplementary Fig. S1. Overexpression of RAS superfamily proteins that do not induce EMT, do not sensitize MCF10A cells to fluvastatin. A-C, Cells with ectopic expression of $RHOA^{G14V}$, $RHOB^{G14V}$, $RAC1^{G12V}$, and $RAP1A^{G12V}$ were assayed for colony formation in soft agar. Without fluvastatin treatment, RHOA, RHOB, and RAP1A transformed MCF10As as assayed by soft agar colony formation assay. Bars are mean + SD, n=3. *, $p<0.05$; **, $p<0.01$ (one-way ANOVA with a Dunnett post-test, comparing all columns vs. vector control column). Fluvastatin treatment had no significant effect on the colony count (B) or size (C). Colonies were treated with 20 μM fluvastatin 2x weekly for 16 days. Bars are mean + SD, n=3. ns, not significant (unpaired, two-tailed *t* test, comparing fluvastatin-treated vs. no treatment control). D, Ectopic expression of these RAS superfamily proteins do not induce EMT, as seen by similar expression levels of E-cadherin and vimentin to the vector control.

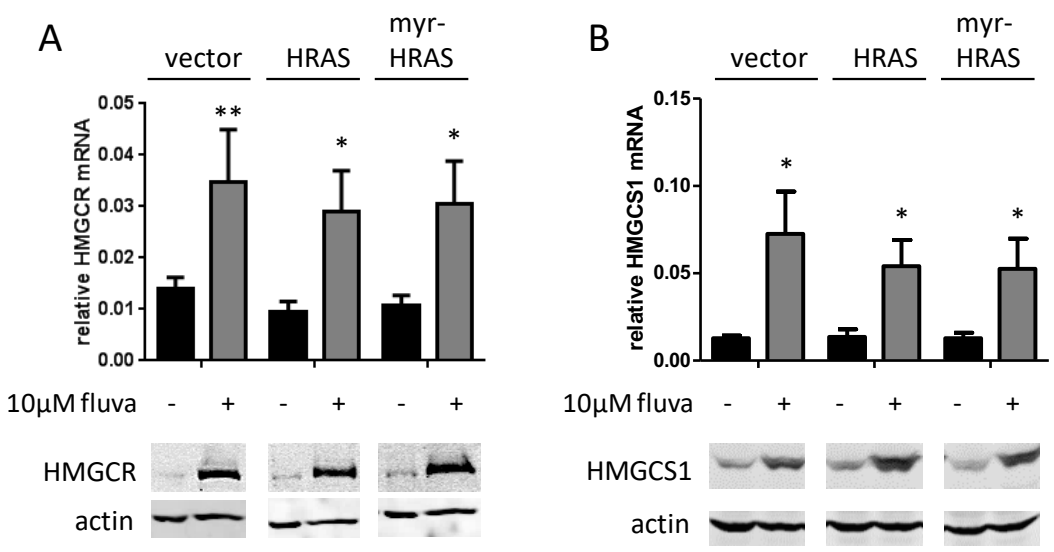

Supplementary Fig. S2. Overexpression of $HRAS^{G12V}$ or myr-$HRAS^{G12V}$ does not alter HMGCR or HMGCS1 expression. A-B, Cells were treated with 10μM fluvastatin for 16 h and analyzed for the mRNA and protein expression of HMGCR (A) and HMGCS1 (B), Bars are mean + SD, n=3. *, $p<0.05$; **, $p<0.01$ (unpaired, two-tailed *t* test, comparing fluvastatin-treated vs. no treatment control).

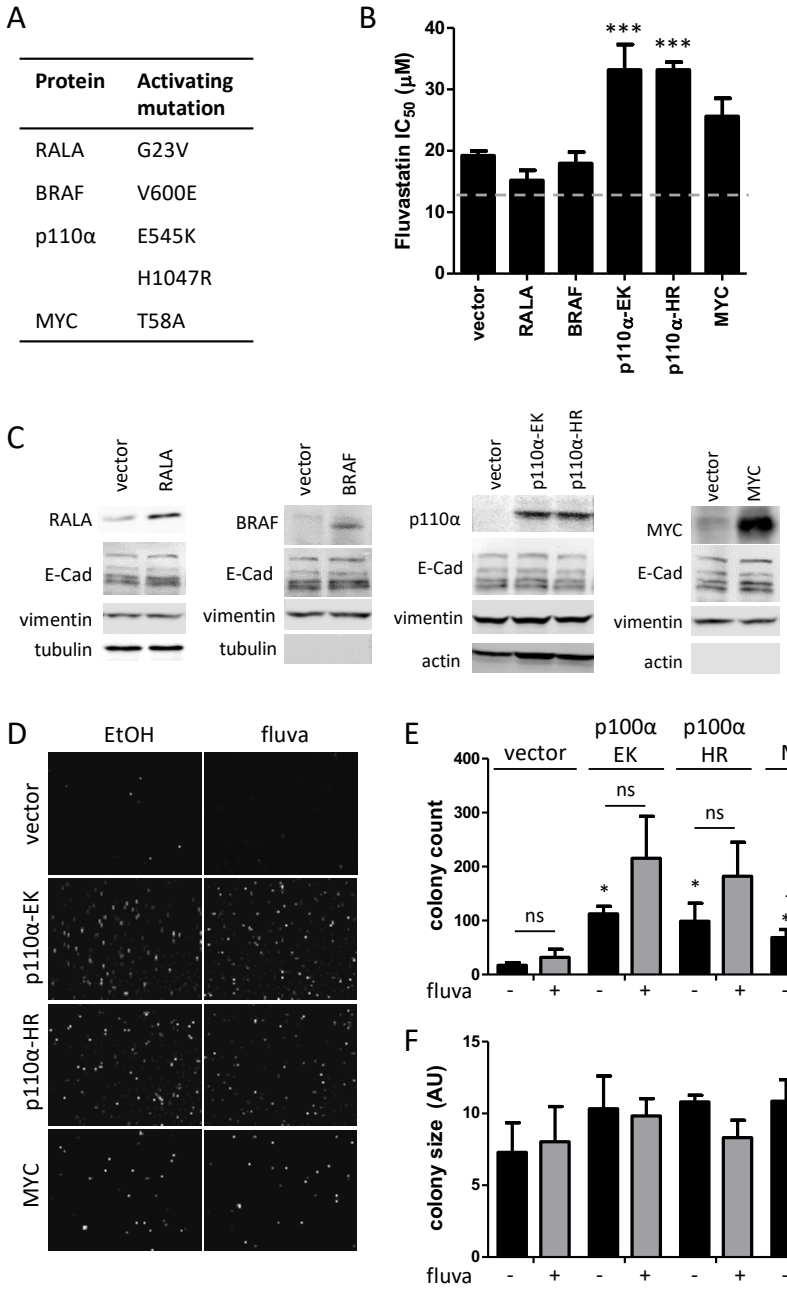

Supplementary Fig. S3. Fluvastatin sensitivity is not mediated by the BRAF, RALA, PI3K, or MYC downstream mediators of RAS signaling. A, ectopic expression of downstream mediators of RAS signaling. B, none of the oncoproteins in panel A sensitized MCF10A cells to fluvastatin; p110α overexpression desensitized MCF10As to fluvastatin. Bars are mean + SD, n=3. ***, $p<0.001$ (one-way ANOVA with a Dunnett post-test, comparing all columns vs. vector control column). C, None of the oncoproteins in panel A induced EMT. D-F, Cells with ectopic expression of PI3K-p110α^{E545K}, PI3K-p110α^{H1047R}, and MYC^{T58A} were assayed for colony formation in soft agar. Without fluvastatin treatment, all three oncogenes transformed MCF10As as assayed by soft agar colony formation assay. Bars are mean + SD, n=3. *, $p<0.05$ (one-way ANOVA with a Dunnett post-test, comparing all columns vs. vector control column). Fluvastatin treatment had no significant effect on the colony count (E) or size (F). Colonies were treated with 20 μM fluvastatin 2x weekly for 18 days. Bars are mean + SD, n=3. ns, not significant (unpaired, two-tailed *t* test, comparing fluvastatin-treated vs. no treatment control).

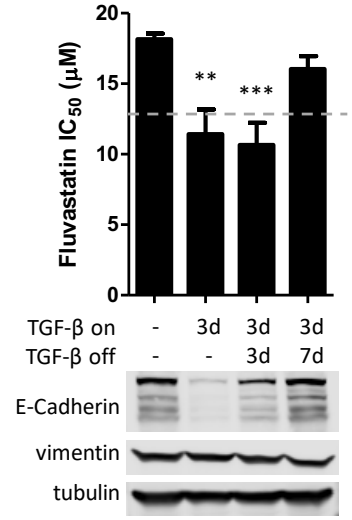

Supplementary Fig. S4. TGF-β induced EMT and fluvastatin sensitivity are both reversible. After 3 days of treatment with 5 ng/mL TGF-β, MCF10A cells undergo EMT and become more sensitive to fluvastatin, as assessed by MTT assays for 72 h. Dashed line represents IC_{50} of $HRAS^{G12V}$-overexpressing cells. Cells gradually reverted to epithelial with continued culturing after TGF-β removal; after 7 days, sensitivity to fluvastatin was restored to control levels. Bars are mean + SD, n=3. **, $p<0.01$; ***, $p<0.001$ (one-way ANOVA with a Dunnett post-test, comparing all columns vs. vector control column).

A

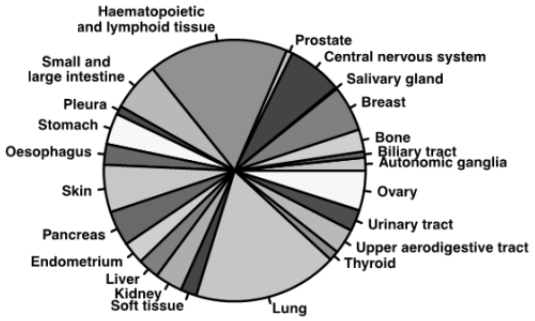

B

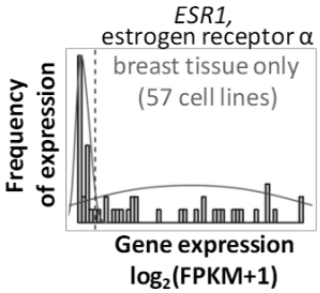

Left peak:
ERα-low cell lines
Right peak:
ERα-high cell lines
- - - - Cutoff

C

	Gene name	Protein name	Bimodality index
controls	POLR2A	RNA polymerase II, subunit A	0.09
controls	ESR1	Estrogen receptor α	0.6
Known EMT-associated genes	VIM	Vimentin	1.9
Known EMT-associated genes	CDH1	E-Cadherin	1.7
Known EMT-associated genes	ZEB1	ZEB1/TCF8	1.6
Known EMT-associated genes	FN1	Fibronectin	1.5
Known EMT-associated genes	CDH2	N-Cadherin	1.5
Known EMT-associated genes	HMGA2	HMGA2	1.3
Known EMT-associated genes	ZEB2	ZEB2/SIP1	1.3
Known EMT-associated genes	SNAI2	SNAIL2/SLUG	1.1
Known EMT-associated genes	TWIST1	TWIST1	1.1
Known EMT-associated genes	SNAI1	SNAIL1	1.0
Known EMT-associated genes	FOXC2	FOXC2	0.7

D

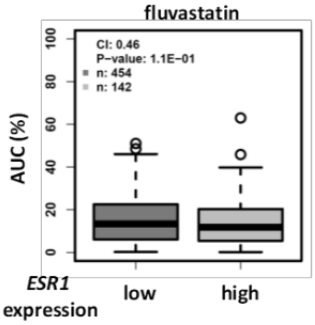

E

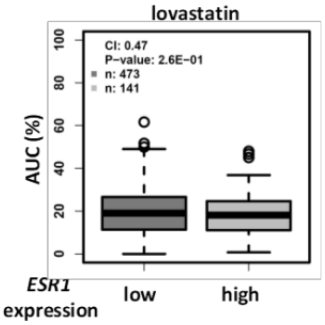

F

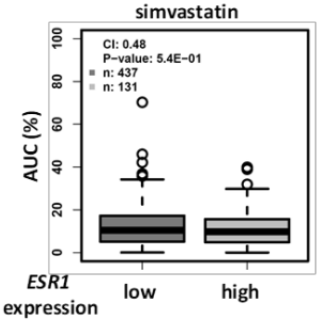

Supplementary Fig. S5. Unimodal and bimodal gene expression in the CCLE database. B, bimodal distribution of *ESR1* in breast cancer cell lines. Gene expression values are $\log_2$(FPKM+1) with FPKM = Fragments Per Kilobase of transcript per Million mapped reads. C, bimodality index of 11 known EMT-associated genes, all scoring higher than *ESR1*. D-F, *ESR1* expression levels are not correlated with sensitivity to three statin family members. AUC, area under the curve (higher values represent higher drug sensitivity); CI, Concordance Index; P-value, Wilcoxon rank sum test, comparing statin response on EMT 'enriched' vs. 'not-enriched' cell lines; n, number of cell lines. The script and data used for the generation of these figures can be downloaded at https://github.com/bhklab/StatinEMT.

Published OnlineFirst February 18, 2021; DOI: 10.1158/0008-5472.CAN-20-2642

CANCER RESEARCH | METABOLISM AND CHEMICAL BIOLOGY

Mevalonate Pathway Inhibition Slows Breast Cancer Metastasis via Reduced *N*-glycosylation Abundance and Branching

Rosemary Yu[1,2], Joseph Longo[1,2], Jenna E. van Leeuwen[1,2], Cunjie Zhang[3], Emily Branchard[1], Mohamad Elbaz[1], David W. Cescon[1], Richard R. Drake[4], James W. Dennis[3,5,6], and Linda Z. Penn[1,2]

ABSTRACT

Aberrant *N*-glycan Golgi remodeling and metabolism are associated with epithelial–mesenchymal transition (EMT) and metastasis in patients with breast cancer. Despite this association, the *N*-glycosylation pathway has not been successfully targeted in cancer. Here, we show that inhibition of the mevalonate pathway with fluvastatin, a clinically approved drug, reduces both *N*-glycosylation and *N*-glycan-branching, essential components of the EMT program and tumor metastasis. This indicates novel cross-talk between *N*-glycosylation at the endoplasmic reticulum (ER) and *N*-glycan remodeling at the Golgi. Consistent with this cooperative model between the two spatially separated levels of protein *N*-glycosylation, fluvastatin-induced tumor cell death was enhanced by loss of Golgi-associated *N*-acetylglucosaminyltransferases MGAT1 or MGAT5. In a mouse model of postsurgical metastatic breast cancer, adjuvant fluvastatin treatment reduced metastatic burden and improved overall survival. Collectively, these data support the immediate repurposing of fluvastatin as an adjuvant therapeutic to combat metastatic recurrence in breast cancer by targeting protein *N*-glycosylation at both the ER and Golgi.

Significance: These findings show that metastatic breast cancer cells depend on the fluvastatin-sensitive mevalonate pathway to support protein *N*-glycosylation, warranting immediate clinical testing of fluvastatin as an adjuvant therapy for breast cancer.

Introduction

The first-line therapy for early-stage breast cancer is surgical removal of the tumor, followed by adjuvant therapies (1). Despite aggressive treatment, 15% to 20% of patients with early-stage breast cancer experience recurrence, often as distant metastases (1). Prevention or delay of metastatic recurrence in breast cancer would represent a key advance in the treatment of this disease. Several retrospective studies have indicated that the risk of postsurgical breast cancer recurrence is reduced by 30% to 60% in patients who are taking statins (2–5), a class of approved drugs that lowers serum cholesterol. Increased duration of adjuvant statin use is associated with decreased risk of recurrence (5), suggesting that long-term intake of statins in the adjuvant setting may prolong patient survival. Preclinically, statins have been shown to inhibit metastasis in a broad range of cancers (6–9); however, the precise mechanism remains unclear. Mechanistic understanding of the effect of fluvastatin on metastatic breast cancer cells may provide the essential insight required to guide the design of clinical trials, identify biomarkers of statin response, and provide a starting point for the development of additional agents to target metastatic recurrence.

Statins inhibit the metabolic conversion of 3-hydroxy-3-methylglutaryl coenzyme A (HMG-CoA) to mevalonate (MVA), the rate-limiting step of the MVA pathway (**Fig. 1A**). The MVA pathway synthesizes cholesterol; farnesyl pyrophosphate (FPP) and geranylgeranyl pyrophosphate (GGPP), required for protein prenylation; coenzyme Q (CoQ), required for the electron transport chain (ETC); and dolichol, required for protein *N*-glycosylation (**Fig. 1A**; ref. 10). Statin-triggered tumor cell death can be rescued by exogenous GGPP; therefore, statin activity has been linked to inhibition of prenylated proteins (11, 12). However, recent interrogation has revealed that statins preferentially target cancer cells with enriched mesenchymal features, but this effect is uncoupled from inhibition of RAS family protein prenylation (11). This suggests an alternative mechanism of action of fluvastatin on cells undergoing EMT, which occurs downstream of GGPP. As disseminated primary tumor cells often gain mesenchymal characteristics while losing epithelial features (13), investigating this novel mechanism is of interest as targeting breast cancer cells with mesenchymal phenotypes may have utility in the adjuvant setting to prevent metastatic recurrence.

Herein, we show that statin-dependent depletion of dolichol selectively inhibits the viability of EMT-induced invasive breast cancer cells. Dolichol is a group of long-chain isoprenoids that comprises the lipid component of lipid-linked oligosaccharides (LLO), essential for *N*-linked glycosylation of nascent peptides translated in the secretory pathway (**Fig. 1A**; ref. 10). The oligosaccharide in LLO is added cotranslationally to asparagine on secretory and membrane proteins at the endoplasmic reticulum (ER), and subsequently processed to more complex structures by glycosidases and glycosyltransferases in the ER and Golgi during transit to the cell surface. Surprisingly, we

[1]Princess Margaret Cancer Centre, University Health Network, Toronto, Ontario, Canada. [2]Department of Medical Biophysics, University of Toronto, Toronto, Ontario, Canada. [3]Lunenfeld-Tanenbaum Research Institute, Mount Sinai Hospital, Toronto, Ontario, Canada. [4]Department of Cell and Molecular Pharmacology and Experimental Therapeutics, Medical University of South Carolina, Charleston, South Carolina. [5]Department of Molecular Genetics, University of Toronto, Toronto, Ontario, Canada. [6]Department of Laboratory Medicine and Pathobiology, University of Toronto, Toronto, Ontario, Canada.

Note: Supplementary data for this article are available at Cancer Research Online (http://cancerres.aacrjournals.org/).

Corresponding Authors: Linda Z. Penn, Princess Margaret Cancer Centre, 13th Floor 13–706, Toronto, Ontario M5G 1L7, Canada. Phone: 416-634-8770; E-mail: Linda.Penn@uhnresearch.ca; and James W. Dennis, Lunenfeld-Tanenbaum Research Institute, Mount Sinai Hospital, 600 University Avenue, R988, Toronto, Ontario M5G 1X5, Canada. Phone: 416-586-8233; E-mail: DENNIS@lunenfeld.ca

Cancer Res 2021;81:2625–35

doi: 10.1158/0008-5472.CAN-20-2642

Published OnlineFirst February 18, 2021; DOI: 10.1158/0008-5472.CAN-20-2642

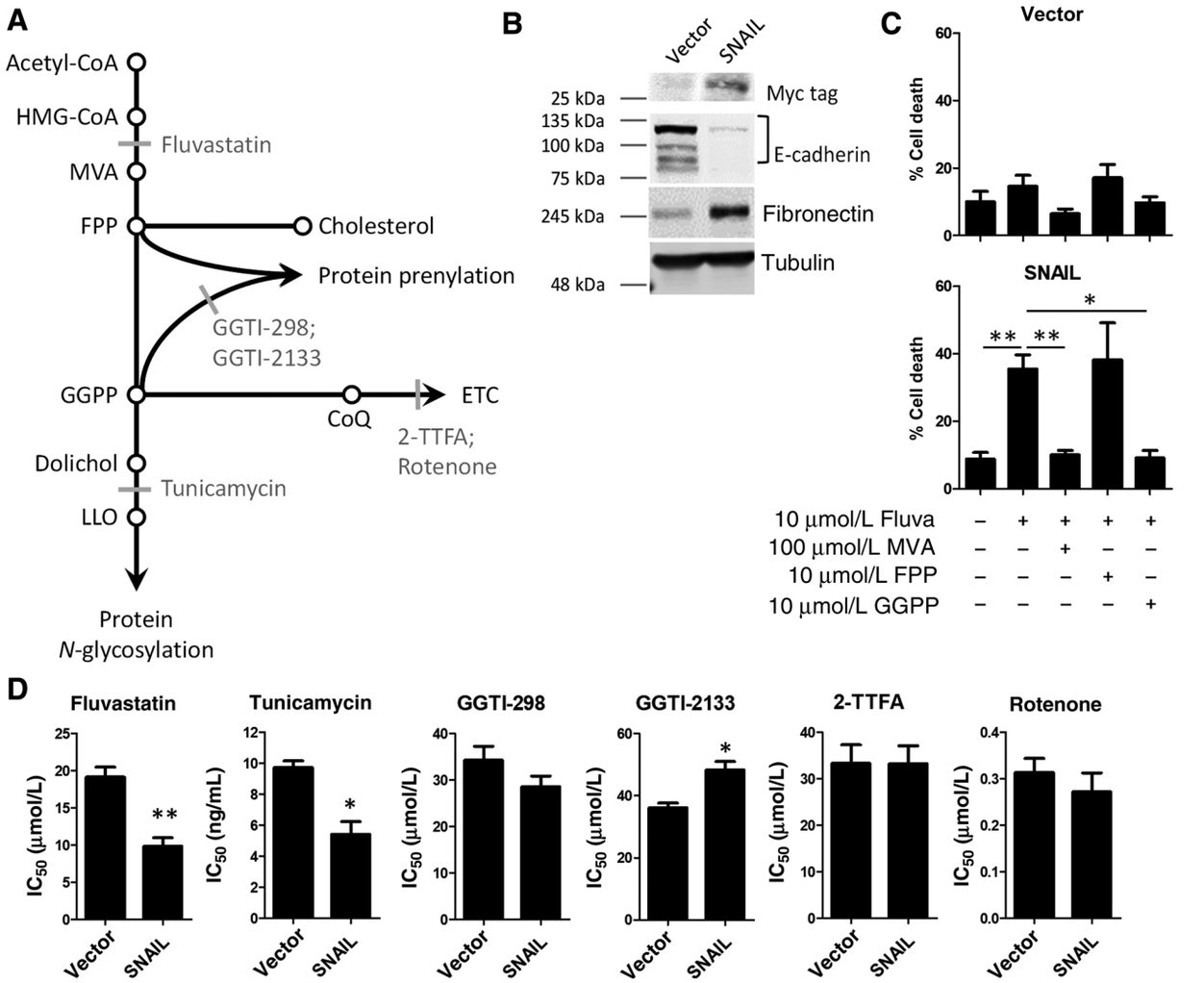

Figure 1.

Induction of EMT by SNAIL overexpression increases cell sensitivity to inhibition of dolichol-dependent protein *N*-glycosylation by fluvastatin and tunicamycin. **A,** A simplified schematic of the MVA pathway. Inhibitors of specific components of the pathway are represented in gray. **B,** Immunoblot of E-cadherin, an epithelial cell marker, and fibronectin, a mesenchymal cell marker, revealed that overexpression of SNAIL induced EMT in MCF10A cells. Tubulin was used as loading control. **C,** Flow cytometric quantification of percentage of dead cells (% pre-G_1 population) with propidium iodide DNA staining after fixation. Fluvastatin treatment for 72 hours induced cell death in MCF10A cells overexpressing SNAIL, but not in vector control cells. Fluvastatin-induced cell death was fully rescued by coadministration with MVA or GGPP, but not FPP, at the indicated doses. Bars, mean + SD, $n = 3$. *, $P < 0.05$; **, $P < 0.01$ (one-way ANOVA with a Dunnett posttest, comparing all columns vs. fluvastatin column). **D,** SNAIL overexpression sensitized cells to fluvastatin and tunicamycin, but not inhibitors of other components of the MVA pathway. IC_{50} values as calculated based on MTT assays after cells were treated with 8 doses of each drug for 72 hours. Bars, mean + SD, $n = 3$–4. *, $P < 0.05$; **, $P < 0.01$ (unpaired, two-tailed *t* test, comparing SNAIL vs. vector columns).

show that in addition to reducing LLO-dependent *N*-glycosylation at the ER, fluvastatin treatment also reduced subsequent branching of complex-type *N*-glycans that occurs in the *medial*-Golgi. Oncogenic mutations induce *N*-glycan branching by increasing expression of MGAT4, MGAT5, and metabolic pathways to nucleotide-sugars, which modify receptor kinases that promote epithelial-to-mesenchymal transition (EMT) and metastasis (14–18). Knockout of MGAT5 in mice has been shown to reduce mammary tumor growth and metastases (19), and knockdown of MGAT1 significantly decreased tumor growth and incidence of lung metastases in a prostate cancer xenograft model (20). Moreover, *N*-glycan branches and the number of glycan-occupied sites in receptors act cooperatively as ligands for multivalent galectins, thereby regulating cell surface residency and signaling (16). To date, however, ER and Golgi levels of protein *N*-glycosylation in cancer metastasis has not been successfully targeted. Here, we show for the first time that aberrant protein *N*-glycosylation in metastatic breast cancer cells can be therapeutically targeted by inhibiting dolichol biosynthesis using fluvastatin, using a model of spontaneous postsurgical metastasis that closely follows the course of human breast cancer progression and treatment (21). Our results demonstrate that postsurgical fluvastatin treatment attenuates the development of breast cancer metastases and improves overall survival by >30%. Taken together, our results support the immediate clinical testing of fluvastatin as a safe and effective therapeutic in the

adjuvant setting, and support the further development of novel therapeutics to combat metastatic recurrence in breast cancer by inhibiting aberrant protein *N*-glycosylation.

Materials and Methods

Reagents

Fluvastatin was purchased from US Biologicals (F5277–76). TGFβ was purchased from PeproTech (100–21). PNGase F was purchased from NEB (P0704). Complete protease inhibitor was purchased from Roche (11697498001). RapiGest SF was purchased from Waters (186001861). Sialidase was purchased from Glyko (GK80040). All other chemicals were purchased from Sigma unless otherwise specified. In the conduct of research involving hazardous organisms or toxins, the investigators adhered to the CDC-NIH Guide for Biosafety in Microbiological and Biomedical Laboratories.

Cell lines

MCF10A cells were a kind gift from Dr. Senthil Muthuswamy. MDA-MB-231 and LM2–4 cells were a kind gift from Dr. Robert Kerbel. All other cell lines were obtained from ATCC. HEK293Tv, LM2–4, MCF-7, MCF10A, and MDA-MB-231 cells were cultured at 37°C in a humidified atmosphere at 5% CO_2 in supplemented growth media (21–23). All cell lines were authenticated by short tandem repeat (STR) profiling and tested to be free of *Mycoplasma* monthly using commercial mycoplasma detection kits. All cell lines were used between 3 to 20 passages after thawing. Transgene expression was stably introduced into MCF10A cells using retroviral insertion with pLPC, a kind gift from Dr. Roberta Maestro, or pBabePuro (22). In the conduct of research utilizing recombinant DNA, the investigators adhered to NIH Guidelines for research involving recombinant DNA molecules.

HeLa Flp-In-TREx cells were transfected with two guide RNA (sgRNA) in the CRISPR/Cas9 px459 vector targeting exon 4 and the flaking intron for removal of 110 bp from the SLC3A2 gene. sgRNA#1: CAGATTCAACCGGAGGTACC, sgRNA#2: CCGCGTTGTCGCGAGCTAC. Deletions were confirmed by sequencing. Inducible expression was restored by transfecting the cells with human SLC3A2 cDNA cloned into the pcDNA5/FRT/TO vector for single site insertion at a preintegrated FRT recombination site. MGAT1 and MGAT5 mutant MDA-MB-231 cells were generated with CRISPR/Cas9 px459 vector using guide RNA for a deletion within the catalytic domain (https://zlab.bio/guide-design-resources). The null mutations were validated by sequencing and LC/MS-MS analysis of glycopeptidase released *N*-glycan.

MTT assays

3-(4,5-dimethylthiazol-2-yl)-2,5-diphenyltetrazolium bromide (MTT) assays were performed as described previously (23). Cells were seeded at 750 to 5,000 cells/well in 96-well plates and treated in triplicate with 8 doses of drugs or the solvent control for 72 hours. IC_{50} values were computed using GraphPad Prism with a bottom constraint equal to 0.

Immunoblotting

Lysates were prepared in RIPA lysis buffer (25 mmol/L Tris pH 7.4, 150 mmol/L NaCl, 0.5% sodium deoxycholate, 1% NP-40, protease inhibitors). Antibodies used were c-MYC (MAb 9E10, in-house), E-cadherin (CST 3195), vimentin (CST 5741), fibronectin (Abcam ab32419), actin (Sigma A2066), tubulin (Millipore CP06), GP130 (SCB sc-655), EGFR (CST 2232), SLC3A2 (SCB sc-7095), and Ku80 (CST 2180).

Immunohistochemistry

For tumors, two sequential slices were stained for hematoxylin and eosin (H&E) or Ki67 (Novus NB110–90592). For lungs, two sequential slices were obtained every 200 μm for three depths containing all five lobes, and stained for H&E or hEGFR (Zymed 28005). Metastatic colonies were identified by hEGFR staining and confirmed by H&E. Total hEGFR positivity was computed using ImageScope.

Cell death assay

Cells were seeded at 250,000/plate overnight, then treated with as indicated for 72 hours. Cells were fixed in 70% ethanol overnight, stained with propidium iodide (Sigma), and analyzed for the sub-diploid DNA ("pre-G1") population as previously described (23).

qRT-PCR

Total RNA was harvested from subconfluent cells using TRIzol Reagent (Invitrogen). cDNA was synthesized from 500 ng of RNA using SuperScript III (Invitrogen). Real-time quantitative RT-PCR was performed using SYBR Green (Applied Biosystems) with the following primers:

BiP_fw 3′-TGACATTGAAGACTTCAAAGCT-5′
BiP_rv 3′-CTGCTGTATCCTCTTCACCAGT-5′
ERdj4_fw 3′-AAAATAAGAGCCCGGATGCT-5′
ERdj4_rv 3′-CGCTTCTTGGATCCAGTGTT-5′
18S_rRNA_fw 5′-GTAACCCGTTGAACCCCATT-3′
18S_rRNA_fw 3′-CCATCCAATCGGTAGTAGCG-3′

Sample preparation for glycopeptide analysis

A total of 1×10^7 cells were harvested after indicated treatment. Cells were lysed in 1 mL IP lysis buffer (1% Triton-100, 20 mmol/L Tris pH 7.5, 150 mmol/L NaCl, 1 mmol/L EDTA, 1 mmol/L EGTA, cOmplete protease inhibitor), and centrifuged at 14,000 rpm for 30 minutes at 4°C. Lysates were normalized to 2.5 mg/mL and 1 mL was incubated with 20 μL of FLAG beads at 4°C overnight. Beads were washed thoroughly in TBS (50 mmol/L Tris pH 7.5, 150 mmol/L NaCl) and 50 mmol/L ammonium bicarbonate and on-bead trypsin digest was carried out using 0.5 μg of trypsin at 37°C overnight. Glycopeptides were extracted using 0.5% formic acid, vacuumed to dry, and desialidated with 0.5 μL of sialidase at 37°C overnight.

Glycopeptide analysis by LC/MS-MS

Peptides were applied to a nano-HPLC Chip using an Agilent 1200 series microwell-plate autosampler, and interface with an Agilent 6550 Q-TOF MS (Agilent Technologies). The reverse-phase nano-HPLC Chip (G4240–62002) had a 40 nL enrichment column and a 75 μmol/L × 150 mm separation column packed with 5 μmol/L Zorbax 300SB-C18. The mobile phase was 0.1% formic acid in water (v/v) as solvent A, and 0.1% formic acid in ACN (v/v) as solvent B. The flow rate at 0.3 μL/min with gradient schedule; 3% B (0−1 minutes); 3%−40% B (1−90 minutes); 40%−80% B (90−95 minutes); 80% B (95−100 minutes), and 80%–3% B (100–105 minutes). Mascot search was used to identify proteins and peptide sequences coverage. Extract glycopeptide were identified by Agilent Masshunter Quanlititive Analysis software by the presence of hexose (Hex) and N-acetylhexosamine (NAc), such as 204 (HexNAc ions), and 366 (Hex-HexNAc ions). Glycan structures were predicted for extracted glycopeptides by online GlycoMod (http://web.expasy.org/glycomod/).

Published OnlineFirst February 18, 2021; DOI: 10.1158/0008-5472.CAN-20-2642

Glycan structure by MS/MS and occupancy of NXS/T(X≠P) N-glycosylation sites were determined manually.

N-glycan extraction

A total of 15 × 10^6cells were seeded overnight and treated as indicated. Cells were harvested, suspended in 1 mL of HEPES homogenization buffer (0.25 mol/L sucrose, 50 mmol/L HEPES pH 7.5, 5 mmol/L NaF, 5 mmol/L EDTA, 2 mmol/L DTT, cOmplete protease inhibitor), and lysed using a probe sonicator. Homogenate was cleared at 2,000 × *g* for 20 minutes at 4°C, then ultracentrifuged at 115,000 × *g* for 70 minutes at 4°C. The pellet was vigorously suspended in 650 μL Tris buffer (0.8% Triton X-114, 50 mmol/L Tris pH 7.5, 0.1 mmol/L NaCl, 5 mmol/L EDTA, 5 mmol/L NaF, 2 mmol/L DTT, cOmplete protease inhibitor). The homogenate was chilled on ice for 10 minutes, incubated at 37°C for 20 minutes, then phase partitioned at 1,950 × *g* for 2 minutes at room temperature. The upper phase was discarded. Membrane proteins in the lower phase was precipitated with 1 mL acetone at −20°C overnight.

Precipitated proteins were suspended in 60 μL of suspension buffer (0.25% RapiGest SF, 50 mmol/L ammonium bicarbonate, 5 mmol/L DTT). The completely dissolved solution was heated for 3 minutes at 85°C. Approximately 30 μg proteins was mixed with 0.5 μL of PNGase F, 0.7 μL of sialidase, and 20 μL of 50 mmol/L ammonium bicarbonate, and incubated at 42°C for 2 hours followed by 37°C overnight. Released *N*-glycans were extracted with 4 to 5 volumes of 100% ethanol at −80°C for 2 hours. The supernatant containing released *N*-glycans was speed vacuumed to dry.

Homemade porous graphitized carbon (PGC) microtips containing 10 mg PGC in a bed volume of 50 μL was washed with 500 μL of ddH_2O, 500 μL of 80% acetonitrile (ACN), and equilibrated with 500 μL 0.1% trifluoroacetic acid (TFA). *N*-glycan pellets were dissolved in 50 μL of 0.1% TFA and slowly loaded into microtips. Microtips were washed with 500 μL 0.1% TFA. *N*-glycans were eluted several times with 500 μL of elution buffer (0.05% TFA, 40% ACN). The eluted *N*-glycans were speed vacuumed to dry.

Global glycan analysis by LC/MS-MS

Analysis of the eluted *N*-glycans was modified from a previous method (24). Total glycan samples were applied to a nano-HPLC Chip using an Agilent 1200 series microwell plate autosampler, and interface with an Agilent 6550 Q-TOF MS (Agilent Technologies). The HPLC PGC-Chip (G4240–64010) had a 40 nL enrichment column and a 75 μmol/L × 43 mm separation column packed with 5 μmol/L porous graphitized carbon as stationary phase. The mobile phase was 0.1% formic acid in water (v/v) as solvent A, and 0.1% formic acid in ACN (v/v) as solvent B. The flow rate at 0.3 μL/minute with gradient schedule; 5% B (0−1 minutes); 5%−20% B (1−15 minutes); 20%−70% B (15−16 minutes); 70% B (16−19 minutes), and 70%–5% B (19–20 minutes). Free glycans released by PNGase F were identified by Agilent Masshunter Quanlititive Analysis software in the presence of hexose and *N*-acetylhexosamine. Glycan structures were predicted by online GlycoMod (http://web.expasy.org/glycomod/). Agilent Masshunter Quantitative Analysis software was used to quantify the extracted glycan peaks.

Animal models

Animal work was carried out with the approval of the Princess Margaret Cancer Centre Ethics Review Board in accordance with the regulations of the Canadian Council on Animal Care. In conducting research using animals, the investigators adhered to the laws of the United States and regulations of the Department of Agriculture. Female SCID mice were obtained from the in-house breeding colony at the Princess Margaret Cancer Centre and at 6 to 8 weeks of age. All mice were maintained under specific pathogen-free conditions with a 12-hour light/dark cycle. Food and water were provided *ad libitum*.

LM2–4 cells (1 × 10^6cells in 50 μL) were implanted subcutaneously in female SCID mice (6–8 weeks), obtained in-house from the University Health Network animal colony. Primary tumors were measured every two days and calculated by (width × width × length)/2. After surgical removal of the primary tumors, animals were monitored daily for endpoint, including signs of metastatic load in the lung (labored breathing). Treatment was given daily orally with PBS or 50 mg/kg/day fluvastatin. Necropsy was performed at endpoint where any tissue with evidence of metastatic disease is rapidly excised and fixed in formalin for histopathology.

Quantification and statistical analysis

Statistical analysis was performed using GraphPad Prism 6 and R software. Statistical testing and significance are performed as indicated in the legend of each figure. Histopathologic analyses were independently reviewed by two personnel blinded to group allocation at the time of analysis. Quantification of histochemical analyses was performed using ImageScope software. *In vitro* experiments were not feasible for randomization or blinding due to the nature of the experiments.

Results

EMT sensitizes breast cancer cells to the inhibition of dolichol synthesis

To delineate the mechanism of statin action on mesenchymal-enriched breast cancer cells, fluvastatin was chosen for our studies based on its favorable pharmacokinetic properties and promising anti–breast cancer activities in the preclinical and clinical preoperative settings (23, 25). We used MCF10A breast epithelial cells as our model system, which allowed for the evaluation of EMT in an isogenic panel of cells in the absence of gross genetic instability (26). Ectopic expression of the EMT-inducing transcription factor SNAIL triggered EMT in MCF10A cells, as shown by downregulation of E-cadherin and upregulation of fibronectin (**Fig. 1B**). Treatment with fluvastatin readily induced cell death in SNAIL-overexpressing cells, but not vector control cells, as assessed by quantification of DNA content following cell fixation and propidium iodide staining (**Fig. 1C**). Fluvastatin-induced cell death in SNAIL-overexpressing cells was fully rescued by coadministration with MVA or GGPP, but not FPP (**Fig. 1C**). FPP and GGPP at the concentrations used have previously been shown to enter the cells and rescue protein prenylation (12, 27). This preferential rescue of statin-induced cell death in tumor cells by GGPP has also been reported in several other cancer cell lines (28, 29), together suggesting that disruption of biological processes downstream of GGPP is critical for statin-induced cell death.

GGPP is required for three biological processes: protein prenylation, synthesis of CoQ used in the ETC, and synthesis of dolichol required for protein *N*-glycosylation (**Fig. 1A**; ref. 10). We tested whether inhibiting any of these pathways individually using specific inhibitors (**Fig. 1A**) could phenocopy statin treatment and preferentially kill breast cancer cells with mesenchymal phenotypes. EMT sensitized cells to fluvastatin, as indicated by a lower IC_{50} value in SNAIL-overexpressing cells (**Fig. 1D**). Consistent with our previous finding (11), EMT did not sensitize cells to geranylgeranyltransferase inhibitors, GGTI-298 or GGTI-2133 (**Fig. 1D**), indicating that fluvastatin-induced cell death in this context is independent from

inhibition of protein prenylation. The IC_{50} for 2-thenoyltrifluoroacetone (2-TTFA) and rotenone, both inhibitors of the ETC, were similar in both vector and SNAIL-overexpressing cell lines (**Fig. 1D**), indicating that EMT does not sensitize cells to inhibition of the ETC. Instead, inhibition of LLO assembly downstream of dolichol synthesis by tunicamycin phenocopied fluvastatin treatment, as evidenced by a lower IC_{50} in SNAIL-overexpressing cells (**Fig. 1D**).

These observations were validated in MCF10A cells overexpressing additional inducers of EMT (SLUG, TWIST, ZEB1), as well as two independent breast cancer cell lines, MDA-MB-231 and MCF-7 (Supplementary Fig. S1A–S1D). Ectopic expression of TWIST or ZEB1 induced EMT in MCF10A cells, as indicated by downregulation of E-cadherin and upregulation of fibronectin or vimentin (Supplementary Fig. S1A). SLUG did not induce EMT in the MCF10A cell system, likely arising from a relatively small increase of SLUG expression in our experiment (Supplementary Fig. S1A) and indicating that a critical level of SLUG expression is needed to induce EMT (30). Consistently, the mesenchymal TWIST- and ZEB1-expressing cells became more sensitive to fluvastatin and tunicamycin compared with the vector control (Supplementary Fig. S1B). The IC_{50} for geranylgeranyltransferase inhibitor (GGTI) and ETC inhibitors were unaffected by EMT (Supplementary Fig. S1B). Similarly, immunoblotting for E-cadherin and vimentin indicated that MCF-7 cells were epithelial and MDA-MB-231 cells were mesenchymal (Supplementary Fig. S1C). MDA-MB-231 cells were 50-fold more sensitive to both fluvastatin and tunicamycin than MCF-7 cells, which could not be phenocopied by GGTI-298, GGTI-2133, 2-TTFA, or rotenone (Supplementary Fig. S1D). Together, these data indicate that breast cancer cells with mesenchymal phenotypes are more sensitive to inhibition of dolichol synthesis and function, by either fluvastatin or tunicamycin.

As tunicamycin is an inhibitor of the first enzyme downstream of dolichol, leading to LLO synthesis, and elicits ER stress as a result of blocking *N*-glycosylation (31), we tested whether its effect is an indirect consequence of ER stress. To this end, we treated cells with thapsigargin, a dolichol-independent inducer of ER stress. Treatment with tunicamycin or thapsigargin upregulated ER stress markers ERdj4 and BiP, in both vector and SNAIL-overexpressing cells following 24 hours of treatment (Supplementary Fig. S2A). In contrast, treatment with fluvastatin displayed only a moderate increase the mRNA expression of ERdj4 and BiP in SNAIL-overexpressing MCF10A cells compared with the vector control cells, after up to 72 hours of treatment (Supplementary Fig. S2B). These data indicate that mesenchymal breast cancer cells are sensitized to fluvastatin treatment by inhibition of *N*-glycosylation, and while tunicamycin also inhibits *N*-glycosylation, the effect is accompanied by elevated levels of ER stress leading to greater toxicity in normal cells, which has limited its clinical development as an anticancer therapeutic (32). In contrast, fluvastatin produces a milder effect on protein *N*-glycosylation by dampening the dolichol synthesis pathway further upstream, which alleviates the induction of a strong ER stress response.

Fluvastatin inhibits ER-associated protein *N*-glycosylation and Golgi-associated *N*-glycan remodeling

Dolichol is a group of hydrophobic long-chain isoprenoid molecules that constitutes the lipid portion of LLOs, an essential component for protein Asn(*N*)-glycosylation (10) that occurs on newly synthesized peptides at the consensus sequence NXS/T(X≠P) (**Fig. 2A**). As dolichol is technically difficult to directly quantify and its only known function is in glycosylation, we validated fluvastatin inhibition of dolichol synthesis by evaluating whether fluvastatin treatment could reduce protein *N*-glycosylation. To this end, we used SLC3A2 as a molecular biomarker of protein glycosylation. SLC3A2 is a single-pass transmembrane glycoprotein with four *N*-glycosylation sites, all modified at the ER and remodeled at the Golgi with complex-type *N*-glycan structures (33). We expressed SLC3A2 in a doxycycline-inducible manner in HeLa cells, where endogenous SLC3A2 has been knocked out. With fluvastatin treatment, doxycycline-induced FLAG-SLC3A2 displayed lower molecular weight immunoblot bands, intermediate in size compared with that of *N*-glycopeptidase-treated samples, indicating reduced occupancy of *N*-glycan sites consistent with suppression of dolichol and, in turn, LLO and *N*-glycosylation (**Fig. 2B**). To examine site occupancy more directly, three peptides containing *N*-glycosylation sites at N365, N381, and N424 in FLAG-SLC3A2 were detected and quantified by LC-MS/MS (Supplementary Table S1). With fluvastatin treatment, an increase in the unoccupied fraction of peptides containing Asn365 and Asn381 was observed (**Fig. 2C**). Interestingly, site occupancy of Asn424 remained unaffected by fluvastatin treatment (**Fig. 2C**), indicating that *N*-glycosylation sites on the same protein can differ in sensitivity to reduced dolichol levels. These results and immunoblotting for additional *N*-glycosylated receptors (Supplementary Fig. S3) are consistent with a partial reduction in *N*-glycosylation in response to fluvastatin treatment.

Complex type *N*-glycans are a major subset of post-Golgi structures on mature cell surface glycoproteins. These *N*-glycans can be further subdivided by *N*-acetylactosamine branching and fucose (F, Fuc) at the core region and on the peripheral branches (**Fig. 2D**, highlighted in box). Analysis of SLC3A2 glycopeptides revealed that, in addition to partial inhibition of glycan transfer from LLO to the protein substrates by oligosaccharyltransferase (OST), fluvastatin treatment altered the Golgi dependent profile of residual *N*-glycans measured in a site-specific manner. Notably, a significant reduction in branched complex *N*-glycans was observed at N381, N424, and N365 sites (**Fig. 2E–G**; Supplementary Table S1). Immunoblotting for three additional membrane proteins (EGFR, GP130, and SLC3A2) in vector and SNAIL-overexpressing MCF10A cells revealed that these proteins became under-glycosylated after 48 to 72 hours of fluvastatin treatment in both cell lines to a similar extent (Supplementary Fig. S3A). Treatment with thapsigargin for up to 72 hours did not result in under-glycosylation of EGFR, GP130, or SLC3A2 in either vector or SNAIL-overexpressing cells, although a slight reduction in total glycoprotein levels were observed (Supplementary Fig. S3B). In contrast, these receptors were markedly under-glycosylated with 24 hours of tunicamycin treatment. As cancer cell metastasis requires increased expression of tetra-antennary complex type *N*-glycans (14–18), we examined whether the transition to EMT was accompanied by increased expression of these glycan structures. To this end, we profiled *N*-glycans released from membranes of control and SNAIL-overexpressing MCF10A cells treated with and without fluvastatin (Supplementary Table S2). The MCF10A glycome consists of 32% high mannose type *N*-glycans and 59% complex type *N*-glycans. The latter can be further subdivided based on branching and fucosylation (F, Fuc) status at the core region and the antennae (**Fig. 3A**). In MCF10A cells, complex type *N*-glycans were commonly expressed in the unfucosylated and singly fucosylated (core) forms, with a small amount of doubly fucosylated (core and antennae) structures (**Fig. 3A**). With induction of EMT, the expression of 12 *N*-glycans structures were significantly upregulated, all of which belonged to the complex type subgroup; 15 structures were downregulated, including all 9 of the doubly fucosylated complex structures detected (**Fig. 3B**; Supplementary Table S2). We then examined the effect of fluvastatin treatment on *N*-glycan profiles and found that 6 of the 12 complex type *N*-glycans that were upregulated following induction of EMT were specifically inhibited by fluvastatin

Published OnlineFirst February 18, 2021; DOI: 10.1158/0008-5472.CAN-20-2642

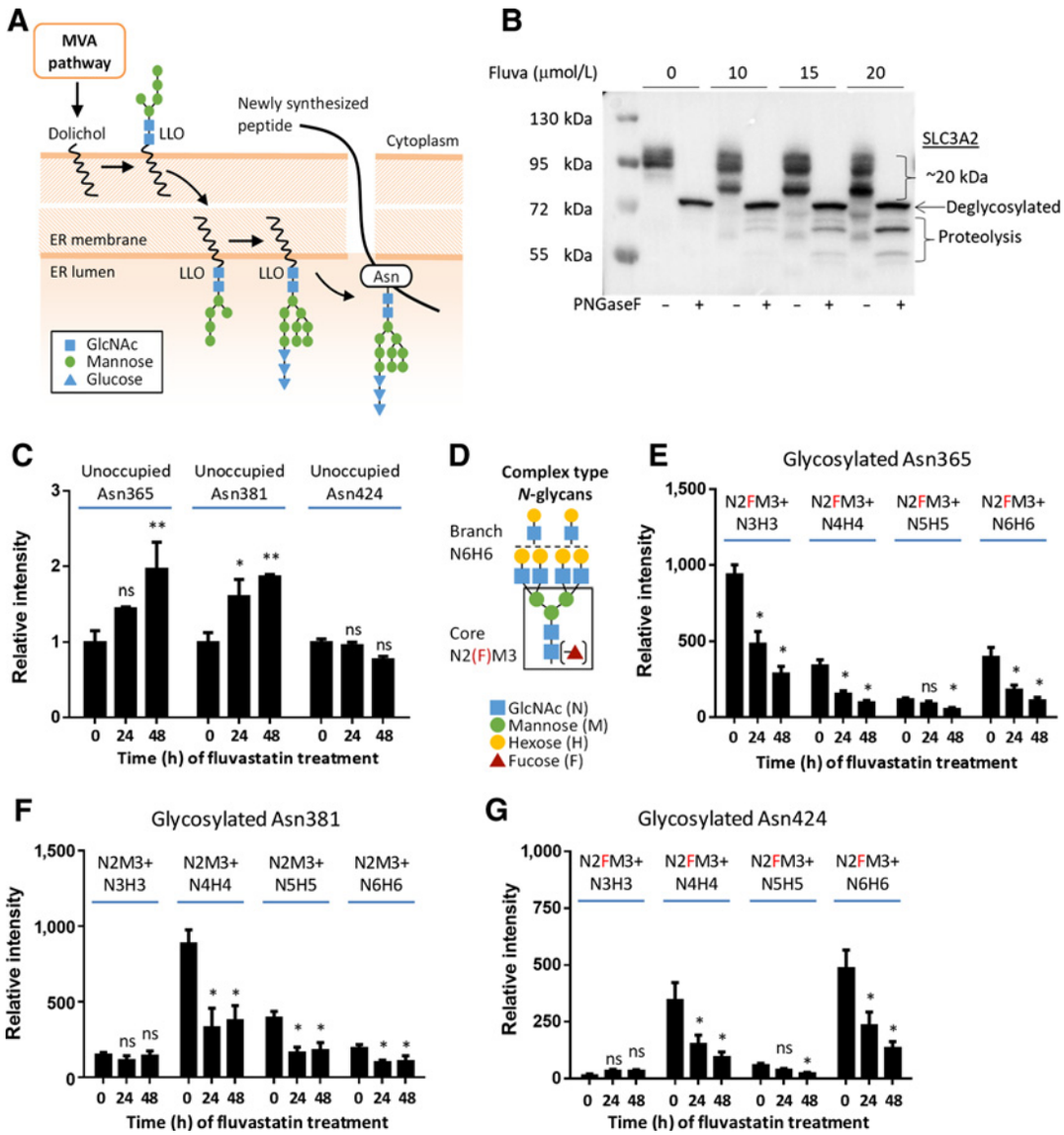

Figure 2.

Fluvastatin treatment blocks dolichol-dependent protein *N*-glycosylation with complex type *N*-glycans. **A,** A simplified schematic of the dolichol-dependent protein *N*-glycosylation process. GlcNAc, *N*-acetylglucosamine; Asn, asparagine. **B,** In HeLa cells with Dox-inducible FLAG-SLC3A2 expression, immunoblot for FLAG indicates that fluvastatin treatment led to partial deglycosylation of SLC3A2 as indicated by the appearance of lower molecular weight bands. Complete deglycosylation with PNGaseF treatment was used as a control. **C,** Relative levels of unoccupied Asn residues at glycosylation sites NXS/T(X≠P) in SLC3A2 were quantified by FLAG-IP, followed by LC/MS-MS. Fluvastatin treatment for up to 48 hours increased the levels of unoccupied Asn at residues 365 and 381, but not 424. Three biological replicates were analyzed with two technical replicates each. ns, not significant; *, $P < 0.05$; **, $P < 0.01$ (two-way ANOVA with a Dunnett posttest, comparing each treatment column vs. control column). **D,** Schematic representation of complex type *N*-glycans that decorate SLC3A2 on Asn residues 365, 381, and 424 that are represented in the following panels. **E–G,** Fluvastatin treatment for up to 48 hours decreases the levels of branched complex type *N*-glycans, triantennary (N3H3) and tetra-antennary (N4H4), and branch elongation (N5H5 and N6H6) at the indicated site in SLC3A2. Bars, mean + SD, $n = 3$. ns, not significant; *, $P < 0.05$ (two-way ANOVA with a Dunnett posttest, comparing each treatment column vs. control column).

treatment in SNAIL-overexpressing cells, but not in control cells (**Fig. 3C**, black arrowheads). Of these, the singly fucosylated triantennary (N2FM3+N3H3) and singly fucosylated tetra-antennary (N2FM3+N4H4) structures, each representing approximately 10% of the total surface glycome, were both upregulated in SNAIL-overexpressing cells, and significantly reduced in response to fluvastatin treatment (**Fig. 3D** and **E**).

Our results suggest that the elevated sensitivity of mesenchymal breast cancer cells to fluvastatin is due to the dual effect of fluvastatin on protein *N*-glycosylation: (i) decreasing the level of *N*-glycosylation at the ER by inhibiting dolichol synthesis; and (ii) decreasing the complex branching of *N*-glycans that occurs at the Golgi. Of note, the second effect occurs on those *N*-glycans that are transferred to proteins in the presence of fluvastatin, the

Published OnlineFirst February 18, 2021; DOI: 10.1158/0008-5472.CAN-20-2642

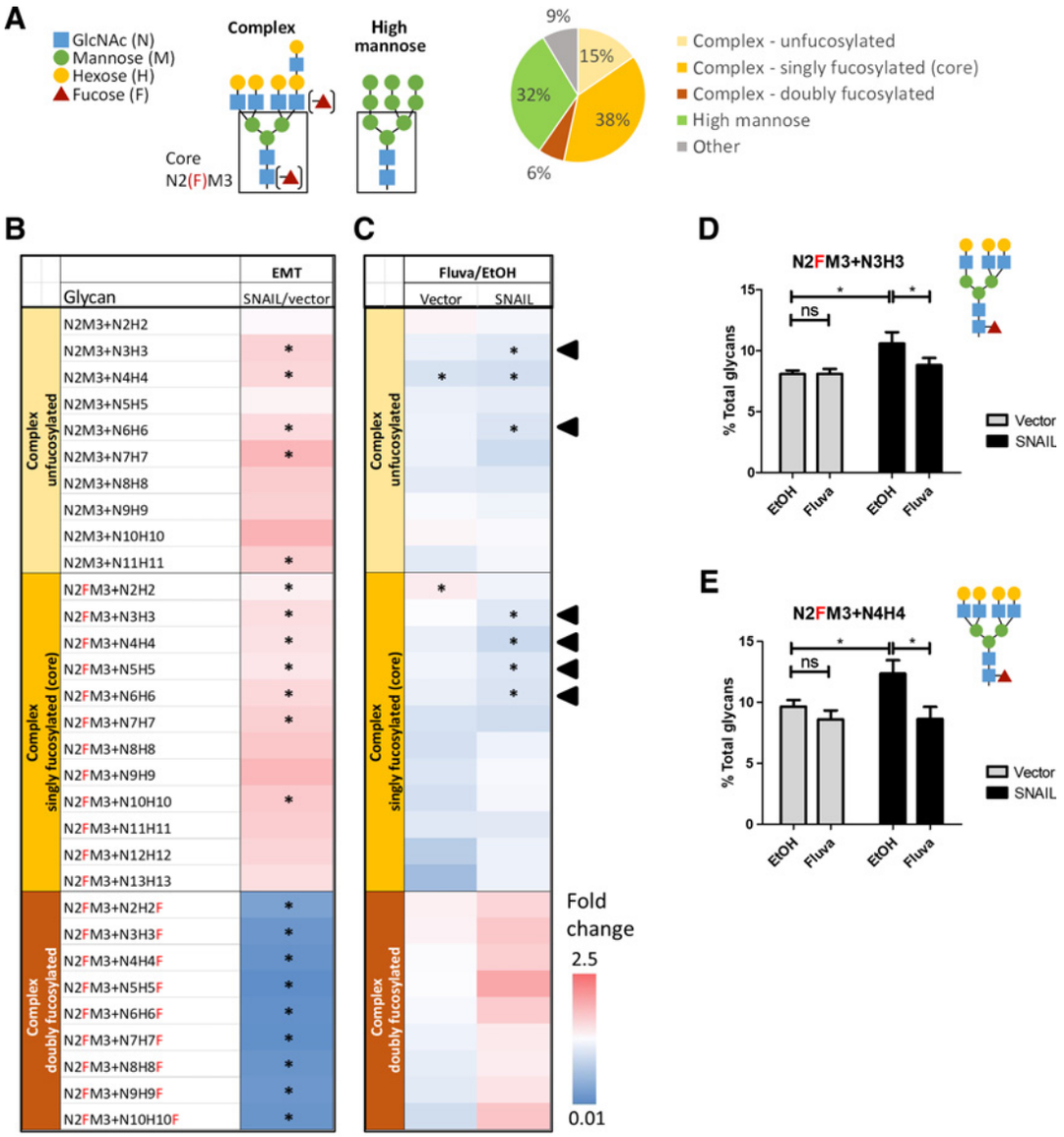

Figure 3.

Fluvastatin treatment decreases complex branched *N*-glycans associated with EMT. **A,** Schematic representation of high mannose type and complex type *N*-glycans, the two major classes of *N*-glycans (top), and distribution of major classes of *N*-glycans in the total cell surface glycome in MCF10A cells quantified by LC/MS-MS (bottom). **B,** Heatmap of the expression of complex *N*-glycans following SNAIL-induced EMT. Data presented are the mean of three biological replicates with one to two technical replicates each. *, $P < 0.0301$ (unpaired, two-tailed *t* test with Benjamini–Hochberg FDR correction). **C,** Heatmap of the expression of complex *N*-glycans following treatment with 20 μmol/L fluvastatin in vector cells (left column) and SNAIL-overexpressing cells (right column). Black arrowheads, glycan species that are significantly upregulated in EMT (**B**) and downregulated by fluvastatin treatment in SNAIL-overexpressing cells (**C,** right column), but not affected by fluvastatin treatment in control cells (**C,** left column). Data presented are the mean of three biological replicates with one to two technical replicates each. EtOH, ethanol (treatment control). *, $P < 0.0108$ (unpaired, two-tailed *t* test with Benjamini–Hochberg FDR correction). **D** and **E,** LC/MS-MS quantification of the fucosylated triantennary (N3H3; **D**) and tetra-antennary (N4H4; **E**) *N*-glycan structures indicating that these *N*-glycans are upregulated in EMT, which is inhibited by 20 μmol/L fluvastatin treatment for 48 hours. Complete data can be found in Supplementary Table S2. Bars, mean + SD, $n = 3$. ns, not significant; *, $P < 0.05$ (one-way ANOVA with a Bonferroni posttest, comparing selected pairs of columns).

mechanism of which remains to be explored. To test this model, we evaluated whether fluvastatin at concentrations that partially inhibit both NXS/T(X≠P) site occupancy and Golgi *N*-glycan branching, may display synergy with loss of the branching enzymes MGAT1 or MGAT5. MGAT1 knockout blocks all branching, whereas MGAT5 knockout eliminates the last branch to be added (Supplementary Fig. S4A–S4C). Consistent with this hypothesis, the IC_{50} for fluvastatin treatment was inversely proportional to levels of complex-type branched *N*-glycans (MDA-MB-231 wild-type > MGAT5 deficient > MGAT1 deficient cells; Supplementary Fig. S4D). The order of interaction between fluvastatin treatment and these Golgi enzymes is consistent with the known effects of

Published OnlineFirst February 18, 2021; DOI: 10.1158/0008-5472.CAN-20-2642

mutating these enzymes in cancer models (19, 20, 34). Taken together, our data suggest that fluvastatin treatment impairs the EMT-driven expression of complex type branched *N*-glycans on multiple cell surface glycoproteins associated with EMT and metastasis (16–18).

Postsurgical adjuvant fluvastatin treatment delays metastatic outgrowth and prolongs survival

As the transition to a more mesenchymal state is associated with cancer metastasis (35), we evaluated the efficacy of fluvastatin treatment against a postsurgical metastatic breast cancer model *in vivo*. We

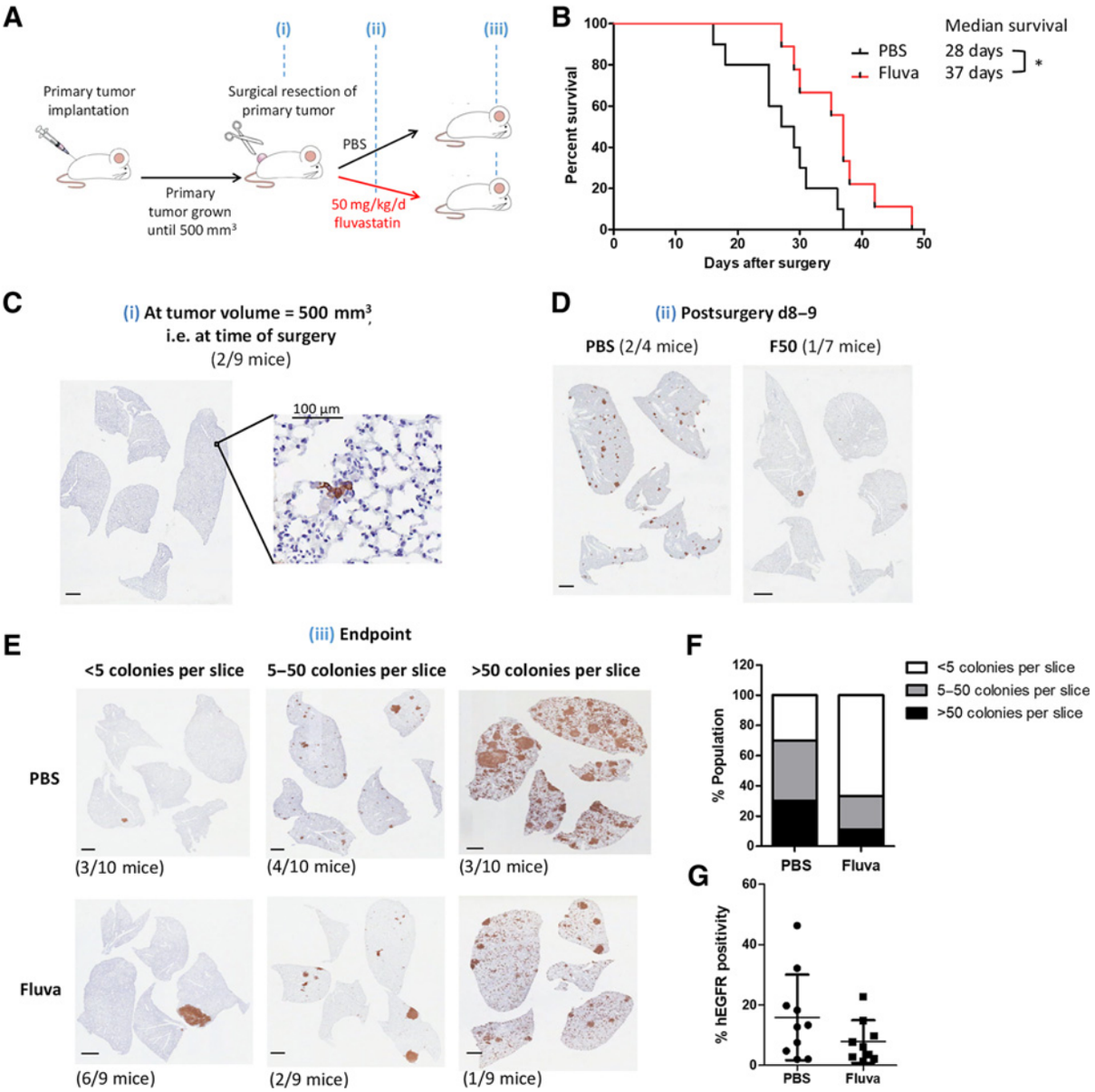

Figure 4.

Postsurgical adjuvant fluvastatin treatment delays metastasis and prolongs survival. **A,** Schematic of the mouse model and the time points where mice were sacrificed. **B,** Fluvastatin treatment at 50 mg/kg/day orally significantly prolonged survival of mice with postsurgical metastatic breast cancer. *, $P < 0.05$ (log-rank test, $n = 12$). **C–E,** At the indicated time point, mice were sacrificed and lungs were resected for FFPE. Two sequential slices were obtained every 200 µm for three depths containing all five lobes and stained for H&E or hEGFR. Metastatic colonies were identified by hEGFR staining and confirmed by H&E. At the time of surgery, mouse lungs were clear of metastatic colonies or had very small lesions (**C**). At 8 to 9 days postsurgery, mice receiving fluvastatin treatment had less metastatic tumor load than mice receiving PBS control (**D**). F50, 50 mg/kg/day fluvastatin treatment group. At endpoint, fluvastatin treatment decreased the proportion of mice with heavy (>50 colonies/slice) or intermediate metastatic burden (5 to 50 colonies/slice). The proportion of mice with light metastatic burden (<5 colonies/slice) were increased (**E**). Each lung slice was independently reviewed by two personnel. Representative images are shown. Scale bars, 1 mm except in **C** inset where it is 100 µm as indicated. **F** and **G,** Quantification of metastatic load by colony count (**F**) or by hEGFR positivity (**G**) both showed lowered metastatic load in fluvastatin-treated mice.

used the LM2–4 model of postsurgical advanced metastatic breast cancer, derived from the MDA-MB-231 cell line, which spontaneously metastasizes to the mouse lung (21). After subcutaneous implantation, we allowed LM2–4 xenografts to reach approximately 500 mm^3, then excised the primary tumors to mimic first-line surgical treatment (**Fig. 4A**; Supplementary Fig. S5A; ref. 21). After surgery, mice were randomly assigned to receive PBS (vehicle control) or 50 mg/kg fluvastatin orally, daily (**Fig. 4A**). Adjuvant fluvastatin treatment significantly prolonged overall survival by >30% in this mouse model (**Fig. 4B**).

To evaluate the potential antimetastatic activity of fluvastatin, we analyzed lung samples at three time points during the course of the experiment: (i) at time of surgery; (ii) at 8 to 9 days postsurgery; and (iii) at endpoint (**Fig. 4A**). Metastases to the mouse lung were identified by lesions that stained positive for human EGFR (hEGFR) and confirmed by H&E (Supplementary Fig. S5B). At time of surgery, most mice (7/9) did not have any observable metastases, and 2 of 9 mice had very small lung lesions (**Fig. 4C**). At 8 to 9 days postsurgery, adjuvant fluvastatin treatment effectively inhibited metastatic outgrowth from disseminated breast cancer cells (**Fig. 4D**). Finally, at endpoint, fluvastatin treatment decreased the proportion of mice with heavy (>50 colonies/slice) or medium (5–50 colonies/slice) metastatic burden, while increasing the proportion of mice with light metastatic burden (<5 colonies/slice; **Fig. 4E–G**). Consistently, autopsy at endpoint indicated that the majority of PBS-treated mice reached endpoint due to lung metastases, whereas fluvastatin-treated mice largely reached endpoint from primary tumor regrowth (Supplementary Fig. S5C). We have thus demonstrated, using an *in vivo* postsurgical metastatic breast cancer model that closely follows the course of human disease, that adjuvant fluvastatin use can delay the development of metastases and prolong overall survival.

Discussion

Metastatic recurrence is the main cause of breast cancer deaths (1). Since statins are already clinically approved, inexpensive, and have excellent safety profiles that permit their long-term use, these drugs are ideal candidates for repurposing as metastasis prevention agents. Identifying the mechanism of the antimetastatic breast cancer activity of statins, also provides an opportunity to identify novel actionable biomarkers that distinguish patients who will benefit from statin treatment. Here, we show that sensitivity to fluvastatin in the context of breast cancer cell EMT is mediated by inhibition of protein *N*-glycosylation, providing a mechanistic explanation for previous observations showing statin treatment can block *N*-glycosylation of specific membrane glycoproteins such as P-gp (36), IGFR (37), EpoR (38), and FLT3 (39). Surprisingly, we also show that fluvastatin exposure impaired Golgi pathway biosynthesis of complex type tri- and tetra-antennary *N*-glycans associated with breast cancer EMT and metastasis (16–18, 40). The cooperative effects of NXS/T(X≠P) site number and Golgi-associated *N*-glycan branching is important for cell surface retention and signaling by growth factor receptors (EGF, TGFβ, FGF), and thereby EMT (16). Indeed, we observed cooperative inhibition of fluvastatin and loss of *N*-glycan branching enzymes MGAT1 or MGAT5 in MDA-MB-231 breast cancer cells. Adjuvant use of fluvastatin delayed breast cancer metastasis and prolonged survival by >30% in a postsurgical model of breast cancer metastasis, supporting the immediate evaluation of fluvastatin in the adjuvant breast cancer space, as well as further development of glycosylation inhibitors to prevent metastatic recurrence in breast cancer (41).

Altered protein *N*-glycosylation, notably the upregulation of tri- and tetra-antennary complex type glycans, is pivotal to EMT (18, 42, 43) and is a potent modulator of metastatic potential (14–18, 40). High levels of tri- and tetra-antennary complex *N*-glycans are associated with disease progression and poor prognosis in breast and colon cancer patients (44, 45). Here, we demonstrate that EMT-associated upregulation of complex *N*-glycans can be targeted by inhibiting the MVA pathway using fluvastatin. The assembly of each *N*-glycan requires 8 dolichol molecules (46). However, dolichol cannot be efficiently recycled (47) and accumulates with aging (48), indicating that cells must continuously synthesize dolichol. Our results show that fluvastatin treatment can exploit this metabolic vulnerability in metastatic breast cancer cells, reducing protein *N*-glycosylation on glycoproteins critical to metastasis.

Strong epidemiologic evidence has shown that the risk of postsurgical breast cancer recurrence is reduced by 30% to 60% in patients who are taking statins (2–5). Here, we used a mouse model of postsurgical metastatic breast cancer that closely mimics first-line treatment and disease progression (21), to test the efficacy of fluvastatin when used in the adjuvant setting to prevent metastasis, where long-term use of this safe and inexpensive drug could have considerable clinical benefit. Adjuvant fluvastatin treatment effectively delayed metastasis and prolonged survival by >30% at a daily dose of 50 mg/kg in the mouse, equivalent to a well-tolerated daily dose of 4 mg/kg in human patients (49). Our results support the immediate clinical evaluation of fluvastatin at this well-tolerated dose in the adjuvant setting in patients with breast cancer patients. Moreover, this work reinforces that targeting aberrant tumor metabolism is a feasible strategy for the development of novel and effective anticancer agents.

Authors' Disclosures

No disclosures were reported.

Authors' Contributions

R. Yu: Investigation, writing–original draft. **J. Longo:** Investigation, writing–review and editing. **J.E. van Leeuwen:** Investigation, writing–review and editing. **C. Zhang:** Investigation, writing–review and editing. **E. Branchard:** Investigation, writing–review and editing. **M. Elbaz:** Investigation, writing–review and editing. **D.W. Cescon:** Investigation, writing–review and editing. **R.R. Drake:** Investigation, writing–review and editing. **J.W. Dennis:** Investigation, writing–review and editing. **L.Z. Penn:** Supervision, investigation, writing–review and editing.

Acknowledgments

The authors thank Drs. Robert Kerbel, Roberta Maestro, and Senthil Muthuswamy for providing reagents, Dr. Meegan Larsen for pathology support, Dr. Thomas Kislinger for helpful discussion, Aaliya Tamachi for technical assistance, and all members of the Penn lab for helpful discussion and critical review of the manuscript. This work was supported by funding from the Canada Research Chairs Program (L.Z. Penn), Canadian Institutes of Health Research (L.Z. Penn), Terry Fox Research Institute (L.Z. Penn and D.W. Cescon), CIHR Canada Graduate Scholarship (R. Yu and J. Longo), and Ontario Student Opportunity Trust Fund (J.E. van Leeuwen). This work was also supported by the Office of the Assistant Secretary of Defense for Health Affairs through the Breast Cancer Research Program under Award No. W81XWH-16-1-0068. Opinions, interpretations, conclusions, and recommendations are those of the author and are not necessarily endorsed by the Department of Defense.

The costs of publication of this article were defrayed in part by the payment of page charges. This article must therefore be hereby marked *advertisement* in accordance with 18 U.S.C. Section 1734 solely to indicate this fact.

Received August 3, 2020; revised December 21, 2020; accepted February 15, 2021; published first February 18, 2021.

References

1. Weigelt B, Peterse JL, van't Veer LJ. Breast cancer metastasis: markers and models. Nat Rev Cancer 2005;5:591–602.
2. Ahern TP, Pedersen L, Tarp M, Cronin-Fenton DP, Garne JP, Silliman RA, et al. Statin prescriptions and breast cancer recurrence risk: a Danish nationwide prospective cohort study. J Natl Cancer Inst 2011;103:1461–8.
3. Boudreau DM, Yu O, Chubak J, Wirtz HS, Bowles EJ, Fujii M, et al. Comparative safety of cardiovascular medication use and breast cancer outcomes among women with early stage breast cancer. Breast Cancer Res Treat 2014;144:405–16.
4. Chae YK, Valsecchi ME, Kim J, Bianchi AL, Khemasuwan D, Desai A, et al. Reduced risk of breast cancer recurrence in patients using ACE inhibitors, ARBs, and/or statins. Cancer Invest 2011;29:585–93.
5. Kwan ML, Habel LA, Flick ED, Quesenberry CP, Caan B. Post-diagnosis statin use and breast cancer recurrence in a prospective cohort study of early stage breast cancer survivors. Breast Cancer Res Treat 2008;109:573–9.
6. Horiguchi A, Sumitomo M, Asakuma J, Asano T, Asano T, Hayakawa M. 3-hydroxy-3-methylglutaryl-coenzyme a reductase inhibitor, fluvastatin, as a novel agent for prophylaxis of renal cancer metastasis. Clin Cancer Res 2004; 10:8648–55.
7. Paragh G, Foris G, Paragh G Jr, Seres I, Karanyi Z, Fulop P, et al. Different anticancer effects of fluvastatin on primary hepatocellular tumors and metastases in rats. Cancer Lett 2005;222:17–22.
8. Yang Z, Su Z, DeWitt JP, Xie L, Chen Y, Li X, et al. Fluvastatin prevents lung adenocarcinoma bone metastasis by triggering autophagy. EBioMedicine 2017; 19:49–59.
9. Beckwitt CH, Brufsky A, Oltvai ZN, Wells A. Statin drugs to reduce breast cancer recurrence and mortality. Breast Cancer Res 2018;20:144.
10. Mullen PJ, Yu R, Longo J, Archer MC, Penn LZ. The interplay between cell signalling and the mevalonate pathway in cancer. Nat Rev Cancer 2016;16: 718–31.
11. Yu R, Longo J, van Leeuwen JE, Mullen PJ, Ba-Alawi W, Haibe-Kains B, et al. Statin-induced cancer cell death can be mechanistically uncoupled from prenylation of RAS family proteins. Cancer Res 2018;78:1347–57.
12. Wong WW, Clendening JW, Martirosyan A, Boutros PC, Bros C, Khosravi F, et al. Determinants of sensitivity to lovastatin-induced apoptosis in multiple myeloma. Mol Cancer Ther 2007;6:1886–97.
13. Giancotti FG. Mechanisms governing metastatic dormancy and reactivation. Cell 2013;155:750–64.
14. Scott DA, Casadonte R, Cardinali B, Spruill L, Mehta AS, Carli F, et al. Increases in tumor N-glycan polylactosamines associated with advanced HER2-positive and triple-negative breast cancer tissues. Proteomics Clin Appl 2019;13: e1800014.
15. Herrera H, Dilday T, Uber A, Scott D, Zambrano JN, Wang M, et al. Core-fucosylated tetra-antennary N-glycan containing a single N-acetyllactosamine branch is associated with poor survival outcome in breast cancer. Int J Mol Sci 2019;20:2528.
16. Lau KS, Partridge EA, Grigorian A, Silvescu CI, Reinhold VN, Demetriou M, et al. Complex N-glycan number and degree of branching cooperate to regulate cell proliferation and differentiation. Cell 2007;129:123–34.
17. Cheung P, Dennis JW. Mgat5 and Pten interact to regulate cell growth and polarity. Glycobiology 2007;17:767–73.
18. Partridge EA, Le Roy C, Di Guglielmo GM, Pawling J, Cheung P, Granovsky M, et al. Regulation of cytokine receptors by Golgi N-glycan processing and endocytosis. Science 2004;306:120–4.
19. Granovsky M, Fata J, Pawling J, Muller WJ, Khokha R, Dennis JW. Suppression of tumor growth and metastasis in Mgat5-deficient mice. Nat Med 2000;6:306–12.
20. Beheshti Zavareh R, Sukhai MA, Hurren R, Gronda M, Wang X, Simpson CD, et al. Suppression of cancer progression by MGAT1 shRNA knockdown. PLoS One 2012;7:e43721.
21. Guerin E, Man S, Xu P, Kerbel RS. A model of postsurgical advanced metastatic breast cancer more accurately replicates the clinical efficacy of antiangiogenic drugs. Cancer Res 2013;73:2743–8.
22. Pandyra AA, Mullen PJ, Goard CA, Ericson E, Sharma P, Kalkat M, et al. Genome-wide RNAi analysis reveals that simultaneous inhibition of specific mevalonate pathway genes potentiates tumor cell death. Oncotarget 2015;6: 26909–21.
23. Goard CA, Chan-Seng-Yue M, Mullen PJ, Quiroga AD, Wasylishen AR, Clendening JW, et al. Identifying molecular features that distinguish fluvastatin-sensitive breast tumor cells. Breast Cancer Res Treat 2014;143:301–12.
24. Abdel Rahman AM, Ryczko M, Nakano M, Pawling J, Rodrigues T, Johswich A, et al. Golgi N-glycan branching N-acetylglucosaminyltransferases I, V and VI promote nutrient uptake and metabolism. Glycobiology 2015;25: 225–40.
25. Garwood ER, Kumar AS, Baehner FL, Moore DH, Au A, Hylton N, et al. Fluvastatin reduces proliferation and increases apoptosis in women with high grade breast cancer. Breast Cancer Res Treat 2010;119:137–44.
26. Soule HD, Maloney TM, Wolman SR, Peterson WD Jr., Brenz R, McGrath CM, et al. Isolation and characterization of a spontaneously immortalized human breast epithelial cell line, MCF-10. Cancer Res 1990;50:6075–86.
27. Finlay GA, Malhowski AJ, Liu Y, Fanburg BL, Kwiatkowski DJ, Toksoz D. Selective inhibition of growth of tuberous sclerosis complex 2 null cells by atorvastatin is associated with impaired Rheb and Rho GTPase function and reduced mTOR/S6 kinase activity. Cancer Res 2007;67:9878–86.
28. Taylor-Harding B, Orsulic S, Karlan BY, Li AJ. Fluvastatin and cisplatin demonstrate synergistic cytotoxicity in epithelial ovarian cancer cells. Gynecol Oncol 2010;119:549–56.
29. Xia Z, Tan MM, Wong WW, Dimitroulakos J, Minden MD, Penn LZ. Blocking protein geranylgeranylation is essential for lovastatin-induced apoptosis of human acute myeloid leukemia cells. Leukemia 2001;15: 1398–407.
30. Vuoriluoto K, Haugen H, Kiviluoto S, Mpindi JP, Nevo J, Gjerdrum C, et al. Vimentin regulates EMT induction by Slug and oncogenic H-Ras and migration by governing Axl expression in breast cancer. Oncogene 2011; 30:1436–48.
31. Shang J, Gao N, Kaufman RJ, Ron D, Harding HP, Lehrman MA. Translation attenuation by PERK balances ER glycoprotein synthesis with lipid-linked oligosaccharide flux. J Cell Biol 2007;176:605–16.
32. Morin MJ, Bernacki RJ. Biochemical effects and therapeutic potential of tunicamycin in murine L1210 leukemia. Cancer Res 1983;43:1669–74.
33. Yanagida O, Kanai Y, Chairoungdua A, Kim DK, Segawa H, Nii T, et al. Human L-type amino acid transporter 1 (LAT1): characterization of function and expression in tumor cell lines. Biochim Biophys Acta 2001;1514:291–302.
34. Mendelsohn R, Cheung P, Berger L, Partridge E, Lau K, Datti A, et al. Complex N-glycan and metabolic control in tumor cells. Cancer Res 2007;67:9771–80.
35. Thiery JP. Epithelial-mesenchymal transitions in tumour progression. Nat Rev Cancer 2002;2:442–54.
36. Atil B, Berger-Sieczkowski E, Bardy J, Werner M, Hohenegger M. *In vitro* and *in vivo* downregulation of the ATP binding cassette transporter B1 by the HMG-CoA reductase inhibitor simvastatin. Naunyn Schmiedebergs Arch Pharmacol 2016;389:17–32.
37. Dricu A, Wang M, Hjertman M, Malec M, Blegen H, Wejde J, et al. Mevalonate-regulated mechanisms in cell growth control: role of dolichyl phosphate in expression of the insulin-like growth factor-1 receptor (IGF-1R) in comparison to Ras prenylation and expression of c-myc. Glycobiology 1997;7:625–33.
38. Hamadmad SN, Hohl RJ. Lovastatin suppresses erythropoietin receptor surface expression through dual inhibition of glycosylation and geranylgeranylation. Biochem Pharmacol 2007;74:590–600.
39. Williams AB, Li L, Nguyen B, Brown P, Levis M, Small D. Fluvastatin inhibits FLT3 glycosylation in human and murine cells and prolongs survival of mice with FLT3/ITD leukemia. Blood 2012;120:3069–79.
40. Scott DA, Drake RR. Glycosylation and its implications in breast cancer. Expert Rev Proteomics 2019;16:665–80.
41. Goss PE, Baker MA, Carver JP, Dennis JW. Inhibitors of carbohydrate processing: A new class of anticancer agents. Clin Cancer Res 1995;1: 935–44.
42. Terao M, Ishikawa A, Nakahara S, Kimura A, Kato A, Moriwaki K, et al. Enhanced epithelial-mesenchymal transition-like phenotype in N-acetylglucosaminyltransferase V transgenic mouse skin promotes wound healing. J Biol Chem 2011;286:28303–11.
43. Miyoshi E, Nishikawa A, Ihara Y, Saito H, Uozumi N, Hayashi N, et al. Transforming growth factor beta up-regulates expression of the N-acetylglucosaminyltransferase V gene in mouse melanoma cells. J Biol Chem 1995;270:6216–20.
44. Fernandes B, Sagman U, Auger M, Demetrio M, Dennis JW. Beta 1–6 branched oligosaccharides as a marker of tumor progression in human breast and colon neoplasia. Cancer Res 1991;51:718–23.

45. Drake RR, Powers TW, Jones EE, Bruner E, Mehta AS, Angel PM. MALDI mass spectrometry imaging of N-linked glycans in cancer tissues. Adv Cancer Res 2017;134:85–116.
46. Varki A, Cummings RD, Esko JD, Freeze HH, Stanley P, Bertozzi CR, et al. Essentials of glycobiology. 2nd ed. Cold Spring Harbor, NY: Cold Spring Harbor Laboratory Press; 2009.
47. Breitling J, Aebi M. N-linked protein glycosylation in the endoplasmic reticulum. Cold Spring Harb Perspect Biol 2013;5:a013359.
48. Parentini I, Cavallini G, Donati A, Gori Z, Bergamini E. Accumulation of dolichol in older tissues satisfies the proposed criteria to be qualified a biomarker of aging. J Gerontol A Biol Sci Med Sci 2005; 60:39–43.
49. Sabia H, Prasad P, Smith HT, Stoltz RR, Rothenberg P. Safety, tolerability, and pharmacokinetics of an extended-release formulation of fluvastatin administered once daily to patients with primary hypercholesterolemia. J Cardiovasc Pharmacol 2001;37:502–11.

Cancer Research
The Journal of Cancer Research (1916–1930) | The American Journal of Cancer (1931–1940)

AACR American Association for Cancer Research

Mevalonate Pathway Inhibition Slows Breast Cancer Metastasis via Reduced *N*-glycosylation Abundance and Branching

Rosemary Yu, Joseph Longo, Jenna E. van Leeuwen, et al.

Cancer Res 2021;81:2625-2635. Published OnlineFirst February 18, 2021.

Computational pharmacogenomic screen identifies drugs that phenocopy dipyridamole and potentiate anti-breast cancer activity of statins

Jenna van Leeuwen[1,2], Wail Ba-Alawi[1,2], Emily Branchard[2], Joseph Longo[1,2], Jennifer Silvester[3], David W. Cescon[2,3,4], Benjamin Haibe-Kains[1,2,5,6,§], Linda Z. Penn[1,2,§], Deena M.A. Gendoo[7,§]

[1]Department of Medical Biophysics, University of Toronto, 101 College Street, Toronto, ON, Canada, M5G 1L7
[2]Princess Margaret Cancer Centre, University Health Network, 101 College Street, Toronto, ON, Canada, M5G 1L7
[3]The Campbell Family Institute for Breast Cancer Research (CFIBCR), 620 University Avenue, Toronto, ON, Canada, M5G 2C1
[4]Division of Medical Oncology and Hematology, Department of Medicine, University of Toronto, 27 King's College Circle, Toronto, ON, Canada, M5S 1A1
[5]Department of Computer Science, University of Toronto, 10 King's College Road, Toronto, ON, Canada, M5S 3G4
[6]Ontario Institute of Cancer Research, 661 University Avenue, Suite 510, Toronto, ON, Canada, M5G 0A3
[7]Centre for Computational Biology, Institute of Cancer and Genomic Sciences, University of Birmingham, Birmingham, Birmingham B15 2TT, United Kingdom

[§] Co-corresponding authors

Address for correspondence: Regarding computational aspects, Dr. Haibe-Kains <Benjamin.Haibe-Kains@uhnresearch.ca> and Dr. Gendoo <d.gendoo@bham.ac.uk>; regarding statin aspects, Dr. Penn <Linda.Penn@uhnresearch.ca>.

Abstract

Statins are a family of FDA-approved cholesterol-lowering drugs that inhibit the rate-limiting enzyme of the metabolic mevalonate pathway, which have been shown to have anti-cancer activity. As therapeutic efficacy increases when drugs are used in combination, we sought to identify agents, like dipyridamole, that potentiate statin-induced tumor cell death. As an antiplatelet agent dipyridamole will not be suitable for all cancer patients. Thus, we developed an integrative pharmacogenomics pipeline to identify agents that were similar to dipyridamole at the level of drug structure, *in vitro* sensitivity and molecular perturbation. To enrich for compounds expected to target the mevalonate pathway, we took a pathway-centric approach towards computational selection, which we called mevalonate drug network fusion (MVA-DNF). We validated two of the top ranked compounds, nelfinavir and honokiol and demonstrated that, like dipyridamole, they synergize with fluvastatin to potentiate tumour cell death by blocking the restorative feedback loop. This is achieved by inhibiting activation of the key transcription factor that induces mevalonate pathway gene transcription, sterol regulatory element-binding protein 2 (SREBP2). Mechanistically, the synergistic response of fluvastatin-nelfinavir and fluvastatin-honokiol was associated with similar transcriptomic and proteomic pathways, indicating a similar mechanism of action between nelfinavir and honokiol when combined with fluvastatin. Further analysis identified the canonical epithelial-mesenchymal transition (EMT) gene, E-cadherin as a biomarker of these synergistic responses across a large panel of breast cancer cell lines. Thus, our computational pharmacogenomic approach can identify novel compounds that phenocopy a compound of interest in a pathway-specific manner.

Key words: Drug combinations; cancer therapy; mevalonate pathway; drug similarity; drug perturbations; pharmacogenomics; breast cancer

Significance Statement:

We provide a rapid and cost-effective strategy to expand a class of drugs with a similar phenotype. Our parent compound, dipyridamole, potentiated statin-induced tumour cell death by blocking the statin-triggered restorative feedback response that dampens statins pro-apoptotic activity. To identify compounds with this activity we performed a pharmacogenomic analysis to distinguish agents similar to dipyridamole in terms of structure, cell sensitivity and molecular perturbations. As dipyridamole has many reported activities, we focused our molecular perturbation analysis on the pathway inhibited by statins, the metabolic mevalonate pathway. Our strategy was successful as we validated nelfinavir and honokiol as dipyridamole-like compounds at both the phenotypic and molecular levels. Our developed approach sets the framework for future pathway-centric identification of drug combinations.

Introduction

Triple-negative breast cancer (TNBC) is an aggressive subtype of breast cancer (BC) that has a poorer prognosis amongst the major breast cancer subtypes[1]. This poor prognosis stems from our limited understanding of the underlying biology, the lack of targeted therapeutics, and the associated risk of distant recurrence occurring predominantly in the first two years after diagnosis[2]. Cytotoxic anthracycline and taxane-based chemotherapy regimens remain the primary option for treating TNBC, with other classes of investigational agents in various stages of development. Therefore, novel and effective therapeutics are urgently needed to combat this difficult-to-treat cancer.

Altered cellular metabolism is a hallmark of cancer[3,4] and targeting key metabolic pathways can provide new anti-cancer therapeutic strategies. Aberrant activation of the metabolic mevalonate (MVA) pathway is a hallmark of many cancers, including TNBC, as the end-products include cholesterol and other non-sterol isoprenoids essential for cellular proliferation and survival[5–7]. The statin family of FDA-approved cholesterol-lowering drugs are potent inhibitors of the rate-limiting enzyme of the MVA pathway, 3-hydroxy-3-methylglutaryl-CoA reductase (HMGCR)[6]. Epidemiological evidence shows that statin-use as a cholesterol control agent is associated with reduced cancer incidence[8] and recurrence[9–13]. Specifically, in BC, a 30-60% reduction in recurrence is evident amongst statin users, and decreased risk is associated with increased statin duration[9,12,14,15]. We and others have shown preclinically that Estrogen Receptor (ER)-negative BC cell lines, including TNBC, are preferentially sensitive to statin-induced apoptosis[16,17]. Moreover, three preoperative clinical trials investigating lipophilic statins (fluvastatin, atorvastatin) in human BC, showed statin use was associated with reduced tumour cell proliferation and increased apoptosis of high-grade BCs[18,19]. Thus, evidence suggests that statins have potential utility in the treatment of BC, including TNBC.

Drug combinations that overcome resistance mechanisms and maximize efficacy have potential advantages as cancer therapy. Blocking the MVA pathway with statins triggers a restorative feedback response that significantly dampens the pro-apoptotic activity of statins[20,21]. Briefly, statin-induced

depletion of intracellular sterols, triggers the inactive cytoplasmic, precursor form of the transcription factor sterol regulatory element-binding protein 2 (SREBP2) to be processed to the active mature nuclear form, which induces transcription of MVA genes, including *HMGCR* and the upstream synthase (*HMGCS1*)[22]. We have shown that inhibiting SREBP2 using RNAi, or blocking SREBP2 processing using the drug dipyridamole, significantly potentiates the ability of statins to trigger tumor cell death[21,23,24].

Dipyridamole is an FDA-approved antiplatelet agent commonly used for secondary stroke prevention, and since statin-dipyridamole has been co-prescribed for other indications, it may be safely used in the treatment of cancer[25]. However, the exact mechanism of dipyridamole action remains unclear as it has been reported to regulate several biological processes. Moreover, the antiplatelet activity of dipyridamole may be a contraindication for some cancer patients. Thus, to expand this dipyridamole-like class of compounds that can potentiate the pro-apoptotic activity of statins, we employed a pathway-centric approach to develop a computational pharmacogenomics pipeline to distinguish compounds that are predicted to behave similarly to dipyridamole in the regulation of MVA pathway genes. Using this strategy, we identified several potential dipyridamole-like compounds including nelfinavir, an FDA-approved antiretroviral drug and honokiol, a compound isolated from *Magnolia spp.*, which synergise with statins to drive tumour cell death by blocking the restorative feedback response. Correlation analysis of the statin-compound combination synergy score, with basal mRNA expression across a large panel of BC cell lines, identified *CDH1* expression as a predictive biomarker of response to these combination therapies. Taken together, we provide a new strategy to identify compounds that behave functionally similar to dipyridamole in an MVA pathway-specific manner and suggest that this approach will have broad utility for compound discovery across a wide variety of drug/pathway interactions.

Results

Computational pharmacogenomic pipeline identifies dipyridamole-like compounds

We developed a computational pipeline that harnesses high-throughput pharmacogenomics analysis to identify dipyridamole-like compounds that synergise with statins by blocking MVA pathway gene

expression to inhibit cancer cell viability (**Figure 1A and 1B**). The LINCS-L1000 (L1000)[26] and NCI-60[27] datasets were chosen for these studies as they contain cellular drug-response data at the molecular and proliferative levels across a panel of cell lines, respectively. From these datasets we extracted drug structure, drug-induced gene perturbation data (gene expression changes after drug treatment) and drug-cell line sensitivity profiles for the 238 compounds common to both datasets. Treating each level of data as a separate layer, we restricted the drug-gene perturbation layer from the L1000 dataset to only include the six MVA pathway genes present in the L1000 landmark gene set, to enrich for compounds that phenocopy the MVA pathway-specific activity of dipyridamole (**Supplemental Figure 1A and Figure 1B**). With dipyridamole as the reference input, we generated an MVA pathway-specific Drug Network Fusion (MVA-DNF) through the integration of three distinct data layers: drug structure, MVA-specific drug perturbation signatures, and drug-cell line sensitivity profiles. For each of the data layers incorporated into MVA-DNF, a 238x238 drug affinity matrix was generated, indicating drug similarity for a selected drug against all other drugs (further described in methods). Briefly, we first computed similarity between pairs of drug structures using the Tanimoto index, prior to generating the structure affinity matrix. We computed the similarity for every pair of drug sensitivity profiles using the pearson correlation coefficient, prior to generating an affinity matrix for the drug sensitivity layer. To create an affinity matrix for the MVA-specific perturbation layer, we first calculated the pearson correlation coefficient on the drug perturbation signatures that were filtered to include only MVA genes (**Figure 1B**). By integrating the three affinity matrices using similarity network fusion, and filtering hits using permutation testing, we subsequently identified 23 potential dipyridamole-like compounds that scored as significant (permutation test p-value <0.05) (**Figure 1B, Supplementary Table 1,** and further explained in methods). Represented as a network, these hits display strong connectivity to dipyridamole as well as to each other.

We assessed the contribution of the different data layers (drug structure, drug-gene perturbation, and drug-cell line sensitivity) within the MVA-DNF for each of these 23 compounds (**Figure 1C**). Drug perturbation played a significant role in the selection of novel dipyridamole-like compounds compared to drug sensitivity and drug structure. This reflects upon the specificity of the MVA-DNF towards the MVA pathway, in comparison to a ‘global’ drug taxonomy that is not MVA pathway-centric. Further assessment of the six MVA-pathway gene expression changes within the drug perturbation signatures highlights

comparable expression profiles between dipyridamole and the novel dipyridamole-like compounds (**Supplementary Figure 1B**).

To prioritize and further interrogate the identified dipyridamole-like hits we annotated the 23 compounds by reported mechanism of action and potential clinical utility. Two compounds were excluded from further analysis as they were not clinically useful: chromomycin A3, a reported toxin[28], and cadmium chloride, an established carcinogen[29]. The remaining 21 compounds segregated into ten distinct categories, demonstrating that dipyridamole-like hits identified through our pharmacogenomics pipeline spanned a diverse chemical and biological space (**Supplemental Figure 1C, Supplemental Table 1**). We sought to validate the five hits that scored as most similar to dipyridamole, which belong to four different categories: RAF/MEK inhibitor (selumetinib); antiretroviral (nelfinavir); anthracycline (doxorubicin, mitoxantrone); and natural product (honokiol). The reliability of our approach is evidenced by previous work by our lab and others that the anthracycline doxorubicin potentiates lovastatin in ovarian cancer cells[30] and RAF/MEK inhibitors such as PD98059 and more recently selumetinib (AZD6244) have been reported to synergise with statins to potentiate cancer cell death[31,32]. The molecular targeted compound (selumetinib) along with the novel three compounds were advanced for further evaluation (nelfinavir, mitoxantrone and honokiol) (**Supplemental Table 1**).

Dipyridamole-like compounds induce apoptosis in combination with fluvastatin and block the sterol-regulated feedback loop of the MVA pathway

To investigate whether the dipyridamole-like compounds could potentiate fluvastatin-induced cell death similar to that of dipyridamole, we first investigated sensitivity to increasing statin exposure in combination with a sub-lethal concentration of the novel dipyridamole-like compounds in two breast cancer cell line models with differential sensitivity to fluvastatin as a single agent (**Supplemental Figure 2**)[16]. As seen with dipyridamole, we observed similar potentiation of fluvastatin (lower IC_{50}) when combined with a sub-lethal concentration of selumetinib, nelfinavir, or honokiol, but not mitoxantrone (**Supplemental Figure 3 and Supplemental Figure 4**). Therefore, mitoxantrone was no longer pursued as a dipyridamole-like compound. To determine the nature of the anti-proliferative activity of the statin-compound combinations, we evaluated cell death by fixed propidium iodide staining and PARP cleavage with selumetinib, nelfinavir, or honokiol. Our data indicate that all three compounds, at

concentrations that have minimal effects as single agents, phenocopy dipyridamole and potentiate statin-induced cell death (**Figure 2**).

Mechanistically, statins induce a feedback response mediated by SREBP2 that has been shown to dampen cancer cell sensitivity to statin exposure. Moreover, blocking the SREBP2-mediated feedback response with dipyridamole enhances statin-induced cancer cell death[21,23]. We have shown that dipyridamole blocks the regulatory cleavage and therefore activation of SREBP2, decreasing mRNA expression of SREBP2-target genes of the MVA pathway. As expected, statin treatment induced the expression of SREBP2-target genes, *INSIG1*, *HMGCR* and *HMGCS1* after 16 hr of treatment, which was blocked by the co-treatment with dipyridamole (**Figure 3A, Supplemental Figure 5A**). Similarly, nelfinavir and honokiol both phenocopy dipyridamole and block the statin-induced expression of MVA pathway genes (**Figure 3A, Supplemental Figure 5A**). By contrast, co-treatment with selumetinib did not block the fluvastatin-induced feedback response. Housekeeping gene RPL13A was used as a reference gene for normalizing mRNA between samples and was not altered in the presence of the compounds (**Supplemental Figure 5B**).

Because SREBP2 is synthesized as an inactive full-length precursor that is activated to the mature nuclear form upon proteolytic cleavage, we used western blot analysis to assess the protein levels of both full-length and mature SREBP2. Nelfinavir and honokiol, but not selumetinib, blocked fluvastatin-induced SREBP2 processing and cleavage similar to that of dipyridamole (**Figure 3B-C**). This suggests that while selumetinib is a strong potentiator of statin-induced cell death, it does not mimic the action of dipyridamole by blocking the restorative feedback response (**Figure 3, Supplemental Figure 5**).

Novel statin-compound combinations phenocopy synergistic activity of fluvastatin-dipyridamole in a breast cancer cell line screen

To investigate whether the potentiation of fluvastatin by nelfinavir and honokiol has broad applicability and examine the determinants of synergy, we further evaluated these statin-compound combinations across a large panel of 47 breast cancer cell lines. A 5-day cytotoxicity assay (sulforhodamine B assay; SRB) in a 6x10 dose matrix was used to assess fluvastatin-compound efficacy. As expected, dipyridamole treatment resulted in a dose-dependent decrease in fluvastatin IC_{50} value (**Supplemental Figure 6A**). Similarly, nelfinavir and honokiol treatment also resulted in a dose-dependent decrease in fluvastatin IC_{50} values

similar to that of dipyridamole (**Supplemental Figure 6A**). This suggests that our computational pharmacogenomic pipeline predicts compounds that potentiate statin activity similarly to dipyridamole across multiple subtypes of breast cancer cell lines.

Next, we evaluated statin-compound synergy using the Bliss Index model derived using SynergyFinder[33] across the panel of breast cancer cell lines. Like the dose-dependent sensitivity data, we observed that the trend in synergy between fluvastatin-dipyridamole across the 47 breast cancer cell lines was also seen with fluvastatin-nelfinavir and fluvastatin-honokiol (**Figure 4A**). Since we had previously identified that the basal subtype of breast cancer cell lines were more sensitive to single agent fluvastatin[16], we evaluated whether basal breast cancer cell lines were similarly more sensitive to the fluvastatin-compound combinations. Using the SCMOD2 subtyping scheme, we evaluated the basal, HER2 and luminal B status of each cell line and determined synergy is independent of BC subtype (**Supplemental Figure 6B**). This suggests these statin-compound combinations can be applied to multiple breast cancer subtypes as therapeutic options, however a biomarker to distinguish those with high-sensitivity remained unclear.

Because the synergy profiles across the three fluvastatin-compound combinations were significantly similar (Fluva-NFV vs Fluva-DP, R_s=0.55, p-value=7.1e-05; Fluva-HNK vs Fluva-DP, R_s=0.62, p-value=5.5e-06; Fluva-NFV vs Fluva-HNK, R_s=0.82, p-value < 2.2e-16), we next interrogated whether baseline gene and/or protein expression profiles across the cell lines for each of the statin-compound combinations was associated with high-sensitivity and the synergistic response. To further interrogate the similarity between the statin-compound combinations, we correlated the RNA-seq and reverse phase protein array (RPPA) profiles of the 47 breast cancer cell lines[34] with their synergy scores for each of the statin-compound combinations. These represent the transcriptomic and proteomic state associations with synergy for each combination. We then evaluated the correlation between these associations across the different combinations (Fluva-DP vs Fluva-NFV; Fluva-DP vs Fluva-HNK; Fluva-NFV vs Fluva-HNK) (**Figure 4B**) and identified a high positive correlation between the combinations on the basis of similar transcriptomic associations (Fluva-NFV vs Fluva-DP, R_s=0.73, p-value < 2.2e-16; Fluva-HNK vs Fluva-DP, R_s=0.77, p-value < 2.2e-16; Fluva-NFV vs Fluva-HNK, R_s=0.87, p-value < 2.2e-16). This high positive correlation was also seen between these combinations using proteomic (RPPA) and synergy data

(**Supplemental Figure 6C**) suggesting that similar pathways were associated with the synergistic response to the three statin-compound combinations.

To compare the overlap in pathways associated with sensitivity to fluvastatin alone, and synergy between the fluvastatin-compound combinations, a Gene Set Enrichment Analysis (GSEA) using the Hallmark Gene Set Collection was performed[35]. These results showed that enriched pathways were highly similar amongst fluvastatin alone and the fluvastatin-compound combinations with one of the highest scoring enriched pathways being epithelial-mesenchymal transition (EMT) (**Figure 4C**). To further support this finding and because of the low agreement amongst EMT gene sets, we also evaluated four additional GSEA EMT pathways and observed similar trends between fluvastatin alone and the fluvastatin-compound combinations for each of the EMT gene sets (**Supplemental Figure 6D**). As we and others have published that mesenchymal-enriched cancer cell lines are more sensitive to statin monotherapy[36,37], this data suggests that fluvastatin is the primary driver of response to these statin-compound combinations. This is consistent with fluvastatin inhibiting the MVA pathway, triggering the SREBP-mediated feedback response, which in turn is inhibited by the second compound (dipyridamole, nelfinavir or honokiol) in these fluvastatin-compound combinations.

We then examined the individual genes within each of the GSEA EMT pathways to identify a biomarker of the synergistic response to the statin-compound combinations. Within the EMT field, gene set signatures have low agreement (**Supplemental Figure 7**). Previously our lab published a binary classifier of five EMT genes to predict increased sensitivity to statins across 631 cell lines representing multiple cancer types[36]. We evaluated whether this binary five-gene classifier could also predict synergy between the different fluvastatin-compound combinations. The five-gene EMT classifier could predict sensitivity to fluvastatin alone across the panel of breast cancer cell lines (**Supplemental Figure 8A**), but failed to predict synergy to the fluvastatin-compound combinations (**Supplemental Figure 8B**). We next interrogated each of the five genes individually. Interestingly, low gene expression and protein levels of E-cadherin (*CDH1*), a canonical epithelial state marker, not only predicted sensitivity to fluvastatin but also demonstrated synergy across all three fluvastatin-compound combinations (**Figure 5A-B and Supplemental Figure 8C**). To validate our findings, we probed for basal E-cadherin protein expression across a panel of nine breast cancer cell lines and showed that synergy to the novel statin-compound combinations is positively associated with low E-cadherin protein expression (**Figure 5C-D**). Overall, this

data validates that our MVA-DNF pharmacogenomics strategy can successfully distinguish compounds that, like-dipyridamole, can synergize with statins to trigger BC tumour cell death.

Discussion

By blocking the statin-induced restorative feedback response, dipyridamole potentiates statin efficacy to drive tumour cell death[21,23]. However, as the platelet-aggregation activity of dipyridamole may preclude its use in some cancer patients, our goal was to expand this class of agents that potentiate the pro-apoptotic activity of statins. To this end, we developed a novel computational pharmacogenomics pipeline that distinguished compounds that are similar to dipyridamole at the level of structure, MVA pathway gene expression perturbation, and anti-proliferative activity. We identified 23 potential dipyridamole-like compounds and then evaluated several of the top hits for their ability to phenocopy dipyridamole. By this approach, we validated that nelfinavir and honokiol sensitize breast cancer cell lines to statin-induced cell death by blocking the statin-induced restorative feedback loop. Analysis of basal RNA and protein expression identified the canonical EMT gene *CDH1* (E-cadherin) as a biomarker of the synergistic response to both statin-nelfinavir and statin-honokiol treatment. Thus, despite the polypharmacology of dipyridamole, the computational pharmacogenomics screen described here successfully identified synergistic statin-compound drug combinations as novel anti-breast cancer therapies.

By integrating a computational pharmacogenomics pipeline and cellular validation, we provide a novel, rapid, broadly-adaptable, and inexpensive strategy to distinguish compounds with similar biological activities. We show here that this approach overcomes a major problem associated with working with drugs, such as dipyridamole, that possess a complex polypharmacology. Dipyridamole was originally identified for its anti-platelet aggregation activity, but its mechanism of action spans a wide variety of functions. Several activities of dipyridamole have been described including an inhibitor of phosphodiesterases[38], nucleoside transport[39] and glucose uptake[40]. By restricting the gene perturbation layer of our pharmacogenomics pipeline to MVA-pathway genes, we successfully circumvented many of these varied functions and focused specifically on identifying dipyridamole-like drugs whose mechanisms

centre on the mevalonate pathway. This highlights that the computational pharmacogenomics pipeline described here is likely tunable to drug-specific structural features, activities and signaling pathways.

The new statin-sensitizing agents identified here using MVA-DNF include nelfinavir and honokiol, which like dipyridamole, inhibit statin-induced SREBP2 cleavage and activation[21,23]. To date, a number of SREBP2 inhibitors have been identified that block SREBP2 processing from its precursor to mature form, including fatostatin, betulin, and xanthohumal (ER-Golgi translocation), PF-429242 (site-1 protease (S1P) cleavage), and nelfinavir and 1,10-phenanthroline (site-2 protease (S2P) cleavage). Additional SREBP2 inhibitors include BF175 and tocotrienols that target SREBP2 transcriptional activity and protein stability, respectively. However, other than nelfinavir, these agents are either under development for clinical application or are only used for research purposes. The S2P protease inhibitor nelfinavir (marketed as Viracept) was approved for use in 1997 as an antiviral for the treatment of HIV, and is under evaluation for its utility as an anti-cancer agent[41–46]. This further reinforces that the novel combination of statin-nelfinavir is immediately actionable and should be evaluated without delay. We suggest the fluvastatin-nelfinavir combination is prefered compared to other statins, as distinct cytochrome P450 enzymes are used to process these agents, thereby preventing adverse drug-drug interactions [47].

To the best of our knowledge, this is the first study to report honokiol to synergize with statins in the context of cancer. Honokiol is a natural product commonly used in traditional medicine and has a number of reported mechanisms of action. How honokiol inhibits SREBP2 remains unknown, but this is the first study to interrogate its activity in SREBP2 translocation and gene expression alone and in combination with statins. As honokiol and its derivatives are presently under development, our findings of this new mechanism for honokiol can be incorporated into future analysis of honokiol's structure-activity relationships. Two additional predicted dipyridamole-like compounds tested in this study include selumetinib and mitoxantrone; the former was observed to sensitize breast cancer cells to statin-induced apoptosis, but the latter did not. Selumetinib functions through an SREBP2-independent mechanism, which suggests that not only is the identification of feedback-dependent mechanisms beneficial for cancer treatment, but that additional feedback-independent classes of statin-sensitizers can be identified. This is

particularly relevant, as some multiple myeloma and prostate cancer cell lines have been shown to lack the feedback response[20,21,48].

The data presented here have important clinical implications for statins as anti-cancer agents. Despite encouraging positive results from window-of-opportunity clinical trials in breast cancer using statins as a single-agent, a modest effect was observed with some but not all patients[18,19]. Accordingly, discovery of novel therapeutic combinations is necessary to achieve significant clinical impact. Since nelfinavir is poised for repurposing, and statins have demonstrated anti-cancer activity in early-phase clinical trials[18,19,49–54], clinical studies to further evaluate the therapeutic benefit of this combination could proceed swiftly. Furthermore, analyses of gene and protein expression data across our large collection of breast cancer cell lines identified a mesenchymal-enriched gene expression profile as highly predictive of sensitivity to all three statin-compound (dipyridamole, nelfinavir or honokiol) combinations. We further showed that *CDH1* expression levels served as a biomarker of synergistic response. This reinforces the dipyridamole-like behaviour of nelfinavir and honokiol, identified by our pharmacogenomics pipeline, and creates opportunities for biomarker-guided clinical studies (**Figure 5E**). We also observed this synergistic response to the combination therapies across multiple subtypes of breast cancer. Previously we had identified the basal-like breast cancer subtype as more sensitive to statins alone; here, we have expanded the scope of statin treatment to encompass the wider breast cancer population which can be distinguished on the basis of *CDH1* expression.

Collectively, our computational pharmacogenomics pipeline underscores the ability to identify compounds that phenocopy our parent compound of interest (dipyridamole), importantly, in a pathway-specific manner (mevalonate). Our study also provides a strong preclinical rationale to warrant further investigation of the fluvastatin-nelfinavir combination, as well as the utility of *CDH1* as a biomarker of response. The availability of these approved, well-tolerated drugs as well as simple methods for assessing *CDH1* expression could enable rapid translation of these findings to improve breast cancer outcomes.

Methods

Our analysis design encompasses both computational identification and refinement of dipyridamole-like compounds, as well as experimental validation of the most promising candidates.

MVA-specific Drug Network Fusion (MVA-DNF).

We developed a computational pharmacogenomic pipeline (MVA-DNF) that facilitates identification of analogues to dipyridamole, by elucidating drug-drug relationships specific to the mevalonate (MVA) pathway. MVA-DNF briefly extends upon some principles of the drug network fusion algorithm we had described previously[55], by utilizing the similarity network fusion algorithm across three drug taxonomies (drug structures, drug perturbation, and drug sensitivity). Drug structure annotations and drug perturbation signatures are obtained from the LINCS-L1000 dataset[26], and drug sensitivity signatures are obtained from the NCI-60 drug panel[27]. Drug structure annotations were converted into drug similarity matrices by calculating tanimoto similarity measures[56] and extended connectivity fingerprints[57] across all compounds, as described previously[55]. We extracted calculated Z-scores from drug-dose response curves for the NCI-60 drug sensitivity profiles, and computed Pearson correlation across these profiles to generate a drug similarity matrix based on sensitivity[27]. We used our PharmacoGx package (version 1.6.1) to compute drug perturbation signatures for the L1000 dataset using a linear regression model, as described previously[58]. The regression model adjusts for cell specific differences, batch effects and experiment duration, to generate a signature for the effect of drug concentration on the transcriptional state of a cell. This facilitates identification of gene expression which has been significantly perturbed due to drug treatment. These signatures indicate transcriptional changes that are induced by compounds on cancer cell lines. We further refined the drug perturbation profiles to a set of six MVA-pathway genes (**Supplementary Figure 1A**) that had been obtained from the literature as well as repositories of pathway-specific gene sets including MSigDB[59], HumanCyc[60] and KEGG[61,62]. These gene sets include ‘mevalonate pathway’ and ‘superpathway of geranylgeranyldiphosphate biosynthesis I (via mevalonate)’ from the HumanCyc[63], and ‘Kegg Terpenoid Backbone Biosynthesis’ from KEGG[61,62]. The filtered

drug-induced gene perturbation signatures were subsequently used to generate a drug perturbation similarity matrix that elucidates drug-drug relationships based on common transcriptional changes across the six MVA-pathway genes. We calculated similarity between estimated standardized coefficients of drug perturbation signatures using the Pearson correlation coefficient. Finally, we used the similarity network fusion algorithm[64] to integrate the affinity matrices for drug structure, drug sensitivity, and MVA-pathway specific drug perturbation profiles, to generate an MVA-pathway specific drug taxonomy (MVA-DNF) spanning 238 compounds.

Identification of analogues to dipyridamole

We interrogated the MVA-DNF taxonomy using a variety of approaches to identify a candidate set of dipyridamole-like compounds. Using MVA-DNF similarity scores, we first generated a ranking of all compounds closest to dipyridamole. We then conducted a permutation test, to assess the statistical relationship of each ranked drug against dipyridamole. Briefly, drug fusion networks were generated 999 times across perturbation, sensitivity, and drug structure profiles, each time using a random set of six genes to generate a 'pathway-centric' drug perturbation similarity matrix. Z-scores and p-values were calculated to determine the statistical relevance of a given dipyridamole-like analog in MVA-DNF, compared to the randomly generated networks. From this, we further ranked a list of dipyridamole-like candidate compounds by their statistical significance within MVA-DNF ($p\text{-value}<0.05$), resulting in identification of 23 candidate dipyridamole analogs.

For each of the dipyridamole analogues we identified, we conducted a similar assessment of significance to identify the relationships of these compounds to dipyridamole and to themselves. A network of dipyridamole-like analogues was rendered using the iGraph R package[65]. Using MVA-DNF similarity scores, we further assessed the contribution of each of the drug layers (structure, sensitivity and perturbation) towards the identification of dipyridamole-like compounds.

We assessed the regulation of gene expression for genes involved in the mevalonate pathway across all of the top-selected dipyridamole analogues, by analyzing the drug-induced transcriptional

profiles (described above) of the selected analogues. To further prioritize the dipyridamole analogues, the candidate compounds were categorized, and compounds that were known toxins or carcinogens were excluded from the analysis (**Supplemental Table 1, Supplemental Figure 1C**). Top hits from the largest categories were selected for further validation.

Cell culture and compounds

All cell lines were cultured as described previously[16,23]. Briefly, MDA-MB-231 and HCC1937 cells were cultured in Dulbecco's Modified Eagle's Medium (DMEM) and Roswell Park Memorial Institute medium (RPMI), respectively. All media was supplemented with 10% fetal bovine serum (FBS), 100 units/mL penicillin and 100 µg/mL streptomycin. Cell lines were routinely confirmed to be mycoplasma-free using the MycoAlert Mycoplasma Detection Kit (Lonza), and their authenticity was verified by short-tandem repeat (STR) profiling at The Centre for Applied Genomics (Toronto, ON, Canada). Fluvastatin (US Biological F5277-76) was dissolved in ethanol and dipyridamole (Sigma), nelfinavir (Sigma), honokiol (Sigma), mitoxantrone (Sigma) and selumetinib (Selleckchem) were dissolved in DMSO.

Breast cancer cell lines panel

The breast cancer cell line[34] panel was a generous gift from Dr. Benjamin Neel. RNAseq quantification was done using Kallisto pipeline[66] using human transcriptome reference hg38.gencodeV23[67]. RPPA processed data was downloaded from Marcotte et al. 2016[34]. SCMOD2[68] breast cancer subtypes of these cell lines were obtained using the genefu R package[69].

Breast cell-line combination viability screen

We used the sulforhodamine B colorimetric (SRB) proliferation assay[70] in 96-well plates to determine the dose-response curves. To test the combinations in the panel of BC cell lines (See Breast cancer cell lines panel), the fluvastatin/dipyridamole, fluvastatin/nelfinavir and fluvastatin/honokiol drug combinations were tested in a 6x10 dose matrix format covering a range of decreasing concentrations of each drug (highest drug dose was 20 µM fluvastatin, 20 µM dipyridamole, 10 µM nelfinavir and 20 µM honokiol), along with

all their pairwise combinations, as well as the negative control (EtOH and DMSO). We subtracted the average phosphate-buffer saline (PBS) wells value from all wells and computed the standard deviation and coefficient for each replicate. All individually treated well values were normalized to the control well values. We used Prism (v8.2.0, GraphPad Software) to compute dose-response curves with a bottom constraint equal to 0.

Cell viability assays

3-(4,5-dimethylthiazol-2-yl)-2,5-diphenyltetrazolium bromide (MTT) assays were performed as previously described[20]. Briefly, BC cells were seeded in 750-15,000 cells/well in 96-well plates overnight, then treated in triplicate with 0-400 μM fluvastatin for 72 hours. Half-maximal inhibitory concentrations (IC_{50}) values were computed from dose-response curves using Prism (v8.2.0, GraphPad Software) with a bottom constraint equal to 0.

Cell death assays

Cells were seeded at $2.5x10^5$ cells/plates and treated the next day as indicated. After 72 hours, cells were fixed in 70% ethanol for >24 h, stained with propidium iodide and analyzed by flow cytometry for the sub-diploid (% pre-G1) DNA population as a measure of cell death as previously described[20].

Immunoblotting

Cell lysates were prepared by washing cells twice with cold PBS and lysing cells in RIPA buffer (50 mM Tris-HCl pH 8.0, 150 mM NaCl, 0.5% sodium deoxycholate, 1% NP-40, 0.1% SDS, 1 mM EDTA, protease inhibitors) on ice for 30 min. Lysates were cleared by centrifugation and protein concentrations were determined using the Pierce 660 nm Protein Assay Kit (Thermo Fisher Scientific). Equal amounts of protein were diluted in Laemmli sample buffer, boiled for 5 min and resolved by SDS-polyacrylamide gel electrophoresis. The resolved proteins were then transferred onto nitrocellulose membranes. Membranes were then blocked for 1 hr in 5% milk in tris-buffered saline/0.1 % Tween-20 (TBS-T) at room

temperature, then probed with the following primary antibodies in 5% milk/TBS-T overnight at 4 °C: SREBP-2 (1:250, BD Biosciences, 557037), p44/42 MAPK (ERK1/2) (1:1000, Cell Signaling Technology, 4695), PARP (1:1000, Cell Signaling Technology, 9542L), α-Tubulin (1:3000, Calbiochem, CP06) and E-cadherin (1:1000, Cell Signaling Technology, 3195). Primary antibodies were detected using IRDye-conjugated secondary antibodies and the Odyssey Classic Imaging System (LI-COR Biosciences). Densitometric analysis was performed using ImageJ 1.47v software.

RNA expression analyses

Total RNA was harvested from sub-confluent cells using TRIzol Reagent (Invitrogen). cDNA was synthesized from 500 ng RNA using SuperScript III (Invitrogen). Quantitative reverse transcription PCR (qRT-PCR) was performed using the ABI Prism 7900HT sequence detection system and TaqMan probes (Applied Biosystems) for *HMGCR* (Hs00168352), *HMGCS1* (Hs00266810), *INSIG1* (Hs01650979) and *RPL13A* (Hs01578913).

Drug combinations synergy analysis

Viability scores were calculated using standard pipelines from PharmacoGx R package[58] and synergy scores represented by Bliss Index were calculated using SynergyFinder R package[33]. Pearson correlation coefficient was used to measure the associations between the transcriptomic and proteomic states of cell lines and the corresponding synergy scores for each of the combinations. The transcriptomic associations were then used to rank genes for GSEA[71]. The Hallmark gene set collection[35] was downloaded from MSigDB[72]. The Piano R package was used to run GSEA analysis[73]. Other EMT related pathways, namely “GO Positive Regulation of Epithelial To Mesenchymal Transition”[74], “GO Epithelial To Mesenchymal Transition”[74], “SARRIO Epithelial Mesenchymal Transition DN”[75], and “SARRIO Epithelial Mesenchymal Transition Up”[75], were also downloaded from MSigDB for analysis.

Data Access

The code and associated tutorial describing how to run the analysis pipeline are publicly available on Github at: https://github.com/DGendoo/MVA_DNF. All software dependencies are available on Bioconductor (BioC) or the Comprehensive Repository R Archive Network (CRAN), and have been listed throughout the methods as applicable.

Authors' contributions

Experimental Design: LZP, DG, BHK, JVL, JS, DWC

Acquisition of data: JVL, EB, JL, JS

Experimental analysis and interpretation: JVL, LZP, BHK, DG, WB, DWC

Conception and design of the pathway-centric MVA-DNF & permutation pipeline: DG, LZP, BHK, JVL, JL

Development of computational methodology: BHK, DG, WB

Bioinformatics data analysis and interpretation: DG, WB, BHK

Code Development: DG, WB

Writing, review, and/or revision of the manuscript: JVL, LZP, DWC, WB, BHK, DG

Study supervision: LZP and BHK

Approved the manuscript: all authors

Conflict of Interest Statement

DWC serves as a consultant for Agendia, Dynamo Therapeutics, AstraZeneca, Exact Sciences, GSK, Merck, Novartis, Pfizer, Puma, Roche; receives research support (to institution) from GSK, Merck and Pfizer and Roche-Genentech, and holds intellectual property as co-inventor on a patent related to biomarkers for TTK inhibitors. All other authors declare that they have no conflicts of interest.

Acknowledgements

This study was conducted with the support of the Terry Fox Research Institute-New Frontiers Program Project Grant (1064; LZP, BHK, WB and DWC), the Canada Research Chairs Program (to LZP; 950-229872) and Canadian Institutes of Health Research (to LZP; MOP-142263). This work was also supported by the Office of the Assistant Secretary of Defense of Health Affairs, through the Breast Cancer Research Program under Award No. W81XWH-16-1-0068 (to LZP and DWC). Opinions, interpretations, conclusions and recommendations are those of the author and are not necessarily endorsed by the Department of Defense. The authors thank all members of the Penn lab for helpful suggestions and critical feedback.

Figure Legends

Fig. 1. A schematic of the mevalonate (MVA) pathway and overview of the computational pharmacogenomics workflow. (A) In response to fluvastatin treatment (labelled with 1), MVA pathway end-product levels decrease, triggering an SREBP-mediated feedback response that activates MVA pathway-associated gene expression to restore cholesterol and other non-sterol end-product levels. Dipyridamole (DP) (labelled with 2) blocks the SREBP-mediated feedback response, thereby potentiating fluvastatin-induced cancer cell death. **(B)** An overview of the computational pharmacogenomics workflow, MVA-DNF, used to identify the top 23 “dipyridamole-like” candidates and visualized as a compound network. MVA-DNF combines drug structure, drug sensitivity, and drug-induced gene perturbation datasets restricted to six MVA pathway-specific genes. Permutation specificity testing was performed to select compounds that have a degree of specificity to the mevalonate pathway and dipyridamole. Statistical significance of compounds similar to dipyridamole was assessed by comparing to 999 networks generated from random selection of six genes within the drug perturbation layer. A network representation of dipyridamole and top 23 statistically-significant (p-value <0.05) “dipyridamole-like” compounds are shown. Each node represents a compound and edges connect compounds based on statistical significance of p-value <0.01. Darker blue nodes and orange edges represent the compounds connected to dipyridamole, and edge thickness represents the associated p-value between the compounds. **(C)** Radar plot of the top 23 dipyridamole-like compounds (p-value <0.05), where the contribution of each individual layer of the MVA-DNF (drug structure, sensitivity, and perturbation) is depicted. Percent contribution of each layer is shown from the center (0%) to the outer edges (100%).

Fig. S1, related to Fig. 1. Additional information regarding drug-induced genotype changes and categorization of top 23 dipyridamole-like compounds. (A) Simplified schematic of the MVA pathway, highlighting the six MVA-pathway genes (in red) in the L1000 database used to restrict the drug-induced gene perturbation layer of the MVA-DNF method. **(B)** Drug perturbation signatures for dipyridamole and dipyridamole-like compounds, plotted for genes pertaining to the MVA pathway. Similarity between

compounds based on their overall expression profiles is rendered in the dendrogram. Dipyridamole- and fluvastatin-induced changes shown on the bottom as reference. **(C)** Categorization of the top 21 dipyridamole-like compounds excluding toxins and carcinogenic compounds.

Fig. S2. MVA-DNF drug-dose response curves for MDA-MB-231 and HCC1937 breast cancer cell lines to identify a sub-lethal dose of top dipyridamole-like compounds. (A) MDA-MB-231 and **(B)** HCC1937 cells were treated with a range of doses for 72 hours, and cell viability was determined using an MTT assay. The drug dose-response curves are plotted with a dashed line at 80% MTT activity indicating a sub-lethal drug dose. Data for an average of three technical replicates are plotted; data reflect the results of a single biological experiment. **(C)** Table of sub-lethal drug dose and interpolated % MTT activity for both MDA-MB-231 and HCC1937.

Fig. S3. MVA-DNF drug-dose response curves, fluvastatin IC_{50} and solvent control values for MDA-MB-231 cells. MDA-MB-231 cells were treated with a range of fluvastatin doses alone or in combination with a sub-lethal dose of dipyridamole (5 μM), selumetinib (0.4 μM), nelfinavir (3 μM), mitoxantrone (0.01 μM) or honokiol (12 μM) for 72 hours, and cell viability was determined using an MTT assay. The drug dose-response curves, fluvastatin IC_{50} values and control values are plotted. Error bars represent the mean +/- SD, n = 3-5, *p <0.05, **p <0.01 (Student *t* test, unpaired, two-tailed).

Fig. S4. MVA-DNF drug-dose response curves, fluvastatin IC_{50} and solvent control values for HCC1937 cells. HCC1937 cells were treated with a range of fluvastatin doses alone or in combination with a sub-lethal dose of dipyridamole (5 μM), selumetinib (1 μM), nelfinavir (3 μM), mitoxantrone (0.001 μM) or honokiol (10 μM) for 72 hours, and cell viability was determined using an MTT assay. The drug dose-response curves, fluvastatin IC_{50} values and control values are plotted. Error bars represent the mean +/- SD, n = 3-6, *p <0.05, **p <0.01, ***p <0.001 (Student *t* test, unpaired, two-tailed).

Fig. 2. Dipyridamole-like compounds potentiate fluvastatin-induced cell death. (A) MDA-MB-231 and HCC1937 cells were treated with solvent controls or fluvastatin +/- dipyridamole (DP), nelfinavir (NFV), honokiol (HNK) or selumetinib (Selu) for 72 hours, fixed in ethanol and assayed for DNA fragmentation (% pre-G1 population) as a marker of cell death by propidium iodide staining. Error bars represent the mean +/- SD, n = 3-4, *p < 0.05, **p < 0.01, ****p < 0.0001 (one-way ANOVA with Bonferroni's multiple comparisons test, where each treatment was compared to the solvent control). **(B)** Cells were treated as in (A), protein isolated and immunoblotting was performed to assay for PARP cleavage. (F) represents full-length PARP and (C) represents cleaved PARP. **(C)** PARP cleavage (cleaved/full-length) shown in (B) was quantified by densitometry and normalized to Tubulin expression. Error bars represent the mean +/- SD, n = 3-5, *p < 0.05, **p<0.005, ***p<0.001, ****p<0.0001 (one-way ANOVA with Bonferroni's multiple comparisons test, where each group was compared to the solvent control within each experiment).

Fig. 3. Nelfinavir and Honokiol block fluvastatin-induced SREBP activation. (A) MDA-MB-231 and HCC1937 cells were exposed to solvent controls, fluvastatin (Flu) +/- dipyridamole (DP), nelfinavir (NFV), honokiol (HNK) or selumetinib (Selu) for 16 hours, and RNA was isolated to assay *INSIG1* expression by qRT-PCR. mRNA expression data are normalized to *RPL13A* expression. Error bars represent the mean +/- SD, n = 3-4, *p < 0.05, **p<0.005, ***p<0.001, ****p<0.0001 (one-way ANOVA with Bonferroni's multiple comparisons test, where each group was compared to the solvent control group within each experiment). **(B)** MDA-MB-231 and HCC1937 cells were treated with fluvastatin +/- dipyridamole, nelfinavir, honokiol or selumetinib for 12 hours, and protein was harvested to assay for SREBP2 expression and cleavage (activation) by immunoblotting. (P) represents precursor, full-length SREBP2 and (M) represents mature, cleaved SREBP2. **(C)** SREBP2 cleavage (cleaved/full-length) was quantified by densitometry and normalized to total ERK expression. Error bars represent the mean +/- SD, n = 3-8, *p < 0.05, **p<0.005, ***p<0.001, ****p<0.0001 (one-way ANOVA with Bonferroni's multiple comparisons test, where each group was compared to the solvent controls group within its experiment).

Fig. S5, related to Fig 3. Nelfinavir and Honokiol block fluvastatin-induced SREBP activation of SREBP2 feedback genes. (A) MDA-MB-231 cells were treated with fluvastatin +/- dipyridamole, nelfinavir, honokiol or selumetinib for 16 hours, and RNA was isolated to assay for *HMGCR* and *HMGCS1* expression by qRT-PCR. mRNA expression data are normalized to *RPL13A* expression. **(B)** RPL13A Ct mean values plotted as a control. Error bars represent the mean +/- SD, n = 3-4, *p < 0.05, **p<0.005, ***p<0.001, ****p<0.0001 (one-way ANOVA with Bonferroni's multiple comparisons test, where each group was compared to the solvent controls group).

Fig. S6, related to Fig 4. High-throughput compound combination screen. (A) Heatmap of Log_{10}(Fluvastatin IC_{50}) values for a high-throughput compound synergy screen against 47 BC cell lines visualizing the 15^{th} to 85^{th} percentile. BC cell lines were treated with a dose matrix of fluvastatin (0-20 μM) +/- dipyridamole (DP) (0-20 μM), nelfinavir (NFV) (0-10 μM) or honokiol (HNK) (0-20 μM). After 5 days of drug treatment, cell viability was assessed by SRB assay. SCMOD2 cell line subtyping was assigned to the BC cell line panel. Data presented are the average of 2 biological replicates (fluvastatin +/- dipyridamole (DP)) or the mean of 3-6 biological replicates (fluvastatin +/- nelfinavir (NFV) and fluvastatin +/- honokiol (HNK)). **(B)** Comparison of synergy scores stratified by BC subtypes across the combinations using wilcoxon paired rank test. Red dash line at synergy threshold where >0 indicates lower synergy and <0 indicates higher synergy. **(C)** Associations of proteomic states[34] with synergy scores across the fluvastatin-compound combinations. Similarity of proteomic states associations were compared across the combinations (Fluva-DP vs Fluva-NFV; Fluva-DP vs Fluva-HNK; Fluva-NFV vs Fluva-HNK) using Pearson correlation coefficient. Top five basally-expressed proteins associated with synergy in either direction are annotated in red. **(D)** Gene set enrichment analysis using five EMT gene set collections and genes ranked by basal mRNA correlated to the fluvastatin IC_{50} (Fluva) value or synergy score (Fluva-DP, Fluva-NFV and Fluva-HNK). Dot size indicates the difference in enrichment scores (ES) of the pathways. Background shading indicates the FDR. X indicates pathway and drug combinations that were not significantly enriched (FDR > 0.05).

Fig. 4. Compound combination synergy analysis. (A) Heatmap of synergy scores (Bliss Index model) for fluvastatin (Fluva) + dipyridamole (DP), nelfinavir (NFV) or honokiol (HNK) in a panel of 47 breast cancer cells lines. Ordered by synergy score of Fluva-DP, from greatest (<0) to least synergy (>0). Breast cancer subtype of each cell line is shown and is based on the SCMOD2 subtyping scheme. **(B)** Basal mRNA expression[34] associations with synergy scores for each drug combination (e.g. Fluva-NFV vs. Fluva-DP, Fluva-HNK vs. Fluva-DP, and Fluva-NFV vs. Fluva-HNK). Associations were calculated using Pearson correlation coefficient. Top five basally-expressed genes associated with synergy in either direction are annotated in red. **(C)** Gene set enrichment analysis (GSEA) using the Hallmark gene set collection, where genes were ranked according to their correlation to the fluvastatin IC_{50} (Fluva) value or to the synergy score (Fluva-DP, Fluva-NFV and Fluva-HNK). Dot plot was restricted to pathways enriched in two out of the four groups. Dot size indicates the difference in enrichment scores (ES) of the pathways. Background shading indicates the FDR. X indicates pathway and drug combinations that were not significantly enriched (FDR > 0.05).

Fig. S7, related to Fig 4. Overlapping genes within the EMT gene sets. (A) Upset plot to visualize the agreement between Yu *et al.* (2018)[36] five-gene classifier and five additional EMT gene sets.

Fig. S8, related to Fig 5. EMT gene expression as a biomarker of sensitivity to fluvastatin and synergistic response to fluvastatin-compound combinations. (A) Five-gene fluvastatin sensitivity gene classifier[36] predicts sensitivity to fluvastatin alone, but **(B)** does not predict synergy to Fluva-DP, Fluva-NFV or Fluva-HNK. **(C)** Basal Vimentin (VIM), N-Cadherin (CDH2), ZEB1 and fibronectin (FN1) mRNA expression do not predict synergy to the drug combinations.

Fig. 5. Basal E-cadherin predicts synergistic response to fluvastatin-compound combinations. (A) Basal E-cadherin mRNA expression between cell lines predicted to be synergistic or not to each drug combination. Synergy was defined by Bliss Index and significance was measured by wilcoxon rank sum test. **(B)** Basal E-cadherin mRNA expression between cell lines predicted to be respondent or not to

fluvastatin. Sensitivity was defined by IC_{50} and significance was measured by wilcoxon rank sum test. **(C)** Protein lysates were isolated from a panel of breast cancer cell lines to assay for basal E-cadherin expression by immunoblotting. **(D)** Densitometry values of normalized E-cadherin expression plotted as a heatmap. E-cadherin expression was quantified by densitometry and normalized individually to Tubulin expression. **(E)** Schematic diagram detailing the potential for fluvastatin (labelled with 1) and nelfinavir (labelled with 2) to block the SREBP2-mediated feedback response and synergize to potentiate fluvastatin-induced cell death.

Table Legends

Supplementary Table 1 - Ranked MVA-DNF compounds. Z-score and p-values are indicated. Compounds are ordered by p-value.

References

1. Canadian Cancer Society. Canadian Cancer Statistics publication. *www.cancer.ca* http://www.cancer.ca/en/cancer-information/cancer-101/canadian-cancer-statistics-publication/?region=on (2019).
2. Lebert, J. M., Lester, R., Powell, E., Seal, M. & McCarthy, J. Advances in the systemic treatment of triple-negative breast cancer. *Curr. Oncol.* **25**, S142–S150 (2018).
3. DeBerardinis, R. J. & Chandel, N. S. Fundamentals of cancer metabolism. *Science Advances* vol. 2 e1600200 (2016).
4. Warburg, O. On the origin of cancer cells. *Science* **123**, 309–314 (1956).
5. Ehmsen, S. *et al.* Increased Cholesterol Biosynthesis Is a Key Characteristic of Breast Cancer Stem Cells Influencing Patient Outcome. *Cell Rep.* **27**, 3927–3938.e6 (2019).
6. Mullen, P. J., Yu, R., Longo, J., Archer, M. C. & Penn, L. Z. The interplay between cell signalling and the mevalonate pathway in cancer. *Nat. Rev. Cancer* **16**, 718–731 (2016).
7. Clendening, J. W. *et al.* Dysregulation of the mevalonate pathway promotes transformation. *Proc. Natl. Acad. Sci. U. S. A.* **107**, 15051–15056 (2010).
8. Boudreau, D. M. *et al.* A validation study of patient interview data and pharmacy records for antihypertensive, statin, and antidepressant medication use among older women. *Am. J. Epidemiol.* **159**, 308–317 (2004).
9. Ahern, T. P. *et al.* Statin prescriptions and breast cancer recurrence risk: a Danish nationwide prospective cohort study. *J. Natl. Cancer Inst.* **103**, 1461–1468 (2011).
10. Cronin-Fenton, D. *et al.* Breast cancer recurrence, bone metastases, and visceral metastases in women with stage II and III breast cancer in Denmark. *Breast Cancer Res. Treat.* **167**, 517–528 (2018).
11. Nielsen, S. F., Nordestgaard, B. G. & Bojesen, S. E. Statin Use and Reduced Cancer-Related Mortality. *New England Journal of Medicine* vol. 367 1792–1802 (2012).
12. Kwan, M. L., Habel, L. A., Flick, E. D., Quesenberry, C. P. & Caan, B. Post-diagnosis statin use and

627 breast cancer recurrence in a prospective cohort study of early stage breast cancer survivors. *Breast*
628 *Cancer Res. Treat.* **109**, 573–579 (2008).
629 13. Brewer, T. M. *et al.* Statin use in primary inflammatory breast cancer: a cohort study. *Br. J. Cancer*
630 **109**, 318–324 (2013).
631 14. Chae, Y. K. *et al.* Reduced risk of breast cancer recurrence in patients using ACE inhibitors, ARBs,
632 and/or statins. *Cancer Invest.* **29**, 585–593 (2011).
633 15. Boudreau, D. M. *et al.* Comparative safety of cardiovascular medication use and breast cancer
634 outcomes among women with early stage breast cancer. *Breast Cancer Res. Treat.* **144**, 405–416
635 (2014).
636 16. Goard, C. A. *et al.* Identifying molecular features that distinguish fluvastatin-sensitive breast tumor
637 cells. *Breast Cancer Res. Treat.* **143**, 301–312 (2014).
638 17. Kimbung, S., Lettiero, B., Feldt, M., Bosch, A. & Borgquist, S. High expression of cholesterol
639 biosynthesis genes is associated with resistance to statin treatment and inferior survival in breast
640 cancer. *Oncotarget* **7**, 59640–59651 (2016).
641 18. Garwood, E. R. *et al.* Fluvastatin reduces proliferation and increases apoptosis in women with high
642 grade breast cancer. *Breast Cancer Res. Treat.* **119**, 137–144 (2010).
643 19. Bjarnadottir, O. *et al.* Targeting HMG-CoA reductase with statins in a window-of-opportunity breast
644 cancer trial. *Breast Cancer Res. Treat.* **138**, 499–508 (2013).
645 20. Clendening, J. W. *et al.* Exploiting the mevalonate pathway to distinguish statin-sensitive multiple
646 myeloma. *Blood* **115**, 4787–4797 (2010).
647 21. Longo, J. *et al.* An actionable sterol-regulated feedback loop modulates statin sensitivity in prostate
648 cancer. *Mol Metab* **25**, 119–130 (2019).
649 22. Brown, M. S. & Goldstein, J. L. The SREBP Pathway: Regulation of Cholesterol Metabolism by
650 Proteolysis of a Membrane-Bound Transcription Factor. *Cell* vol. 89 331–340 (1997).
651 23. Pandyra, A. *et al.* Immediate utility of two approved agents to target both the metabolic mevalonate
652 pathway and its restorative feedback loop. *Cancer Res.* **74**, 4772–4782 (2014).
653 24. Pandyra, A. A. *et al.* Genome-wide RNAi analysis reveals that simultaneous inhibition of specific

mevalonate pathway genes potentiates tumor cell death. *Oncotarget* **6**, 26909–26921 (2015).

25. Ye, Y. *et al.* Enhanced cardioprotection against ischemia-reperfusion injury with a dipyridamole and low-dose atorvastatin combination. *Am. J. Physiol. Heart Circ. Physiol.* **293**, H813–8 (2007).
26. Subramanian, A. *et al.* A Next Generation Connectivity Map: L1000 Platform and the First 1,000,000 Profiles. *Cell* **171**, 1437–1452.e17 (2017).
27. Shoemaker, R. H. The NCI60 human tumour cell line anticancer drug screen. *Nat. Rev. Cancer* **6**, 813–823 (2006).
28. Samal, B. *et al.* Chromomycin A3 for advanced breast cancer: a Southwest Oncology Group study. *Cancer Treat. Rep.* **62**, 19–22 (1978).
29. Godt, J. *et al.* The toxicity of cadmium and resulting hazards for human health. *J. Occup. Med. Toxicol.* **1**, 22 (2006).
30. Martirosyan, A., Clendening, J. W., Goard, C. A. & Penn, L. Z. Lovastatin induces apoptosis of ovarian cancer cells and synergizes with doxorubicin: potential therapeutic relevance. *BMC Cancer* **10**, 103 (2010).
31. Wu, J., Wong, W. W.-L., Khosravi, F., Minden, M. D. & Penn, L. Z. Blocking the Raf/MEK/ERK pathway sensitizes acute myelogenous leukemia cells to lovastatin-induced apoptosis. *Cancer Res.* **64**, 6461–6468 (2004).
32. McGregor, G. H. *et al.* Targeting the Metabolic Response to Statin-Mediated Oxidative Stress Produces a Synergistic Antitumor Response. *Cancer research* vol. 80 175–188 (2020).
33. Ianevski, A., He, L., Aittokallio, T. & Tang, J. SynergyFinder: a web application for analyzing drug combination dose-response matrix data. *Bioinformatics* **33**, 2413–2415 (2017).
34. Marcotte, R. *et al.* Functional Genomic Landscape of Human Breast Cancer Drivers, Vulnerabilities, and Resistance. *Cell* **164**, 293–309 (2016).
35. Liberzon, A. *et al.* The Molecular Signatures Database (MSigDB) hallmark gene set collection. *Cell Syst* **1**, 417–425 (2015).
36. Yu, R. *et al.* Statin-Induced Cancer Cell Death Can Be Mechanistically Uncoupled from Prenylation of RAS Family Proteins. *Cancer Res.* **78**, 1347–1357 (2018).

37. Viswanathan, V. S. *et al.* Dependency of a therapy-resistant state of cancer cells on a lipid peroxidase pathway. *Nature* **547**, 453–457 (2017).
38. Bender, A. T. & Beavo, J. A. Cyclic Nucleotide Phosphodiesterases: Molecular Regulation to Clinical Use. *Pharmacological Reviews* vol. 58 488–520 (2006).
39. King, A. E., Ackley, M. A., Cass, C. E., Young, J. D. & Baldwin, S. A. Nucleoside transporters: from scavengers to novel therapeutic targets. *Trends Pharmacol. Sci.* **27**, 416–425 (2006).
40. Steinfelder, H. J. & Joost, H. G. Inhibition of insulin-stimulated glucose transport in rat adipocytes by nucleoside transport inhibitors. *FEBS Letters* vol. 227 215–219 (1988).
41. Chow, W. A., Jiang, C. & Guan, M. Anti-HIV drugs for cancer therapeutics: back to the future? *Lancet Oncol.* **10**, 61–71 (2009).
42. Guan, M., Su, L., Yuan, Y.-C., Li, H. & Chow, W. A. Nelfinavir and nelfinavir analogs block site-2 protease cleavage to inhibit castration-resistant prostate cancer. *Sci. Rep.* **5**, 9698 (2015).
43. Soprano, M. *et al.* Oxidative Stress Mediates the Antiproliferative Effects of Nelfinavir in Breast Cancer Cells. *PLoS One* **11**, e0155970 (2016).
44. Hitz, F. *et al.* Nelfinavir and lenalidomide/dexamethasone in patients with lenalidomide-refractory multiple myeloma. A phase I/II Trial (SAKK 39/10). *Blood Cancer J.* **9**, 70 (2019).
45. Rengan, R. *et al.* Clinical Outcomes of the HIV Protease Inhibitor Nelfinavir With Concurrent Chemoradiotherapy for Unresectable Stage IIIA/IIIB Non--Small Cell Lung Cancer: A Phase 1/2 Trial. *JAMA oncology* **5**, 1464–1472 (2019).
46. Blumenthal, G. M. *et al.* A phase I trial of the HIV protease inhibitor nelfinavir in adults with solid tumors. *Oncotarget* **5**, 8161–8172 (2014).
47. Hsyu, P.-H., Schultz-Smith, M. D., Lillibridge, J. H., Lewis, R. H. & Kerr, B. M. Pharmacokinetic Interactions between Nelfinavir and 3-Hydroxy-3-Methylglutaryl Coenzyme A Reductase Inhibitors Atorvastatin and Simvastatin. *Antimicrobial Agents and Chemotherapy* vol. 45 3445–3450 (2001).
48. Longo, J. *et al.* The mevalonate pathway is an actionable vulnerability of t(4;14)-positive multiple myeloma. *Leukemia* (2020) doi:10.1038/s41375-020-0962-2.
49. Goss, G. D. *et al.* A phase I study of high-dose rosuvastatin with standard dose erlotinib in patients

with advanced solid malignancies. *J. Transl. Med.* **14**, 83 (2016).

50. Hus, M. *et al.* Thalidomide, dexamethasone and lovastatin with autologous stem cell transplantation as a salvage immunomodulatory therapy in patients with relapsed and refractory multiple myeloma. *Ann. Hematol.* **90**, 1161–1166 (2011).
51. Knox, J. J. *et al.* A Phase I trial of prolonged administration of lovastatin in patients with recurrent or metastatic squamous cell carcinoma of the head and neck or of the cervix. *Eur. J. Cancer* **41**, 523–530 (2005).
52. Kornblau, S. M. *et al.* Blockade of adaptive defensive changes in cholesterol uptake and synthesis in AML by the addition of pravastatin to idarubicin + high-dose Ara-C: a phase 1 study. *Blood* **109**, 2999–3006 (2007).
53. Longo, J. *et al.* A pilot window-of-opportunity study of preoperative fluvastatin in localized prostate cancer. *Prostate Cancer Prostatic Dis.* (2020) doi:10.1038/s41391-020-0221-7.
54. Murtola, T. J. *et al.* Atorvastatin Versus Placebo for Prostate Cancer Before Radical Prostatectomy—A Randomized, Double-blind, Placebo-controlled Clinical Trial. *Eur. Urol.* **74**, 697–701 (2018).
55. El-Hachem, N. *et al.* Integrative Cancer Pharmacogenomics to Infer Large-Scale Drug Taxonomy. *Cancer Res.* **77**, 3057–3069 (2017).
56. Tanimoto, T. T. *An Elementary Mathematical Theory of Classification and Prediction*. (International Business Machines Corporation, 1958).
57. Guha, R. & Others. Chemical informatics functionality in R. *J. Stat. Softw.* **18**, 1–16 (2007).
58. Smirnov, P. *et al.* PharmacoGx: an R package for analysis of large pharmacogenomic datasets. *Bioinformatics* **32**, 1244–1246 (2016).
59. Subramanian, T. & Others. Molecular Signatures Database (MSigDB). *Proc. Natl. Acad. Sci. U. S. A.* **102**, 15545–15550 (2005).
60. Romero, P. *et al.* Computational prediction of human metabolic pathways from the complete human genome. *Genome Biol.* **6**, R2 (2005).
61. Kanehisa, M. & Goto, S. KEGG: kyoto encyclopedia of genes and genomes. *Nucleic Acids Res.* **28**,

27–30 (2000).

62. Du, J. *et al.* KEGG-PATH: Kyoto encyclopedia of genes and genomes-based pathway analysis using a path analysis model. *Mol. Biosyst.* **10**, 2441–2447 (2014).
63. Caspi, R. *et al.* The MetaCyc database of metabolic pathways and enzymes and the BioCyc collection of pathway/genome databases. *Nucleic Acids Res.* **44**, D471–80 (2016).
64. Wang, B. *et al.* Similarity network fusion for aggregating data types on a genomic scale. *Nat. Methods* **11**, 333–337 (2014).
65. Csardi, G., Nepusz, T. & Others. The igraph software package for complex network research. *InterJournal, complex systems* **1695**, 1–9 (2006).
66. Bray, N. L., Pimentel, H., Melsted, P. & Pachter, L. Near-optimal probabilistic RNA-seq quantification. *Nat. Biotechnol.* **34**, 525–527 (2016).
67. Frankish, A. *et al.* GENCODE reference annotation for the human and mouse genomes. *Nucleic Acids Res.* **47**, D766–D773 (2019).
68. Wirapati, P. *et al.* Meta-analysis of gene expression profiles in breast cancer: toward a unified understanding of breast cancer subtyping and prognosis signatures. *Breast Cancer Res.* **10**, R65 (2008).
69. Gendoo, D. M. A. *et al.* Genefu: an R/Bioconductor package for computation of gene expression-based signatures in breast cancer. *Bioinformatics* **32**, 1097–1099 (2016).
70. Vichai, V. & Kirtikara, K. Sulforhodamine B colorimetric assay for cytotoxicity screening. *Nat. Protoc.* **1**, 1112–1116 (2006).
71. Subramanian, A. *et al.* Gene set enrichment analysis: a knowledge-based approach for interpreting genome-wide expression profiles. *Proc. Natl. Acad. Sci. U. S. A.* **102**, 15545–15550 (2005).
72. Liberzon, A. *et al.* Molecular signatures database (MSigDB) 3.0. *Bioinformatics* **27**, 1739–1740 (2011).
73. Väremo, L., Nielsen, J. & Nookaew, I. Enriching the gene set analysis of genome-wide data by incorporating directionality of gene expression and combining statistical hypotheses and methods. *Nucleic Acids Res.* **41**, 4378–4391 (2013).

74. Ashburner, M. *et al.* Gene ontology: tool for the unification of biology. The Gene Ontology Consortium. *Nat. Genet.* **25**, 25–29 (2000).

75. Sarrió, D. *et al.* Epithelial-mesenchymal transition in breast cancer relates to the basal-like phenotype. *Cancer Res.* **68**, 989–997 (2008).

FIGURE 1

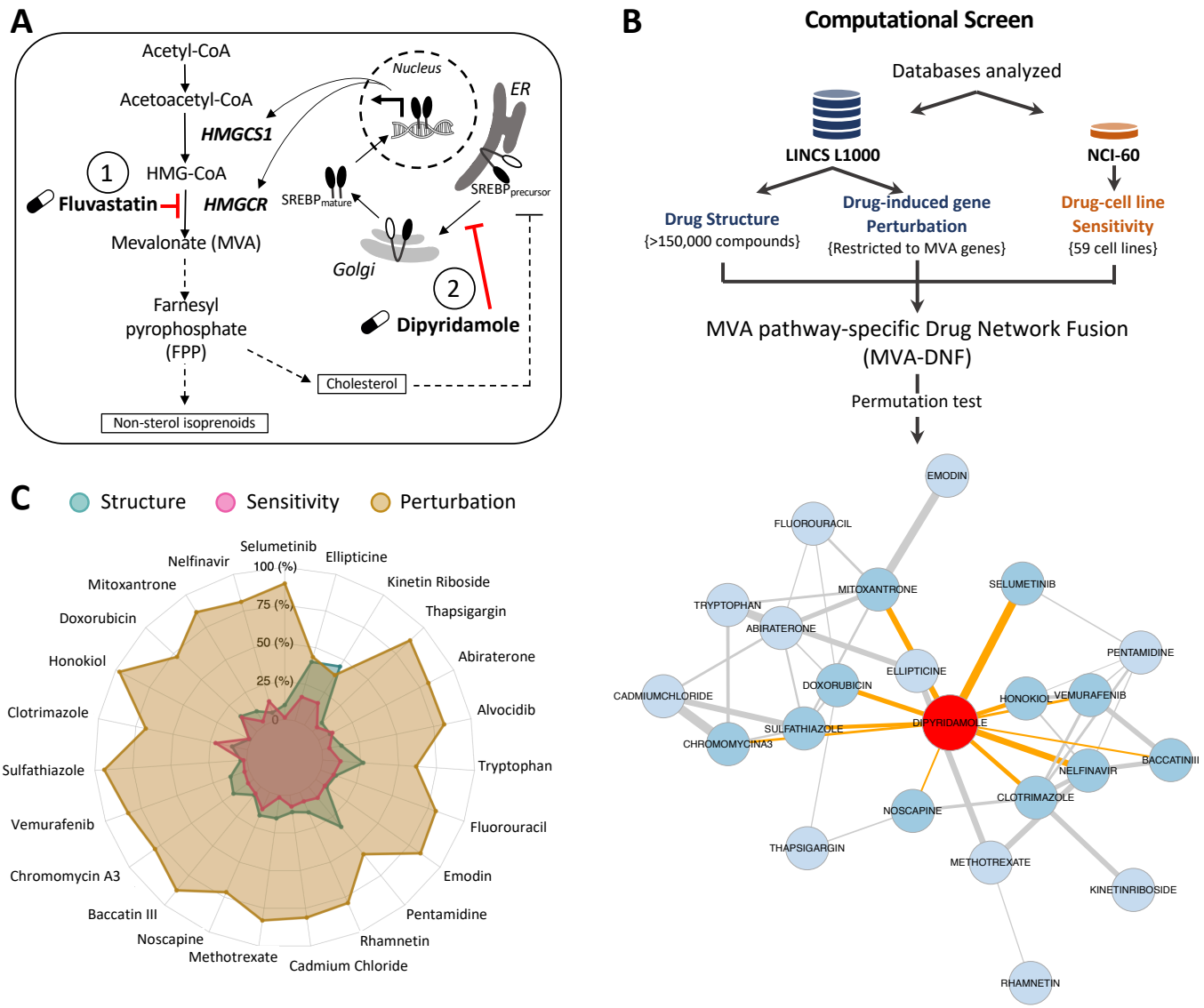
A
Acetyl-CoA
Acetoacetyl-CoA
HMGCS1
1
HMG-CoA
Fluvastatin
HMGCR
Mevalonate (MVA)
Farnesyl pyrophosphate (FPP)
Non-sterol isoprenoids
Cholesterol
Nucleus
ER
SREBP mature
SREBP precursor
Golgi
2
Dipyridamole
B
Computational Screen
Databases analyzed
LINCS L1000
NCI-60
Drug Structure
{>150,000 compounds}
Drug-induced gene Perturbation
{Restricted to MVA genes}
Drug-cell line Sensitivity
{59 cell lines}
MVA pathway-specific Drug Network Fusion (MVA-DNF)
Permutation test
EMODIN
FLUOROURACIL
MITOXANTRONE
SELUMETINIB
TRYPTOPHAN
ABIRATERONE
PENTAMIDINE
ELLIPTICINE
DOXORUBICIN
CADMIUMCHLORIDE
HONOKIOL
VEMURAFENIB
DIPYRIDAMOLE
SULFATHIAZOLE
CHROMOMYCINA3
BACCATINIII
NELFINAVIR
CLOTRIMAZOLE
NOSCAPINE
THAPSIGARGIN
METHOTREXATE
KINETINRIBOSIDE
RHAMNETIN
C
Structure
Sensitivity
Perturbation
100 (%)
75 (%)
50 (%)
25 (%)
0
Selumetinib
Ellipticine
Kinetin Riboside
Thapsigargin
Abiraterone
Alvocidib
Tryptophan
Fluorouracil
Emodin
Pentamidine
Rhamnetin
Cadmium Chloride
Methotrexate
Noscapine
Baccatin III
Chromomycin A3
Vemurafenib
Sulfathiazole
Clotrimazole
Honokiol
Doxorubicin
Mitoxantrone
Nelfinavir

SUPP FIGURE 1

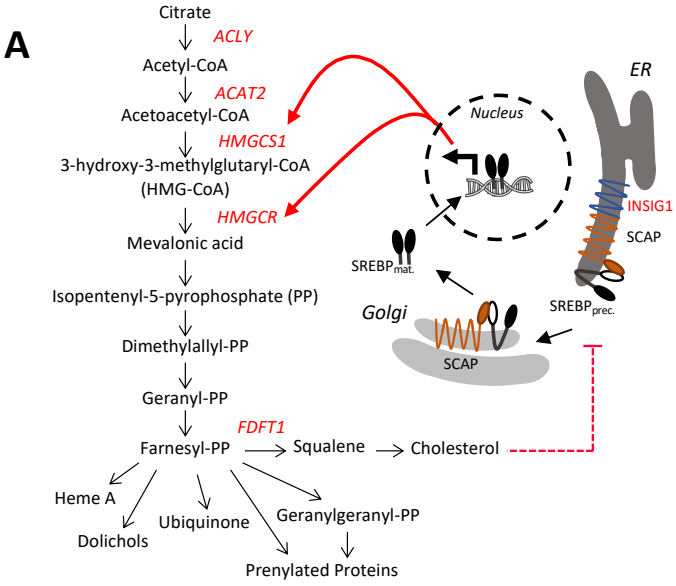

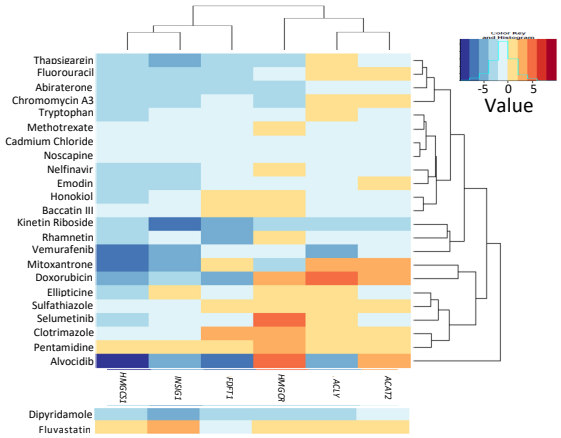

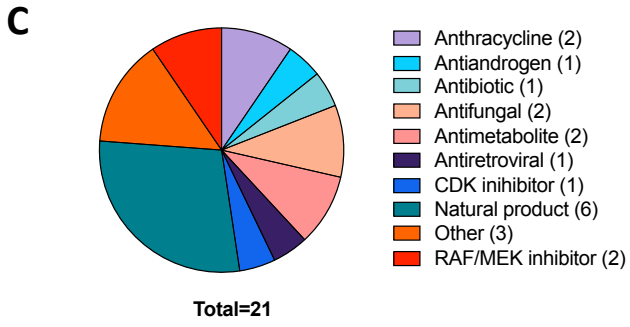

SUPP FIGURE 2

A

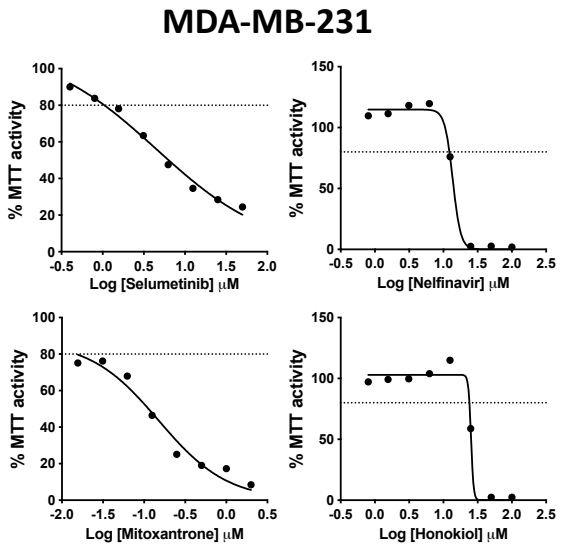

B

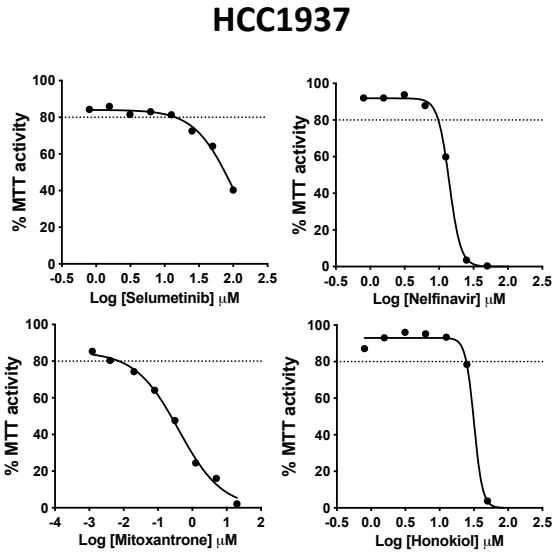

C

	MDA-MB-231		HCC1937	
Drug	**Dose**	**Interpolated MTT activity**	**Dose**	**Interpolated MTT activity**
Selumetinib	0.4 μM	91.92%	1 μM	83.97%
Nelfinavir	3 μM	114.8%	3 μM	91.8%
Mitoxantrone	0.01 μM	~80%	0.001 μM	85.4%
Honokiol	12 μM	102.99%	10 μM	92.97%

SUPP FIGURE 3 (MDA-MB-231)

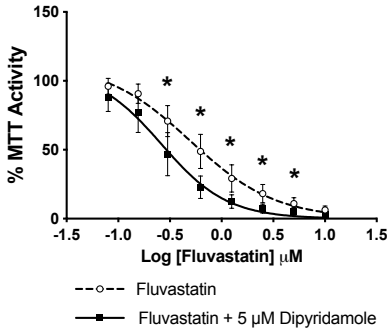

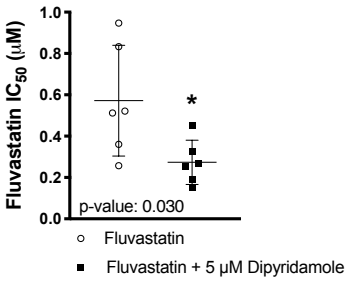

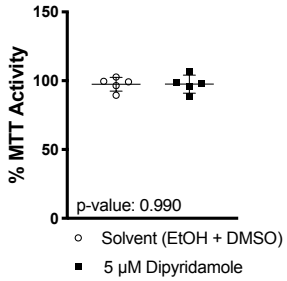

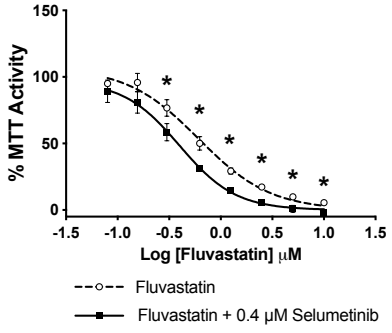

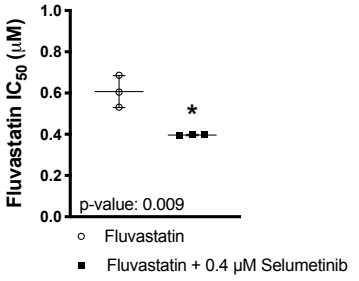

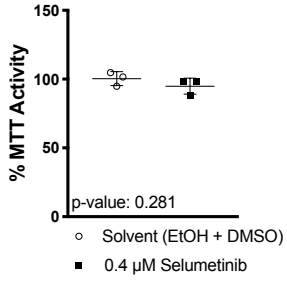

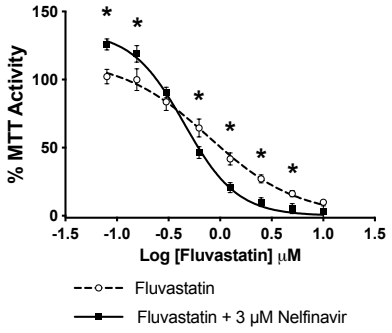

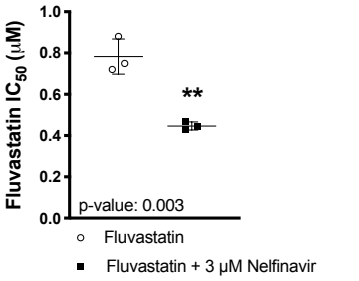

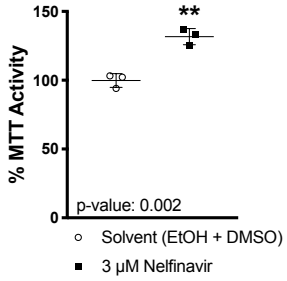

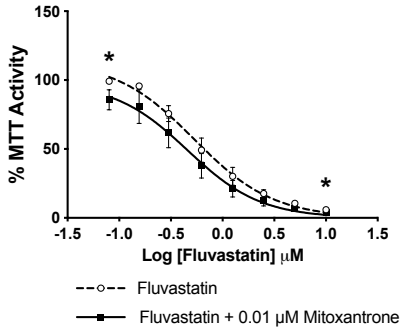

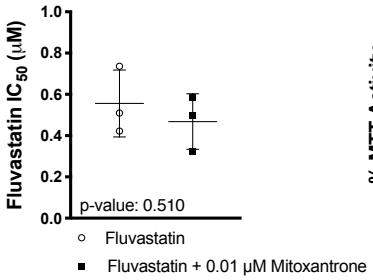

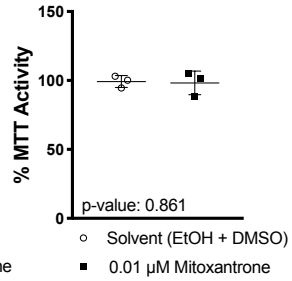

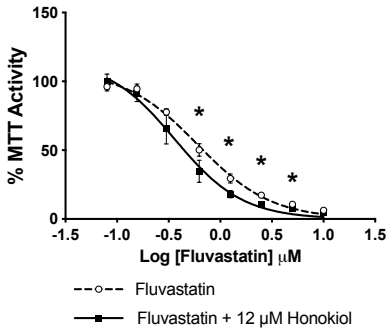

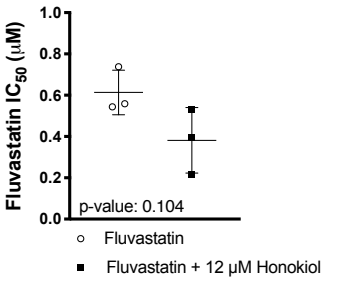

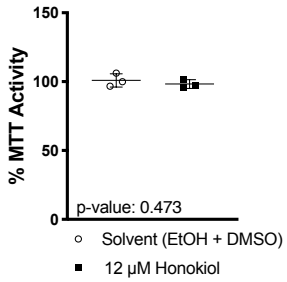

SUPP FIGURE 4 (HCC1937)

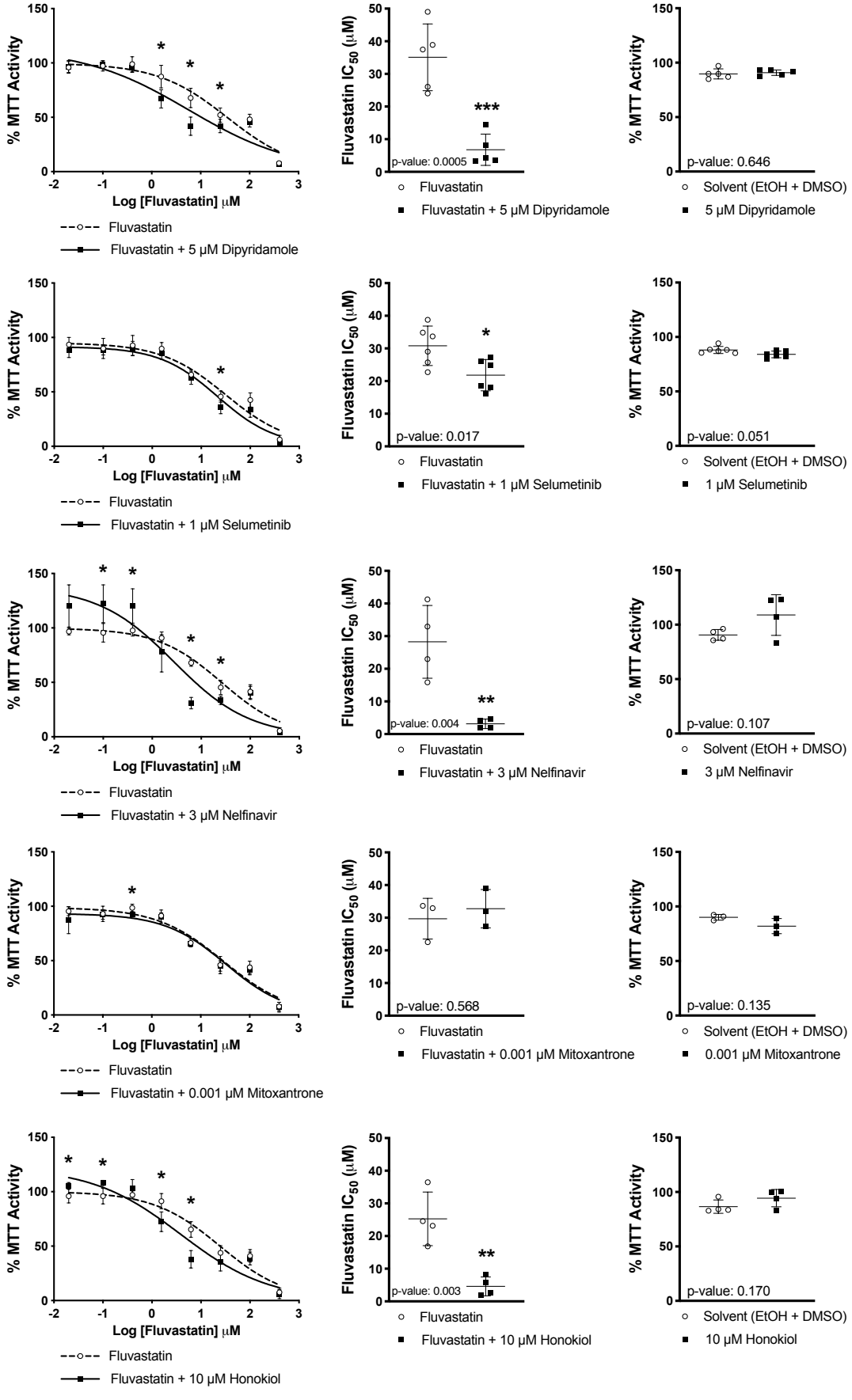

FIGURE 2

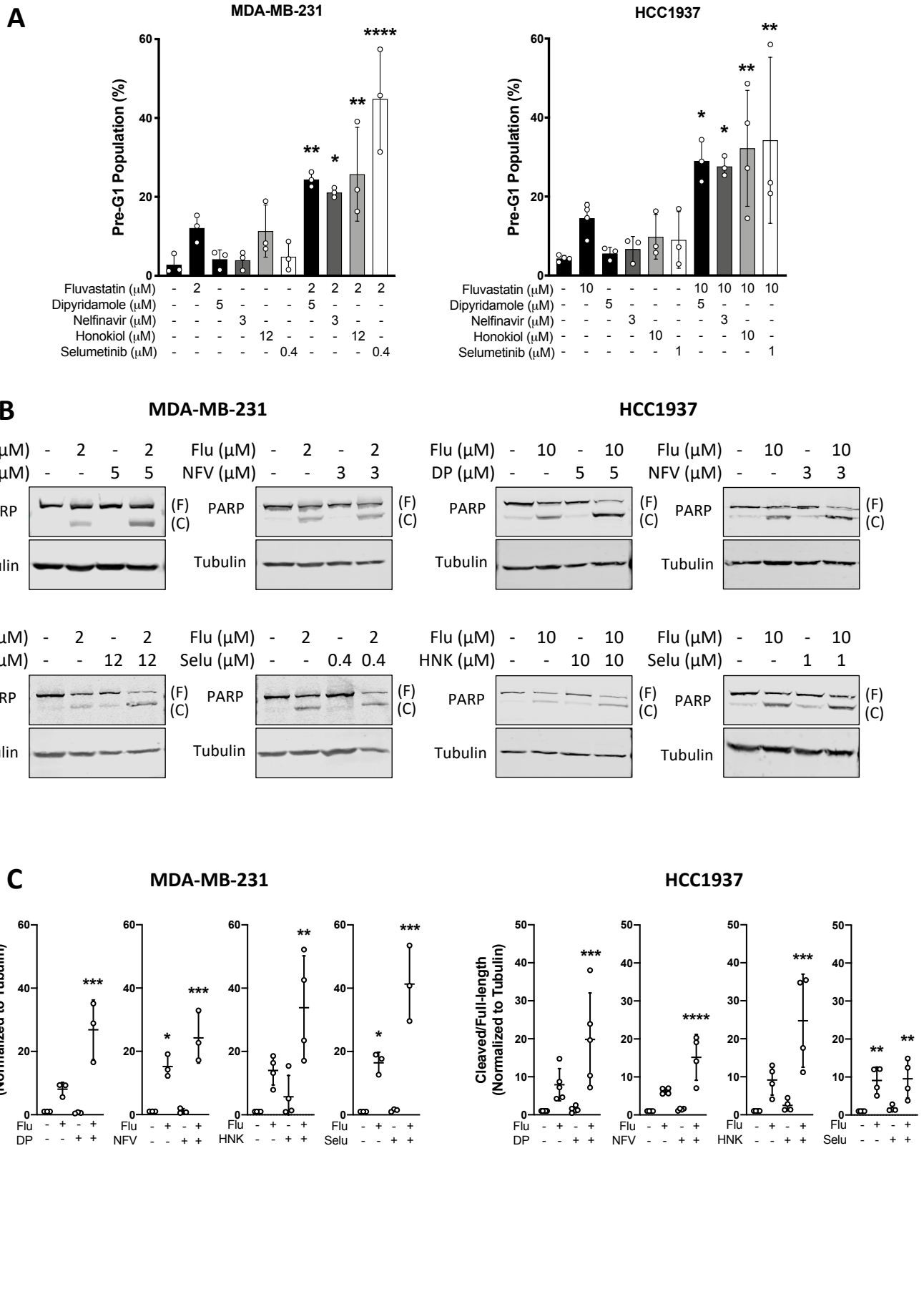
A
MDA-MB-231
Pre-G1 Population (%)
Fluvastatin (μM) - 2 - - - - 2 2 2 2
Dipyridamole (μM) - - 5 - - - 5 - - -
Nelfinavir (μM) - - - 3 - - - 3 - -
Honokiol (μM) - - - - 12 - - - 12 -
Selumetinib (μM) - - - - - 0.4 - - - 0.4
HCC1937
Pre-G1 Population (%)
Fluvastatin (μM) - 10 - - - - 10 10 10 10
Dipyridamole (μM) - - 5 - - - 5 - - -
Nelfinavir (μM) - - - 3 - - - 3 - -
Honokiol (μM) - - - - 10 - - - 10 -
Selumetinib (μM) - - - - - 1 - - - 1
B
MDA-MB-231
Flu (μM) - 2 - 2
DP (μM) - - 5 5
NFV (μM) - - 3 3
HNK (μM) - - 12 12
Selu (μM) - - 0.4 0.4
PARP
(F)
(C)
Tubulin
HCC1937
Flu (μM) - 10 - 10
DP (μM) - - 5 5
NFV (μM) - - 3 3
HNK (μM) - - 10 10
Selu (μM) - - 1 1
C
MDA-MB-231
Cleaved/Full-length (Normalized to Tubulin)
Flu
DP
NFV
HNK
Selu
HCC1937

FIGURE 3

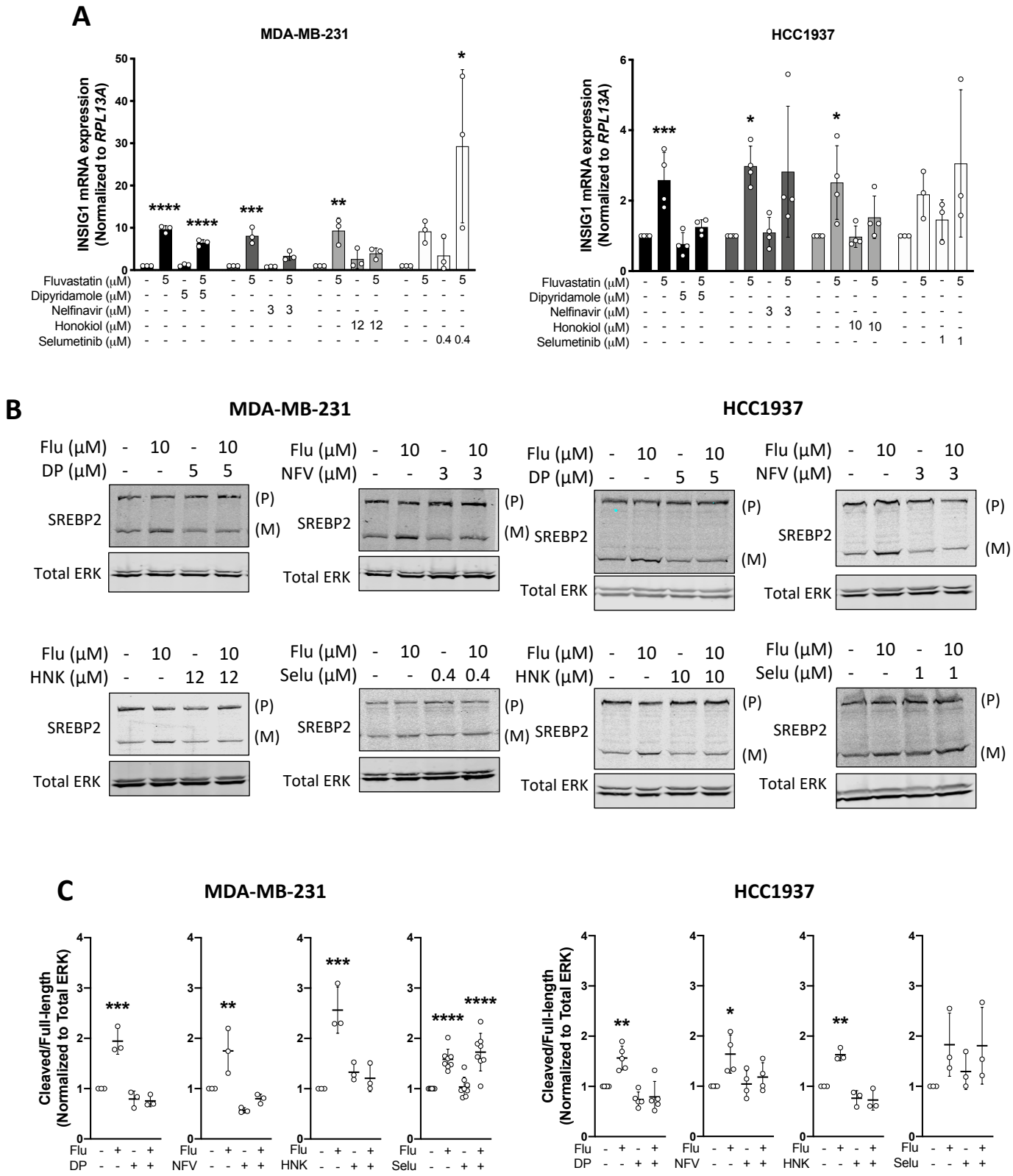
A
MDA-MB-231
HCC1937
INSIG1 mRNA expression (Normalized to RPL13A)
Fluvastatin (μM)
Dipyridamole (μM)
Nelfinavir (μM)
Honokiol (μM)
Selumetinib (μM)
B
MDA-MB-231
HCC1937
Flu (μM)
DP (μM)
NFV (μM)
HNK (μM)
Selu (μM)
SREBP2
(P)
(M)
Total ERK
C
MDA-MB-231
HCC1937
Cleaved/Full-length (Normalized to Total ERK)
Flu
DP
NFV
HNK
Selu

SUPP FIGURE 5

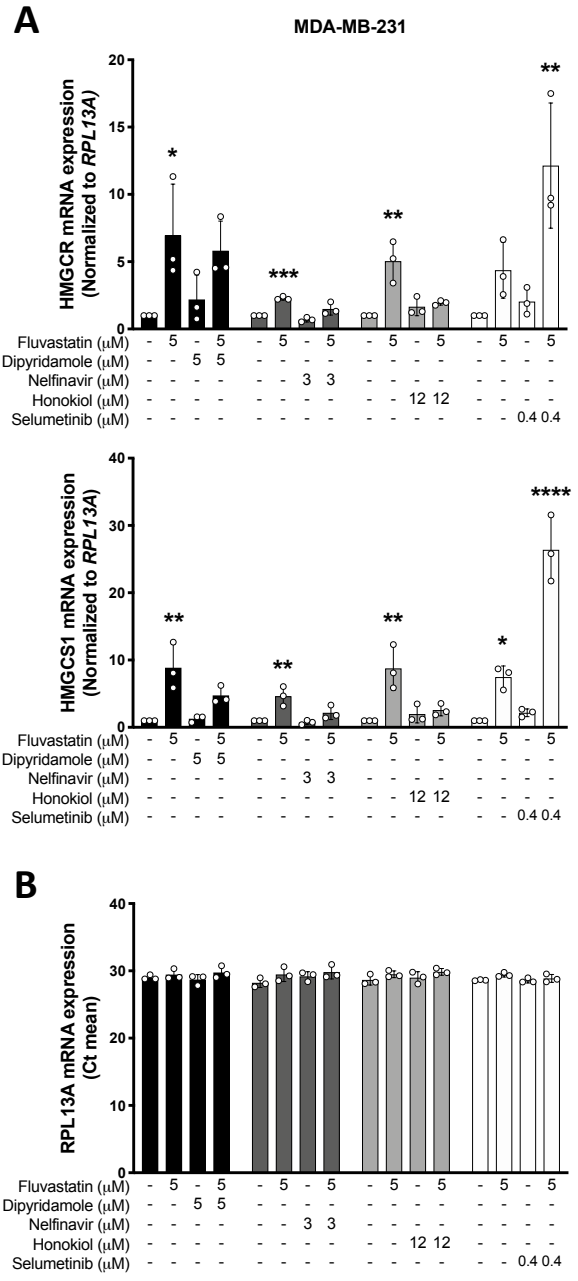

SUPP FIG 6

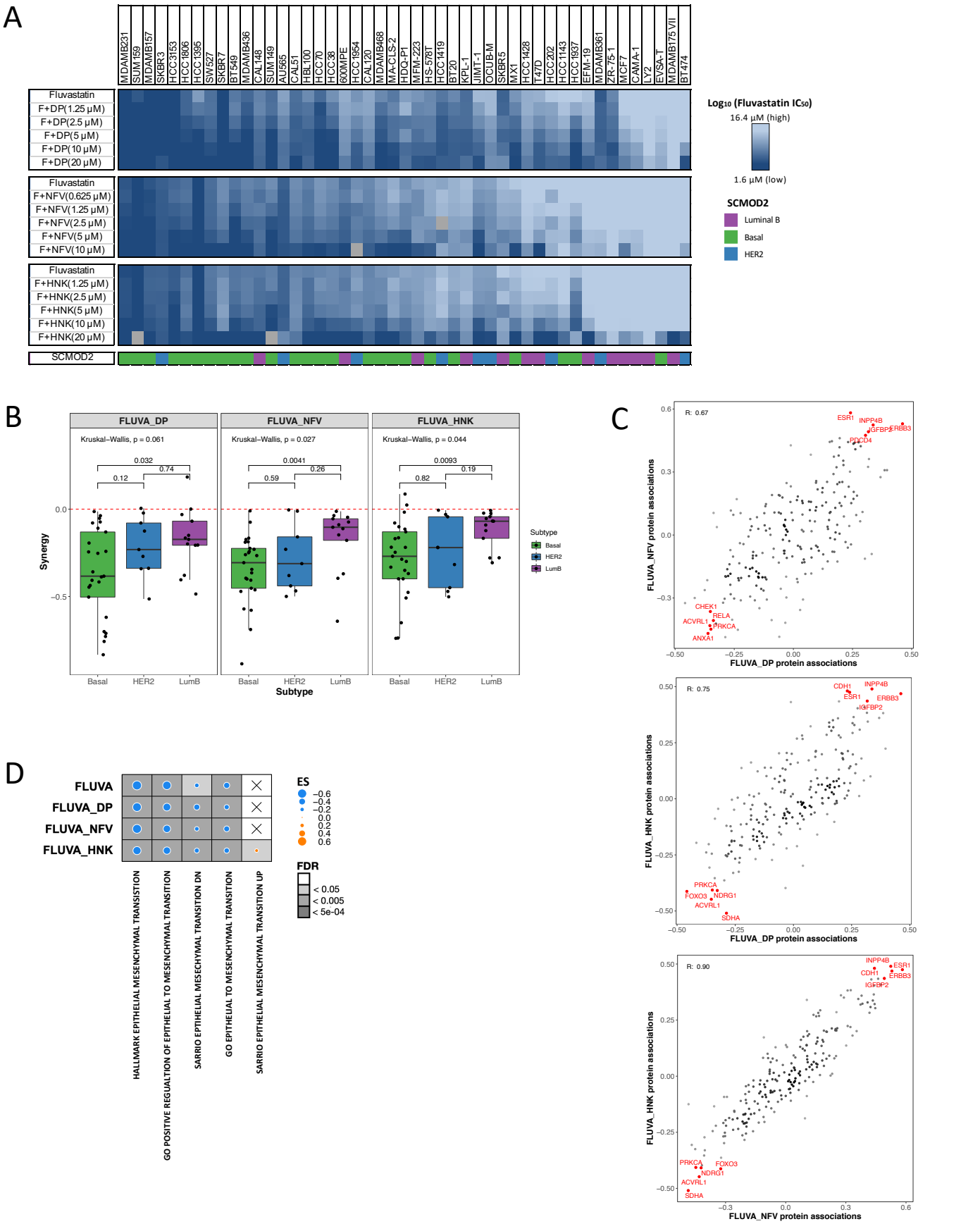
A
MDAMB231
SUM159
MDAMB157
SKBR3
HCC3153
HCC1806
HCC1395
SW527
SKBR7
BT549
MDAMB436
CAL148
SUM149
AU565
CAL51
HBL100
HCC70
HCC38
600MPE
HCC1954
CAL120
MDAMB468
MA-CLS-2
HDQ-P1
MFM-223
HS-578T
HCC1419
BT20
KPL-1
JIMT-1
OCUB-M
SKBR5
MX1
HCC1428
T47D
HCC202
HCC1143
HCC1937
EFM-19
MDAMB361
ZR-75-1
MCF7
CAMA-1
LY2
EVSA-T
MDAMB175.VII
BT474
Fluvastatin
F+DP(1.25 μM)
F+DP(2.5 μM)
F+DP(5 μM)
F+DP(10 μM)
F+DP(20 μM)
F+NFV(0.625 μM)
F+NFV(1.25 μM)
F+NFV(2.5 μM)
F+NFV(5 μM)
F+NFV(10 μM)
F+HNK(1.25 μM)
F+HNK(2.5 μM)
F+HNK(5 μM)
F+HNK(10 μM)
F+HNK(20 μM)
SCMOD2
Log10 (Fluvastatin IC50)
16.4 μM (high)
1.6 μM (low)
SCMOD2
Luminal B
Basal
HER2
B
FLUVA_DP
FLUVA_NFV
FLUVA_HNK
Kruskal–Wallis, p = 0.061
Kruskal–Wallis, p = 0.027
Kruskal–Wallis, p = 0.044
0.032
0.74
0.12
0.0041
0.26
0.59
0.0093
0.19
0.82
Synergy
Basal
HER2
LumB
Subtype
C
R: 0.67
FLUVA_NFV protein associations
FLUVA_DP protein associations
ESR1
INPP4B
IGFBP2
ERBB3
PDCD4
CHEK1
RELA
ACVRL1
PRKCA
ANXA1
R: 0.75
FLUVA_HNK protein associations
CDH1
PRKCA
FOXO3
NDRG1
ACVRL1
SDHA
R: 0.90
D
FLUVA
FLUVA_DP
FLUVA_NFV
FLUVA_HNK
ES
FDR
< 0.05
< 0.005
< 5e-04
HALLMARK EPITHELIAL MESENCHYMAL TRANSITION
GO POSITIVE REGULATION OF EPITHELIAL TO MESENCHYMAL TRANSITION
SARRIO EPITHELIAL MESECHYMAL TRANSITION DN
GO EPITHELIAL TO MESENCHYMAL TRANSITION
SARRIO EPITHELIAL MESENCHYMAL TRANSITION UP

FIGURE 4

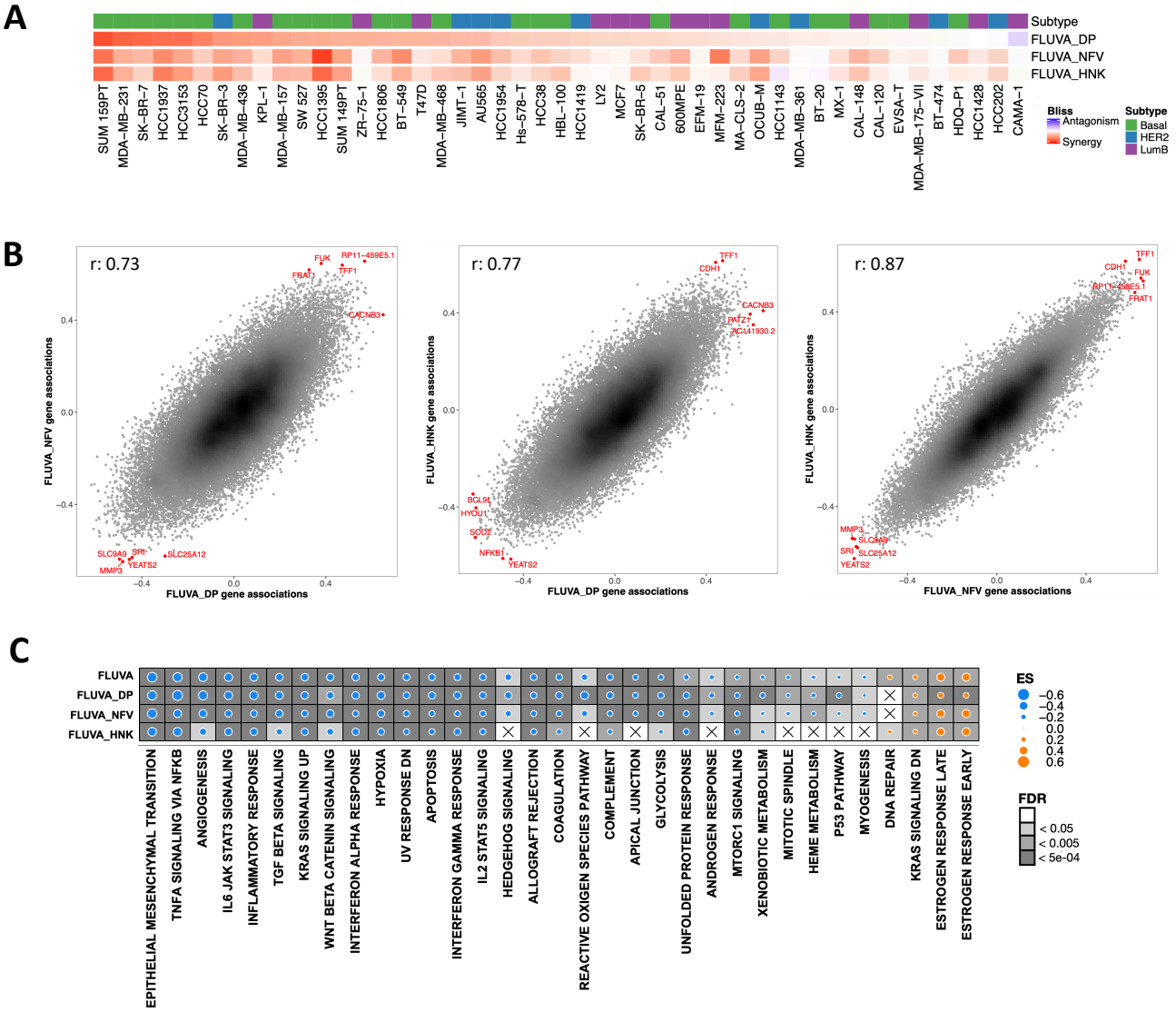
A
Subtype
FLUVA_DP
FLUVA_NFV
FLUVA_HNK
SUM 159PT
MDA−MB−231
SK−BR−7
HCC1937
HCC3153
HCC70
SK−BR−3
MDA−MB−436
KPL−1
MDA−MB−157
SW 527
HCC1395
SUM 149PT
ZR−75−1
HCC1806
BT−549
T47D
MDA−MB−468
JIMT−1
AU565
HCC1954
Hs−578−T
HCC38
HBL−100
HCC1419
LY2
MCF7
SK−BR−5
CAL−51
600MPE
EFM−19
MFM−223
MA−CLS−2
OCUB−M
HCC1143
MDA−MB−361
BT−20
MX−1
CAL−148
CAL−120
EVSA−T
MDA−MB−175−VII
BT−474
HDQ−P1
HCC1428
HCC202
CAMA−1
Bliss
Antagonism
Synergy
Subtype
Basal
HER2
LumB
B
r: 0.73
FLUVA_NFV gene associations
FLUVA_DP gene associations
FUK
RP11−459E5.1
FRAT1
TFF1
CACNB3
SLC9A9
SRI
SLC25A12
YEATS2
MMP3
r: 0.77
FLUVA_HNK gene associations
FLUVA_DP gene associations
TFF1
CDH1
CACNB3
RAPZ1
AC141930.2
BCL9L
HYOU1
SCD2
NFKB1
YEATS2
r: 0.87
FLUVA_HNK gene associations
FLUVA_NFV gene associations
TFF1
CDH1
FUK
RP11−459E5.1
FRAT1
MMP3
SLC9A9
SRI
SLC25A12
YEATS2
C
FLUVA
FLUVA_DP
FLUVA_NFV
FLUVA_HNK
EPITHELIAL MESENCHYMAL TRANSITION
TNFA SIGNALING VIA NFKB
ANGIOGENESIS
IL6 JAK STAT3 SIGNALING
INFLAMMATORY RESPONSE
TGF BETA SIGNALING
KRAS SIGNALING UP
WNT BETA CATENIN SIGNALING
INTERFERON ALPHA RESPONSE
HYPOXIA
UV RESPONSE DN
APOPTOSIS
INTERFERON GAMMA RESPONSE
IL2 STAT5 SIGNALING
HEDGEHOG SIGNALING
ALLOGRAFT REJECTION
COAGULATION
REACTIVE OXIGEN SPECIES PATHWAY
COMPLEMENT
APICAL JUNCTION
GLYCOLYSIS
UNFOLDED PROTEIN RESPONSE
ANDROGEN RESPONSE
MTORC1 SIGNALING
XENOBIOTIC METABOLISM
MITOTIC SPINDLE
HEME METABOLISM
P53 PATHWAY
MYOGENESIS
DNA REPAIR
KRAS SIGNALING DN
ESTROGEN RESPONSE LATE
ESTROGEN RESPONSE EARLY
ES
−0.6
−0.4
−0.2
0.0
0.2
0.4
0.6
FDR
< 0.05
< 0.005
< 5e-04

SUPP FIG 7

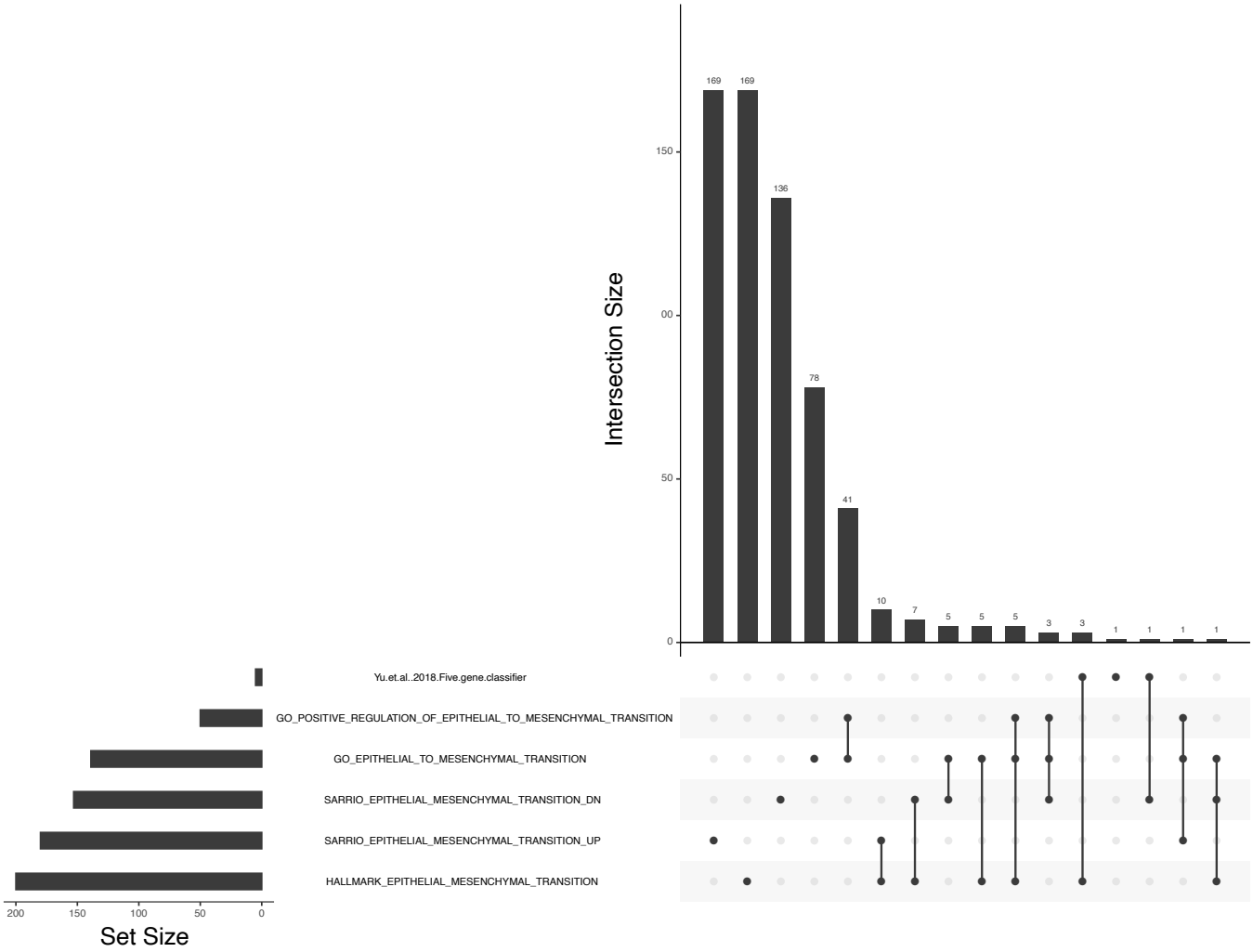
Intersection Size
169
169
136
78
41
10
7
5
5
5
3
3
1
1
1
1
150
00
50
0
Yu.et.al..2018.Five.gene.classifier
GO_POSITIVE_REGULATION_OF_EPITHELIAL_TO_MESENCHYMAL_TRANSITION
GO_EPITHELIAL_TO_MESENCHYMAL_TRANSITION
SARRIO_EPITHELIAL_MESENCHYMAL_TRANSITION_DN
SARRIO_EPITHELIAL_MESENCHYMAL_TRANSITION_UP
HALLMARK_EPITHELIAL_MESENCHYMAL_TRANSITION
200
150
100
50
0
Set Size

SUPP FIG 8

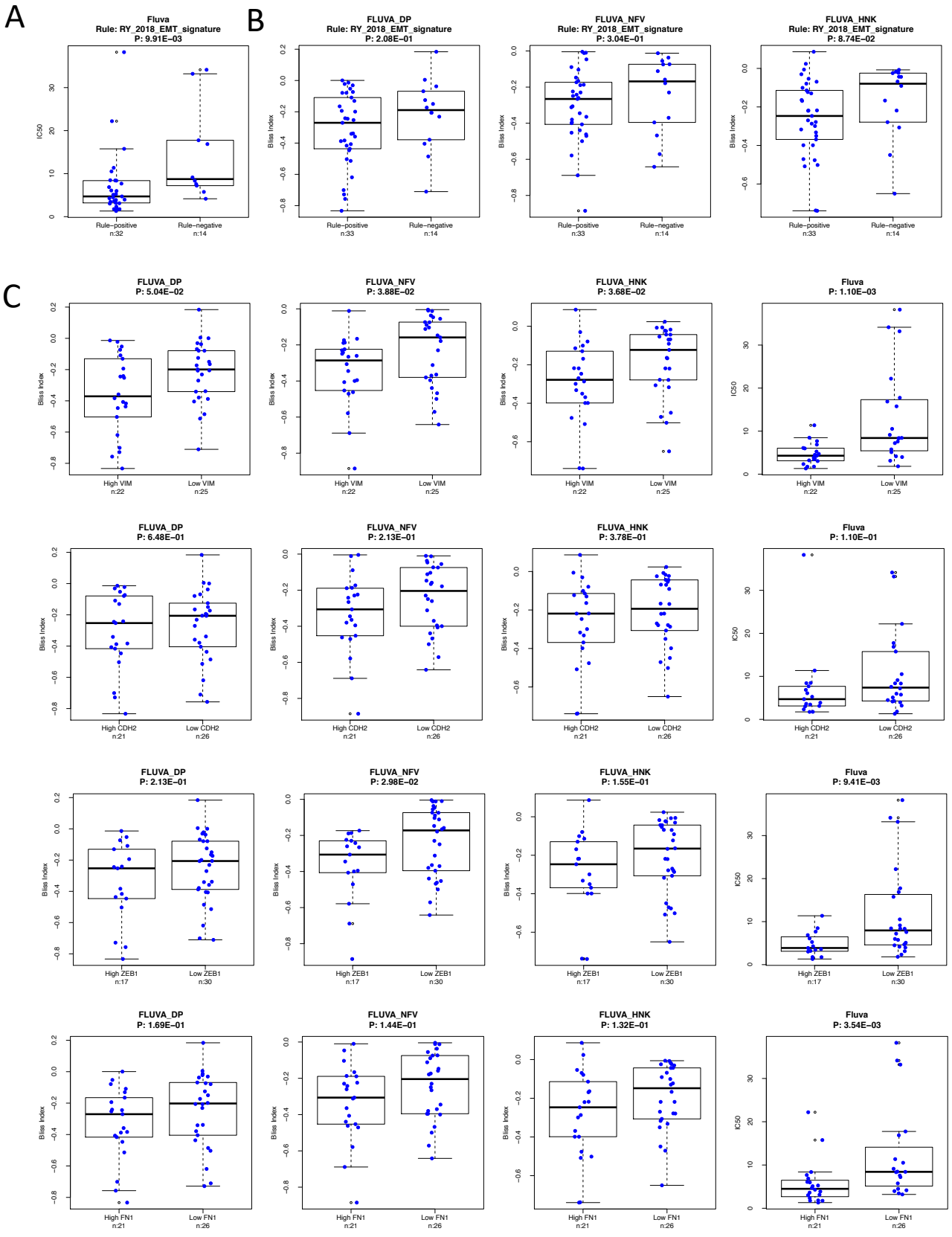
A
Fluva
Rule: RY_2018_EMT_signature
P: 9.91E−03
IC50
Rule−positive
n:32
Rule−negative
n:14
B
FLUVA_DP
Rule: RY_2018_EMT_signature
P: 2.08E−01
FLUVA_NFV
Rule: RY_2018_EMT_signature
P: 3.04E−01
FLUVA_HNK
Rule: RY_2018_EMT_signature
P: 8.74E−02
Bliss Index
Rule−positive
n:33
Rule−negative
n:14
C
FLUVA_DP
P: 5.04E−02
FLUVA_NFV
P: 3.88E−02
FLUVA_HNK
P: 3.68E−02
Fluva
P: 1.10E−03
High VIM
n:22
Low VIM
n:25
FLUVA_DP
P: 6.48E−01
FLUVA_NFV
P: 2.13E−01
FLUVA_HNK
P: 3.78E−01
Fluva
P: 1.10E−01
High CDH2
n:21
Low CDH2
n:26
FLUVA_DP
P: 2.13E−01
FLUVA_NFV
P: 2.98E−02
FLUVA_HNK
P: 1.55E−01
Fluva
P: 9.41E−03
High ZEB1
n:17
Low ZEB1
n:30
FLUVA_DP
P: 1.69E−01
FLUVA_NFV
P: 1.44E−01
FLUVA_HNK
P: 1.32E−01
Fluva
P: 3.54E−03
High FN1
n:21
Low FN1
n:26

FIGURE 5

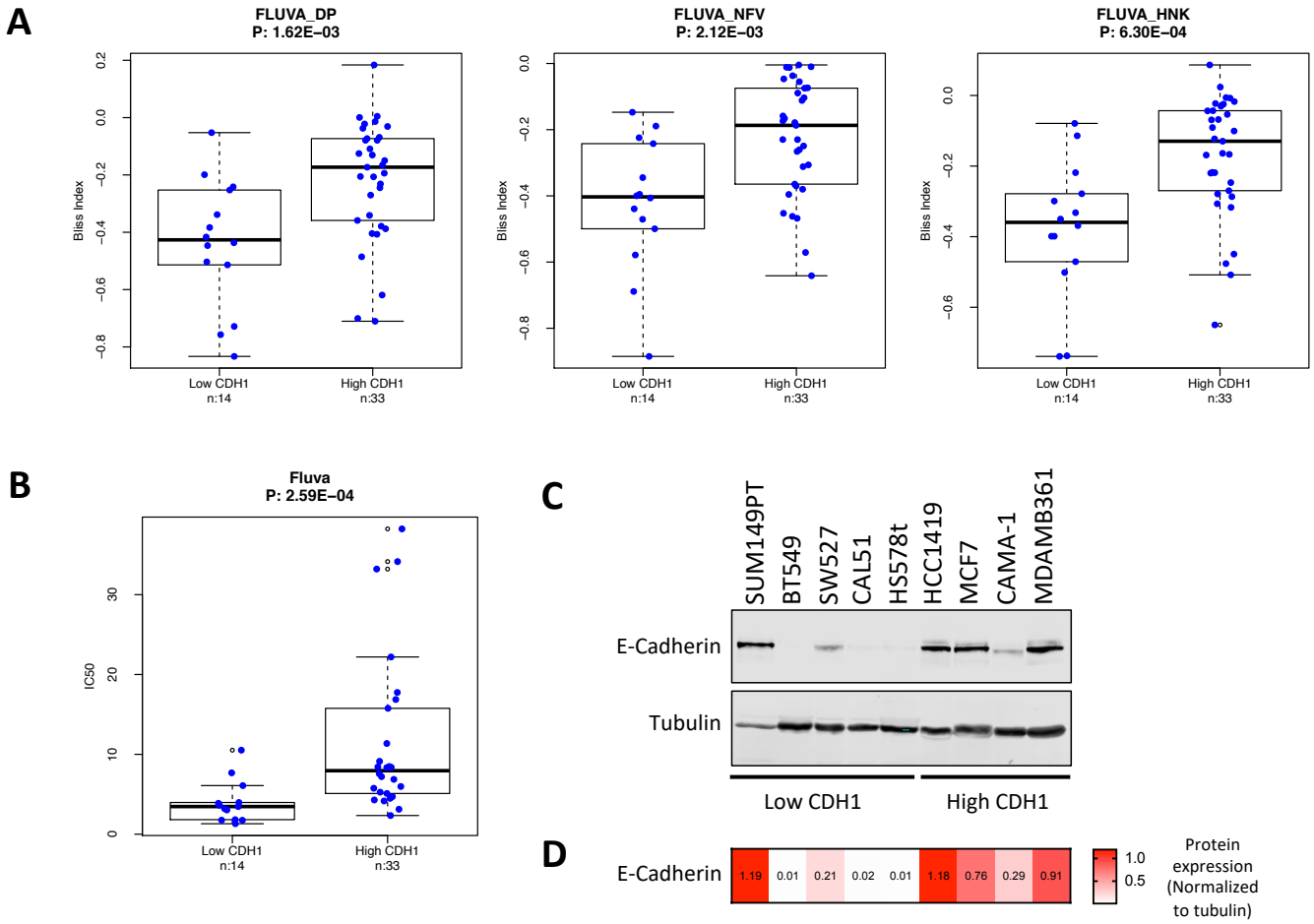
A
FLUVA_DP
P: 1.62E−03
FLUVA_NFV
P: 2.12E−03
FLUVA_HNK
P: 6.30E−04
Bliss Index
Low CDH1
n:14
High CDH1
n:33
B
Fluva
P: 2.59E−04
IC50
C
SUM149PT
BT549
SW527
CAL51
HS578t
HCC1419
MCF7
CAMA-1
MDAMB361
E-Cadherin
Tubulin
Low CDH1
High CDH1
D
E-Cadherin
1.19
0.01
0.21
0.02
0.01
1.18
0.76
0.29
0.91
1.0
0.5
Protein expression (Normalized to tubulin)

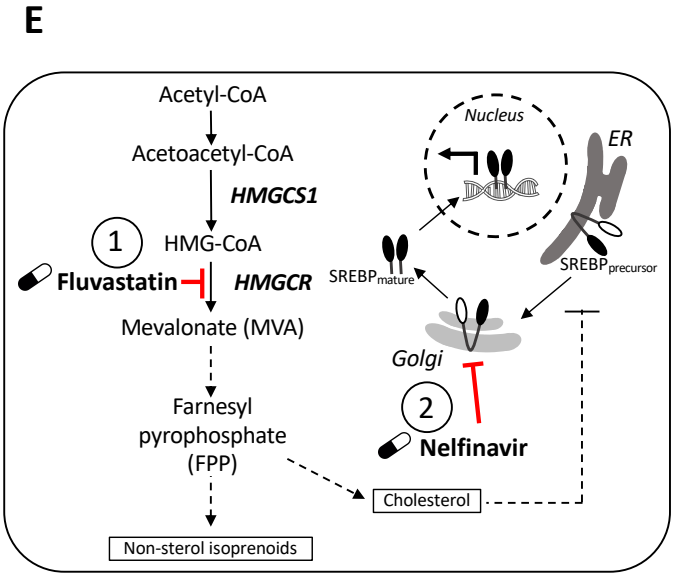
E
Acetyl-CoA
Acetoacetyl-CoA
HMGCS1
1
HMG-CoA
Fluvastatin
HMGCR
Mevalonate (MVA)
Farnesyl pyrophosphate (FPP)
Non-sterol isoprenoids
Nucleus
ER
SREBP mature
SREBP precursor
Golgi
2
Nelfinavir
Cholesterol

SUPP TABLE 1

Hits	Permutation Test		Currently used in humans	Currently used in cancer treatment	In clincal trials for cancer treatment	Pre-clinical	Research tool	Exclude	Classification
	Z-Score	P-Value*							
SELUMETINIB	-3.57	1.77E-04	+		+				RAF/MEK inhibitor
NELFINAVIR	-3.28	5.18E-04	+		+				Antiretroviral
MITOXANTRONE	-3.20	6.82E-04	+	+	+				Anthracycline
DOXORUBICIN	-3.03	1.22E-03	+	+	+				Anthracycline
HONOKIOL	-2.96	1.53E-03				+			Natural product
CLOTRIMAZOLE	-2.95	1.57E-03	+						Antifungal
SULFATHIAZOLE	-2.89	1.90E-03				+			Antibiotic
VEMURAFENIB	-2.67	3.79E-03	+	+	+				RAF/MEK inhibitor
CHROMOMYCINA3	-2.64	4.13E-03				+	+	Toxin	Antibiotic
BACCATINIII	-2.53	5.69E-03				+			Natural product
NOSCAPINE	-2.51	6.11E-03			+	+			Natural product
METHOTREXATE	-2.29	1.11E-02	+	+	+				Antimetabolite
CADMIUMCHLORIDE	-2.22	1.33E-02				+	+	Carcinogen	Other
RHAMNETIN	-2.18	1.45E-02				+			Natural product
PENTAMIDINE	-2.18	1.46E-02	+		+				Antifungal
EMODIN	-2.16	1.55E-02				+			Natural product
FLUOROURACIL	-2.11	1.75E-02	+	+	+				Antimetabolite
TRYPTOPHAN	-1.92	2.76E-02	+		+				Other
ALVOCIDIB	-1.82	3.44E-02	+	+	+				CDK inhibitor
ABIRATERONE	-1.77	3.81E-02	+	+	+				Antiandrogen
THAPSIGARGIN	-1.71	4.36E-02				+			Other
KINETINRIBOSIDE	-1.66	4.84E-02				+			Other
ELLIPTICINE	-1.65	4.92E-02				+			Natural product

* Table ordered by p-value

Molecular Oncology

FEBS PRESS science publishing by scientists

Cyclic AMP-hydrolyzing phosphodiesterase inhibitors potentiate statin-induced cancer cell death

Joseph Longo[1,2], Aleksandra A. Pandyra[1,2,3,4], Paweł Stachura[3], Mark D. Minden[1,2], Aaron D. Schimmer[1,2] and Linda Z. Penn[1,2]

1 Princess Margaret Cancer Centre, University Health Network, Toronto, Canada
2 Department of Medical Biophysics, University of Toronto, Toronto, Canada
3 Department of Molecular Medicine II, Medical Faculty, Heinrich Heine University, Düsseldorf, Germany
4 Department of Gastroenterology, Hepatology, and Infectious Diseases, Heinrich Heine University, Düsseldorf, Germany

Keywords
cilostazol; dipyridamole; mevalonate pathway; phosphodiesterase inhibitor; SREBP2; statins

Correspondence
L. Z. Penn, Princess Margaret Cancer Centre, University Health Network, Princess Margaret Cancer Research Tower, 101 College Street, 13-706, Toronto, ON M5G 1L7, Canada
Tel: +1 416 634 8770
E-mail: lpenn@uhnresearch.ca

Joseph Longo and Aleksandra A. Pandyra contributed equally to this work

(Received 17 February 2020, revised 13 July 2020, accepted 30 July 2020)

doi:10.1002/1878-0261.12775

Dipyridamole, an antiplatelet drug, has been shown to synergize with statins to induce cancer cell-specific apoptosis. However, given the polypharmacology of dipyridamole, the mechanism by which it potentiates statin-induced apoptosis remains unclear. Here, we applied a pharmacological approach to identify the activity of dipyridamole specific to its synergistic anticancer interaction with statins. We evaluated compounds that phenocopy the individual activities of dipyridamole and assessed whether they could potentiate statin-induced cell death. Notably, we identified that a phosphodiesterase (PDE) inhibitor, cilostazol, and other compounds that increase intracellular cyclic adenosine monophosphate (cAMP) levels potentiate statin-induced apoptosis in acute myeloid leukemia and multiple myeloma cells. Additionally, we demonstrated that both dipyridamole and cilostazol further inhibit statin-induced activation of sterol regulatory element-binding protein 2, a known modulator of statin sensitivity, in a cAMP-independent manner. Taken together, our data support that PDE inhibitors such as dipyridamole and cilostazol can potentiate statin-induced apoptosis via a dual mechanism. Given that several PDE inhibitors are clinically approved for various indications, they are immediately available for testing in combination with statins for the treatment of hematological malignancies.

1. Introduction

The synthesis of cholesterol and other isoprenoids via the mevalonate (MVA) pathway is tightly regulated to maintain homeostasis. In many cancer cells, an increased dependency on isoprenoid biosynthesis for growth and survival confers sensitivity to the statin family of drugs, which inhibits the rate-limiting enzyme of the MVA pathway, HMG-CoA reductase (HMGCR) [1]. However, in normal cells and many cancer cells, treatment with statins activates the transcription factor sterol regulatory element-binding protein 2 (SREBP2), which functions to upregulate genes involved in MVA metabolism to restore homeostasis. Activation of this feedback response has been associated with statin resistance in cancer cells [2–4]. In contrast, subsets of cancer cells that do not induce this feedback loop following statin treatment readily undergo apoptosis [2,4].

Abbreviations
AML, acute myeloid leukemia; ANOVA, analysis of variance; cAMP, cyclic adenosine monophosphate; cGMP, cyclic guanosine monophosphate; GGPP, geranylgeranyl pyrophosphate; HMG-CoA, 3-hydroxy-3-methylglutaryl coenzyme A; HMGCR, HMG-CoA reductase; MM, multiple myeloma; MVA, mevalonate; PDE, phosphodiesterase; PKA, protein kinase A; qRT–PCR, quantitative reverse transcription–PCR; SD, standard deviation; sgRNAs, small guide RNAs; SREBP, sterol regulatory element-binding protein.

We previously demonstrated that inhibition of this feedback response via RNAi-mediated knockdown of SREBP2 potentiates statin-induced cell death in lung and breast cancer cell lines [5]. Moreover, through a drug screening approach, our laboratory identified that the drug dipyridamole, an antiplatelet agent approved for secondary stroke prevention, can synergize with statins to induce apoptosis in acute myeloid leukemia (AML) and multiple myeloma (MM) cells [6]. We further demonstrated that dipyridamole inhibits statin-induced SREBP2 cleavage and activation, thus abrogating the restorative feedback loop of the MVA pathway (Fig. 1) [6]. Since these initial observations in AML and MM, dipyridamole has been shown to inhibit statin-induced SREBP2 activation and potentiate statin-induced cell death in breast [3] and prostate [4] cancer; however, the mechanism by which dipyridamole inhibits SREBP2 and potentiates statin-induced cancer cell death remains poorly characterized.

In this manuscript, we present data to suggest that the synergistic anticancer interaction between statins and dipyridamole is twofold. In part, the ability of dipyridamole to function as a phosphodiesterase (PDE) inhibitor and increase cyclic adenosine monophosphate (cAMP) levels sensitizes cancer cells to statin-induced apoptosis. Additionally, dipyridamole and another cAMP-hydrolyzing PDE inhibitor, cilostazol, are able to inhibit statin-induced SREBP2 activity, and thus potentiate the proapoptotic activity of statins through a second, cAMP-independent mechanism. Collectively, these data warrant further investigation into the combination of a statin and cAMP-hydrolyzing PDE inhibitor for the treatment of hematological malignancies.

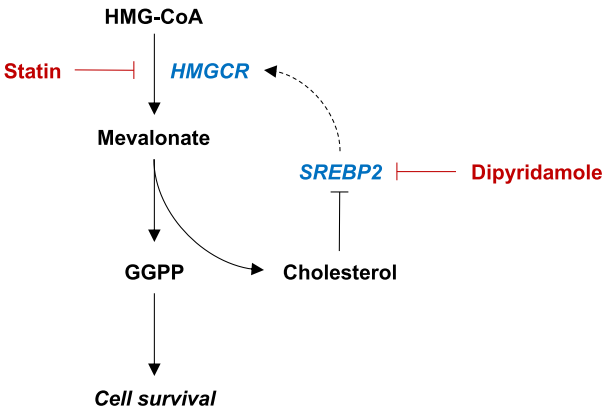

Fig. 1. Dipyridamole inhibits the sterol-regulated feedback loop of the MVA pathway. Schematic representation of the MVA pathway. Statins inhibit the rate-limiting enzyme of the pathway, HMGCR, which catalyzes the conversion of HMG-CoA to MVA. MVA is subsequently used to synthesize various metabolites that are important for cell growth and survival, including GGPP and cholesterol. Statin-mediated cholesterol depletion induces the cleavage and activation of SREBP2, which in turn induces the transcription of genes involved in MVA metabolism to restore homeostasis. We previously identified that the drug dipyridamole can inhibit statin-induced SREBP2 activation; however, the mechanism by which dipyridamole inhibits SREBP2 cleavage remains poorly understood.

2. Materials and methods

2.1. Cell culture and compounds

KMS11, LP1, OCI-AML-2, and OCI-AML-3 cell lines were cultured as described previously [6]. S49 wild-type (CCLZR352) and kin- (CCLZR347) cells were purchased from the University of California, San Francisco (UCSF) Cell Culture Facility and were cultured in Dulbecco's modified Eagle medium supplemented with 10% heat-inactivated horse serum, 100 units·mL^{-1} penicillin, and 100 μg·mL^{-1} streptomycin. Cell lines were routinely confirmed to be mycoplasma-free using the MycoAlert Mycoplasma Detection Kit (Lonza, Mississauga, Canada). Atorvastatin calcium (21CEC Pharmaceuticals Ltd., Markham, Canada) and fluvastatin sodium (US Biological, Burlington, Canada) were dissolved in ethanol. Dipyridamole (Sigma, Oakville, Canada), cilostazol (Tocris Bioscience, Burlington, Canada), *S*-(4-nitrobenzyl)-6-thioinosine (NBMPR) (Tocris Bioscience), 4-{[3′,4′-(methylenedioxy)benzyl] amino}-6-methoxyquinazoline (MBMQ) (Calbiochem, Oakville, Canada), fasentin (Sigma), and forskolin (Sigma) were dissolved in DMSO. Mevalonate and dibutyryl-cAMP (db-cAMP) were purchased from Sigma and dissolved in water. Geranylgeranyl pyrophosphate (GGPP) (methanol : ammonia solution) was purchased from Sigma.

2.2. Cell viability assays

3-(4,5-Dimethylthiazol-2-yl)-2,5-diphenyltetrazolium bromide (MTT) assays were performed as previously described [7]. Briefly, cells were seeded at 15 000–20 000 cells/well in 96-well plates and treated as indicated for 48 h. Percent cell viability was calculated relative to cells treated with solvent control(s). Fluvastatin dose–response curves were plotted, and area under the dose–response curve (AUC) values were computed using GRAPHPAD PRISM v6 software (San Diego, CA, USA).

2.3. Cell death assays

Cells were seeded at 750 000 cells/well in 6-well plates and treated as indicated for 48 h. For propidium

iodide (PI) staining, cells were fixed in 70% ethanol for at least 24 h, stained with PI, and analyzed by flow cytometry for the % pre-G1 DNA population as a measure of cell death, as previously described [2]. For Annexin V staining, cells were processed and stained using the Annexin V-FITC Apoptosis Kit (BioVision Inc., Burlington, Canada) as per the manufacturer's protocol, or washed and stained as indicated in Annexin V Binding Buffer (BD Biosciences, Mississauga, Canada). Apoptosis assays using primary AML cells were performed as described previously [6]. Patient samples were obtained with informed consent under a protocol approved by the University Health Network Research Ethics Board in accordance with the Declaration of Helsinki.

2.4. CCLE data mining

RNA sequencing data for the selected AML and MM human cell lines from the Cancer Cell Line Encyclopedia (CCLE) [8] were analyzed using the UCSC Xena Functional Genomics Explorer (https://xenabrowser.net/) [9].

2.5. CRISPR/Cas9-mediated gene knockout

Independent small guide RNAs (sgRNAs) that target *PRKACA* were cloned into lentiCRISPR v2 (Addgene plasmid #52961, Watertown, MA, USA). A sgRNA targeting a random locus on chromosome 10 was used as a negative control. HEK-293Tv cells were co-transfected with the sgRNA constructs, pMD2.G and psPAX2 using calcium-phosphate. LP1 cells were transduced with the lentiviral supernatants in the presence of 8 $\mu g \cdot mL^{-1}$ polybrene, after which they were selected with 1 $\mu g \cdot mL^{-1}$ puromycin. The sequences for the sgRNAs were obtained from Ref. [10] and are as follows:

gC10 Random: AAACATGTATAACCCTGCGC
gPRKACA #1: ACGAATCAAGACCCTCGGCA
gPRKACA #2: AGATGTTCTCACACCTACGG

2.6. Immunoblotting

For proteins other than HMGCR, immunoblotting was performed as previously described [4], using the following primary antibodies: SREBP2 (1 : 250; BD Biosciences, 557037), Actin (1 : 3000; Sigma, A2066), PKA C-α (1 : 1000; Cell Signaling Technology, #4782), α-Tubulin (1 : 3000; Calbiochem, CP06), and Ku80 (1 : 3000; Cell Signaling Technology, #2180). For HMGCR immunoblots, cells were seeded at 750 000 cells/well in 6-well plates and treated as indicated for 24 h. Whole cell lysates were prepared by washing cells twice with cold PBS and lysing cells in ~ 80 μL of buffer (20 mM Tris pH 7.5, 150 mM NaCl, 1 mM EDTA, 1 mM EGTA, 0.5% Triton X-100, protease inhibitors) on ice for 30 min. Lysates were cleared by centrifugation and protein concentrations determined using the Pierce 660 nm Protein Assay Kit (Thermo Fisher Scientific). Dithiothreitol (DTT) was added to a final concentration of 1 M. 4x Laemmli sample buffer was then added to the DTT-containing lysates at room temperature. Samples were not boiled to limit aggregation of membrane proteins. Blots were probed with primary antibodies against HMGCR (A9) (1 : 1000; prepared in-house) and actin.

2.7. Quantitative RT–PCR

Total RNA was isolated using TRIzol Reagent (Invitrogen, Mississauga, Canada). cDNA was synthesized from 500 ng RNA using SuperScript III (Invitrogen), or RNA was directly used for RT–PCR analysis using the iTaq Universal Probe One-Step Kit (Bio-Rad, Mississauga, Canada), according to the manufacturer's instructions. Quantitative reverse transcription–PCR (qRT–PCR) was performed using TaqMan probes (Applied Biosystems, Mississauga, Canada) for the following genes: *HMGCR* (Hs00168352), *HMGCS1* (Hs00266810), *INSIG1* (Hs01650979), and *GAPDH* (Hs99999905).

2.8. Intracellular cAMP quantification

Intracellular levels of cAMP were measured using the Cyclic AMP Chemiluminescent Immunoassay Kit (Cell Technology, Hayward, CA, USA) as per the manufacturer's protocol. Briefly, 1.5×10^6 cells/well (6-well plate) were incubated with the compounds as indicated, washed with PBS, and lysed in 150 μL of the provided lysis buffer.

3. Results

3.1. The cAMP-hydrolyzing PDE3 inhibitor cilostazol phenocopies dipyridamole to potentiate statin-induced cancer cell death

Dipyridamole has been reported to have multiple targets and can function as an inhibitor of nucleoside transport [11], glucose uptake [12], and PDEs [13] (Fig. 2A). To test which, if any, of these reported functions of dipyridamole are important for

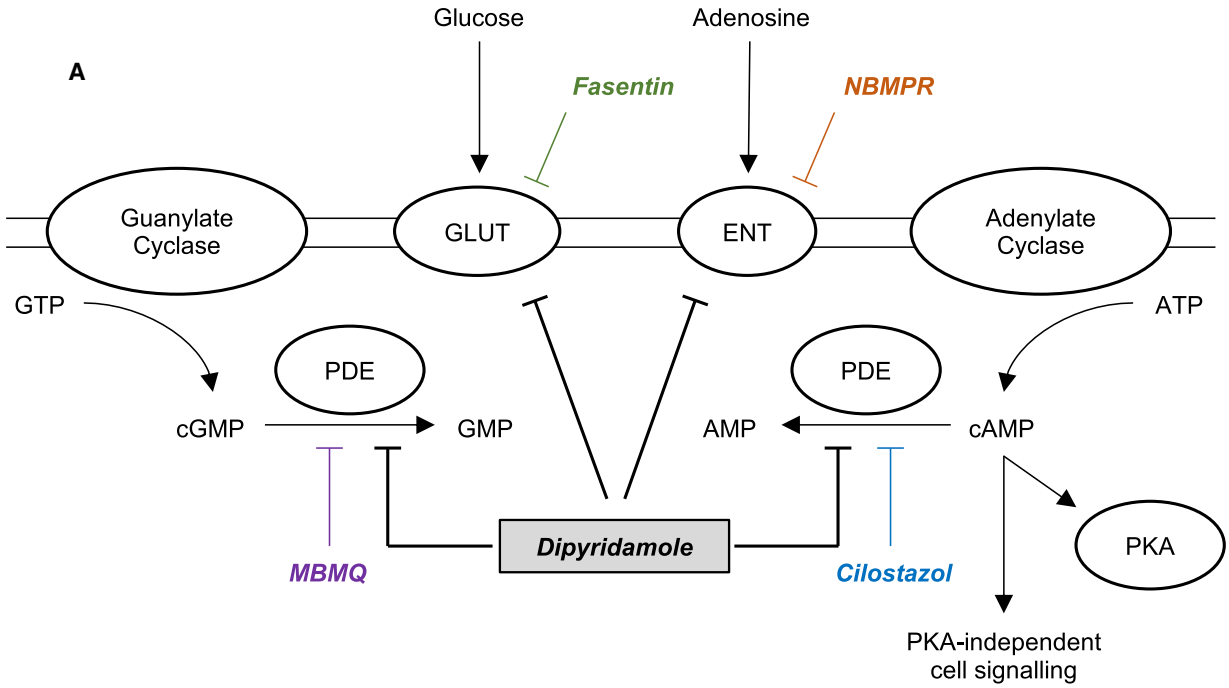

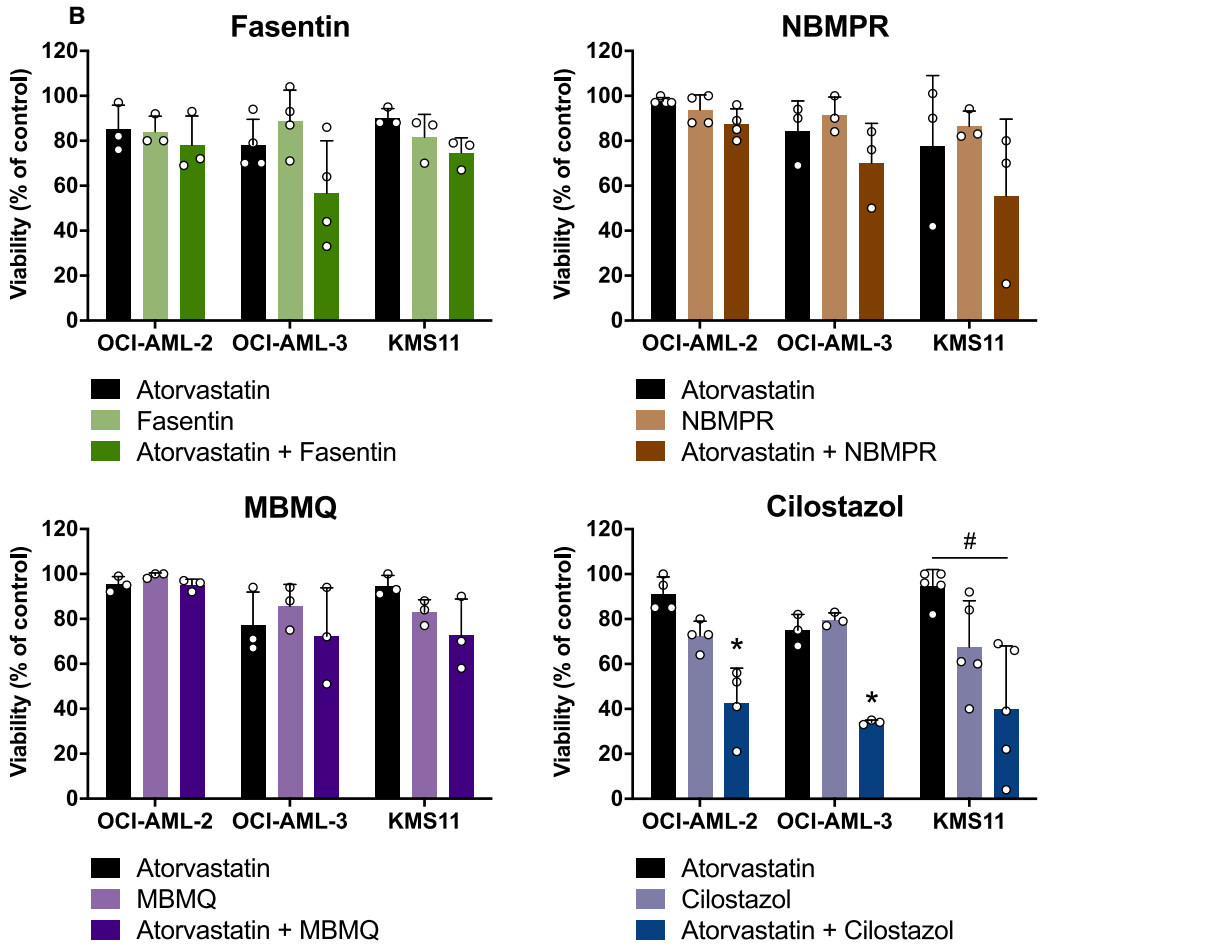

Fig. 2. The cAMP-hydrolyzing PDE3 inhibitor cilostazol phenocopies dipyridamole to potentiate statin-induced cancer cell death. (A) Schematic representation of the reported targets of dipyridamole and additional compounds that target these proteins. ENT, equilibrative nucleoside transporter; GLUT, glucose transporter; PDE, phosphodiesterase; PKA, protein kinase A. (B) OCI-AML-2, OCI-AML-3, and KMS11 cells were treated with atorvastatin (4, 2 and 4 μM for OCI-AML-2, OCI-AML-3, and KMS11 cells, respectively) ± a glucose uptake inhibitor (fasentin; 12.5, 6.3, and 12.5 μM for OCI-AML-2, OCI-AML-3, and KMS11 cells, respectively), ENT inhibitor (NBMPR; 20 μM), cGMP-hydrolyzing PDE5 inhibitor (MBMQ; 10 μM), or cAMP-hydrolyzing PDE3 inhibitor (cilostazol; 25, 12.5, and 25 μM for OCI-AML-2, OCI-AML-3, and KMS11 cells, respectively). After 48 h, cell viability was evaluated by MTT assays. Data are represented as the mean + SD. $*P < 0.05$ (one-way ANOVA with Tukey's multiple comparisons test, where the indicated groups were compared to the other groups of that cell line). $^{\#}P < 0.05$ (one-way ANOVA with Tukey's multiple comparisons test, comparing the two indicated groups).

potentiating statin-induced cancer cell death, we assayed additional compounds with similar activities for their ability to phenocopy dipyridamole. For these experiments, we evaluated the following compounds: NBMPR [equilibrative nucleoside transporter 1 (ENT1) inhibitor], fasentin [glucose transporter 1 (GLUT1) inhibitor], MBMQ (PDE5 inhibitor), and cilostazol (PDE3 inhibitor). AML (OCI-AML-2, OCI-AML-3) and MM (KMS11) cells were treated with each compound alone or in combination with atorvastatin. The concentrations of each compound were chosen such that they had minimal single-agent effects on cell viability (< 20%), but were still within the range known to inhibit the target under investigation [14–20]. Of the four compounds evaluated, only the combination of atorvastatin and cilostazol was observed to decrease AML and MM cell viability in all three cell lines (Fig. 2B). We further demonstrated that these effects were on-target and not specific to atorvastatin, as a similar decrease in cell viability was observed when cilostazol was combined with fluvastatin, another statin drug (Fig. S1). Moreover, the addition of exogenous MVA or GGPP was able to fully rescue the decrease in cell viability caused by the statin–cilostazol combination (Fig. S1), further supporting that these effects were due to MVA pathway inhibition.

3.2. Compounds that increase cAMP levels phenocopy dipyridamole to potentiate statin-induced apoptosis

PDEs catalyze the hydrolysis of cAMP and cyclic guanosine monophosphate (cGMP) (Fig. 2A), thereby regulating the intracellular concentrations of these secondary messengers. There are 11 PDE proteins that can be expressed in mammalian cells, which differ in their cellular functions, structures, expression patterns, and affinities for cAMP and cGMP [21,22]. Dipyridamole is known to inhibit multiple cAMP- and cGMP-hydrolyzing PDEs with varying affinities [13,22]. In contrast, cilostazol is reported to be a specific inhibitor of PDE3, which is a cAMP-hydrolyzing PDE [13,21]. Given our observation that the statin–cilostazol combination was uniquely able to decrease the viability of AML and MM cells, we hypothesized that inhibition of cAMP hydrolysis by dipyridamole may be responsible, at least in part, for its ability to synergize with statins to induce cancer cell death. Indeed, dipyridamole treatment, at the concentration used throughout this study (5 μM), resulted in a 2.5-fold increase in intracellular cAMP levels (Fig. S2).

To evaluate whether the PDEs targeted by dipyridamole and cilostazol are expressed in AML and MM cells, we mined the Cancer Cell Line Encyclopedia (CCLE) database [8]. Indeed, multiple PDEs, including isoforms of PDE3, PDE5, PDE6, PDE7, and PDE8, are highly and consistently expressed in a panel of AML and MM cell lines, including previously characterized statin-sensitive (e.g., KMS11, OCI-AML-3) and insensitive (e.g., LP1) cell lines (Fig. 3A) [6,23,24]. We subsequently evaluated the ability of an adenylate cyclase activator (forskolin) and cell-permeable analog of cAMP (db-cAMP) to potentiate statin-induced apoptosis in AML cells. The combination of fluvastatin and dipyridamole, cilostazol, forskolin, or db-cAMP significantly induced apoptosis in OCI-AML-2 and OCI-AML-3 cells, whereas no significant apoptosis was observed in response to treatment with each cAMP-modulating compound on its own (Fig. 3B). To determine whether primary cells were similarly sensitive to the combination of a statin and PDE inhibitor, we treated primary AML cells with fluvastatin and/or cilostazol for 48 h, after which apoptosis was quantified by Annexin V staining using flow cytometry. Indeed, the fluvastatin–cilostazol combination significantly induced apoptosis in these cells (Fig. 3C). This is consistent with our previous report that the statin–dipyridamole combination can induce apoptosis in primary AML cells [6]. Notably, we evaluated the statin–cilostazol combination in primary cells from three of the same patients as in our previous report with dipyridamole, and observed concordant results [6]. Collectively, these data suggest that elevating intracellular levels of cAMP may be an effective way to

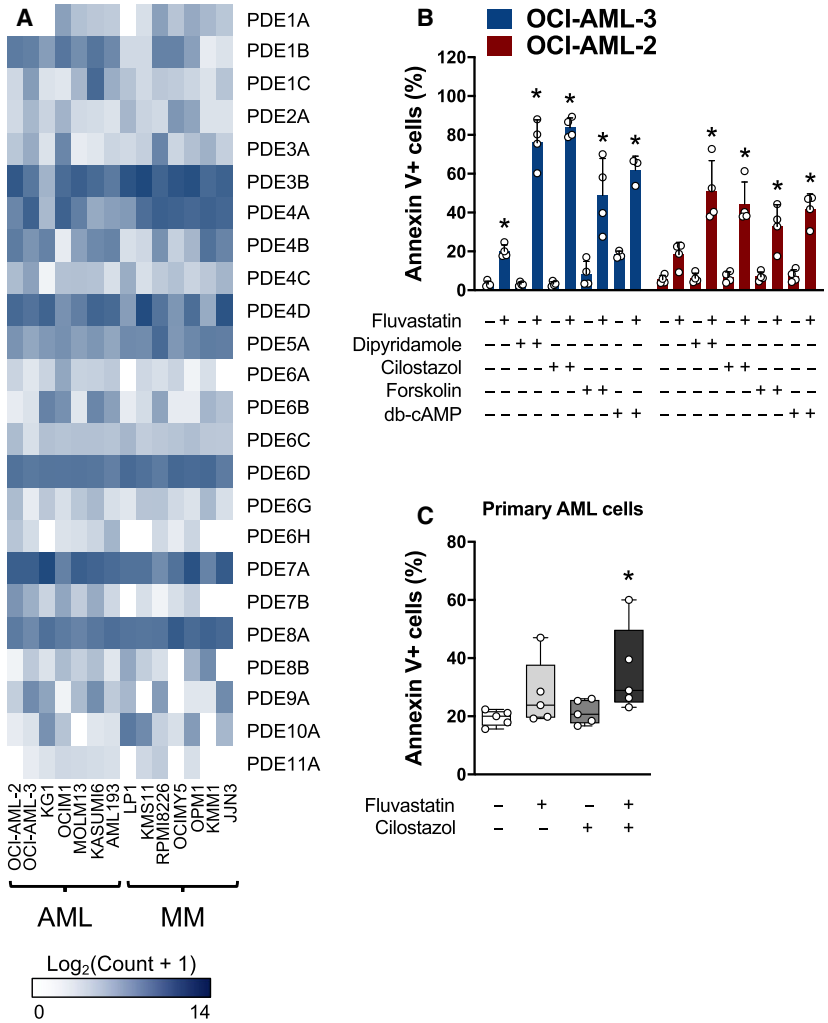

Fig. 3. Compounds that increase cAMP levels phenocopy dipyridamole to potentiate statin-induced apoptosis. (A) RNA expression of the different PDEs in a panel of human AML and MM cell lines. Data were mined from the CCLE database. (B) OCI-AML-2 and OCI-AML-3 cells were treated with fluvastatin (4 μM for OCI-AML-2 and 2 μM for OCI-AML-3) ± a PDE3 inhibitor (cilostazol; 20 μM), an adenylate cyclase activator (forskolin; 10 μM) or db-cAMP (0.1 mM). After 48 h, cells were labeled with FITC-conjugated Annexin V and apoptotic cells were quantified by flow cytometry. $*P < 0.05$ (one-way ANOVA with Dunnett's multiple comparisons test, where the indicated groups were compared to the solvent controls group of that cell line). Data are represented as the mean + SD. (C) Primary AML cells were cultured in the presence of solvent controls, 5 μM fluvastatin, 20 μM cilostazol, or the combination. After 48 h, cells were labeled with FITC-conjugated Annexin V and analyzed by flow cytometry. Data from four independent AML patient samples are represented as box plots with whiskers depicting the maximum and minimum values. $*P < 0.05$ (one-way ANOVA with Dunnett's multiple comparisons test, where the indicated group was compared to the solvent controls group).

sensitize hematological cancer cells to statin-induced apoptosis.

3.3. Compounds that increase cAMP levels differentially modulate sterol metabolism

We previously demonstrated that dipyridamole inhibits statin-induced SREBP2 cleavage and activation, which sensitizes cancer cells to statin-induced apoptosis [4,6]. To test whether compounds that increase cAMP levels similarly inhibit the induction of sterol metabolism gene expression in response to statin treatment, we treated LP1 cells with fluvastatin as a single agent or in combination with a PDE inhibitor (dipyridamole or cilostazol), forskolin or db-cAMP, and then evaluated the expression of three SREBP2 target genes by qRT–PCR: *HMGCR*, HMG-CoA synthase 1 (*HMGCS1*), and insulin-induced gene 1 (*INSIG1*). We chose LP1

cells for these experiments because we previously demonstrated that this cell line robustly activates SREBP2 in response to statin exposure, and cotreatment with dipyridamole sensitizes them to statin-induced apoptosis [6]. As expected, treatment of LP1 cells with fluvastatin resulted in the induction of all three sterol-regulated genes, a response which was completely blocked by dipyridamole cotreatment (Fig. 4A). Cilostazol similarly inhibited fluvastatin-induced expression of these SREBP2 target genes (Fig. 4A). In contrast, forskolin and db-cAMP had weaker, if any, effects on the expression of these sterol-regulated genes in this cell line, and yet both compounds potentiated statin-induced apoptosis (Figs 3B and 4A, Fig. S3). Concordantly, only dipyridamole and cilostazol decreased statin-induced HMGCR protein expression (Fig. 4B), which was associated with the inhibition of SREBP2 cleavage following statin treatment (Fig. 4C).

cAMP can regulate several effectors, the most well studied of which is cAMP-dependent protein kinase A (PKA). PKA phosphorylates a multitude of proteins with diverse roles in signal transduction, metabolism, ion transport, and transcription regulation [25]. In particular, PKA has been shown to phosphorylate and negatively regulate SREBP1 (the master transcriptional regulator of fatty acid biosynthesis) *in vitro* at a residue that is conserved between SREBP1 and SREBP2 [26]. However, given our observation that db-cAMP did not inhibit statin-induced SREBP2 target gene expression (Fig. 4A), we reasoned that the effects of dipyridamole and cilostazol on SREBP2 were likely independent of cAMP/PKA signaling. To validate this model, we knocked out the alpha catalytic subunit of PKA (PKA Cα, encoded by *PRKACA*) in LP1 cells and evaluated the subsequent effects on dipyridamole and cilostazol activity. Consistent with a cAMP/PKA-independent mechanism, both dipyridamole and cilostazol retained their ability to inhibit SREBP2 and potentiate statin-induced cell death in PKA-depleted LP1 cells (Figs S4 and S5).

To further confirm the above observation, we evaluated dipyridamole and cilostazol activity in isogenic wild-type and PKA-null (kin-) S49 cells [27]. S49 kin- cells have no detectable PKA activity due to improper *cis*-autophosphorylation at serine 338 during translation, which renders the catalytic subunit of PKA insoluble [28]. Indeed, dipyridamole and cilostazol potentiated statin-induced cell death in both S49 wild-type and kin- cells (Fig. S4).

Taken together, these data suggest that compounds that increase cAMP levels, including PDE inhibitors and forskolin, can sensitize hematological cancer cells to statin-induced apoptosis. Furthermore, PDE inhibitors such as dipyridamole and cilostazol further possess cAMP/PKA-independent activity against statin-induced SREBP2 activation (Fig. 5).

4. Discussion

Our laboratory previously reported a novel role for the drug dipyridamole as an inhibitor of the SREBP family of transcription factors [4,6]. As a result, dipyridamole can sensitize certain cancer cells to statin-induced apoptosis (Fig. 1) [4,6]. However, given the polypharmacology of dipyridamole, the mechanism by which it inhibits the SREBP proteins and synergizes with statins remains to be fully understood. As a step toward elucidating this mechanism, we evaluated individual compounds that phenocopied the different known functions of dipyridamole for their ability to sensitize AML and MM cell lines to statin-induced cell death. Through this approach, we were able to dissect the polypharmacology of dipyridamole and implicate its role as a cAMP-hydrolyzing PDE inhibitor in potentiating statin-induced apoptosis.

Our study revealed that cAMP-hydrolyzing PDE inhibitors, including dipyridamole and cilostazol, sensitize hematological cancer cells to statin-induced apoptosis via a dual mechanism (Fig. 5). By inhibiting PDE activity, dipyridamole and cilostazol increase intracellular cAMP levels (Fig. S2) [18]. We demonstrated

Fig. 4. Compounds that increase cAMP levels differentially modulate sterol metabolism. (A) LP1 cells were treated with 4 μM fluvastatin ± 5 μM dipyridamole, 20 μM cilostazol, 10 μM forskolin, or 0.1 mM db-cAMP for 16 h, and RNA was isolated to assay for *HMGCR*, *HMGCS1* and *INSIG1* expression by qRT–PCR. mRNA expression data are normalized to *GAPDH* expression. Data are represented as the mean + SD. $^{*}P < 0.05$ (one-way ANOVA with Tukey's multiple comparisons test, where the indicated groups were compared to the solvent controls group), $^{\#}P < 0.05$ (one-way ANOVA with Tukey's multiple comparisons test, comparing the two indicated groups). (B) LP1 cells were treated with 4 μM fluvastatin ± 5 μM dipyridamole, 20 μM cilostazol, 10 μM forskolin, or 0.1 mM db-cAMP for 24 h, and protein was isolated to assay for HMGCR expression by immunoblotting. 1 = HMGCR oligomer, 2 = HMGCR monomer. Immunoblots are representative of three independent experiments. (C) LP1 cells were treated with 4 μM fluvastatin ± 5 μM dipyridamole or 20 μM cilostazol for 8 h, and protein was isolated to assay for SREBP2 cleavage (activation) by immunoblotting. F, full-length SREBP2; C, cleaved SREBP2. Immunoblots are representative of three independent experiments.

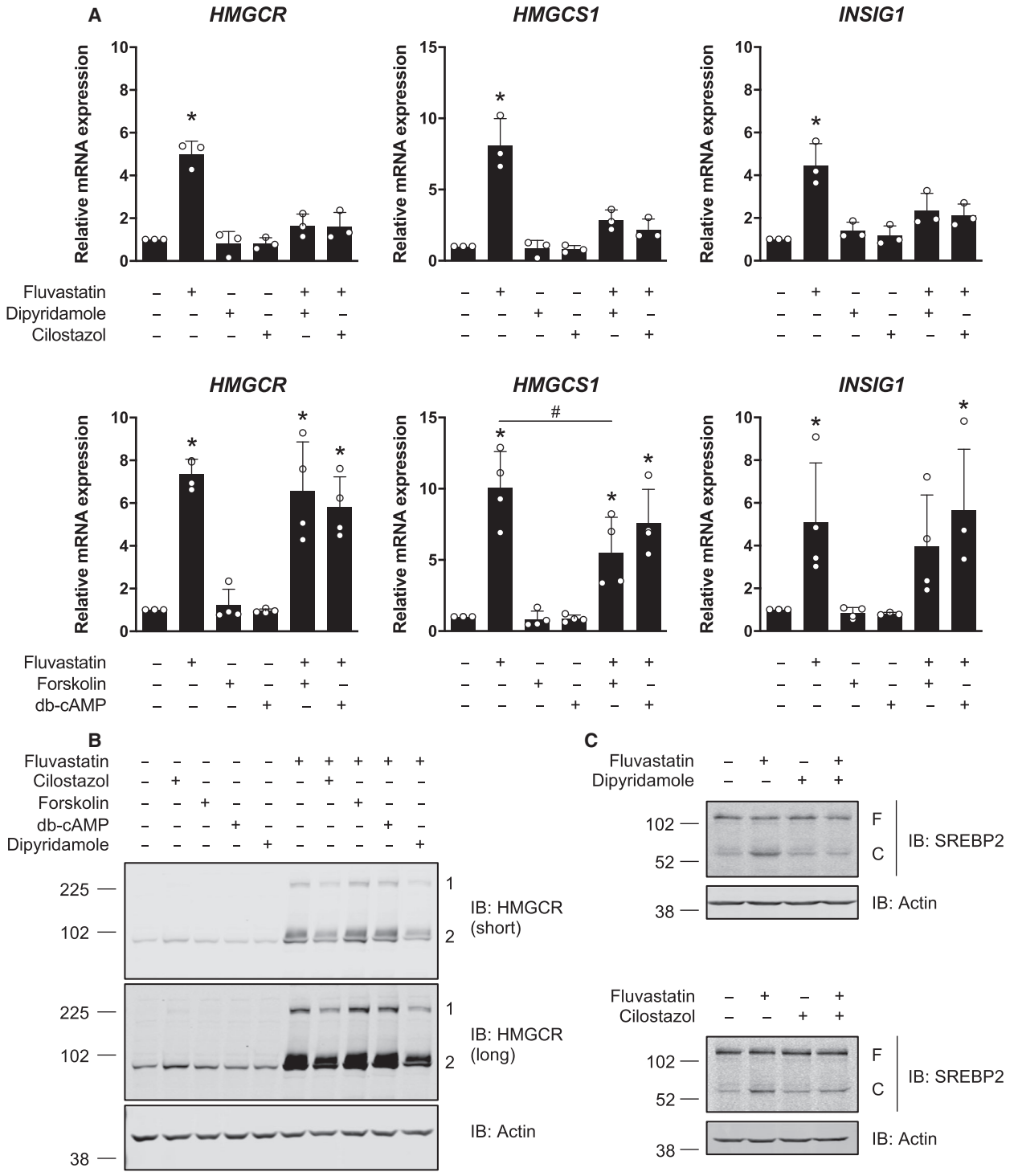

that other compounds that increase cAMP levels, including forskolin, similarly sensitize cancer cells to statin-induced cell death. Importantly, cotreatment with a statin and cAMP-modulating agent was effective at potentiating cell death in both statin-sensitive (e.g., KMS11, OCI-AML-3) and statin-insensitive (e.g., LP1) cell lines (Fig. 3B, Figs S1, S3,and S4D). Our data are consistent with a previous report, where the combination of lovastatin and db-cAMP was shown to enhance differentiation and cytotoxicity in

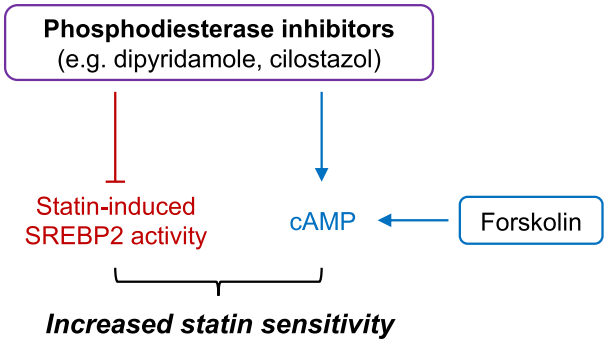

Fig. 5. Proposed model for how cAMP-hydrolyzing PDE inhibitors potentiate statin-induced cancer cell death. Compounds that increase intracellular cAMP levels, including PDE inhibitors (e.g., dipyridamole, cilostazol) and forskolin, can sensitize cancer cells to statin-induced apoptosis. Dipyridamole and cilostazol also inhibit statin-induced activation of SREBP2 through a cAMP-independent mechanism, which abrogates the restorative feedback loop of the MVA pathway and further sensitizes cancer cells to statin-induced apoptosis.

embryonal carcinoma and neuroblastoma cell lines [29]. However, the critical cAMP-regulated effector that modulates statin sensitivity in cancer cells remains to be identified. In the present study, we found that dipyridamole and cilostazol potentiate statin-induced cell death in a PKA-independent manner (Fig. S4). In addition to PKA, cAMP also regulates specific ion channels and the EPAC (exchange protein directly activated by cAMP) proteins, which are cAMP-dependent guanine nucleotide exchange factors for the RAP GTPases [30]. Future work is required to delineate the mechanism by which elevated cAMP levels sensitize cancer cells to statin-induced apoptosis.

We further demonstrated that the PDE inhibitors dipyridamole and cilostazol inhibit the SREBP2-regulated feedback mechanism of the MVA pathway via an additional, cAMP-independent mechanism (Fig. 4). Interestingly, cilostazol has previously been reported to inhibit insulin-induced expression of SREBP1 [31], but the potential involvement of cAMP signaling was not explored. Data in the literature are conflicting as to the effects of PDE inhibitors on lipid metabolism. A recent study demonstrated that combined inhibition of PDE4 and PDE8 in Leydig cells promotes SREBP2 signaling, cholesterol metabolism, and steroidogenesis [32]. In contrast, data from a randomized controlled trial in patients with type 2 diabetes revealed that cilostazol treatment significantly lowered serum triglyceride and low-density lipoprotein (LDL) cholesterol levels [33]. The data we present here clearly show that dipyridamole (a pan-PDE inhibitor) and cilostazol (a PDE3 inhibitor) can abrogate SREBP2 cleavage and activation in AML and MM cells exposed to a statin. It is therefore possible that different PDEs play unique roles in regulating SREBP2 signaling and sterol metabolism and that PDE-mediated regulation of SREBP2 is tissue type- and context-dependent. In the context of cancer, dipyridamole has been shown to inhibit statin-induced SREBP2 cleavage and activation in AML, MM, breast cancer, and prostate cancer cells [3,4,6], suggesting similar regulation in many different cell types. A rigorous analysis of the effects of different PDE inhibitors on lipid metabolism and investigation into the mechanism(s) by which these clinically approved drugs act to modulate cancer cell metabolism should be a focus of future studies. Interestingly, unlike many other PDE inhibitors, dipyridamole and cilostazol also inhibit adenosine uptake [11,34]. While we did not observe enhanced cell death when the adenosine reuptake inhibitor NBMPR was combined with a statin (Fig. 2B), it remains possible that dipyridamole and cilostazol inhibit sterol metabolism via a PDE-independent mechanism or through simultaneous modulation of multiple targets.

The data presented here may have important clinical implications, as many cAMP-hydrolyzing PDE inhibitors are approved for several nononcology indications [21]. For example, cilostazol (marketed as Pletal) is currently approved and widely used to treat intermittent claudication. The overexpression of several PDEs has been observed in solid and hematological tumors, and the possibility of cAMP-hydrolyzing PDE inhibition as an anticancer strategy has been preclinically explored alone or in combination with chemo- and targeted molecular therapies [35–40]. In hematological malignancies, primary chronic lymphocytic leukemia patient samples were found to have PDE7B overexpression and noted to be sensitive to PDE7 inhibition in a cAMP-dependent manner [38]. Another study found a strong synergistic combinatorial effect between adenosine A2A receptor agonists and cAMP-hydrolyzing PDE inhibitors in MM and diffuse large B-cell lymphoma cell lines and primary patient samples [41]. Given that a number of PDE inhibitors are poised for repurposing and that statins have demonstrated anticancer activity in early-phase clinical trials [42–49], further studies are needed to evaluate the therapeutic benefit of a statin-PDE inhibitor combination for the treatment of cancer. As the combination of cilostazol and statins has already been evaluated clinically in healthy subjects [50,51] and in patients with cardiovascular indications [52,53] without added adverse effects, there is the possibility of fast-tracking these agents to phase II trials in AML and MM.

5. Conclusion

In summary, we propose a working model whereby cAMP-hydrolyzing PDE inhibitors, such as dipyridamole and cilostazol, increase cAMP levels and inhibit SREBP2 activation via independent mechanisms, both of which converge to potentiate statin-induced apoptosis in hematological cancer cells (Fig. 5). Given that statins and a number of PDE inhibitors are already approved for various nononcology indications, future studies are needed to thoroughly evaluate the potential therapeutic benefit of these agents for the treatment of hematological malignancies. Moreover, our experimental approach to dissect the polypharmacology of dipyridamole is one that may be useful when interrogating novel functions of other repurposed drugs.

Acknowledgements

We thank all members of the Penn laboratory for helpful discussions. LZP holds a Tier 1 Canada Research Chair in Molecular Oncology. This work was supported by funding from the Canadian Institutes of Health Research (CIHR) (FRN: 142263; LZP), Canadian Cancer Society (Grant #706394; LZP), and Office of the Assistant Secretary of Defense for Health Affairs, through the Breast Cancer Research Program (Award No. W81XWH-16-1-0068; LZP). Opinions, interpretations, conclusions, and recommendations are those of the author and are not necessarily endorsed by the Department of Defense. JL and AAP were supported by CIHR Doctoral Research Awards. AAP was further supported by a Canadian Breast Cancer Foundation Doctoral Award.

Conflict of interest

The authors declare no conflict of interest.

Author contributions

JL, AAP, and LZP conceived and designed the study. JL, AAP, and PS performed experiments, as well as analyzed and interpreted the experimental data. MDM and ADS provided the primary AML cells and clinical expertise. JL, AAP, and LZP wrote the manuscript. All authors read and approved the manuscript. LZP supervised the study.

Data accessibility

The RNA expression data in Fig. 3A were obtained through the CCLE database [8]. All other raw data are available from the corresponding author upon reasonable request.

References

1 Mullen PJ, Yu R, Longo J, Archer MC & Penn LZ (2016) The interplay between cell signalling and the mevalonate pathway in cancer. *Nat Rev Cancer* **16**, 718–731.

2 Clendening JW, Pandyra A, Li Z, Boutros PC, Martirosyan A, Lehner R, Jurisica I, Trudel S & Penn LZ (2010) Exploiting the mevalonate pathway to distinguish statin-sensitive multiple myeloma. *Blood* **115**, 4787–4797.

3 Göbel A, Breining D, Rauner M, Hofbauer LC & Rachner TD (2019) Induction of 3-hydroxy-3-methylglutaryl-CoA reductase mediates statin resistance in breast cancer cells. *Cell Death Dis* **10**, 91.

4 Longo J, Mullen PJ, Yu R, van Leeuwen JE, Masoomian M, Woon DTS, Wang Y, Chen EX, Hamilton RJ, Sweet JM *et al.* (2019) An actionable sterol-regulated feedback loop modulates statin sensitivity in prostate cancer. *Mol Metab* **25**, 119–130.

5 Pandyra AA, Mullen PJ, Goard CA, Ericson E, Sharma P, Kalkat M, Yu R, Pong JT, Brown KR, Hart T *et al.* (2015) Genome-wide RNAi analysis reveals that simultaneous inhibition of specific mevalonate pathway genes potentiates tumor cell death. *Oncotarget* **6**, 26909–26921.

6 Pandyra A, Mullen PJ, Kalkat M, Yu R, Pong JT, Li Z, Trudel S, Lang KS, Minden MD, Schimmer AD *et al.* (2014) Immediate utility of two approved agents to target both the metabolic mevalonate pathway and its restorative feedback loop. *Cancer Res* **74**, 4772–4782.

7 Dimitroulakos J, Ye LY, Benzaquen M, Moore MJ, Kamel-Reid S, Freedman MH, Yeger H & Penn LZ (2001) Differential sensitivity of various pediatric cancers and squamous cell carcinomas to lovastatin-induced apoptosis: therapeutic implications. *Clin Cancer Res* **7**, 158–167.

8 Barretina J, Caponigro G, Stransky N, Venkatesan K, Margolin AA, Kim S, Wilson CJ, Lehár J, Kryukov GV, Sonkin D *et al.* (2012) The Cancer Cell Line Encyclopedia enables predictive modelling of anticancer drug sensitivity. *Nature* **483**, 603–607.

9 Goldman M, Craft B, Hastie M, Repečka K, Kamath A, McDade F, Rogers D, Brooks AN, Zhu J & Haussler D (2019) The UCSC Xena platform for cancer genomics data visualization and interpretation. *bioRxiv*. https://doi.org/10.1101/326470

10 Hart T, Chandrashekhar M, Aregger M, Steinhart Z, Brown KR, MacLeod G, Mis M, Zimmermann M, Fradet-Turcotte A, Sun S *et al.* (2015) High-resolution CRISPR screens reveal fitness genes and genotype-specific cancer liabilities. *Cell* **163**, 1515–1526.

11 King AE, Ackley MA, Cass CE, Young JD & Baldwin SA (2006) Nucleoside transporters: from scavengers to novel therapeutic targets. *Trends Pharmacol Sci* **27**, 416–425.
12 Steinfelder HJ & Joost HG (1988) Inhibition of insulin-stimulated glucose transport in rat adipocytes by nucleoside transport inhibitors. *FEBS Lett* **227**, 215–219.
13 Bender AT & Beavo JA (2006) Cyclic nucleotide phosphodiesterases: molecular regulation to clinical use. *Pharmacol Rev* **58**, 488–520.
14 Wood TE, Dalili S, Simpson CD, Hurren R, Mao X, Saiz FS, Gronda M, Eberhard Y, Minden MD, Bilan PJ *et al.* (2008) A novel inhibitor of glucose uptake sensitizes cells to FAS-induced cell death. *Mol Cancer Ther* **7**, 3546–3555.
15 Boleti H, Coe IR, Baldwin SA, Young JD & Cass CE (1997) Molecular identification of the equilibrative NBMPR-sensitive (es) nucleoside transporter and demonstration of an equilibrative NBMPR-insensitive (ei) transport activity in human erythroleukemia (K562) cells. *Neuropharmacology* **36**, 1167–1179.
16 Hourani SMO, Boon K, Fooks HM & Prentice DJ (2001) Role of cyclic nucleotides in vasodilations of the rat thoracic aorta induced by adenosine analogues. *Br J Pharmacol* **133**, 833–840.
17 Kim M-J, Park K-G, Lee K-M, Kim H-S, Kim S-Y, Kim C-S, Lee S-L, Chang Y-C, Park J-Y, Lee K-U *et al.* (2005) Cilostazol inhibits vascular smooth muscle cell growth by downregulation of the transcription factor E2F. *Hypertension* **45**, 552–556.
18 Shakur Y, Fong M, Hensley J, Cone J, Movsesian MA, Kambayashi J-I, Yoshitake M & Liu Y (2002) Comparison of the effects of cilostazol and milrinone on cAMP-PDE activity, intracellular cAMP and calcium in the heart. *Cardiovasc Drugs Ther* **16**, 417–427.
19 Bouley R, Pastor-Soler N, Cohen O, McLaughlin M, Breton S & Brown D (2005) Stimulation of AQP2 membrane insertion in renal epithelial cells in vitro and in vivo by the cGMP phosphodiesterase inhibitor sildenafil citrate (Viagra). *Am J Physiol Ren Physiol* **288**, F1103–F1112.
20 Lu J, Montgomery BK, Chatain GP, Bugarini A, Zhang Q, Wang X, Edwards NA, Ray-Chaudhury A, Merrill MJ, Lonser RR *et al.* (2018) Corticotropin releasing hormone can selectively stimulate glucose uptake in corticotropinoma via glucose transporter 1. *Mol Cell Endocrinol* **470**, 105–114.
21 Maurice DH, Ke H, Ahmad F, Wang Y, Chung J & Manganiello VC (2014) Advances in targeting cyclic nucleotide phosphodiesterases. *Nat Rev Drug Discov* **13**, 290–314.
22 Baillie GS, Tejeda GS & Kelly MP (2019) Therapeutic targeting of 3′,5′-cyclic nucleotide phosphodiesterases: inhibition and beyond. *Nat Rev Drug Discov* **18**, 770–796.
23 Wong WW-L, Clendening JW, Martirosyan A, Boutros PC, Bros C, Khosravi F, Jurisica I, Stewart AK, Bergsagel PL & Penn LZ (2007) Determinants of sensitivity to lovastatin-induced apoptosis in multiple myeloma. *Mol Cancer Ther* **6**, 1886–1897.
24 Dimitroulakos J, Nohynek D, Backway KL, Hedley DW, Yeger H, Freedman MH, Minden MD & Penn LZ (1999) Increased sensitivity of acute myeloid leukemias to lovastatin-induced apoptosis: a potential therapeutic approach. *Blood* **93**, 1308–1318.
25 Sassone-Corsi P (2012) The cyclic AMP pathway. *Cold Spring Harb Perspect Biol* **4**, a011148.
26 Lu M & Shyy JYJ (2006) Sterol regulatory element-binding protein 1 is negatively modulated by PKA phosphorylation. *Am J Physiol Cell Physiol* **290**, 1477–1486.
27 Orellana SA & McKnight GS (1990) The S49 Kin- cell line transcribes and translates a functional mRNA coding for the catalytic subunit of cAMP-dependent protein kinase. *J Biol Chem* **265**, 3048–3053.
28 Keshwani MM, Klammt C, von Daake S, Ma Y, Kornev AP, Choe S, Insel PA & Taylor SS (2012) Cotranslational cis-phosphorylation of the COOH-terminal tail is a key priming step in the maturation of cAMP-dependent protein kinase. *Proc Natl Acad Sci USA* **109**, E1221–E1229.
29 Arnold DE, Gagne C, Niknejad N, McBurney MW & Dimitroulakos J (2010) Lovastatin induces neuronal differentiation and apoptosis of embryonal carcinoma and neuroblastoma cells: enhanced differentiation and apoptosis in combination with dbcAMP. *Mol Cell Biochem* **345**, 1–11.
30 Bos JL (2006) Epac proteins: multi-purpose cAMP targets. *Trends Biochem Sci* **31**, 680–686.
31 Jung YA, Kim HK, Bae KH, Seo HY, Kim HS, Jang BK, Jung GS, Lee IK, Kim MK & Park KG (2014) Cilostazol inhibits insulin-stimulated expression of sterol regulatory binding protein-1c via inhibition of LXR and Sp1. *Exp Mol Med* **46**, e73.
32 Shimizu-Albergine M, Van Yserloo B, Golkowski MG, Ong SE, Beavo JA & Bornfeldt KE (2016) SCAP/SREBP pathway is required for the full steroidogenic response to cyclic AMP. *Proc Natl Acad Sci USA* **113**, E5685–E5693.
33 Katakami N, Kim YS, Kawamori R & Yamasaki Y (2010) The phosphodiesterase inhibitor cilostazol induces regression of carotid atherosclerosis in subjects with type 2 diabetes mellitus: principal results of the Diabetic Atherosclerosis Prevention by Cilostazol (DAPC) study: a randomized trial. *Circulation* **121**, 2584–2591.
34 Sun B, Le SN, Lin S, Fong M, Guertin M, Liu Y, Tandon NN, Yoshitake M & Kambayashi J (2002) New mechanism of action for cilostazol: interplay

between adenosine and cilostazol in inhibiting platelet activation. *J Cardiovasc Pharmacol* **40**, 577–585.
35 Moon EY & Lerner A (2003) PDE4 inhibitors activate a mitochondrial apoptotic pathway in chronic lymphocytic leukemia cells that is regulated by protein phosphatase 2A. *Blood* **101**, 4122–4130.
36 Noonan KA, Ghosh N, Rudraraju L, Bui M & Borrello I (2014) Targeting immune suppression with PDE5 inhibition in end-stage multiple myeloma. *Cancer Immunol Res* **2**, 725–731.
37 Lerner A & Epstein PM (2006) Cyclic nucleotide phosphodiesterases as targets for treatment of haematological malignancies. *Biochem J* **393**, 21–41.
38 Zhang L, Murray F, Zahno A, Kanter JR, Chou D, Suda R, Fenlon M, Rassenti L, Cottam H, Kipps TJ *et al.* (2008) Cyclic nucleotide phosphodiesterase profiling reveals increased expression of phosphodiesterase 7B in chronic lymphocytic leukemia. *Proc Natl Acad Sci USA* **105**, 19532–19537.
39 Lin DC, Xu L, Ding LW, Sharma A, Liu LZ, Yang H, Tan P, Vadgama J, Karlan BY, Lester J *et al.* (2013) Genomic and functional characterizations of phosphodiesterase subtype 4D in human cancers. *Proc Natl Acad Sci USA* **110**, 6109–6114.
40 Zhou S, Xu H, Tang Q, Xia H & Bi F (2020) Dipyridamole enhances the cytotoxicities of trametinib against colon cancer cells through combined targeting of HMGCS1 and MEK pathway. *Mol Cancer Ther* **19**, 135–146.
41 Rickles RJ, Pierce LT, Giordano TP, Tam WF, McMillin DW, Delmore J, Laubach JP, Borisy AA, Richardson PG & Lee MS (2010) Adenosine A2A receptor agonists and PDE inhibitors: a synergistic multitarget mechanism discovered through systematic combination screening in B-cell malignancies. *Blood* **116**, 593–602.
42 Kornblau SM, Banker DE, Stirewalt D, Shen D, Lemker E, Verstovsek S, Estrov Z, Faderl S, Cortes J, Beran M *et al.* (2007) Blockade of adaptive defensive changes in cholesterol uptake and synthesis in AML by the addition of pravastatin to idarubicin + high-dose Ara-C: a phase 1 study. *Blood* **109**, 2999–3006.
43 Knox JJ, Siu LL, Chen E, Dimitroulakos J, Kamel-Reid S, Moore MJ, Chin S, Irish J, LaFramboise S & Oza AM (2005) A phase I trial of prolonged administration of lovastatin in patients with recurrent or metastatic squamous cell carcinoma of the head and neck or of the cervix. *Eur J Cancer* **41**, 523–530.
44 Hus M, Grzasko N, Szostek M, Pluta A, Helbig G, Woszczyk D, Adamczyk-Cioch M, Jawniak D, Legiec W, Morawska M *et al.* (2011) Thalidomide, dexamethasone and lovastatin with autologous stem cell transplantation as a salvage immunomodulatory therapy in patients with relapsed and refractory multiple myeloma. *Ann Hematol* **90**, 1161–1166.
45 Goss GD, Jonker DJ, Laurie SA, Weberpals JI, Oza AM, Spaans JN, la Porte C & Dimitroulakos J (2016) A phase I study of high-dose rosuvastatin with standard dose erlotinib in patients with advanced solid malignancies. *J Transl Med* **14**, 83.
46 Bjarnadottir O, Romero Q, Bendahl PO, Jirström K, Rydén L, Loman N, Uhlén M, Johannesson H, Rose C, Grabau D *et al.* (2013) Targeting HMG-CoA reductase with statins in a window-of-opportunity breast cancer trial. *Breast Cancer Res Treat* **138**, 499–508.
47 Murtola TJ, Syvälä H, Tolonen T, Helminen M, Riikonen J, Koskimäki J, Pakarainen T, Kaipia A, Isotalo T, Kujala P *et al.* (2018) Atorvastatin versus placebo for prostate cancer before radical prostatectomy – a randomized, double-blind, placebo-controlled clinical trial. *Eur Urol* **74**, 697–701.
48 Garwood ER, Kumar AS, Baehner FL, Moore DH, Au A, Hylton N, Flowers CI, Garber J, Lesnikoski BA, Hwang ES *et al.* (2010) Fluvastatin reduces proliferation and increases apoptosis in women with high grade breast cancer. *Breast Cancer Res Treat* **119**, 137–144.
49 Longo J, Hamilton RJ, Masoomian M, Khurram N, Branchard E, Mullen PJ, Elbaz M, Hersey K, Chadwick D, Ghai S *et al.* (2020) A pilot window-of-opportunity study of preoperative fluvastatin in localized prostate cancer. *Prostate Cancer Prostatic Dis.* https://doi.org/10.1038/s41391-020-0221-7.
50 Bramer SL, Brisson J, Corey AE & Mallikaarjun S (1999) Effect of multiple cilostazol doses on single dose lovastatin pharmacokinetics in healthy volunteers. *Clin Pharmacokinet* **37**, 69–77.
51 Kim J-R, Jung JA, Kim S, Huh W, Ghim J-L, Shin J-G & Ko J-W (2019) Effect of cilostazol on the pharmacokinetics of simvastatin in healthy subjects. *Biomed Res Int* **2019**, 1365180.
52 Hiatt WR, Money SR & Brass EP (2008) Long-term safety of cilostazol in patients with peripheral artery disease: the CASTLE study (Cilostazol: a study in long-term effects). *J Vasc Surg* **47**, 330–336.
53 Ari H, Emlek N, Ari S, Coşar S, Doğanay K, Aydin C, Tenekecioğlu E, Tütüncü A, Yontar OC, Gürdoğan M *et al.* (2015) The effect of high dose cilostazol and rosuvastatin on periprocedural myocardial injury in patients with elective percutaneous coronary intervention. *Acta Cardiol Sin* **31**, 292–300.

Supporting information

Additional supporting information may be found online in the Supporting Information section at the end of the article.

Fig. S1. Statin-cilostazol-induced cancer cell death can be rescued by exogenous MVA or GGPP. KMS11 and

OCI-AML-3 cells were treated as indicated with fluvastatin (2 μM for KMS11 and 0.5 μM for OCI-AML-3 cells), cilostazol (12.5 μM), mevalonate (0.2 mM) and/or GGPP (2 μM). After 48 hr, cell viability was evaluated by MTT assays. Data are represented as the mean + SD. *$p < 0.05$ (one-way ANOVA with Tukey's multiple comparisons test, where the indicated groups were compared to the other groups of that cell line).

Fig. S2. Dipyridamole treatment increases intracellular cAMP. OCI-AML-3 cells were treated with 2 μM fluvastatin ± 5 μM dipyridamole for 15 min and intracellular cAMP levels were quantified. Data are represented as the mean + SD. *$p < 0.05$ (one-way ANOVA with Dunnett's multiple comparisons test, where the indicated groups were compared to the solvent controls group).

Fig. S3. Forskolin and db-cAMP sensitize LP1 cells to fluvastatin-induced apoptosis. LP1 cells were treated with 4 μM fluvastatin ± 10 μM forskolin or 0.1 mM db-cAMP for 48 hr, after which apoptotic cells (double Annexin V-positive and 7AAD-positive cells) were quantified by flow cytometry. Data are represented as the mean + SD. *$p < 0.05$ (one-way ANOVA with Dunnett's multiple comparisons test, where the indicated groups were compared to the solvent controls group).

Fig. S4. Potentiation of statin-induced cancer cell death by dipyridamole and cilostazol is independent of PKA. (A) Immunoblot for PKA C-α expression in LP1 cells expressing Cas9 and a sgRNA to a random locus on chromosome 10 (gC10 Random) or one of two different locations within *PRKACA* (representative of three independent experiments). (B) LP1 gC10 Random and gPRKACA sublines were treated with a range of fluvastatin concentrations (0-24 μM) ± 5 μM dipyridamole or 10 μM cilostazol. After 48 hr, cell viability was evaluated by MTT assays. The area under each fluvastatin dose-response curve is plotted. Data are represented as the mean + SD. *$p < 0.05$ (one-way ANOVA with Dunnett's multiple comparisons test, where the indicated groups were compared to the fluvastatin alone group of that subline). (C) Immunoblot for PKA C-α expression in S49 wildtype (WT) or kin- (PKA-null) cells (representative of three independent experiments). (D) S49 WT and kin- cells were treated with 5 μM fluvastatin ± 2.5 μM dipyridamole or 5 μM cilostazol for 48 hr, fixed in ethanol and assayed for DNA fragmentation (% pre-G1 population) as a marker of cell death by propidium iodide staining. Data are represented as the mean + SD. *$p < 0.05$ (one-way ANOVA with Dunnett's multiple comparisons test, where the indicated groups were compared to the solvent controls group of that cell line).

Fig. S5. Dipyridamole and cilostazol inhibit the sterol-regulated feedback loop of the MVA pathway independent of PKA. (A) LP1 gPRKACA sublines were treated with 4 μM fluvastatin ± 5 μM dipyridamole or 20 μM cilostazol for 16 hr, and RNA was isolated to assay for *HMGCS1* expression by qRT-PCR. mRNA expression data are normalized to *GAPDH* expression. Data are represented as the mean + SD. *$p < 0.05$ (one-way ANOVA with Sidak's multiple comparisons test, where the indicated groups were compared to the solvent controls group of that subline). (B) LP1 gC10 Random or gPRKACA #1 cells were treated with 4 μM fluvastatin ± 5 μM dipyridamole or 20 μM cilostazol for 8 hr, and protein was isolated to assay for SREBP2 cleavage (activation) by immunoblotting. F = full-length SREBP2, C = cleaved SREBP2. Immunoblots are representative of three independent experiments.

Published OnlineFirst September 4, 2020; DOI: 10.1158/1078-0432.CCR-20-1967

CLINICAL CANCER RESEARCH | REVIEW

Statins as Anticancer Agents in the Era of Precision Medicine

Joseph Longo[1,2], Jenna E. van Leeuwen[1,2], Mohamad Elbaz[1], Emily Branchard[1], and Linda Z. Penn[1,2]

ABSTRACT

Statins are widely prescribed cholesterol-lowering drugs that inhibit HMG-CoA reductase (HMGCR), the rate-limiting enzyme of the mevalonate metabolic pathway. Multiple lines of evidence indicate that certain cancers depend on the mevalonate pathway for growth and survival, and, therefore, are vulnerable to statin therapy. However, these immediately available, well-tolerated, and inexpensive drugs have yet to be successfully repurposed and integrated into cancer patient care. In this review, we highlight recent advances and outline important considerations for advancing statins to clinical trials in oncology.

Introduction

Since their approval by the FDA in the late 1980s, statins have revolutionized the clinical management of high cholesterol. Statins are specific inhibitors of the mevalonate pathway, which is responsible for the *de novo* synthesis of cholesterol and nonsterol isoprenoids (**Fig. 1**). Specifically, statins inhibit the conversion of HMG-CoA to mevalonate by inhibiting the rate-limiting enzyme of the mevalonate pathway, HMG-CoA reductase (HMGCR). In addition to its important roles in normal physiology, the mevalonate pathway supports tumorigenesis and is known to be deregulated in human cancers (1–4). As such, there is significant interest in repurposing statins as anticancer agents. Statins have been shown to induce potent tumor-specific apoptosis (5–7). Moreover, many retrospective studies have reported that statin use is associated with reduced cancer risk (8–11), lower cancer grade and stage at diagnosis (12, 13), and reduced recurrence and/or cancer-specific mortality (14–18). Given that statins are FDA-approved, well-tolerated, and are available as generic drugs, they offer an immediate, safe, and inexpensive opportunity to improve cancer patient care and treatment outcomes.

Despite these promising observations, statins have yet to be repurposed and integrated into cancer patient care. Emerging evidence suggests that certain molecular subtypes of cancer are more susceptible to statin therapy than others, highlighting the importance of predictive biomarkers for patient stratification. Moreover, recent clinical trials have provided important insights into how to realistically use these agents in an oncology setting. In this review, we highlight the gaps in knowledge that have precluded the repurposing of statins as anticancer agents, as well as recent advances that will help inform future clinical trial design.

Statin Mechanism of Action

Statins compete with HMG-CoA for binding to the active site of HMGCR, thereby reducing mevalonate synthesis. As a consequence, statins deplete intracellular cholesterol, which triggers a homeostatic feedback mechanism governed by the sterol regulatory element-binding protein (SREBP) family of transcription factors (**Fig. 1**). Activation of the SREBPs results in the increased expression of mevalonate pathway and sterol metabolism genes, including *HMGCR* and the low-density lipoprotein (LDL) receptor (*LDLR*). Increased membrane expression of LDLR leads to enhanced LDL cholesterol (LDL-C) uptake from the bloodstream, thus effectively lowering serum cholesterol levels. As a result, statins are commonly prescribed to reduce the risk of cardiovascular disease or improve survival in patients with cardiovascular disease.

Cholesterol has also been shown to play multifaceted roles in tumorigenesis (reviewed in refs. 1, 19). In specific contexts, statins have been shown to elicit their anticancer effects through the depletion of cholesterol. For example, one study demonstrated that simvastatin decreases the cholesterol content of lipid rafts in prostate cancer cells, which hinders AKT signaling and induces apoptosis (20). Moreover, in a subset of medulloblastoma driven by aberrant Hedgehog signaling, the depletion of cholesterol impairs signal transduction and inhibits cancer cell growth (21). However, in the majority of other reports, exogenous cholesterol is unable to rescue statin-induced apoptosis, highlighting a role for other end products of the mevalonate pathway in cancer cell survival.

In addition to cholesterol, statins also reduce the synthesis of nonsterol isoprenoids, including geranylgeranyl pyrophosphate (GGPP; **Fig. 1**). Several studies have shown that statin-induced apoptosis can be consistently and fully rescued by exogenous mevalonate or mevalonate-derived GGPP (22–25). These studies not only support that statin-induced apoptosis is an on-target effect, but also reveal that certain cancers rely on GGPP synthesis for survival. GGPP can serve as a substrate for protein prenylation, or as a precursor for the synthesis of other metabolites, such as coenzyme Q (CoQ) and dolichols (1). In recent years, it has become apparent that different cancer cell types have a dependency on distinct fates of GGPP (22–24, 26, 27). In acute myeloid leukemia and multiple myeloma cells, statin-induced apoptosis can be phenocopied by prenylation inhibitors, which suggests that these cancers rely on GGPP synthesis, at least in part, for protein prenylation (22, 23, 28). However, in other cancers where statin-induced cell death can be rescued by exogenous GGPP, statin sensitivity can be uncoupled from effects on protein prenylation (24). Indeed, recent studies have shown that

[1]Princess Margaret Cancer Centre, University Health Network, Toronto, Ontario, Canada. [2]Department of Medical Biophysics, University of Toronto, Toronto, Ontario, Canada.

J.E. van Leeuwen, M. Elbaz, and E. Branchard contributed equally to this article.

Corresponding Author: Linda Z. Penn, Princess Margaret Cancer Centre, 13th Floor 13-706, 101 College St., Toronto, Ontario, M5G 1L7, Canada. Phone: 416-634-8770; E-mail: lpenn@uhnres.utoronto.ca

Clin Cancer Res 2020;26:5791–800

doi: 10.1158/1078-0432.CCR-20-1967

Published OnlineFirst September 4, 2020; DOI: 10.1158/1078-0432.CCR-20-1967

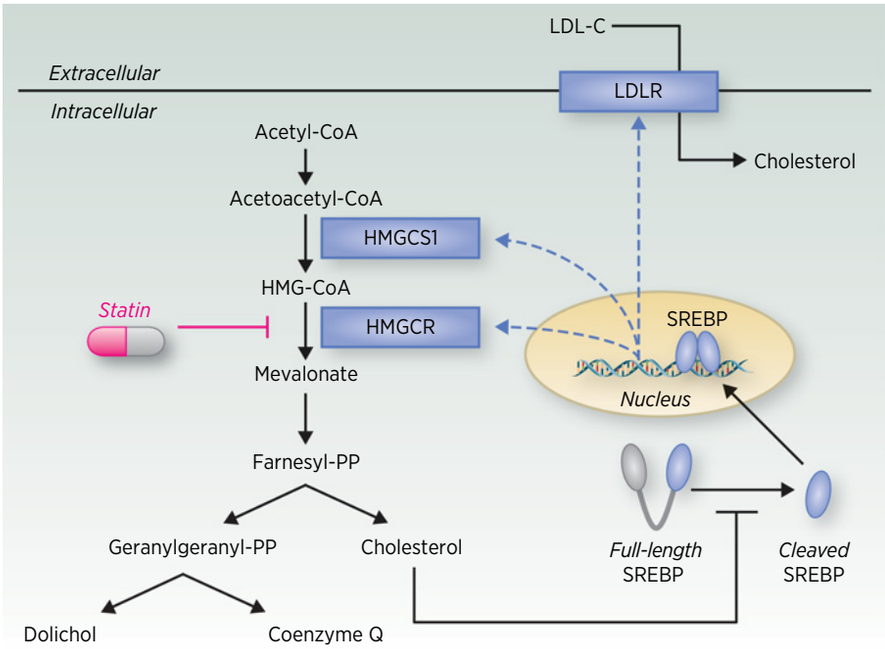

Figure 1.
Schematic of the mevalonate pathway and its SREBP-mediated feedback response. The mevalonate pathway converts acetyl-CoA to cholesterol and a number of non-sterol isoprenoids that play important roles in cell growth and survival. Under homeostatic conditions, intracellular cholesterol retains the SREBPs in their full-length, inactive form. In response to cholesterol depletion, such as when cells are treated with a statin, the SREBPs are cleaved, thus liberating the active transcription factor. Nuclear SREBP induces the transcription of genes involved in the mevalonate pathway and cholesterol transport. HMGCS1, HMG-CoA synthase 1.

certain tumors rely on the mevalonate pathway for the synthesis GGPP-derived CoQ (26, 27). In these cells, statin treatment leads to oxidative stress and apoptosis (26, 27), which can be rescued by exogenous CoQ (26).

Despite numerous studies implicating the direct, intratumoral inhibition of HMGCR as the mechanism by which statins elicit their anticancer effects, systemic contributions are also likely. It is important to note that, unlike in humans, statin treatment does not reduce serum cholesterol levels in mice (20, 29). While reducing circulating cholesterol levels may add to the benefit of statin therapy in patients with cancer, evidence from preclinical studies support a direct mechanism. Thus, in this review, we focus primarily on the direct effects of statins on cancer cells.

Identifying Statin Vulnerable Tumors

While many epidemiologic studies report positive associations between statin use and cancer patient outcomes, the extent to which statin use confers a benefit is variable between studies (14–18). Several factors might explain this heterogeneity, including interpatient differences in the type of statin, dose, and duration of statin use (discussed further in the next section). Furthermore, it is possible that not all patients with cancer benefit equally from statin therapy. Consistent with this hypothesis, highly heterogeneous responses to statin exposure across panels of cancer cell lines have been reported (23, 24, 30–32), and biomarkers of statin sensitivity have recently been described (**Fig. 2**). Hence, different tumor subtypes are not equally vulnerable to statin therapy.

If statins are to be repurposed for the precise treatment of cancer, we must first identify which tumor subtypes are vulnerable to statin-mediated HMGCR inhibition. In breast cancer, for example, statin sensitivity has been associated with estrogen receptor (ER) status, where ER-negative breast cancer cells are particularly sensitive to statin exposure (31). These preclinical observations are further supported by clinical data demonstrating greater tumor cell apoptosis after fluvastatin treatment in women with ER-negative breast cancer (33). Independent studies have demonstrated that tumor cells of various origins with higher expression of mesenchymal cell markers (e.g., vimentin) and/or lower expression of epithelial cell markers (e.g., E-cadherin) are highly sensitive to statin treatment (24, 34, 35). Furthermore, statins have been shown to preferentially kill cells induced to undergo epithelial-to-mesenchymal transition (24), suggesting that they may be effective at impairing metastatic disease. Whether ER-negative breast tumors are more sensitive to statins because they are more mesenchymal remains to be determined. Moreover, it remains poorly understood why cancer cells in a mesenchymal state are vulnerable to HMGCR inhibition. Nonetheless, these data further support the concept that statin sensitivity can be stratified by tumor subtype.

Aberrant sterol metabolism

In some cancer cells, statin sensitivity is inversely associated with the ability to activate a feedback mechanism in response to mevalonate pathway inhibition. In response to cholesterol depletion, the SREBP family of transcription factors is activated to restore homeostasis (**Fig. 1**). In certain cancer cells, this feedback mechanism is impaired, which renders them vulnerable to HMGCR inhibition. In multiple myeloma, for example, it was shown that a subset of cell lines and primary patient-derived cells fail to induce the expression of SREBP target genes following statin treatment and readily undergo apoptosis (36). In contrast, cell lines and primary cells with robust statin-induced SREBP activation were resistant to statin exposure (36). Statin sensitivity has subsequently been associated with impaired feedback regulation of the mevalonate pathway in other cancer types, including prostate cancer (32). Further research is required to better understand why some cancer cells have impaired feedback regulation of the mevalonate pathway, and to identify a clinically amenable biomarker that can stratify patients on the basis of this dampened homeostatic response.

In breast cancer, statin sensitivity has been inversely associated with high basal expression of cholesterol biosynthesis genes, including *HMGCR* (37). This is consistent with a report that acquired resistance to statin exposure *in vitro* is associated with significantly elevated

Published OnlineFirst September 4, 2020; DOI: 10.1158/1078-0432.CCR-20-1967

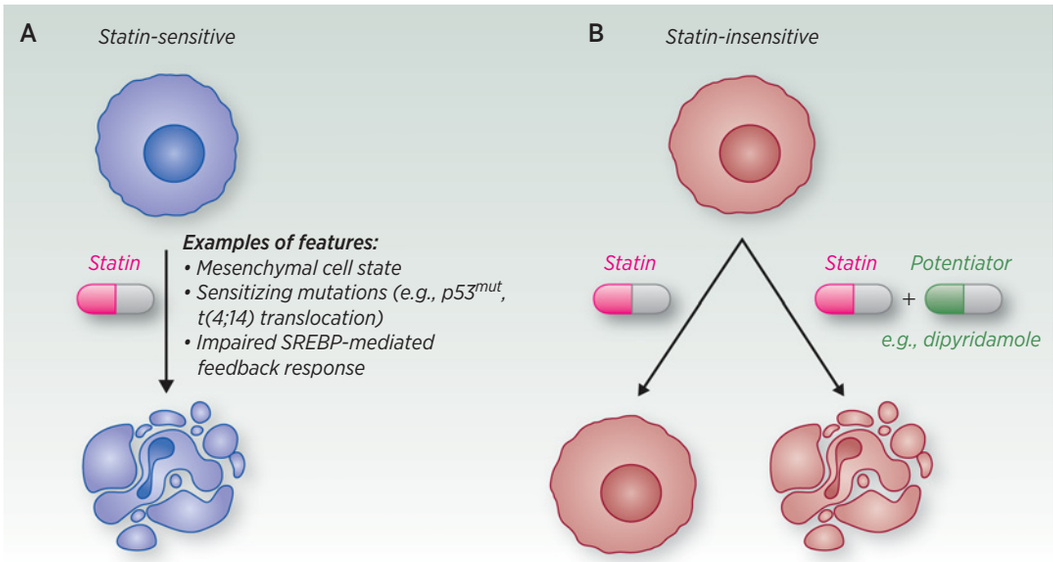

Figure 2.

Identifying statin vulnerable tumors. Cancer cells display a wide range of statin drug sensitivities, highlighting that not all tumors are vulnerable to mevalonate pathway inhibition. **A,** Statin sensitivity has been associated with various molecular features, including tumor-specific genetic lesions and deficiencies in regulating the mevalonate pathway. Treatment of these tumor cells induces cell death in a dose- and time-dependent manner. **B,** In other tumor cells, a statin alone is insufficient to induce cell death; however, cotreatment with additional targeted agents can sensitize these cells to statin treatment. For example, the drug dipyridamole prevents the compensatory activation of the SREBPs following statin treatment, thereby potentiating statin-induced cell death.

HMGCR expression (38). However, studies that have evaluated HMGCR expression as a predictive biomarker of statin sensitivity have yielded conflicting results (31, 36–39). This is likely due, in part, to the lack of specificity of many commercially available HMGCR antibodies (2, 37, 40). These observations also suggest that there is a complex relationship between HMGCR expression and statin sensitivity in cancer. On one hand, elevated HMGCR expression and deregulated mevalonate pathway activity can support tumorigenesis and render cancer cells vulnerable to statin treatment (2, 41). In these tumors, elevated HMGCR expression may indicate a tumor dependency, whereby even a slight dampening of mevalonate pathway activity is sufficient to induce tumor-specific cell death. On the other hand, as HMGCR expression continues to increase (e.g., via elevated SREBP activity), higher statin drug concentrations are required to inhibit the mevalonate pathway, thereby decreasing statin sensitivity (32, 36, 38, 42). Hence, careful consideration is required when evaluating the utility of HMGCR expression as a predictive biomarker of statin sensitivity in cancer.

Mutations and altered cell signaling

There is extensive interplay between the mevalonate pathway and signal transduction in cancer (reviewed in ref. 1), and, therefore, aberrant cell signaling in tumors may confer increased sensitivity to statin therapy. For example, mevalonate-derived farnesyl pyrophosphate (FPP) and GGPP serve as substrates for the posttranslational prenylation of oncoproteins such as RAS and RHO, which is important for their proper localization and function (43). As such, it has long been hypothesized that RAS mutations may be potential biomarkers of statin sensitivity. While activated RAS can sensitize some cells to statins (24, 44), preclinical studies have shown that statin-induced apoptosis is independent of RAS localization and function (23, 24, 44). Moreover, several clinical trials have evaluated statin therapy in patients with RAS-mutant tumors, but the majority of trials failed to demonstrate promising therapeutic responses (45–48). Hence, despite the interplay between RAS and the mevalonate pathway in cancer, RAS status is a poor predictor of statin sensitivity.

A number of recent studies have also implicated *TP53* status in modulating cancer cell sensitivity to statins. While wild-type p53 represses the mevalonate pathway (49), loss of p53 and certain gain-of-function p53 mutants have been shown to induce the expression of mevalonate pathway genes (41, 49, 50). Consistently, it has been demonstrated that these p53-null (26) or -mutant (50–52) tumors are dependent on the mevalonate pathway and particularly vulnerable to statin treatment. The latter has been attributed to the roles of the mevalonate pathway in the stability of mutant p53 protein (51–53).

Cancer type–specific biomarkers of statin sensitivity may also exist. For example, in clear-cell renal cell carcinoma, cells driven by loss of the tumor suppressor, von Hippel-Lindau (*VHL*; ∼90% of tumors), were found to be dependent on the mevalonate pathway for proper RHO and RHO kinase (ROCK) signaling, and were more sensitive to statin treatment compared with *VHL* wild-type cells (54). Moreover, in multiple myeloma, cancer cells driven by a t(4;14) chromosomal translocation are highly dependent on GGPP synthesis and more sensitive to statin-induced apoptosis compared with other multiple myeloma subtypes (55). While *TP53, VHL*, and t(4;14) status can potentially predict statin sensitivity, further validation in patients will be required before these biomarkers can be used clinically.

Considerations for Advancing Statins to Clinical Trials in Oncology

After identifying which patients with cancer might benefit from the addition of a statin to their treatment regimen, the next step is

Published OnlineFirst September 4, 2020; DOI: 10.1158/1078-0432.CCR-20-1967

evaluating how best to prescribe these drugs as anticancer agents. Data from epidemiologic, preclinical, and early-phase clinical studies have demonstrated that statin type, dose, and treatment duration are all important variables to consider when evaluating statins as anticancer agents. While all FDA-approved statins are effective in lowering serum cholesterol by inhibiting HMGCR activity in the liver (**Table 1**), their ability to directly inhibit HMGCR in extrahepatic tumor tissues may be statin type specific. It has been hypothesized that the lipophilic statin drugs are more likely to reach and readily enter extrahepatic cells, whereas hydrophilic statins are more hepatoselective (56). Consistent with this hypothesis, epidemiologic studies have reported that lipophilic, but not hydrophilic, statin use is associated with reduced cancer incidence (10) and recurrence (15) in patients with breast cancer.

Recent clinical studies have reported that the lipophilic statins, atorvastatin (57) and fluvastatin (58), are measurable in prostatic tissue at low nanomolar concentrations after short-term treatment with a typical cholesterol-lowering dose (80 mg/day). While these concentrations are less than those evaluated in most *in vitro* studies, these lower concentrations, when prescribed in the neoadjuvant setting (discussed further in the next section), were shown to reduce tumor cell proliferation (59) or induce apoptosis (58) in a time-dependent manner. These observations are consistent with epidemiologic (60, 61), preclinical (30, 31, 58, 62), and clinical (33, 58, 59) data, all of which indicate that the anticancer effects of statins are both dose- and time-dependent. This implies that comparable anticancer responses may be achieved using lower statin doses over longer durations versus higher statin doses over a shorter period of time. Phase I dose escalation studies have indeed demonstrated that statins are well-tolerated at doses much higher than typically prescribed for cholesterol management (~10–30 × higher), at least for defined periods of time (63–66).

Interestingly, while similar concentrations of atorvastatin and fluvastatin were measured in prostatic tissue following acute treatment, only atorvastatin was found to accumulate within the prostate relative to the serum (57, 58). This may have important implications for longer treatment schedules, as the pharmacokinetic properties of specific statins may enable higher achievable drug concentrations within certain tumor tissues over time. The choice of statin and dosing schedule will likely depend on the type of cancer being treated.

Neoadjuvant statin therapy

A promising therapeutic space for the use of statins is soon after diagnosis to delay the need for more aggressive treatment and/or improve the outcome of first-line therapy. In a series of window-of-opportunity trials in breast and prostate cancer, lipophilic statin treatment showed evidence of reduced tumor cell proliferation and increased apoptosis in a subset of patients. In these studies, short-term neoadjuvant treatment (between 1.5 and 12 weeks) with a cholesterol-lowering dose of either fluvastatin (33, 58) or atorvastatin (39, 59) was evaluated. In all four studies, pretreatment biopsy samples were compared with surgical material obtained after statin treatment. Immunohistochemistry was then performed to evaluate markers of tumor cell proliferation (Ki67) and/or apoptosis (cleaved caspase-3). Fluvastatin treatment was reported to increase tumor cell apoptosis in patients with high-grade breast cancer (33) and localized prostate cancer (58), where greater increases were observed in patients on a higher dose (33) or treated for longer durations (58). Similarly, neoadjuvant atorvastatin therapy was shown to reduce tumor cell proliferation in patients with primary invasive breast cancer (39). Subsequent microarray analysis in these same paired clinical samples revealed atorvastatin-induced effects on genes associated with apoptosis and reduced MAPK signaling (67). While neoadjuvant atorvastatin therapy was not found to reduce intratumoral Ki67 staining in patients with prostate cancer overall, a significant decrease in Ki67 was observed in patients on atorvastatin for greater than 28 days (59); however, a similar response in Ki67 was not observed following fluvastatin therapy (58).

Not only do these studies reinforce that the anticancer effects of statins are both dose- and time-dependent, but they further highlight that certain subgroups of patients may benefit more than others. For example, neoadjuvant fluvastatin treatment in breast cancer was found to decrease Ki67 and increase cleaved caspase-3 expression in patients with ER-negative, high-grade tumors (33), which is consistent with ER-negative breast cancer cells being particularly vulnerable to statin exposure (31). Future studies are needed to evaluate the potential long-term benefits that these effects may have on disease progression.

Statins in combination with standard chemotherapy

In phase I/II studies that have evaluated statins in combination with various standard-of-care therapies, promising responses have been reported in some patients, ranging from stable disease to complete responses (64, 66, 68, 69). While it is premature to draw conclusions about statin efficacy from these studies, these data provide important information that should be considered when designing future randomized controlled trials (RCTs). For example, the variable responses observed when considering mixed patient populations suggest that there are likely specific subsets of patients with cancer who might

Table 1. Properties of different statin drugs.

Statin drug (trade name)	Human dose (mg; ref. 103) Low (↓ LDL-C <30%)	Moderate (↓ LDL-C 30%–49%)	High (↓ LDL-C ≥50%)	Metabolism (104)	Solubility (104)
Atorvastatin (Lipitor)	N/A	10–20	40–80	CYP3A4	Lipophilic
Rosuvastatin (Crestor)	N/A	5–10	20–40	Non-CYP450 (limited CYP2C9/8)	Hydrophilic
Simvastatin (Zocor)	10	20–40	N/A	CYP3A4	Lipophilic
Pravastatin (Pravachol)	10–20	40–80	N/A	Non-CYP450	Hydrophilic
Lovastatin (Mevacor)	20	40–80	N/A	CYP3A4	Lipophilic
Fluvastatin (Lescol)	20–40	40 mg 2 ×/day or XL 80 mg	N/A	CYP2C9	Lipophilic
Pitavastatin (Livalo)	N/A	1–4	N/A	Non-CYP450 (limited CYP2C9/19)	Lipophilic

Abbreviation: XL, extended release.

Published OnlineFirst September 4, 2020; DOI: 10.1158/1078-0432.CCR-20-1967

Table 2. Summary of RCTs of statins combined with other therapies in oncology.

Cancer type	Statin (dose)	Type of study	Other therapies	Outcome	Reference
Lung (SCLC)	Pravastatin (40 mg/day)	Phase III, double-blind, placebo-controlled	Etoposide plus cisplatin or carboplatin	Pravastatin + standard chemotherapy did not offer additional benefit compared with chemotherapy alone	70
Lung (NSCLC)	Simvastatin (40 mg/day)	Phase II	Gefitinib	Simvastatin + gefitinib resulted in higher tumor response rates and longer PFS compared with gefitinib alone only in subgroup of patients with $EGFR^{WT}$ nonadenocarcinomas	92
	Simvastatin (40 mg/day)	Phase II	Afatinib	Simvastatin + afatinib was well-tolerated, but did not improve response rates compared with afatinib alone in patients with nonadenocarcinomas	93
Hepatocellular	Pravastatin (40 mg/day)	Phase II	Transcatheter arterial embolization followed by fluorouracil	Pravastatin + standard therapy prolonged OS compared with standard therapy alone	105
	Pravastatin (40 mg/day)	Phase III	Sorafenib	Pravastatin + sorafenib did not improve OS or PFS compared with sorafenib alone	72
Gastric	Pravastatin (40 mg/day)	Phase II	Epirubicin, cisplatin and capecitabine	Pravastatin + standard chemotherapy was well-tolerated, but did not improve progression-free rate at 6 months compared with chemotherapy alone	106
	Simvastatin (40 mg/day)	Phase III, double-blind, placebo-controlled	Capecitabine and cisplatin	Simvastatin + capecitabine–cisplatin did not increase PFS compared with capecitabine–cisplatin alone	73
Colorectal	Simvastatin (40 mg/day)	Phase III, double-blind, placebo-controlled	FOLFIRI/XELIRI	Simvastatin + FOLFIRI/XELIRI did not increase PFS compared with FOLFIRI/XELIRI alone	71
Pancreatic	Simvastatin (40 mg/day)	Phase II, double-blind, placebo-controlled	Gemcitabine	Simvastatin + gemcitabine was well-tolerated, but did not decrease TTP compared with gemcitabine alone	48
Multiple myeloma	Lovastatin (0.5–2 mg/kg)	Phase II	Thalidomide and dexamethasone	Lovastatin + thalidomide–dexamethasone prolonged OS and PFS compared with thalidomide–dexamethasone alone	68

Abbreviations: OS, overall survival; TTP, time to progression.

benefit from statin therapy, highlighting the need for predictive biomarkers to inform patient stratification.

Statin therapy has been evaluated in a number of RCTs (**Table 2**), including phase III trials in patients with small-cell lung cancer (SCLC; ref. 70), metastatic colorectal cancer (71), advanced hepatocellular carcinoma (72), or advanced gastric cancer (73). In these studies, the addition of 40 mg/day pravastatin (70, 72) or simvastatin (71, 73) to standard chemotherapy offered no additional benefit compared with chemotherapy alone. While disappointing, these studies were designed and initiated prior to evidence demonstrating that specific tumor subtypes are more vulnerable to statins than others. No phase III study to date has stratified patients on the basis of molecular markers predictive of statin sensitivity; however, *post hoc* analyses may uncover that a particular subgroup of patients benefited from statin therapy in these phase III trials. Moreover, given our increasing understanding of the differences between statin drugs and their differential ability to accumulate in extrahepatic tissues (57, 58, 74), choice of statin drug is an important factor. Both pravastatin and simvastatin at 40 mg/day are moderate-intensity prescriptions (**Table 1**), and, therefore, higher doses or prescription of a higher intensity statin might have yielded greater responses in these studies. Drug combination strategies to potentiate the anticancer activity of statin drugs might also be considered for future RCTs.

Combining Statins With Molecular-targeted Therapies

Statins have been evaluated in combination with various classes of other anticancer agents, including targeted therapeutics against different oncogenic signaling pathways and epigenetic modifiers (**Table 3**). Combining a statin with other targeted therapies can enhance their anticancer activity and overcome potential drug resistance mechanisms.

As with any combination therapy approach, not only is there the potential for synergistic anticancer activity, but there is also the possibility of drug–drug interactions that lead to increased toxicity. Hence, careful consideration must be given to drug selection. In addition to differences in solubility, statins also differ from one another in how they are metabolized (**Table 1**). For example, atorvastatin is highly lipophilic, but is primarily metabolized by cytochrome P450 (CYP450) 3A4 (CYP3A4). CYP3A4 function is modulated by certain foods and several commonly prescribed medications (including many chemotherapeutics), and, therefore, lipophilic statins metabolized by other enzymes, such as fluvastatin or pitavastatin, may offer a lower potential for unwanted drug–drug interactions (75). Moreover, some statins, such as lovastatin, have been shown to interact with and modulate P-glycoprotein activity (a major drug efflux pump; refs. 30, 76). These factors must be considered when evaluating statins in combination with other targeted therapies.

Published OnlineFirst September 4, 2020; DOI: 10.1158/1078-0432.CCR-20-1967

Table 3. Statin combinations with small-molecule inhibitors to increase anticancer efficacy.

Agent	Molecular target(s)	Cancer type(s)	Proposed mechanism(s) of interaction	Reference
Dipyridamole	Polypharmacology with activity against SREBP	Multiple cancer types, including AML, multiple myeloma, prostate, and breast	Dipyridamole inhibits statin-induced SREBP activation and potentiates statin-induced apoptosis of tumor cells	32, 38, 42
Zoledronic acid	FPP synthase	Multiple cancer types, including lymphoma, breast, and ovarian	Combined inhibition of the mevalonate pathway	52, 107, 108
Abiraterone acetate Enzalutamide	AR	Prostate	Enhanced suppression of AR signaling; statins reduce AR expression and activity	82–84
Venetoclax	BCL2	Hematologic cancers	Statins suppress protein geranylgeranylation, resulting in PUMA upregulation and venetoclax sensitization	109
Selumetinib	MEK, Cys-Glu antiporter	Pancreatic	Enhanced oxidative stress	27
Erlotinib Gefitinib	EGFR	Multiple cancer types, including NSCLC and HNSCC	Enhanced suppression of EGFR signaling; statins inhibit ligand-induced EGFR activation and AKT signaling	87–91
Vismodegib	Smoothened	Medulloblastoma	Enhanced suppression of Hedgehog signaling	21
JQ1	BET bromodomains	Pancreatic	Combined inhibition of processes downstream of acetyl-CoA	3
Vorinostat Panobinostat	HDACs	Multiple cancer types, including renal and breast	Impaired autophagic flux, AMPK activation	94–96
Celecoxib	COX2	Multiple cancer types, including prostate and colorectal	Unknown	110–112
Metformin	Polypharmacology, indirect activation of AMPK	Multiple cancer types, including prostate and endometrial	Unknown; possibly enhanced AMPK activation	113, 114
Anti-PD-1 antibody	PD-1	Multiple cancer types, including melanoma	Enhanced T-cell activation and antitumor immunity	102

Abbreviations: AML, acute myeloid leukemia; HNSCC, head and neck squamous cell carcinoma.

SREBP inhibition

One approach to potentiate statin-induced apoptosis is via combination treatment with SREBP inhibitors. Similar to normal cells, statin treatment triggers the activation of the SREBPs in most cancer cells (**Fig. 1**). Statin-mediated activation of the SREBPs, particularly SREBP2, results in the induction of mevalonate pathway gene expression, including the upregulation of HMGCR. Knockdown of *SREBF2* (the gene that encodes SREBP2) via RNAi suppresses this feedback loop and sensitizes cancer cells to statin-induced death (32, 77). Consistent with this result, our group identified that the drug dipyridamole, an agent approved for the secondary prevention of cerebral ischemia, could synergize with statins to induce apoptosis in hematologic cancer (42) and prostate cancer (32) cells. Mechanistically, we and others have shown that dipyridamole inhibits statin-induced SREBP activation, thereby preventing the upregulation of mevalonate pathway genes in response to statin exposure (32, 38, 42). By impairing this feedback mechanism, dipyridamole significantly reduces the concentration of statin drug needed to inhibit the mevalonate pathway and induce apoptosis. Because both statins and dipyridamole are FDA-approved drugs, there is interest in advancing this drug combination to clinical trials in oncology.

Antiandrogen therapy

Epidemiologic evidence supports a positive association between statin use and response to antiandrogen therapy in patients with prostate cancer (78–81). These data are further supported by preclinical studies showing that the combination of a statin with either abiraterone acetate or enzalutamide enhances cytotoxicity in prostate cancer cell lines (82, 83). Moreover, enzalutamide-resistant prostate cancer cells upregulate HMGCR expression, and treatment with simvastatin resensitizes these cells to enzalutamide (84).

A number of mechanisms have been proposed for the interaction between statins and antiandrogen therapy. First, cholesterol is a precursor for androgen biosynthesis, and, therefore, statin-mediated cholesterol depletion may also reduce intratumoral androgen levels. Consistent with this hypothesis, statins have been shown to inhibit androgen receptor (AR) activity in prostate cancer cell lines (82–85). In these same studies, statins were also found to reduce AR expression (82–85), possibly via the inhibition of AKT/mTOR signaling (84). Moreover, statin use has been associated with reduced serum PSA levels in patients with prostate cancer (86), which is regulated by AR. Finally, certain statin drugs can compete with dehydroepiandrosterone sulfate, a testosterone precursor, for binding to a transporter at the surface of prostate cancer cells, and, therefore, block androgen uptake (78). Taken together, statins can enhance antiandrogen therapy through multiple mechanisms. Prospective clinical trials are warranted to evaluate the combination of a statin and antiandrogen therapy in patients with advanced prostate cancer and other steroid hormone–driven malignancies.

EGFR inhibitors

Given the interplay between the mevalonate pathway and oncogenic signal transduction (1), numerous studies have evaluated the combination of a statin with various agents that target cell signaling (**Table 3**). For example, statins synergize with EGFR inhibitors, including erlotinib and gefitinib, to induce cell death in a number of different cancer

Published OnlineFirst September 4, 2020; DOI: 10.1158/1078-0432.CCR-20-1967

cell types *in vitro* (87). Statins have been shown to inhibit ligand-induced EGFR activation and downstream AKT signaling, which can be reversed by exogenous GGPP (88, 89). Statin-mediated inhibition of AKT has further been implicated as a mechanism for overcoming resistance to EGFR inhibitors in non–small cell lung cancer (NSCLC) cells (90, 91). Combined treatment with a statin and EGFR inhibitor has been evaluated in phase II RCTs in patients with NSCLC (**Table 2**). Simvastatin (40 mg/day) in combination with gefitinib resulted in higher tumor response rates and longer progression-free survival (PFS) compared with gefitinib alone in patients with EGFR wild-type nonadenocarcinomas (92); however, similar responses were not observed when simvastatin was combined with afatinib, a second-generation EGFR inhibitor (93).

Epigenetic inhibitors

An emerging area of investigation is the combination of statins and epigenetic inhibitors, including histone deacetylase (HDAC) and bromodomain inhibitors (refs. 3, 94–96; **Table 3**). A series of dual-action compounds has also been developed, where the hydroxamate group of vorinostat, an HDAC inhibitor, was fused to lovastatin (97). The resulting HMGCR-HDAC dual inhibitors have been shown to possess potent and selective anticancer activity (98, 99). In mouse models of colorectal cancer, treatment with a dual HMGCR-HDAC inhibitor significantly reduced intestinal inflammation, decreased tumor burden, and impaired metastasis (98).

The mechanism by which statins and different epigenetic inhibitors interact remains poorly characterized. However, given that acetyl-CoA is required for both protein acetylation and mevalonate metabolism, it is possible that simultaneously inhibiting multiple acetyl-CoA–dependent processes is detrimental to tumor cells. Indeed, both histone acetylation and mevalonate pathway gene expression are upregulated in pancreatic adenocarcinoma (PDAC) tumors, and cotreatment with atorvastatin and a bromodomain inhibitor, JQ1, significantly impairs PDAC cell growth (3).

Immunotherapy

Statins have also been shown to elicit immunomodulatory effects (reviewed in ref. 100). High cholesterol in the tumor microenvironment and in tumor-infiltrating $CD8^+$ T cells is associated with elevated expression of immune checkpoint proteins and enhanced T-cell exhaustion, which allows tumor cells to escape immune surveillance (101). Importantly, reducing cholesterol levels in the tumor microenvironment or in $CD8^+$ T cells restores T-cell anti-tumor activity (101). These critical observations highlight the potential for statins to be combined with immunotherapy for the treatment of cancer. An independent study that evaluated the vaccine adjuvant activity of statins revealed that lipophilic statins, such as simvastatin, induce a strong Th1 and cytotoxic T-cell response in mice and enhance the therapeutic response to cancer vaccination (102). In particular, the inhibition of protein prenylation in antigen-presenting cells enhanced antigen presentation and T-cell activation (102). This favorable antitumor response was further potentiated by programmed cell death protein-1 (PD-1) blockade, which resulted in prolonged survival in mice inoculated with melanoma or human papillomavirus–associated tumors (102). As most preclinical studies to date have evaluated the anticancer activity of statins *in vitro* or in immunocompromised animal models, future investigation into the immunomodulatory properties of statins will undoubtably open exciting avenues of research with important clinical implications.

Outlook

If statins are to be integrated into cancer patient care, a precision medicine approach is necessary. In this review, we highlighted recent advances and outlined important considerations for advancing statins to clinical trials in oncology. We also proposed key questions that should be the focus of future research (**Table 4**). As not all tumors are vulnerable to statin-mediated mevalonate pathway inhibition, the development of predictive biomarkers of statin sensitivity is crucial for patient stratification. We have highlighted some promising preclinical biomarkers of statin sensitivity, which can be validated in future clinical trials by enriching for patients with these tumor features. In addition, *post hoc* analyses of completed, unbiased RCTs may similarly reveal novel biomarkers of statin response. However, few statin RCTs in oncology have been performed to date, and those that have been performed evaluated moderate-intensity statin regimens. Given the increasing evidence that certain statins may be better suited as anticancer agents than others, coupled with data indicating that statin-induced apoptosis is both dose- and time-dependent, careful consideration is required when deciding which statin(s) and dosing schedules to evaluate clinically. It is also unlikely that statins will be prescribed as a monotherapy, and, therefore, further investigation into drug combination strategies will remain an important area of research. As a number of preclinical potentiators of statin-induced cancer cell death have already been described, many of which are FDA-approved, immediate phase I/II studies are possible. The outcome of these studies will provide important insights into how to realistically use these immediately available, well-tolerated, and inexpensive agents as precision anticancer therapeutics.

Table 4. Future research.

(i)	With improvements in reagents to study the mevalonate pathway, including validated HMGCR antibodies, further research into the mechanisms of mevalonate pathway deregulation in cancer is needed.
(ii)	Promising predictive biomarkers have been described in cell line models, which warrant further characterization and validation in relevant patient-derived models and clinical trials. These may inform patient inclusion in future RCTs.
(iii)	Impaired feedback regulation of the mevalonate pathway has been described as a feature of statin sensitivity in different cancer cell lines; however, the extent of this deregulation in human tumors remains to be characterized. A better understanding of the mechanisms behind this impairment will allow for the development of additional predictive biomarkers of statin sensitivity.
(iv)	As some statin drugs may have a greater propensity to accumulate in certain tumor tissues than others, a direct comparison of the achievable concentrations of different statins in distinct tissues is needed.
(v)	Studies are required to evaluate and compare the efficacy of different statins as anticancer agents at various doses (typical cholesterol-lowering doses vs. dose escalation) and treatment durations. The development of dynamic biomarkers of statin response will facilitate real-time monitoring of treatment efficacy.
(vi)	A better understanding of the mechanisms by which different classes of agents potentiate the anticancer activity of statins will allow for the future development of effective drug combinations.
(vii)	A number of preclinical potentiators of statin-induced cell death have been described and need to be evaluated in RCTs.
(viii)	Statins have known immunomodulatory properties, which to date have been poorly studied in the context of cancer. Further research in this area is imperative. How these properties influence their interaction with different immunotherapies should also be explored.

Published OnlineFirst September 4, 2020; DOI: 10.1158/1078-0432.CCR-20-1967

Disclosure of Potential Conflicts of Interest

No potential conflicts of interest were disclosed.

Disclaimer

Opinions, interpretations, conclusions, and recommendations are those of the authors and are not necessarily endorsed by the Department of Defense.

Acknowledgments

We thank all members of the Penn laboratory, Drs. Rebecca Gladdy, Benjamin Haibe-Kains, Rob Hamilton, and David Hedley for helpful discussions and critical review of this article. L.Z. Penn holds a Tier 1 Canada Research Chair in Molecular Oncology. The Penn laboratory was supported by funding from the Canadian Institutes of Health Research (CIHR; FRN: 142263), Terry Fox Research Institute (New Frontiers PPG-1064), Canadian Cancer Society (grant #706394), and the Office of the Assistant Secretary of Defense for Health Affairs, through the Breast Cancer Research Program (award no., W81XWH-16-1-0068). J. Longo was supported by a CIHR Doctoral Research award, J.E. van Leeuwen was supported by a Princess Margaret Hospital Foundation Graduate Fellowship in Cancer Research, and M. Elbaz was supported by a George Knudson Memorial Fellowship.

The costs of publication of this article were defrayed in part by the payment of page charges. This article must therefore be hereby marked *advertisement* in accordance with 18 U.S.C. Section 1734 solely to indicate this fact.

Received May 21, 2020; revised July 29, 2020; accepted September 1, 2020; published first September 4, 2020.

References

1. Mullen PJ, Yu R, Longo J, Archer MC, Penn LZ. The interplay between cell signalling and the mevalonate pathway in cancer. Nat Rev Cancer 2016;16:718–31.
2. Clendening JW, Pandyra A, Boutros PC, El Ghamrasni S, Khosravi F, Trentin GA, et al. Dysregulation of the mevalonate pathway promotes transformation. Proc Natl Acad Sci U S A 2010;107:15051–6.
3. Carrer A, Trefely S, Zhao S, Campbell SL, Norgard RJ, Schultz KC, et al. Acetyl-CoA metabolism supports multistep pancreatic tumorigenesis. Cancer Discov 2019;9:416–35.
4. Duncan RE, El-Sohemy A, Archer MC. Mevalonate promotes the growth of tumors derived from human cancer cells *in vivo* and stimulates proliferation *in vitro* with enhanced cyclin-dependent kinase-2 activity. J Biol Chem 2004; 279:33079–84.
5. Newman A, Clutterbuck RD, Powles RL, Catovsky D, Millar JL. A comparison of the effect of the 3-hydroxy-3-methylglutaryl coenzyme A (HMG-CoA) reductase inhibitors simvastatin, lovastatin and pravastatin on leukaemic and normal bone marrow progenitors. Leuk Lymphoma 1997;24:533–7.
6. Dimitroulakos J, Nohynek D, Backway KL, Hedley DW, Yeger H, Freedman MH, et al. Increased sensitivity of acute myeloid leukemias to lovastatin-induced apoptosis: a potential therapeutic approach. Blood 1999;93:1308–18.
7. Wong WWL, Tan MM, Xia Z, Dimitroulakos J, Minden MD, Penn LZ. Cerivastatin triggers tumor-specific apoptosis with higher efficacy than lovastatin. Clin Cancer Res 2001;7:2067–75.
8. Graaf MR, Beiderbeck AB, Egberts ACG, Richel DJ, Guchelaar HJ. The risk of cancer in users of statins. J Clin Oncol 2004;22:2388–94.
9. Poynter JN, Gruber SB, Higgins PDR, Almog R, Bonner JD, Rennert HS, et al. Statins and the risk of colorectal cancer. N Engl J Med 2005;352:2184–92.
10. Cauley JA, McTiernan A, Rodabough RJ, LaCroix A, Bauer DC, Margolis KL, et al. Statin use and breast cancer: prospective results from the Women's Health Initiative. J Natl Cancer Inst 2006;98:700–7.
11. Kuoppala J, Lamminpää A, Pukkala E. Statins and cancer: a systematic review and meta-analysis. Eur J Cancer 2008;44:2122–32.
12. Jacobs EJ, Rodriguez C, Bain EB, Wang Y, Thun MJ, Calle EE. Cholesterol-lowering drugs and advanced prostate cancer incidence in a large U.S. cohort. Cancer Epidemiol Biomarkers Prev 2007;16:2213–7.
13. Kumar AS, Benz CC, Shim V, Minami CA, Moore DH, Esserman LJ. Estrogen receptor-negative breast cancer is less likely to arise among lipophilic statin users. Cancer Epidemiol Biomarkers Prev 2008;17:1028–33.
14. Nielsen SF, Nordestgaard BG, Bojesen SE. Statin use and reduced cancer-related mortality. N Engl J Med 2012;367:1792–802.
15. Ahern TP, Pedersen L, Tarp M, Cronin-Fenton DP, Garne JP, Silliman RA, et al. Statin prescriptions and breast cancer recurrence risk: a Danish nationwide prospective cohort study. J Natl Cancer Inst 2011;103:1461–8.
16. Park HS, Schoenfeld JD, Mailhot RB, Shive M, Hartman RI, Ogembo R, et al. Statins and prostate cancer recurrence following radical prostatectomy or radiotherapy: a systematic review and meta-analysis. Ann Oncol 2013;24:1427–34.
17. Sanfilippo KM, Keller J, Gage BF, Luo S, Wang TF, Moskowitz G, et al. Statins are associated with reduced mortality in multiple myeloma. J Clin Oncol 2016; 34:4008–14.
18. Zhong S, Zhang X, Chen L, Ma T, Tang J, Zhao J. Statin use and mortality in cancer patients: systematic review and meta-analysis of observational studies. Cancer Treat Rev 2015;41:554–67.
19. Riscal R, Skuli N, Simon MC. Even cancer cells watch their cholesterol! Mol Cell 2019;76:220–31.
20. Zhuang L, Kim J, Adam RM, Solomon KR, Freeman MR. Cholesterol targeting alters lipid raft composition and cell survival in prostate cancer cells and xenografts. J Clin Invest 2005;115:959–68.
21. Gordon RE, Zhang L, Peri S, Kuo YM, Du F, Egleston BL, et al. Statins synergize with hedgehog pathway inhibitors for treatment of medulloblastoma. Clin Cancer Res 2018;24:1375–88.
22. Xia Z, Tan MM, Wong WW, Dimitroulakos J, Minden MD, Penn LZ. Blocking protein geranylgeranylation is essential for lovastatin-induced apoptosis of human acute myeloid leukemia cells. Leukemia 2001;15:1398–407.
23. Wong WW-L, Clendening JW, Martirosyan A, Boutros PC, Bros C, Khosravi F, et al. Determinants of sensitivity to lovastatin-induced apoptosis in multiple myeloma. Mol Cancer Ther 2007;6:1886–97.
24. Yu R, Longo J, van Leeuwen JE, Mullen PJ, Ba-Alawi W, Haibe-Kains B, et al. Statin-induced cancer cell death can be mechanistically uncoupled from prenylation of RAS family proteins. Cancer Res 2018;78:1347–57.
25. Taylor-Harding B, Orsulic S, Karlan BY, Li AJ. Fluvastatin and cisplatin demonstrate synergistic cytotoxicity in epithelial ovarian cancer cells. Gynecol Oncol 2010;119:549–56.
26. Kaymak I, Maier CR, Schmitz W, Campbell AD, Dankworth B, Ade CP, et al. Mevalonate pathway provides ubiquinone to maintain pyrimidine synthesis and survival in p53-deficient cancer cells exposed to metabolic stress. Cancer Res 2020;80:189–203.
27. McGregor GH, Campbell AD, Fey SK, Tumanov S, Sumpton D, Blanco GR, et al. Targeting the metabolic response to statin-mediated oxidative stress produces a synergistic antitumor response. Cancer Res 2020;80:175–88.
28. van de Donk NWCJ, Kamphuis MMJ, van Kessel B, Lokhorst HM, Bloem AC. Inhibition of protein geranylgeranylation induces apoptosis in myeloma plasma cells by reducing Mcl-1 protein levels. Blood 2003;102:3354–62.
29. Sparrow CP, Burton CA, Hernandez M, Mundt S, Hassing H, Patel S, et al. Simvastatin has anti-inflammatory and antiatherosclerotic activities independent of plasma cholesterol lowering. Arterioscler Thromb Vasc Biol 2001;21:115–21.
30. Martirosyan A, Clendening JW, Goard CA, Penn LZ. Lovastatin induces apoptosis of ovarian cancer cells and synergizes with doxorubicin: potential therapeutic relevance. BMC Cancer 2010;10:103.
31. Goard CA, Chan-Seng-Yue M, Mullen PJ, Quiroga AD, Wasylishen AR, Clendening JW, et al. Identifying molecular features that distinguish fluvastatin-sensitive breast tumor cells. Breast Cancer Res Treat 2014;143:301–12.
32. Longo J, Mullen PJ, Yu R, van Leeuwen JE, Masoomian M, Woon DTS, et al. An actionable sterol-regulated feedback loop modulates statin sensitivity in prostate cancer. Mol Metab 2019;25:119–30.
33. Garwood ER, Kumar AS, Baehner FL, Moore DH, Au A, Hylton N, et al. Fluvastatin reduces proliferation and increases apoptosis in women with high grade breast cancer. Breast Cancer Res Treat 2010;119:137–44.
34. Warita K, Warita T, Beckwitt CH, Schurdak ME, Vazquez A, Wells A, et al. Statin-induced mevalonate pathway inhibition attenuates the growth of mesenchymal-like cancer cells that lack functional E-cadherin mediated cell cohesion. Sci Rep 2014;4:1–8.
35. Viswanathan VS, Ryan MJ, Dhruv HD, Gill S, Eichhoff OM, Seashore-Ludlow B, et al. Dependency of a therapy-resistant state of cancer cells on a lipid peroxidase pathway. Nature 2017;547:453–7.
36. Clendening JW, Pandyra A, Li Z, Boutros PC, Martirosyan A, Lehner R, et al. Exploiting the mevalonate pathway to distinguish statin-sensitive multiple myeloma. Blood 2010;115:4787–97.

37. Kimbung S, Lettiero B, Feldt M, Bosch A, Borgquist S. High expression of cholesterol biosynthesis genes is associated with resistance to statin treatment and inferior survival in breast cancer. Oncotarget 2016;7:59640–51.
38. Göbel A, Breining D, Rauner M, Hofbauer LC, Rachner TD. Induction of 3-hydroxy-3-methylglutaryl-CoA reductase mediates statin resistance in breast cancer cells. Cell Death Dis 2019;10:91.
39. Bjarnadottir O, Romero Q, Bendahl PO, Jirström K, Rydén L, Loman N, et al. Targeting HMG-CoA reductase with statins in a window-of-opportunity breast cancer trial. Breast Cancer Res Treat 2013;138:499–508.
40. Bjarnadottir O, Feldt M, Inasu M, Bendahl PO, Elebro K, Kimbung S, et al. Statin use, HMGCR expression, and breast cancer survival – The Malmö Diet and Cancer Study. Sci Rep 2020;10:558.
41. Freed-Pastor WA, Mizuno H, Zhao X, Langerød A, Moon SH, Rodriguez-Barrueco R, et al. Mutant p53 disrupts mammary tissue architecture via the mevalonate pathway. Cell 2012;148:244–58.
42. Pandyra A, Mullen PJ, Kalkat M, Yu R, Pong JT, Li Z, et al. Immediate utility of two approved agents to target both the metabolic mevalonate pathway and its restorative feedback loop. Cancer Res 2014;74:4772–82.
43. Wang M, Casey PJ. Protein prenylation: unique fats make their mark on biology. Nat Rev Mol Cell Biol 2016;17:110–22.
44. DeClue JE, Vass WC, Papageorge AG, Lowy DR, Willumsen BM. Inhibition of cell growth by lovastatin is independent of ras function. Cancer Res 1991;51:712–7.
45. Lee J, Hong YS, Hong JY, Han SW, Kim TW, Kang HJ, et al. Effect of simvastatin plus cetuximab/irinotecan for KRAS mutant colorectal cancer and predictive value of the RAS signature for treatment response to cetuximab. Invest New Drugs 2014;32:535–41.
46. Baas JM, Krens LL, Ten Tije AJ, Erdkamp F, Van Wezel T, Morreau H, et al. Safety and efficacy of the addition of simvastatin to cetuximab in previously treated KRAS mutant metastatic colorectal cancer patients. Invest New Drugs 2015;33:1242–7.
47. Baas JM, Krens LL, Bos MM, Portielje JEA, Batman E, Van Wezel T, et al. Safety and efficacy of the addition of simvastatin to panitumumab in previously treated KRAS mutant metastatic colorectal cancer patients. Anticancer Drugs 2015;26:872–7.
48. Hong JY, Nam EM, Lee J, Park JO, Lee SC, Song SY, et al. Randomized double-blinded, placebo-controlled phase II trial of simvastatin and gemcitabine in advanced pancreatic cancer patients. Cancer Chemother Pharmacol 2014;73:125–30.
49. Moon SH, Huang CH, Houlihan SL, Regunath K, Freed-Pastor WA, Morris JP, et al. p53 represses the mevalonate pathway to mediate tumor suppression. Cell 2019;176:564–80.
50. Turrell FK, Kerr EM, Gao M, Thorpe H, Doherty GJ, Cridge J, et al. Lung tumors with distinct p53 mutations respond similarly to p53 targeted therapy but exhibit genotype-specific statin sensitivity. Genes Dev 2017;31:1339–53.
51. Parrales A, Ranjan A, Iyer SV, Padhye S, Weir SJ, Roy A, et al. DNAJA1 controls the fate of misfolded mutant p53 through the mevalonate pathway. Nat Cell Biol 2016;18:1233–43.
52. Tutuska K, Parrilla-Monge L, Di Cesare E, Nemajerova A, Moll UM. Statin as anti-cancer therapy in autochthonous T-lymphomas expressing stabilized gain-of-function mutant p53 proteins. Cell Death Dis 2020;11:274.
53. Ingallina E, Sorrentino G, Bertolio R, Lisek K, Zannini A, Azzolin L, et al. Mechanical cues control mutant p53 stability through a mevalonate-RhoA axis. Nat Cell Biol 2018;20:28–35.
54. Thompson JM, Alvarez A, Singha MK, Pavesic MW, Nguyen QH, Nelson LJ, et al. Targeting the mevalonate pathway suppresses VHL-deficient CC-RCC through an HIF-dependent mechanism. Mol Cancer Ther 2018;17:1781–92.
55. Longo J, Smirnov P, Li Z, Branchard E, van Leeuwen JE, Licht JD, et al. The mevalonate pathway is an actionable vulnerability of t(4;14)-positive multiple myeloma. Leukemia 2020.
56. Duncan RE, El-Sohemy A, Archer MC. Statins and the risk of cancer. JAMA 2006;295:2720–2.
57. Knuuttila E, Riikonen J, Syvälä H, Auriola S, Murtola TJ. Access and concentrations of atorvastatin in the prostate in men with prostate cancer. Prostate 2019;79:1412–9.
58. Longo J, Hamilton RJ, Masoomian M, Khurram N, Branchard E, Mullen PJ, et al. A pilot window-of-opportunity study of preoperative fluvastatin in localized prostate cancer. Prostate Cancer Prostatic Dis 2020.
59. Murtola TJ, Syvälä H, Tolonen T, Helminen M, Riikonen J, Koskimäki J, et al. Atorvastatin versus placebo for prostate cancer before radical prostatectomy-a randomized, double-blind, placebo-controlled clinical trial. Eur Urol 2018;74:697–701.
60. Platz EA, Leitzmann MF, Visvanathan K, Rimm EB, Stampfer MJ, Willett WC, et al. Statin drugs and risk of advanced prostate cancer. J Natl Cancer Inst 2006;98:1819–25.
61. Hamilton RJ, Banez LL, Aronson WJ, Terris MK, Platz EA, Kane CJ, et al. Statin medication use and the risk of biochemical recurrence after radical prostatectomy: results from the Shared Equal Access Regional Cancer Hospital (SEARCH) database. Cancer 2010;116:3389–98.
62. Jiang P, Mukthavaram R, Chao Y, Nomura N, Bharati IS, Fogal V, et al. *In vitro* and *in vivo* anticancer effects of mevalonate pathway modulation on human cancer cells. Br J Cancer 2014;111:1562–71.
63. Thibault A, Samid D, Tompkins AC, Figg WD, Cooper MR, Hohl RJ, et al. Phase I study of lovastatin, an inhibitor of the mevalonate pathway, in patients with cancer. Clin Cancer Res 1996;2:483–91.
64. Knox JJ, Siu LL, Chen E, Dimitroulakos J, Kamel-Reid S, Moore MJ, et al. A phase I trial of prolonged administration of lovastatin in patients with recurrent or metastatic squamous cell carcinoma of the head and neck or of the cervix. Eur J Cancer 2005;41:523–30.
65. van der Spek E, Bloem AC, van de Donk NWCJ, Bogers LH, van der Griend R, Kramer MH, et al. Dose-finding study of high-dose simvastatin combined with standard chemotherapy in patients with relapsed or refractory myeloma or lymphoma. Haematologica 2006;91:542–5.
66. Kornblau SM, Banker DE, Stirewalt D, Shen D, Lemker E, Verstovsek S, et al. Blockade of adaptive defensive changes in cholesterol uptake and synthesis in AML by the addition of pravastatin to idarubicin + high-dose Ara-C: a phase 1 study. Blood 2007;109:2999–3006.
67. Bjarnadottir O, Kimbung S, Johansson I, Veerla S, Jönsson M, Bendahl PO, et al. Global transcriptional changes following statin treatment in breast cancer. Clin Cancer Res 2015;21:3402–11.
68. Hus M, Grzasko N, Szostek M, Pluta A, Helbig G, Woszczyk D, et al. Thalidomide, dexamethasone and lovastatin with autologous stem cell transplantation as a salvage immunomodulatory therapy in patients with relapsed and refractory multiple myeloma. Ann Hematol 2011;90:1161–6.
69. Goss GD, Jonker DJ, Laurie SA, Weberpals JI, Oza AM, Spaans JN, et al. A phase I study of high-dose rosuvastatin with standard dose erlotinib in patients with advanced solid malignancies. J Transl Med 2016;14:83.
70. Seckl MJ, Ottensmeier CH, Cullen M, Schmid P, Ngai Y, Muthukumar D, et al. Multicenter, phase III, randomized, double-blind, placebo-controlled trial of pravastatin added to first-line standard chemotherapy in small-cell lung cancer (LUNGSTAR). J Clin Oncol 2017;35:1506–14.
71. Lim SH, Kim TW, Hong YS, Han SW, Lee KH, Kang HJ, et al. A randomised, double-blind, placebo-controlled multi-centre phase III trial of XELIRI/FOLFIRI plus simvastatin for patients with metastatic colorectal cancer. Br J Cancer 2015;113:1421–6.
72. Jouve JL, Lecomte T, Bouché O, Barbier E, Khemissa Akouz F, Riachi G, et al. Pravastatin combination with sorafenib does not improve survival in advanced hepatocellular carcinoma. J Hepatol 2019;71:516–22.
73. Kim ST, Kang JH, Lee J, Park SH, Park JO, Park YS, et al. Simvastatin plus capecitabine-cisplatin versus placebo plus capecitabine-cisplatin in patients with previously untreated advanced gastric cancer: a double-blind randomised phase 3 study. Eur J Cancer 2014;50:2822–30.
74. Chen C, Lin J, Smolarek T, Tremaine L. P-glycoprotein has differential effects on the disposition of statin acid and lactone forms in mdr1a/b knockout and wild-type mice. Drug Metab Dispos 2007;35:1725–9.
75. Kapur NK, Musunuru K. Clinical efficacy and safety of statins in managing cardiovascular risk. Vasc Health Risk Manag 2008;4:341–53.
76. Goard CA, Mather RG, Vinepal B, Clendening JW, Martirosyan A, Boutros PC, et al. Differential interactions between statins and P-glycoprotein: implications for exploiting statins as anticancer agents. Int J Cancer 2010;127:2939–48.
77. Pandyra AA, Mullen PJ, Goard CA, Ericson E, Sharma P, Kalkat M, et al. Genome-wide RNAi analysis reveals that simultaneous inhibition of specific mevalonate pathway genes potentiates tumor cell death. Oncotarget 2015;6:26909–21.
78. Harshman LC, Wang X, Nakabayashi M, Xie W, Valenca L, Werner L, et al. Statin use at the time of initiation of androgen deprivation therapy and time to progression in patients with hormone-sensitive prostate cancer. JAMA Oncol 2015;1:495–504.
79. Di Lorenzo G, Sonpavde G, Pond G, Lucarelli G, Rossetti S, Facchini G, et al. Statin use and survival in patients with metastatic castration-resistant prostate cancer treated with abiraterone acetate. Eur Urol Focus 2018;4:874–9.

80. Gordon JA, Buonerba C, Pond G, Crona D, Gillessen S, Lucarelli G, et al. Statin use and survival in patients with metastatic castration-resistant prostate cancer treated with abiraterone or enzalutamide after docetaxel failure: the international retrospective observational STABEN study. Oncotarget 2018;9:19861–73.
81. Anderson-Carter I, Posielski N, Liou J-I, Khemees TA, Downs TM, Abel EJ, et al. The impact of statins in combination with androgen deprivation therapy in patients with advanced prostate cancer: a large observational study. Urol Oncol 2019;37:130–7.
82. Miller DR, Ingersoll MA, Chou Y-W, Wakefield CB, Tu Y, Lin F-F, et al. Anti-androgen abiraterone acetate improves the therapeutic efficacy of statins on castration-resistant prostate cancer cells. J Oncol Res Ther 2017;3:1173–8.
83. Syvälä H, Pennanen P, Bläuer M, Tammela TLJ, Murtola TJ. Additive inhibitory effects of simvastatin and enzalutamide on androgen-sensitive LNCaP and VCaP prostate cancer cells. Biochem Biophys Res Commun 2016;481:46–50.
84. Kong Y, Cheng L, Mao F, Zhang Z, Zhang Y, Farah E, et al. Inhibition of cholesterol biosynthesis overcomes enzalutamide resistance in castration-resistant prostate cancer (CRPC). J Biol Chem 2018;293:14328–41.
85. Yang L, Egger M, Plattner R, Klocker H, Eder IE. Lovastatin causes diminished PSA secretion by inhibiting AR expression and function in LNCaP prostate cancer cells. Urology 2011;77:1508.
86. Hamilton RJ, Goldberg KC, Platz EA, Freedland SJ. The influence of statin medications on prostate-specific antigen levels. J Natl Cancer Inst 2008;100:1511–8.
87. Dimitroulakos J, Lorimer IA, Goss G, Lynch T, Heymach J, Eisen T, et al. Strategies to enhance epidermal growth factor inhibition: targeting the mevalonate pathway. Clin Cancer Res 2006;12:4426–32.
88. Mantha AJ, Hanson JEL, Goss G, Lagarde AE, Lorimer IA, Dimitroulakos J. Targeting the mevalonate pathway inhibits the function of the epidermal growth factor receptor. Clin Cancer Res 2005;11:2398–407.
89. Zhao TT, Le Francois BG, Goss G, Ding K, Bradbury PA, Dimitroulakos J. Lovastatin inhibits EGFR dimerization and AKT activation in squamous cell carcinoma cells: potential regulation by targeting rho proteins. Oncogene 2010;29:4682–92.
90. Hwang KE, Kwon SJ, Kim YS, Park DS, Kim BR, Yoon KH, et al. Effect of simvastatin on the resistance to EGFR tyrosine kinase inhibitors in a non-small cell lung cancer with the T790M mutation of EGFR. Exp Cell Res 2014;323:288–96.
91. Chen J, Bi H, Hou J, Zhang X, Zhang C, Yue L, et al. Atorvastatin overcomes gefitinib resistance in KRAS mutant human non-small cell lung carcinoma cells. Cell Death Dis 2013;4:e814.
92. Han JY, Lee SH, Yoo NJ, Lee SH, Moon YJ, Yun T, et al. A randomized phase II study of gefitinib plus simvastatin versus gefitinib alone in previously treated patients with advanced non-small cell lung cancer. Clin Cancer Res 2011;17:1553–60.
93. Lee Y, Lee KH, Lee GK, Lee SH, Lim KY, Joo J, et al. Randomized phase II study of afatinib plus simvastatin versus afatinib alone in previously treated patients with advanced nonadenocarcinomatous non-small cell lung cancer. Cancer Res Treat 2017;49:1001–11.
94. Kou X, Yang Y, Jiang X, Liu H, Sun F, Wang X, et al. Vorinostat and simvastatin have synergistic effects on triple-negative breast cancer cells via abrogating Rab7 prenylation. Eur J Pharmacol 2017;813:161–71.
95. Okubo K, Isono M, Miyai K, Asano T, Sato A. Fluvastatin potentiates anticancer activity of vorinostat in renal cancer cells. Cancer Sci 2020;111:112–26.
96. Lin Z, Zhang Z, Jiang X, Kou X, Bao Y, Liu H, et al. Mevastatin blockade of autolysosome maturation stimulates LBH589-induced cell death in triple-negative breast cancer cells. Oncotarget 2017;8:17833–48.
97. Chen J-B, Chern TR, Wei TT, Chen CC, Lin JH, Fang JM. Design and synthesis of dual-action inhibitors targeting histone deacetylases and 3-hydroxy-3-methylglutaryl coenzyme a reductase for cancer treatment. J Med Chem 2013;56:3645–55.
98. Wei TT, Lin YT, Chen WS, Luo P, Lin YC, Shun CT, et al. Dual targeting of 3-hydroxy-3-methylglutaryl coenzyme a reductase and histone deacetylase as a therapy for colorectal cancer. EBioMedicine 2016;10:124–36.
99. Wei TT, Lin YT, Tseng RY, Shun CT, Lin YC, Wu MS, et al. Prevention of colitis and colitis-associated colorectal cancer by a novel polypharmacological histone deacetylase inhibitor. Clin Cancer Res 2016;22:4158–69.
100. Thurnher M, Gruenbacher G. T lymphocyte regulation by mevalonate metabolism. Sci Signal 2015;8:1–10.
101. Ma X, Bi E, Lu Y, Su P, Huang C, Liu L, et al. Cholesterol induces CD8+ T cell exhaustion in the tumor microenvironment. Cell Metab 2019;30:143–56.
102. Xia Y, Xie Y, Yu Z, Xiao H, Jiang G, Zhou X, et al. The mevalonate pathway is a druggable target for vaccine adjuvant discovery. Cell 2018;175:1059–73.
103. Grundy SM, Stone NJ, Bailey AL, Beam C, Birtcher KK, Blumenthal RS, et al. 2018 AHA/ACC/AACVPR/AAPA/ABC/ACPM/ADA/AGS/APhA/ASPC/NLA/PCNA guideline on the management of blood cholesterol: a report of the American College of Cardiology/American Heart Association Task Force on Clinical Practice Guidelines. Circulation 2019;139:E1082–143.
104. Ward NC, Watts GF, Eckel RH. Statin toxicity: mechanistic insights and clinical implications. Circ Res 2019;124:328–50.
105. Kawata S, Yamasaki E, Nagase T, Inui Y, Ito N, Matsuda Y, et al. Effect of pravastatin on survival in patients with advanced hepatocellular carcinoma. A randomized controlled trial. Br J Cancer 2001;84:886–91.
106. Konings IRHM, Van Der Gaast A, Van Der Wijk LJ, De Jongh FE, Eskens FALM, Sleijfer S. The addition of pravastatin to chemotherapy in advanced gastric carcinoma: a randomised phase II trial. Eur J Cancer 2010;46:3200–4.
107. Göbel A, Thiele S, Browne AJ, Rauner M, Zinna VM, Hofbauer LC, et al. Combined inhibition of the mevalonate pathway with statins and zoledronic acid potentiates their anti-tumor effects in human breast cancer cells. Cancer Lett 2016;375:162–71.
108. Abdullah MI, Abed MN, Richardson A. Inhibition of the mevalonate pathway augments the activity of pitavastatin against ovarian cancer cells. Sci Rep 2017;7:8090.
109. Lee JS, Roberts A, Juarez D, Vo TTT, Bhatt S, Herzog LO, et al. Statins enhance efficacy of venetoclax in blood cancers. Sci Transl Med 2018;10:eaaq1240.
110. Zheng X, Cui XX, Avila GE, Huang MT, Liu Y, Patel J, et al. Atorvastatin and celecoxib inhibit prostate PC-3 tumors in immunodeficient mice. Clin Cancer Res 2007;13:5480–7.
111. Xiao H, Zhang Q, Lin Y, Reddy BS, Yang CS. Combination of atorvastatin and celecoxib synergistically induces cell cycle arrest and apoptosis in colon cancer cells. Int J Cancer 2008;122:2115–24.
112. Zheng X, Cui XX, Gao Z, Zhao Y, Lin Y, Shih WJ, et al. Atorvastatin and celecoxib in combination inhibits the progression of androgen-dependent LNCaP xenograft prostate tumors to androgen independence. Cancer Prev Res 2010;3:114–24.
113. Babcook MA, Shukla S, Fu P, Vazquez EJ, Puchowicz MA, Molter JP, et al. Synergistic simvastatin and metformin combination chemotherapy for osseous metastatic castration-resistant prostate cancer. Mol Cancer Ther 2014;13:2288–302.
114. Kim JS, Turbov J, Rosales R, Thaete LG, Rodriguez GC. Combination simvastatin and metformin synergistically inhibits endometrial cancer cell growth. Gynecol Oncol 2019;154:432–40.

AACR American Association for Cancer Research

Clinical Cancer Research

Statins as Anticancer Agents in the Era of Precision Medicine

Joseph Longo, Jenna E. van Leeuwen, Mohamad Elbaz, et al.

Clin Cancer Res 2020;26:5791-5800. Published OnlineFirst September 4, 2020.

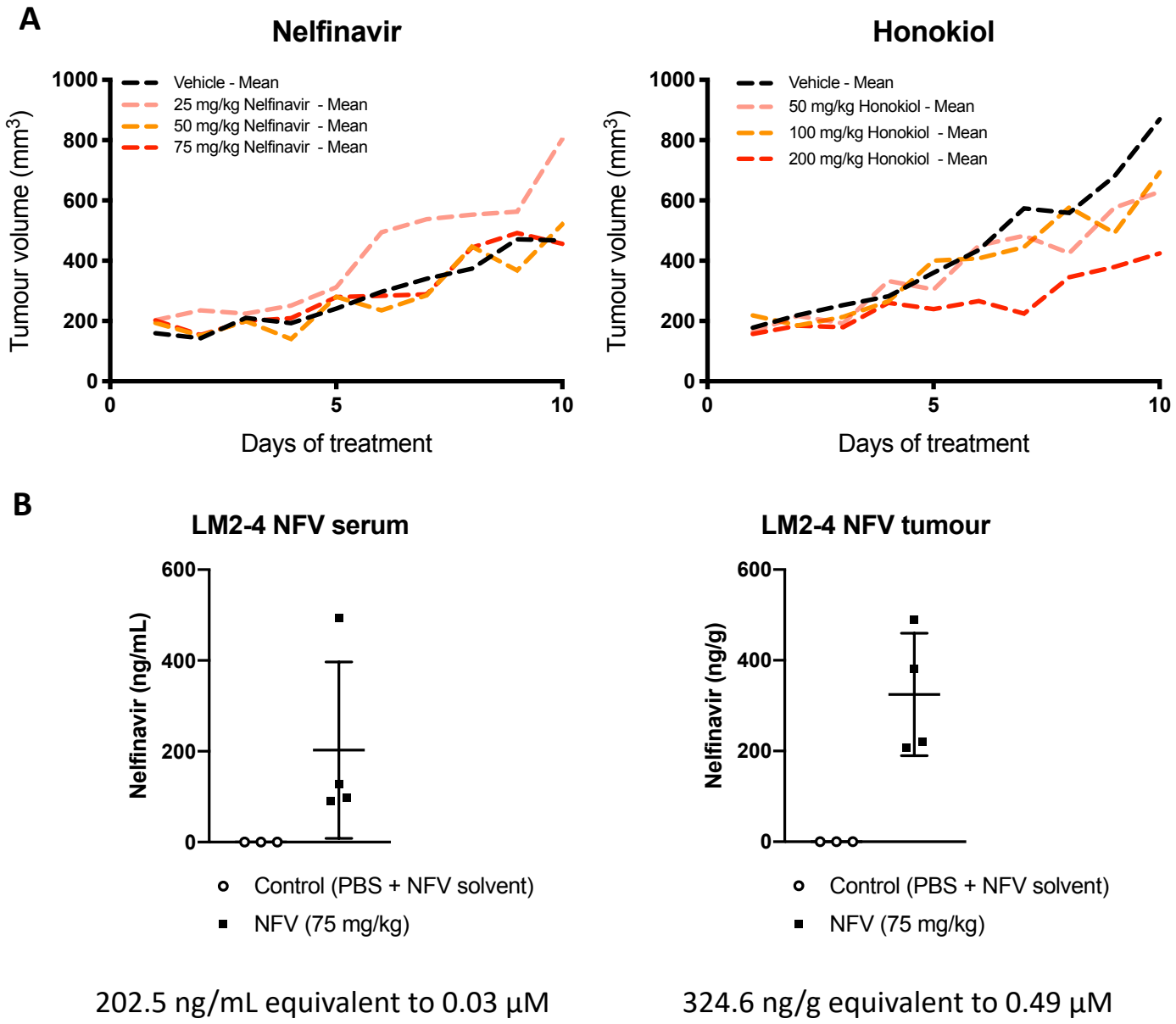

202.5 ng/mL equivalent to 0.03 µM

324.6 ng/g equivalent to 0.49 µM

Figure 1. (A) Pilot experiments to establish dose of single-agent Nelfinavir and Honokiol in LM2-4 cell line xenograft mouse models of breast cancer (n=3 mice per group. Nelfinavir – 1x daily IP injection (Control = 4% DMSO, 5% PEG, 5% Tween80 in saline) Honokiol – 1x daily IP injection (Control = EtOH in 20% intralipid) **(B)** Nelfinavir measured by HPLC in the serum and tumor of the mice. These experiments pilot further evaluation of efficacy in PDO and PDX as outlined for work to perform during the next 12 months as part of our no-cost-extension.